ABSTRACT

LAI, YEN-HAO. Mechanisms and Models of Pain in Head and Neck Cancer Irradiation. (Under the direction of Dr. Michael W. Nolan and Dr. B. Duncan X. Lascelles).

Four out of every five head and neck cancer (HNC) patients treated with (chemo)radiotherapy experience severe and painful oral mucositis. This radiotherapy-associated pain (RAP) significantly reduces the patients' quality of life (QOL). Opioids are commonly used for managing severe pain; because RAP can be long-lasting, patients are at increased risk of chronic opioid use that can lead to dependency, misuse, and/or abuse. Understanding the mechanism(s) of severe acute orofacial RAP will help us to develop safer alternatives that effectively control RAP.

Transient receptor potential vanilloid (TRPV) 1-4 are temperature sensitive ion channels; when located on sensory neurons, these channels can be used by the body to regulate various forms of orofacial pain. Our laboratory's previously published work demonstrated that in mice with severe radiation-induced glossitis, a high proportion of trigeminal sensory neurons are responsive to both a TRPV1 agonist (capsaicin), and a partial TRPV4 agonist (histamine). We therefore hypothesized that orofacial irradiation activates both TRPV1 and TRPV4 on trigeminal afferent neurons; we theorized that the channels become activated before glossitis is clinically evident, and that the activation persists long after glossitis has clinically resolved. We also hypothesized that this channel activation is accompanied by overexpression of TRPV1 and TRPV4.

Our pilot studies (Chapter 2) confirmed that with slight methodologic modifications, a single fraction of 27 Gy induces severe but recoverable glossitis in mice. Furthermore, the low doses of radiation that scatter to distant parts of the body during this high-dose lingual irradiation do not impact the expression or function of TRPV1 on trigeminal neurons. Subsequent

experiments (Chapter 3) characterized the biological changes that occur in mice over the first 45 days following high-dose lingual irradiation. Via *ex vivo* calcium imaging experiments, we found that in tongue-irradiated mice, a high proportion of trigeminal sensory neurons are responsive to various pain stimuli as early as one day post-irradiation; these changes persist for up to 21 days. For reference, glossitis begins 7 days post-irradiation, is most severe at 11-12 days, and resolves by day 15. Accompanying these changes in neuronal function, we also found that tongue-irradiation causes upregulation of the TRPV1 and TRPV4 proteins in trigeminal ganglia and irradiated tongue tissue, respectively. Corresponding to these results, quantitative reverse transcriptase PCR (qPCR) of trigeminal ganglia demonstrated a radiation-induced overexpression of various pain-related TRP genes including *Trpv1*, *Trpa1* and *Trpm8*. Expression of the *Gfrα3* gene was also increased in trigeminal ganglia of mice with radiation-induced glossitis; this is interesting because GFRα3 is the receptor for artemin, which is a protein that potentiates TRPV1 and TRPM8 channel responses. Finally, in the irradiated tongue tissue, we demonstrated increased expression of the Trpv2 and Trpv4 genes. Together, these results suggest that various TRP channels may serve as valuable targets for RAP mitigation.

To build our capacity for preclinical testing of putative RAP therapeutics, Chapter 4 explores the potential for modeling cancer and cancer treatment associated pain in domesticated pet cats. Cats spontaneously develop oral cancers (squamous cell carcinoma; SCC) that closely recapitulate various features of HPV-negative human HNC; here, we began evaluating feline oral SCC as a model of cancer and cancer treatment-associated pain. A battery of pain assessments was performed on 5 cats with sublingual SCC, and 12 healthy pet cats (controls) using various testing instruments. Testing included: (1) an owner-reported quality of life questionnaire; (2) a clinician-based pain scale; and (3) mechanical quantitative sensory testing (mQST: electronic

von Frey and Cochet-Bonnet Aesthesiometer). We evaluated the test – re-test reliability, as well as the discriminatory and responsiveness validity of each assay. Each instrument successfully distinguished cats with sublingual SCC from controls. Opioid administration resulted in non-statistically significant reductions in both the pain scale and mQST; this finding provides provisional evidence for assay sensitivity.

In summary, experiments performed in the murine RAP model suggest that TRPV1 and TRPV4 could be therapeutic targets for RAP mitigation. Tools developed in the feline study enable testing of TRPV1- and TRPV4-targeting drugs in pet cats that develop RAP as part of their routine clinical cancer treatment.

Mechanisms and Models of Pain in Head and Neck Cancer Irradiation

by
Yen-Hao Lai

A dissertation submitted to the Graduate Faculty of
North Carolina State University
in partial fulfillment of the
requirements for the degree of
Doctor of Philosophy

Comparative Biomedical Sciences

Raleigh, North Carolina
2020

APPROVED BY:

_____	_____
Dr. Michael W. Nolan Committee Co-Chair	Dr. B. Duncan X. Lascelles Committee Co-Chair
_____	_____
Dr. David C. Dorman	Dr. Santosh K. Mishra

DEDICATION

This dissertation is devoted to my fiancé, my family, and my friends, for their continued support during this research.

BIOGRAPHY

Yen-Hao Lai (Erik) was born in Taichung City, Taiwan. He attended the College of Veterinary Medicine at National Chung-Hsing University (NCHU) in Taichung, Taiwan, and obtained his Doctorate of Veterinary Medicine in 2013. After graduation from vet school, he completed a Master's degree at NCHU; the program focused on small animal oncology. He became fascinated by oncology and cancer research during his graduate studies. Following this program, he worked in a private veterinary hospital as a general practitioner, but mainly in cancer patient management. In 2016, he began his PhD in Comparative Biomedical Sciences with a concentration of cell biology at the College of Veterinary Medicine, NC State University. Under the mentorship of Dr. Michael Nolan and Dr. B. Duncan X. Lascelles, the research focus has been on radiation-associated pain, and head and neck cancer pain. Upon completion of his PhD studies, he is planning to apply for a radiation oncology residency. Complementing his training in research, he wants to discipline himself to be a clinician-scientist.

ACKNOWLEDGMENTS

I would like to thank my mentor, Dr. Michael Nolan and Dr. Duncan Lascelles, for all of their support, guidance, encouragement, and time during my studies. I cannot thank Dr. Nolan enough for providing me opportunities and giving me support in accomplishing my doctoral studies. I would also like to thank my committee members, Drs. David Dorman and Santosh Mishra, for their thoughtful advice in my research, sharing their knowledge and experience. Without their dedication to me, I would not have been able to complete this work.

I would like to thank all the members, and former members, of the Nolan laboratory. Thank you to Karen Marcus for her assistance in my various projects, including coming early in the morning for radiation experiments. Thank you to Tammy Hawkes for instructing me on how to operate the linear accelerator. I thank Jenna Washburn and Constanza Meneses-Evans for helping me in the experiments and sharing thoughts during our discussions.

Thank you to Drs. Wolfgang Bäumer and Jenny Wilzopolski for training in calcium imaging and neuron culture. I would like to thank Brittany Vallette, Joshua Wheeler, Saumitra Pitake, and Chie Tamamoto-Mochizuki for helping me to develop protocols for molecular assays. I also thank the Clinical Studies Core and Lascelles Lab for helping me in the cat clinical study, especially Carrie Emke, Andrea Thomson, Jonathan Hash and Masataka Enomoto, for their kindness and assistance. Additionally, I would like to thank Pei-Ning Huang, Annie Wang, Paul Cray, Jocsa Cortes, Sarah Quinlan, Laura Minnema, Morika Williams, Timothy Su and Mouta Tung, for their warm support during my studies, far away from my home country.

I would like to thank the Ministry of Education of Taiwan, American College Veterinary Radiology Foundation, and Winn Feline Foundation for providing me support and scholarship to complete my graduate work.

TABLE OF CONTENTS

LIST OF TABLES

CHAPTER 1

CHAPTER 2

CHAPTER 3

CHAPTER 4

LIST OF FIGURES

CHAPTER 2

CHAPTER 3

CHAPTER 4

CHAPTER 1: Orofacial pain related to head and neck cancers and radiotherapy: prevalence, mechanisms and measurement

Introduction

Pain is common in head and neck cancer (HNC) patients, and can be induced by cancer or cancer treatments, such as radiation therapy. However, the molecular mechanisms of head and neck cancer pain and radiation-associated pain are not well understood. In this literature review, we first discuss the epidemiology and challenges of pain in HNC patients; we then explore the mechanisms of orofacial pain induced by cancer and radiation therapy. Among the molecular pathways, we focused the review on the potential role of nociceptive transient receptor potential (TRP) ion channels. Lastly, we review the methodology of orofacial pain assessment in animal models and clinical patients. The purpose of this review is to give an overview of current understanding of pain and pain assessment in HNC patients and animal models, to identify gaps in knowledge related to radiation-associated pain, and methodologies of measuring orofacial pain.

Prevalence and challenges of orofacial pain in HNC patients

Prevalence of orofacial pain related to head and neck cancers

Orofacial pain is a significant problem in head and neck cancer (HNC) patients. Orofacial pain is defined by The International Association for the Study of Pain (IASP) as pain perceived in the face and/or oral cavity [155]; orofacial pain may also affect the eyes, teeth, tongue, sinuses, ears, regional muscles, and temporomandibular joints. HNC is defined by the National Cancer Institute as cancers that arise in the oral cavity, pharynx (including tonsils), larynx, nasal cavity, and salivary glands [14]. The spectrum of HNC includes adenocarcinoma,

mucoepidermoid carcinoma, adenoid carcinoma, acinic cell carcinoma, and other malignant salivary tumors, lymphoma, sarcoma and melanoma [224]. In a report written in 2019, it was stated that there are 650,000 newly diagnosed HNC patients globally every year [209] and the majority (90%) of HNC are squamous cell carcinomas (HNSCC) [235]. In oral SCC, 68%-86% patients report pain [25,199]. A prospective study using multivariate analysis to investigate the predictors of pain in HNC patients [208] found that patients who had pre-treatment pain; were less educated (high school or less); had undergone neck dissection; had a feeding tube; xerostomia; depressive symptoms; frequently use pain medications; undertook less physical activity; and had poor sleep quality, were all more likely to suffer pain with HNC [208]. In the same study, tumors of the oral cavity or larynx (versus pharynx); the primary surgery site; and having a tracheotomy were also associated with pain when analyzed using bivariate analysis but not in multivariance analysis. In HNC patients, pain not only decreases the quality of life, but it also impacts survival time. Significantly shorter survival has been shown in patients who had severe pain (overall 5-year survival rate = 31-33%) compared to patients without severe pain (overall 5-year survival rate = 52-53%) [193]. HNC patients have a significantly higher likelihood of being prescribed opioid pain medication than lung or colon cancer patients [205]. We will discuss the current challenges of managing head and neck cancer pain in a later section.

Pain induced by the therapeutic radiation

More than half of HNC patients receive radiation therapy as part of treatment [33]. After radiation therapy, pain seems to be associated with the presence of mucositis and xerostomia [37,75,134], but pain can last even after the problems have resolved [11]. The management of painful mucositis induced by radiation therapy is challenging. The risk of acute mucositis is 98-

99% in oral/oropharynx HNC patients treated with definitive radiotherapy, and approximately 80% of these patients report severe mouth and throat soreness [68,83]. Similarly, in HNC patients who have radiation therapy, 48% report pain before the treatment, increasing to 75% during radiation therapy [11]. Radiation-associated pain (RAP) can lead to breaks in, or delays in, treatment and this can impede the efficacy of radiotherapy [228]. Studies have found that the probability of tumor control was decreased by 1.4 - 2% per day of radiotherapy interruption in HNC patients [16,21,87,154]. The most commonly used class of analgesics used to manage severe painful mucositis is opioids (approximately 70%) but it comes with undesirable side effects [83].

Challenges of managing pain in HNC patients

A report in 2008 showed 43.4% of cancer patients had undertreated pain [66]. Although pain management has been improved in the past decade, nearly one-third of cancer patients still do not receive adequate pain medication [98]. Nonsteroidal anti-inflammatory drugs, anticonvulsants, antidepressants, selective serotonin and norepinephrine reuptake inhibitors, opioids and the local anesthetic agents such as lidocaine are commonly used to reduce cancer pain [53,196]. However, in human medicine, it is clear that efficacy is suboptimal, and they can be associated with side effects [222]. Most side effects are associated with opioids. Patients taking opioids can suffer CNS toxicity such as cognitive impairment, hallucination or confusion, and other side effects such as urinary retention, constipation, nausea, vomiting, or pruritis [20,32,122,162]. Opioids have been used for long-term pain control in cancer patients during/after their cancer treatment [162]. In radiation-treated patients, persistent pain is not uncommon; a study has reported that approximately 65% of patients have persistent RAP 3

months after the last radiation treatment [11]. Another study showed 63% of the radiation-treated patients continued using opioids 3 months after the completion of the treatment [130]. With long-term use of opioids, radiation-treated patients are at a high risk of addiction and abuse.

Although pain management protocols in cancer patients have been described in the literature [169,196], studies evaluating efficacy are few. Most pain management protocols appear to be based on the clinicians' experience and varies from institute to institute. Common to all of the protocols and recommendations is an over-reliance on opioids. This has continued because of the lack of novel, effective analgesic drugs. Understanding the mechanisms of pain induced by radiotherapy is needed for alternative therapeutics to be developed. It is unclear if it is nociceptive, inflammatory, functional and/or neuropathic pain (see later for description) that contributes to RAP, and which mechanisms play major roles. By understanding underlying pain mechanisms, we may be able to develop a safer and more effective pain medication to replace or reduce the use of opioids. In the following sections, we will review the general mechanisms of orofacial pain, then to specific cancer pain and RAP.

Mechanisms and pathways of orofacial pain

Orofacial pain- neurophysiology and anatomical pathway

Nociception and the perception of pain are evoked when noxious stimuli (e.g., temperature approximately > 40 °C or < 15 °C, intense pressure, or chemicals) activate peripheral sensory neurons [77]. When stimulation reaches a threshold, the primary afferent sensory neurons transmit all-or-none action potentials to the cell body, then onwards. At the central terminal of the primary afferent fiber, neurotransmitters are stored in the synaptic vesicles close to the cell membrane. When the action potential reaches the central terminal, calcium

influx occurs and neurotransmitters are released and bind with the receptors on the post-synaptic membrane, and the signal is propagated to the second order neuron. The perception of pain results if the signal is transmitted to the somatosensory cortex of the brain, and the final experience of pain is created. The actual experience felt is dependent on influences from many other areas of the brain. In the orofacial region, the trigeminal nerve (cranial nerve [CN] V) and facial nerve (CN VII) play important roles in sensation. These two nerves have an extensive network of nerve fibers in the head and neck area [88]. The trigeminal nerve is the most commonly affected nerve in HNC patients due to the anatomical distribution of the three branches of the trigeminal nerve (i.e., ophthalmic, maxillary and mandibular division). For example, the maxillary branch is usually affected by nasopharyngeal tumors and the mandibular branch is usually affected by tumors from lower lip, mandible, or tongue [88].

At the peripheral terminal of the afferent nerve, noxious stimuli (the types of cancer-related stimuli will be discussed later) evoke the initial impulse. Impulses travel to the cell body (in the trigeminal ganglia), then to the central nervous system and synapse onto to the secondary-order neuron in the spinal trigeminal nucleus in the brainstem. The signal then travels in the counter lateral trigeminal thalamic tract. Afterward, it joins other fibers from the trigeminal nucleus to trigeminal lemniscus. The secondary-order neuron terminates in the thalamus and transmits the impulse to third-order neuron then transmits the impulse to the primary somatosensory cortex, where it can be interpreted as the ‘perception of pain’ [236]. The anatomical pathway is crucial for investigators to understand. It helps us to decide where and how to measure the pain, and ultimately, we may be able to identify the target to block pain signal transduction.

There are four major categories of pain – nociceptive, inflammatory, neuropathic and dysfunctional pain, as defined in **(Table 1.1)**. [128,245]. Nociceptive pain can be further classified as somatic pain and visceral pain, but somatic pain may be more common in HNC patients due to the affected soft tissues (e.g., gingiva, tongue) and invaded nearby bones (e.g., mandible, maxilla). Visceral caner pain is related to tumors located in internal organs such as cardiovascular, respiratory, gastrointestinal, and genitourinary systems. Although visceral pain might present in HNC patients have distant metastasis, it has been shown that lung metastasis does not induce significant pain symptoms in those patients [241]. Nevertheless, even though somatic and visceral nerves innervate different types of organs, they share similar nociceptors that can be activated by noxious stimuli [106].

Inflammatory pain is induced by the activation of immune cells in response to tissue injuries or infection [245]. Inflammation is an underlying hallmark of cancer and is involved in enabling and promoting tumor growth [107]. Tumor growth also induces inflammation; the expansion of HNC, such as SCC of the oral mucosa, destroys normal tissue and with that, induces inflammation. As tumors grow, cancer cells release cytokines and chemokines that attract leukocytes and monocytes [55]. Inflammatory mediators produced from the infiltrating immune cells (discussed below) then sensitize and stimulate nociceptors [246]. Lowering the threshold for nociceptor activation means that a mild noxious stimulus can become highly noxious, which is called hyperalgesia; additionally, non-noxious stimuli may produce action potentials in sensory neurons encoding pain, and this is called allodynia [156,204]. Other central changes (central algoplasticity) are thought to be responsible for widespread hyperalgesia and allodynia across the body, such as has been shown in bone cancer patients [113,198].

Neuropathic pain results from direct injury to the somatosensory nervous system. The injuries result in (1) ectopic action potential discharge in the nerve fiber (2) hyperexcitability of nerve fibers in response to stimuli (3) changes in transmitter synthesis and signaling (4) peripheral and central axon growth; these events promote pain signal transmission [54,117]. Neuropathic pain in HNC patients can be induced by tumor compression, but chemotherapy or radiation therapy can also induce painful peripheral neuropathy [12,67]. We will have further discussion of radiation-induced neuropathy in the section entitled "Radiation-induced cell damage and pain".

Dysfunctional pain occurs when there is no damage of the nervous system, and pain is instead evoked by abnormal central processing. The characteristics of dysfunctional pain are widespread or regional hyperalgesia and allodynia [170]. In dysfunctional pain, it is the input into the CNS that is causing plastic changes in the neurobiological function and architecture of the CNS, resulting in facilitation of throughput of signals, and amplification of signals [198,232,244].

Peripheral nerve sensitizers and activators associated with head and neck cancer pain

Peripheral nerves can be sensitized or activated by various kinds of stimuli. In cancer patients, mediators of noxious stimuli are released from tumors, damaged cells or infiltrating immune cells. Tissue damage in cancer patients can be due to tumor invasion, tumor necrosis, or cancer treatment such as radiation therapy, which will be described in the next section. As we mentioned previously, injured cells release mediators that can attract immune cells to release other pro-nociceptive and pro-inflammatory mediators. The released mediators produce varying effects on sensory neurons.

Protons (acid) and adenosine triphosphate (ATP) are nociceptor activators that initiate the noxious signaling. The pH of the intratumoral microenvironment tends to be lower than nearby normal tissues due to hypoxia and compensatory energy production of anaerobic glycolysis [69,100]. Local acidosis also occurs due to the accumulation of protons that are released by inflammatory cells, and intracellular ions that are released during cancer cell death [156]. In HNSCC, the pH in the biopsied samples has shown to be lower than the paired normal tissues [151]. The local acidity causes activation of 2 different types of ion channels that are called transient receptor potential vanilloid 1 (TRPV1) and acid-sensing ion channel-3 (ASIC-3) [44,178,226] that can lead to a noxious stimulus (action potential) being produced. The TRP channels have been widely reviewed for pain treatment [145,187], but the literature of TRP channels related to cancer pain is limited. We will further review the potential role of TRP channels in HNC pain later in the section entitled "Transient receptor potential channels and orofacial pain". Another nociceptor activator is ATP. Cytoplasmic ATP is a well-known cellular energy source, but extracellular ATP contributes to nociception [8,79]. Ye *et al.* have shown that the level of ATP is significantly increased in human HNSCC tissues [251]. ATP binds to P2X2 and P2X3 receptors on sensory neurons and initiates action potentials [229,251].

In the microenvironment of head and neck cancers, numerous nociceptor sensitizers are generated by solid tumors, damaged cells, and infiltrating immune cells. For example, increased interleukin (IL)-1β, IL-6 and TNF-α were detected in solid tumors and/or the serum from HNSCC patients [50,85,195,214,247]. Those mediators may contribute to orofacial hyperalgesia because majority of the sensory neurons possess receptors for IL-1 [22,60], -6 [9,119], and TNF-α [59,115,142] and these result in sensory nerve sensitization. Infiltrat and activated immune cells such as macrophages, neutrophils, dendritic cells, eosinophils, mast cells, as well as

lymphocytes produce various mediators including IL-1, -6, epidermal growth factor (EGF), transforming growth factor (TGF)-β, platelet-derived growth factor, and prostaglandins that promote inflammation and pain [55,156]. Here we review the nociceptor sensitizers that are present in head and neck cancer microenvironments (**Table 1.2**):

Endothelin-1 is a potent vasoactive peptide, but it also directly excites sensory fibers to induce pain [64,95]. In normal cells, endothelin-1 is produced by epithelial cells, endothelial cells, cardiomyocytes, leukocytes, or macrophages [124]. Certain malignancies such as epithelial tumors, prostate cancers, bone cancers, or bone-metastatic cancers (e.g. breast and prostate cancers) also produce endothelin-1 [41,172]. The antagonism of the endothelin-1 receptor (ET_AR) on peripheral sensory neurons reduces mechanical sensitivity in bone cancer patients [181]. Published studies have revealed elevated endothelin-1 production in lingual and esophageal SCC cells [13,184], which suggests that endothelin-1 could contribute to orofacial pain in HNSCC patients.

Another vasoactive peptide that can contribute to the generation of noxious signals from the periphery is bradykinin [156]. The concentration of bradykinin in the tumor microenvironment is increased due to the cancer cell mutation; bradykinin receptor expression is increased and bradykinin production is stimulated in an autocrine manner [34,219]. Bradykinin acts on constitutively expressed B_2 and injury-induced B_1 receptors on peripheral primary sensory neurons to contribute to the peripheral generation of noxious signals (pain) by sensitizing neurons [197]. The bradykinin B_2 receptor is upregulated in HNSCC cells [19], however, how it is related to orofacial pain still needs to be investigated. Other work has shown that bradykinin can promote tumor cell survival, so it has been suggested that both tumor and pain control may be achieved by blocking bradykinin receptors [19].

Substance P (SP) is a neuropeptide that can be released from both normal tissue cells and tumor cells after the activation of protease-activated receptor-2 (PAR-2) [202]. Substance P contributes to the noxious transmission by binding to neurokinin-1 (NK_1) receptors [1,2,109]. In a rodent model, systemically administered NK_1 receptor blockade therapy resulted in a reduction of orofacial heat hyperalgesia induced by carrageenan injection [223]. Substance P has been shown to promote cell proliferation and prevent cells from undergoing apoptosis [56]. The expression of SP and NK_1 are significantly increased in oral SCC, and the higher expression level is correlated with poorly differentiated tumors [26,163]. The fact that SP is overexpressed by certain tumors, contributes to aggressive tumor behavior, and contributes to pain, together suggest that SP inhibitors could be another potential drug to ameliorate cancer pain and tumor progression in HNC patients [255]. Upstream of SP, PAR-2 may also regulate cancer pain [132]. Lam and Schmidt have shown that HNSCC cells have more proteolytic activity than normal cell controls; in their study, the inhibition of PAR-2 reduced the mechanical allodynia that is caused by the injection of SCC cancer cell supernatant [133].

Nerve growth factor (NGF) is a potential target to treat pain due to its critical role in mediating pain [46,239]. NGF was first discovered in the 1950s as a soluble factor produced from tumors, and it can promote sensory ganglia growth and differentiation [143,144]. It is now recognized as a neurotrophic factor released by tissues after injury or stimulation by inflammatory cytokines (i.e., IL-1 and TNF-α) [157]. NGF binds to TrkA and also to p75, however, the main pronociceptive effects are via binding to TrkA [190,227]. After binding to its main receptor TrkA, it initially alters the sensitivity of the nerve by sensitizing (e.g., by phosphorylating) other receptors such as TRPV1 and ASICs. Then the complex NGF-trkA is internalized and transported to sensory neuron ganglion cell bodies, where it alters gene

transcription, resulting in (1) modulation of the production of 'pain receptors' that are expressed on the peripheral end of the nerve; (2) alteration of the peripheral production of SP and calcitonin gene-related peptide (CGRP) in response to nerve stimulation (neurogenic inflammation); and (3) alteration of the central production of neurotransmitters such as SP, CGRP, brain-derived neurotrophic factors (BDNF) and glutamate [46,157]. In oral SCC, the mRNA transcripts and protein levels of NGF are significantly increased [250]. Treatment with anti-NGF antibody in the mouse xenograft oral SCC cancer model resulted in decreased TRPV1, TRPA1, and PAR-2 expression in trigeminal ganglia [250]. Targeting NGF seems to be a promising therapeutic in the management of osteoarthritis pain, [203] although the clinical trials to date in cancer pain have shown mixed results.

Radiation-induced cell damage and pain

Current radiation therapy for head and neck cancers

Among cancer treatments, radiotherapy is one of the most common therapeutics for HNC; among all HNC survivors in the United States, more than half of the patients (55%) receive radiation therapy at some point during their illness, as reported in 2016 [33]. Radiation therapy is used as primary treatment, adjuvant therapy with surgery, combined with chemotherapy, and/or used for palliation. Conventional radiotherapy for HNSCC uses 50-70 Gy in 33-35 fractions, with 5 or 6 fractions per week. The relatively small dose per fraction allows normal (late-responding) tissues to recover, while remaining lethal to cancer cells. Even with that relative sparing of late-responding normal tissues, close to 100% of HNC patients undergoing full course radiation therapy suffer from acute oral mucositis [83]. A published meta-analysis showed hyperfractionated radiation protocols to be superior to the conventional protocol in

treating HNSCC in terms of local control and reduced cancer mortality [131]. The hyperfractionated protocol used a higher total dose than the conventional treatment and applied twice daily fractions with the same overall treatment time. This protocol allowed smaller doses per fraction that reduced late toxicity, higher total dose to achieve better tumor control, and the twice fraction per day limited the tumor repopulation [58,131]. However, it also induced a significantly higher rate of acute mucositis, resulting in pain and the need for feeding tube placement during the treatment [131].

Tissue injury and inflammatory responses

After exposure to ionizing irradiation, acute injury occurs in tissues with a rapid turnover and happens within a few days or weeks; in contrast, late effects occur after months or years and occur predominantly in slowly proliferating tissues (late effects will be discussed in next section). Radiation-induced tissue injury and cell killing in the acute phase is related to DNA damage, which is induced when photons directly interact with DNA, or indirectly interact by inducing free radicals (e.g., reactive oxygen species, ROS) that are released from the irradiated molecules in the cell. In response to DNA damage, cells activate DNA repair and cell cycle arrest immediately as a protective mechanism to promote its recovery [24]. If the DNA lesion is irreparable, the cell undergoes apoptosis or mitotic cell death: cell apoptosis is mainly executed via the activation of caspases, which is regulated by DNA damage-induced p53 activation; mitotic cell death happens when cells attempt to divide but have aberrant chromosome.

Radiation-induced mitotic cell death occurs earlier in rapidly divided cells (i.e. normal endothelial, epithelial cells and cancer cells) and with head and neck radiation therapy, this results in mucositis. Mucositis is defined as the reactive inflammatory process of the oral and

oropharyngeal mucous membranes during radiotherapy [15]. The process is characterized by atrophy of squamous epithelial tissue, absence of vascular damage, and the infiltration of inflammatory cells at the basement layer [108]. The mitotic death of epithelial basal cells occurs within a few hours but the breakdown of epithelial tissues happens at about 4 days after radiotherapy, which is the renewal cycle of the keratinocytes [168]. The tissue injury, and death of cells, leads to an inflammatory response and pain. Inflammatory cell infiltration at irradiated mucosa starts to increase from day 5 to day 15 and then decreases [211].

As was described above for cancer pain, the mediators produced from infiltrating immune cells can contribute to the generation of noxious signals from the periphery [65,206]. TNF-α, IL-1β, IL-6, and CRP are pro-inflammatory factors that are consistently detected in the local mucosa and/or peripheral blood after radiation therapy [48,140,189,210,211]. Accumulated evidence shows a pivotal role of TNF-α in the peripheral and central pain processes [142]. TNF-α released from immune cells (e.g. T cells and macrophages) increases neuron membrane K^+, Na^+ and Ca^{+2} ion channel conduction, leading to neuronal hyperexcitability [61,118,142,210]. Interference of TNF-α production was shown to reduce the severity of mucositis in hamsters, thus TNF-α production was considered to be a potential target to prevent mucositis after radiotherapy [210,211]. However, the preclinical trial using a mouse model to treat radiation-induced mucositis with TNF-α inhibitors or COX-2 inhibitors did not result in better mitigation of mucositis [105]. In contrast, another study using pentoxifylline (a non-selective TNF-α inhibitor), showed improved mucositis in mice after irradiation [101]. However, neither of the studies assessed changes in orofacial pain or sensitivity. Although there is a concern of TNF-α inhibition that may suppress anti-tumor immunity, a murine study showed TNF-α inhibitor markedly reduce tumor size and number in the colonic tumor model [139,185].

IL-1β modulates neuronal excitability by sensitizing TRPV1 and sodium channels in the periphery, and increasing N-methyl-D-aspartate (NMDA) potentiation, and reducing gamma-aminobutyric acid (GABA) receptor current centrally [201]. IL-1β has shown to reduce carrageenan-induced spinal inflammatory pain in a rat model and the IL-1β agonist and anti-IL-1β antibody have been used to treat inflammatory pain in human clinical trials [71,213]. Another cytokine, IL-6, acts presynaptically and also activates postsynaptic NMDA or glutamate receptors, to contribute to pain [146]. Patients with orofacial muscle pain had increased intramuscular IL-6 [152]. Upregulated IL-6 has also been associated with bone cancer pain and peripheral nerve injuries in murine models [74,254]. A recently published patent has shown that an anti-IL-6 antibody can prevent severe radiation-induced mucositis development in a clinical trial, and the study is still in progress [116].

C-reactive protein (CRP) has been used as a robust inflammatory or infection biomarker in the acute phase [51]. The production of CRP can be induced by IL-6 via promoting *CRP* gene expression or hepatic biosynthesis [186,216,240]. Increased levels of CRP have been shown to be associated with higher cold sensitivity in a study that was conducted in 198 female twins [3]. In cancer patients, increased serum CRP has been found in people have HNC and breast cancers [176,217]. Radiation-associated pain could also relate to increased CRP; breast cancer patients who had a higher pre-radiotherapy CRP were shown to in a significantly higher risk of suffering radiation-related pain [140].

Inflammatory mediators are released from immune cells when the irradiated cells are injured or die. Tissue repair then follows the acute injury. However, during this process, pain can be ongoing, which may be induced by different mechanisms.

Pain induced by tissue repair process

The cell death of epithelium and the loss of mucosal integrity result in pain in the acute injury phase. The apoptotic cell death can promote tissue regeneration that is so-called "Phoenix Rising" pathway [147]. The phoenix rising pathway depends on caspase 3 and 7, protease activation during the cell apoptosis. The activated caspase 3 and 7 leads to an increase in synthesis and release of arachidonic acid from apoptotic cells. Arachidonic acid then serves as a precursor for prostaglandin E2 (PGE_2) synthesis and stimulates stem cell proliferation and wound repair [256]. Clearly, PGE_2 may contribute to pain via sensory nerve sensitization. As tissue repairs, nerve compression caused by indirect radiation-induced fibrosis could contribute to the generation of pain [40]. Because the repair process may take months to years after radiation therapy, it is named "late effect". The late effects include tissue fibrosis, vascular damage, tissue hypoxia, atrophy, and neural damage. Vascular damage can occur within days to weeks after radiotherapy. Approximately 90% of endothelial cells experience mitotic cell death in response to conventional fractionated irradiation, whereas a large single dose can induce cell apoptosis [233]. The vascular damage can lead to decreased blood perfusion in tissues. As blood flow and oxygen supply decrease due to radiation injury, tissue ischemia, myopathy, and bone necrosis (osteoradionecrosis) can occur and these can contribute to pain [242]. It is believed that an osteoblast can sustain 30 Gy of radiation but proliferative ability is impaired at 50 Gy [242]. For head and neck cancer treatment, temporal bone necrosis usually happens in treating cancers at the parotid site [183], and sternocleidomastoid muscle necrosis has been reported in a laryngopharyngeal SCC patient seven months after radiotherapy [188]. Although osteoradionecrosis and myopathy are relatively rare adverse events, they can contribute to pain.

Neuronal sensitization, activation and injury associated with radiation

In addition to the inflammatory mediators (previously discussed in the section: "Tissue injury and inflammatory response") that can sensitize/activate neurons, ionizing irradiation and released ROS can have direct effects on neurons. In a guinea pig study, gamma-ray doses of 5 and 10 Gy impaired synaptic function of hippocampal neurons shortly after (30 minutes) radiation exposure [180]. Another study showed that even 0.1 or 2 Gy can alter the gene expression in the mouse brain 30 minutes post-irradiation [252]. There is also evidence that ionizing radiation can directly affect peripheral sensory function in terms of signal transmission, nociceptor protein expression, and electrophysiology [92].

Reactive oxygen species are mediators in multiple downstream biological events including cell death and inflammatory responses [210]. In a Drosophila model, it was shown that endogenous ROS induced by short-wavelength ultraviolet (UVC) irradiation can activate the nociceptors in neurons [125]. They found after UVC irradiation, larva with transgenic overexpression of antioxidant enzymes showed significantly less writhing behavior in response to noxious heat. Additionally, production of ROS after ionizing radiation can promote the release of TNF-α and IL-1 outside of the irradiated area, which contributes to non-target (abscopal) effects and this is thought to contribute to pain generalization and hyperalgesia [237,238]. ROS also plays an important role as a secondary messenger that contribute to synaptic transmission. As one example, increased ROS can increase pain sensitivity by reducing GABA release [253].

After ionizing irradiation, transcription factors such as NF-κB, AP-1, and p53 are activated in mammalian cells due to DNA damage or ROS [57]. Those transcription factors regulate numerous inflammatory cytokines and chemokines related to pain. The activation of NF-κB can upregulate IL-1β and COX-2, which can result in inflammatory pain hypersensitivity

[141]. In the AP-1 transcription factor family, c-FOS and c-JUN have been indicated as messengers in signal transduction in pain the process [171]. After *in vivo* high dose γ-irradiation (8 to 48 Gy) of pig skin, both c-FOS and c-JUN gene were upregulated in the skin within a few hours [159]. This team further investigated a low dose (0.5 Gy) and found c-FOS was induced but not c-JUN [159]. Another upregulated transcription factor, p53, is thought to be associated with persistent pain and is induced by radiation therapy. Recently, the overexpression of p53 was shown to induce increased apoptosis of neurons and result in chronic neuropathic pain in a murine sciatic nerve injury model [89].

Late radiation induced fibrosis and soft tissue ischemia cause peripheral nervous system dysfunction that results in pain, sensory loss and weakness [221]. Stoll found 73% of breast cancer patients treated with megavoltage x-ray had neurological symptoms and peripheral nerve injury, 3.5 weeks after radiotherapy [220]. Most of those patients had paresthesia, and pathological examination revealed fibrous tissue replacement and demyelination. It has been shown that TGF-β and connective tissue growth factor (CTGF) are highly related to late-effect fibrosis. A recent study indicated that TGF-β is involved in chronic pain (osteoarthritis) [23]. Other factors such as TNF-α and IFN-γ released from macrophages and T cells in the repair phase after radiation therapy, have been shown to downregulate TGF-β [104,138]. Therefore, the inflammatory mediators may play multiple roles in RAP during the acute and late phases.

Transient receptor potential channels and orofacial pain

Among all the noxious stimuli activated receptors, the transient receptor potential (TRP) cation channels have received a lot of focus in the past two decades as targets for novel analgesics [145]. TRP channels are membrane proteins that are gated by temperature, light,

pressure or chemical stimuli. There are six subfamilies of TRP channels in mammals: TRPC (canonical), TRPV (vanilloid), TRPM (melastatin), TRPP (polycystin), TRPML (mucolipin), and TRPA (ankyrin) [43]. Six thermal sensitive TRP ion channels including TRP-V1, -V2, -V3, -V4, -M8 and -A1, are especially attractive as putative analgesic targets because they have been shown to mediate pain and sensory neuronal sensitization [103,114,145,225] (**Table 1.3**). The heat generated during radiation therapy could potentially affect those thermal-activated nociceptors. This review will focus on TRPV1, TRPV4, and TRPA1 since other work has shown their activity is associated with orofacial pain [49,78,112,179]. Additionally, and interestingly, the upregulation of TRPV1 and TRPA1 has been shown to be correlated with malignancy or tumor progression in prostate cancers, lung cancers [62,76,200], as well as HNSCC [158]. Although the expression of the TRP in cancer cells does not necessarily relate to pain, the blockade of TRP channels have the potential of serving a dual purpose – inhibition of tumor growth and reduction of orofacial pain. Several compounds have been shown to bind to the TRP channels to reduce orofacial or cancer pain. For example, frutalin is a lectin that is isolated from the seeds of breadfruit, and has been shown to have anti-nociceptive effects mediated by TRPA1, TRPV1, and TRPM8 in a rodent model of orofacial pain [63]. In a murine cancer model, it was shown the blockade of TRPV1 can reduce bone cancer pain [91]. However, the role of TRP channels in HNC-induced cancer pain has not been investigated, and it is unknown if therapeutic irradiation activates any of the TRP channels.

TRPV1

TRPV1 is expressed in approximately 25-50% of nociceptive C fibers but it can also be expressed on Aδ fibers [38,234]. Both types of fibers are primary afferent nociceptive nerves

with nociceptors at the free ending. Aδ fibers convey fast nerve impulses whereas C fibers transmit nerve impulses much more slowly [90]. Protons, heat (> 43 °C), and capsaicin activate TRPV1 that induce calcium ion influx into neurons and trigger the impulse [202]. In preclinical work, the administration of TRPV1 antagonists has been shown to significantly attenuate pain related to nociceptive behavior in mice with bone cancers [91]. Rats with SCC at the paw had upregulated TRPV1 in dorsal root ganglia and accompanying mechanical allodynia and thermal hyperalgesia [207]. In the radiotherapy or radiation injuries, the heat and inflammation may activate TRPV1 at the free nerve ending of afferent neurons, but research in this area has been limited. A recently published paper found that radiation-induced mucositis in mice resulted in sensitization of capsaicin-responsive trigeminal sensory neurons [174], but the direct evidence of TRPV1 expression on these neurons was not evaluated. Another study investigating orofacial inflammation (dental pulpitis) showed that TRPV1 in trigeminal neurons was upregulated by oxidative enzymes [78]. Other upstream molecules, including TNF-α and artemin, have been shown to promote the overexpression of TRPV1 [82,123]. Artemin is a member of glial cell line-derived neurotrophic factor that can induce overexpression of TRPV1 and TRPA1 in afferent sensory neurons, thus increasing the sensitivity to capsaicin and mustard oil [81].

TRPV4

TRPV4 was first identified as an osmolality sensor [149] and related to pain induced by hypertonic or hypotonic stimuli [5,47]. Approximately 35% of peripheral sensory neurons express TRPV4 [6]. This Ca^{2+}-permeable, nonselective cation ion channel can be evoked by temperature > 27ºC. TRPV4 KO mice demonstrate diminished noxious mechanical and thermal responses [150]. Activation of TRPV4 induces mechanical hyperalgesia that is mediated by

protease during inflammation [97]. Mechanical evoked visceral pain can be enhanced by TRPV4 agonists, but mitigated by the deletion of TRPV4 or non-selective TRP channel inhibitors [27]. In rodent models, TRPV4 upregulation in trigeminal ganglia is associated with temporomandibular joint pain and responsive to airborne irritants [49,148]. With formalin irritant injection in the whisker pad, it has shown that the presence of TRPV4 is critical for nocifensive behavior [248]. Inflammatory or neuropathic pain induced by chemotherapy is also found to be associated with higher TRPV4 expression [4]. Those emerging TRPV4 studies regarding pain indicate TRPV4 antagonist can be a potential treatment for orofacial pain and soothing the irritation on trigeminally innervated epithelia. A compound that can selectively block TRPV4 was discovered and has been shown to co-inhibit TRPA1 [120], with the hope to provide a novel therapeutic to attenuate trigeminal and inflammatory pain.

TRPA1

Burning sensation in patients with mucositis after radiation therapy presumably reflects hot thermosensation, but it is unknown whether, or to what extent those patients are sensitive to cold or mechanical stimulation. A cooling agent may be able to soothe the burning sensation, but cold stimuli can also induce pain, particularly in certain pain conditions such as neuropathic pain [231]. Both TRPA1 and TRPM8 respond to cold, and TRPA1 is also excited by the irritants mustard or garlic [18,127,182]. TRPA1 channel is involved in cold hyperalgesia following inflammation and nerve injuries [175] and it is upregulated by nerve growth factor in trigeminal ganglia in a rodent model [72]. The inhibition of TRPA1 significantly reduces noxious cold thermosensation and mechanosensation [182]. However, the role of TRPA1 in cold sensation is controversial [42]. The cold response of TRPA1 is believed to be activated indirectly; the

increase of intracellular Ca^{2+} during the cooling process activates TRPA1 in cells, hence promote the cold response [42].

Evaluation of orofacial discomfort

Orofacial pain evaluation in research animal models

Spontaneous behaviors have been used as measures of pain. Mouse models have been developed for investigating temporomandibular joint disorder pain [49,52] and trigeminal neuralgia [45]. Home cage monitoring such as facial or mouth rubbing/scratching counting, grooming activity monitoring, and vocalization have been used for evaluating spontaneous pain behavior in orofacial pain models in animals [7,35,70]. Facial expression in the mouse, rat, and rabbit have been used to measure spontaneous pain in lab animals, and so-called 'grimace scales' have been developed [135,137,165,177,212]. Grimace scales involve scoring facial expressions from images that captured when the animal is directly facing the camera. The evaluator scores the orbital tightening (narrowing of the orbital area or eye squeezed), nose bulge, cheek bulge, ear position, and whisker position [135]. By scoring facial expression, the grimace scale has shown to be an effective tool for detecting spontaneous orofacial pain induced by temporomandibular joint disorder in a rat model [215]. Recently, the automation of facial expression analysis has been described for mice [230]. Another spontaneous behavior assay is purported to measure masticatory pain [73]. The assays rely on the inherent behavior of a mouse to chew through anything blocking its path. In this assay, the mouse is placed into a tube with a dowel as an obstacle. The gnawing time of dowel is measured to quantify the gnawing function as an indirect index of masticatory / oral pain. A commercialized orofacial stimulation assay was designed for measuring sensitivity of the orofacial region in rodents [45,173]. The assembly has

a drinking window in a cage that can create a thermal or mechanical stimulus-response on the facial region. Another common assay, the "bite force assay", was developed to quantify the biting force of the mouse on a transducer [243]. Reduced bite force indicates an increase of bite-evoked pain, which mimics the orofacial pain induced by chewing food in humans. Interpretation of the results of spontaneous behavioral assays can be controversial [194]. For example, spontaneous pain tests may not necessarily measure pain but rather overall discomfort or overall well-being. Therefore, it is critical to define and assess pain by several different behavioral assays, and in association with evidence of neurophysiological changes such as activation of nociceptors or neuropathic lesions.

In reflexive tests, behavioral responses are evoked by applying stimuli (i.e. heat, cold mechanical, electrical, or chemical) and measuring the threshold or latency at which a response occurs [99]. For example, von Frey filament is one of the quantitative sensory testing (QST) tools that can be applied to the whisker pad to measure the mechanical stimulation threshold [167]. Such tests can detect hyperalgesia or allodynia by applying noxious stimuli or innocuous stimuli. Similarly, thermal stimuli (heat and cold) have been used in rodent models to evaluate orofacial sensitivity [129]. The major concern of the reflexive tests is that they measure sensitivity, not pain. Additionally, as with all behavioral assays, the response of the subjects can be affected by many external factors. The pros and cons of spontaneous reflexive assays are listed in **Table 1.4**.

However, regardless of the pros and cons of reflexive assays, very little work has been done applying these assays to measure oral sensitivity in general, and there is only one study evaluating such assays in a model of radiation associated oral pain [174].

Spontaneous tumor models of orofacial pain

Common head and neck cancers in dogs and cats include SCC, malignant melanoma, soft tissue sarcoma, and adenocarcinoma [31]. Animals with oral cancer may present with various behavioral changes such as eating less, lethargy, reluctant to be touched around the mouth, licking, ptyalism, chattering (jaw shakes), and rubbing their oral region. However, without a validated instrument to evaluate the multi-dimensional impact of pain, it is difficult to assess the severity of the discomfort and the efficacy of pain medication adequately.

Companion animals have been used as a comparative model for investigating pain such as osteoarthritis and bone cancer pain [136]. The incidence and severity of cancer pain are not well documented in veterinary medicine [160]. In veterinary medicine, physical examination plays an important role in evaluating pain and quality of life. The presence of pain can be assessed by the clinician based on animals' behavior and the palpation [164]. Holton *et al.* used simple descriptive, numerical rating, and visual analogue to evaluate postoperative pain in dogs but showed significant variability among observers [111]. In the past decade, several pain scales (clinical metrology instruments) have been developed for acute pain assessment [29,36,110,191]. For example, the Glasgow Composite Measures Pain Scale has been partially validated for dogs and also been adapted for cats (see further details in the introduction of Chapter 4). Botucatu Multidimensional Composite Pain Scale (MCPS) is another pain scale specific for cats that was developed and validated for evaluating acute pain after ovariohysterectomy [29,30]. Those pain scales could potentially be used in measuring cancer pain in pet animals but have not been validated yet. However, the aforementioned scales are 'acute' pain scales, and cancer pain is often more long-standing than classic acute pain. Moreover, none of those scales were designed for orofacial pain assessment. Recently, Stathopoulou *et al*. used a modified Botucatu MCPS and

successfully detect reduced pain after the application of opioids in cats with gingivostomatitis [218]. Their work indicates that the modified Botucatu MCPS might be able to be used to measure pain in cats with oral cancers. Another instrument, the Feline Grimace Scale, evaluates ear position, orbital tightening, the shape of the muzzle and position of the head and whiskers [84,166]. While this grimace scale has been shown to be a valid and reliable tool for evaluating post-operative pain in cats, the validity of measuring head and neck cancer pain should be confirmed.

Owner-reported questionnaires have been used to measure QOL and pain-associated behaviors in canine cancer patients [93,94,153,192,249]. Pet-owner completed questionnaires are thought to be more useful the more 'chronic' a pain condition becomes, as they evaluate often subtle behaviors in the home environment, rather than having a clinician try to assess such behaviors in the unfamiliar surroundings of a hospital where behaviors are often markedly altered. However, these pain and/or QOL questionnaires were not designed for animals with oral/nasal cancers.

Mechanical/thermal QST is used for quantifying local tissue sensitivity induced by injuries and the sensitivity remote from the injured tissues [28,126,161]. Cold and mechanical QST has shown to be a feasible and reliable instrument for assessing somatosensory changes in dogs with osteoarthritis-associated pain [28,126]. Similarly, such methodology could be useful for detecting orofacial hypersensitivity in veterinary patients.

Orofacial pain evaluation in clinical patients

Quantitative sensory testing may be applicable in clinical patients. Neurophysiological investigations like pain-related evoked potentials or laser-evoked potentials have been used for

assessing nociception in human objectives [96,121]. Brain imaging such as positron emission tomography (PET), functional magnetic resonance imaging (MRI), or magnetoencephalography have been used in humans, but a major challenge of using such measurements is the cost and the availability of the equipment. For practical use by a clinician, tools should be easy to use, available and affordable. Most importantly, the ideal tool should be reliable, repeatable and valid.

Orofacial pain assessment in clinical situations is usually based on the history and physical examination. From the medical history, the onset, location, intensity, and frequency of the pain can be recorded for pain evaluation. The discussion can further investigate the triggers of the pain and what factors alleviate the discomfort. The symptoms associated with orofacial pain such as dizziness, running nose, nausea, or hypersalivation can also be helpful to evaluate the origin of the pain and determine if the pain treatment is effective. Visual analogue scales (VAS), the verbal rating scale (VRS), and numerical rating scale (NRS) are the self-reported systems regularly used in evaluations [39,196]. A standardized self-reported questionnaire can be another comprehensive and useful tool for evaluating pain and quality of life, but it is important to know that the physical pain can be influenced by the psychological status of the patient, particularly with respect to knowing the stage of the disease or the treatment response. It is also important to understand that, because of the varied multidimensional nature of pain, not all patients will describe the same symptoms. Additionally, the perception and interpretation of, and communication about, pain can vary greatly from individual to individual and culture to culture. For instance, African Americans and Latin Americans reported a higher level of clinical pain and less tolerance than European descendants [80,86]. The translated language of the survey may also affect the results [102]. Moreover, the self-reported evaluation can be limited by impaired cognition or impaired communication ability due to the age or the end stage of life in cancer

patients. Therefore, multiple physiological or psychological evaluations should be applied to correctly interpret the patients' quality of life and pain in the orofacial region.

Conclusion

In conclusion, orofacial pain produced by cancers and radiotherapy significantly impacts the quality of life of human and animal patients. Effective management of this pain is limited due to a lack of therapeutic options, and this may be partly due to a lack of knowledge of the mechanisms involved. Although the mechanisms of orofacial pain are very poorly understood, TRP channels may be promising targets for ameliorating cancer and radiation-associated pain. By characterizing the role of the nociceptors in orofacial pain, we may uncover novel potential therapeutic strategies. Approaches to measuring orofacial cancer pain in animal models are not particularly well developed, but crucial for both research and the clinical veterinary management of orofacial cancer pain. The following chapters attempt to increase our understanding of the mechanisms of RAP, and explore a spontaneous feline model of RAP.

REFERENCES

[1] AbbadieC, BrownJL, MantyhPW, BasbaumAI. Spinal cord substance P receptor immunoreactivity increases in both inflammatory and nerve injury models of persistent pain. Neuroscience 1996.

[2] AbbadieC, TraftonJ, LiuH, MantyhPW, BasbaumAI. Inflammation increases the distribution of dorsal horn neurons that internalize the neurokinin-1 receptor in response to noxious and non-noxious stimulation. J Neurosci 1997.

[3] AfariN, MostoufiS, NoonanC, PoeschlaB, SuccopA, ChopkoL, StrachanE. C-reactive protein and pain sensitivity: Findings from female twins. Ann Behav Med 2011.

[4] Alessandri-HaberN. Transient Receptor Potential Vanilloid 4 Is Essential in Chemotherapy-Induced Neuropathic Pain in the Rat. J Neurosci 2004.

[5] Alessandri-HaberN, JosephE, DinaOA, LiedtkeW, LevineJD. TRPV4 mediates pain-related behavior induced by mild hypertonic stimuli in the presence of inflammatory mediator. Pain 2005.

[6] Alessandri-HaberN, YehJJ, BoydAE, ParadaCA, ChenX, ReichlingDB, LevineJD. Hypotonicity induces TRPV4-mediated nociception in rat. Neuron 2003.

[7] AlvarezP, SaavedraG, HernándezA, PaeileC, PelissierT. Synergistic antinociceptive effects of ketamine and morphine in the orofacial capsaicin test in the rat. Anesthesiology 2003.

[8] AmayaF, IzumiY, MatsudaM, SasakiM. Tissue Injury and Related Mediators of Pain Exacerbation. Curr Neuropharmacol 2013.

[9] AndersonLC, RaoRD. Interleukin-6 and nerve growth factor levels in peripheral nerve and brainstem after trigeminal nerve injury in the rat. Arch Oral Biol 2001.

[10] Andrew Baranowski, Chairman of PUGO's Classification Committee, Paul Abrams, Richard Berger, Tony Buffington, Beverly Collett, Anton Emmanuel, Magnus Fall, Phil Hanno, Fred Howard, John Hughes, Curtis Nickel, Jorgen Nordling, Dean Tripp, Katy Vincent, Urs and AC de CW. IASP Terminology. n.d. Available: https://www.iasp-pain.org/PublicationsNews/Content.aspx?ItemNumber=1673&navItemNumber=677.

[11] AstrupGL, RustøenT, MiaskowskiC, PaulSM, BjordalK. Changes in and predictors of pain characteristics in patients with head and neck cancer undergoing radiotherapy. Pain 2015.

[12] AuthierN, BalayssacD, MarchandF, LingB, ZangarelliA, DescoeurJ, CoudoreF, BourinetE, EschalierA. Animal Models of Chemotherapy-Evoked Painful Peripheral Neuropathies. Neurotherapeutics 2009.

[13] AwanoS, DawsonLA, HunterAR, TurnerAJ, UsmaniBA. Endothelin system in oral squamous carcinoma cells: Specific siRNA targeting of ECE-1 blocks cell proliferation. Int J Cancer 2006.

[14] BaganJ, SarrionG, JimenezY. Oral cancer: Clinical features. Oral Oncol 2010;46:414–417.

[15] BakerDG. The Radiobiological Basis for Tissue Reactions in the Oral Cavity Following Therapeutic X-Irradiation: A Review. Arch Otolaryngol 1982.

[16] BartonMB, KeaneTJ, GadallaT, MakiE. The effect of treatment time and treatment interruption on tumour control following radical radiotherapy of laryngeal cancer. Radiother Oncol 1992.

[17] BassoL, AltierC. Transient Receptor Potential Channels in neuropathic pain. Curr Opin Pharmacol 2017.

[18] BautistaDM, JordtSE, NikaiT, TsurudaPR, ReadAJ, PobleteJ, YamoahEN, BasbaumAI, JuliusD. TRPA1 Mediates the Inflammatory Actions of Environmental Irritants and Proalgesic Agents. Cell 2006.

[19] BeckC, PiontekG, HaugA, BasM, KnopfA, StarkT, MißlbeckM, RudeliusM, ReiterR, BrandstetterM, PickhardA. The kallikrein-kinin-system in head and neck squamous cell carcinoma (HNSCC) and its role in tumour survival, invasion, migration and response to radiotherapy. Oral Oncol 2012.

[20] BenyaminR, TrescotAM, DattaS, BuenaventuraR, AdlakaR, SehgalN, GlaserSE, VallejoR. Opioid complications and side effects. Pain Physician 2008.

[21] BeseNS, HendryJ, JeremicB. Effects of Prolongation of Overall Treatment Time Due To Unplanned Interruptions During Radiotherapy of Different Tumor Sites and Practical Methods for Compensation. Int J Radiat Oncol Biol Phys 2007.

[22] BianchiM, DibB, PaneraiAE. Interleukin-1 and nociception in the rat. J Neurosci Res 1998.

[23] Blaney DavidsonEN, vanCaamAPM, VittersEL, BenninkMB, ThijssenE, van denBergWB, KoendersMI, vanLentPLEM, van deLooFAJ, van derKraanPM. TGF-β is a potent inducer of Nerve Growth Factor in articular cartilage via the ALK5-Smad2/3 pathway. Potential role in OA related pain? Osteoarthr Cartil 2015.

[24] BorgesHL, LindenR, WangJYJ. DNA damage-induced cell death: Lessons from the central nervous system. Cell Res 2008.

[25] BreivikH, ChernyN, CollettB, deConnoF, FilbetM, FoubertAJ, CohenR, DowL. Cancer-related pain: A pan-European survey of prevalence, treatment, and patient attitudes. Ann Oncol 2009.

[26] BrenerS, González-MolesMA, TostesD, EstebanF, Gil-MontoyaJA, Ruiz-ÁvilaI, BravoM, MuñozM. A role for the substance P/NK-1 receptor complex in cell proliferation in oral squamous cell carcinoma. Anticancer Res 2009.

[27] BrierleySM, PageAJ, HughesPA, AdamB, LiebregtsT, CooperNJ, HoltmannG, LiedtkeW, BlackshawLA. Selective Role for TRPV4 Ion Channels in Visceral Sensory Pathways. Gastroenterology 2008.

[28] BrileyJD, WilliamsMD, FreireM, GriffithEH, LascellesBDX. Feasibility and repeatability of cold and mechanical quantitative sensory testing in normal dogs. Vet J 2014.

[29] BrondaniJT, LunaSPL, PadovaniCR. Refinement and initial validation of a multidimensional composite scale for use in assessing acute postoperative pain in cats. Am J Vet Res 2011.

[30] BrondaniJT, MamaKR, LunaSPL, WrightBD, NiyomS, AmbrosioJ, VogelPR, PadovaniCR. Validation of the English version of the UNESP-Botucatu multidimensional composite pain scale for assessing postoperative pain in cats. BMC Vet Res 2013.

[31] BrøndenLB, EriksenT, KristensenAT. Oral malignant melanomas and other head and neck neoplasms in Danish dogs--data from the Danish Veterinary Cancer Registry. Acta Vet Scand 2009.

[32] BrueraE, SchoellerT, MontejoG. Organic hallucinosis in patients receiving high doses of opiates for cancer pain. Pain 1992.

[33] BryantAK, BanegasMP, MartinezME, MellLK, MurphyJD. Trends in radiation therapy among cancer survivors in the United States, 2000-2030. Cancer Epidemiol Biomarkers Prev 2017.

[34] BunnPA, ChanD, DienhartDG, TolleyR, TagawaM, JewettPB. Neuropeptide Signal Transduction in Lung Cancer: Clinical Implications of Bradykinin Sensitivity and Overall Heterogeneity. Cancer Res 1992.

[35] CallahanBL, GilASC, LevesqueA, MogilJS. Modulation of Mechanical and Thermal Nociceptive Sensitivity in the Laboratory Mouse by Behavioral State. J Pain 2008.

[36] CalvoG, HoldenE, ReidJ, ScottEM, FirthA, BellA, RobertsonS, NolanAM. Development of a behaviour-based measurement tool with defined intervention level for assessing acute pain in cats. J Small Anim Pract 2014.

[37] CAMPOSMIDC, CAMPOSCN, AARESTRUPFM, AARESTRUPBJV. Oral mucositis in cancer treatment: Natural history, prevention and treatment. Mol Clin Oncol 2014.

[38] CaoE, Cordero-MoralesJF, LiuB, QinF, JuliusD. TRPV1 Channels Are Intrinsically Heat Sensitive and Negatively Regulated by Phosphoinositide Lipids. Neuron 2013.

[39] CaraceniA, ChernyN, FainsingerR, KaasaS, PoulainP, RadbruchL, DeConnoF. Pain measurement tools and methods in clinical research in palliative care: Recommendations of an Expert Working Group of the European Association of Palliative Care. J Pain Symptom Manage 2002.

[40] CaraceniA, PortenoyRK. An international survey of cancer pain characteristics and syndromes. IASP Task Force on Cancer Pain. International Association for the Study of Pain. Pain 1999;82:263–74. doi:10.1016/S0304-3959(99)00073-1.

[41] CarducciMA, JimenoA. Targeting bone metastasis in prostate cancer with endothelin receptor antagonists. Clin Cancer Res 2006.

[42] CaspaniO, HeppenstallPA. TRPA1 and cold transduction: An unresolved issue? J Gen Physiol 2009.

[43] CaterinaMJ. Transient receptor potential ion channels as participants in thermosensation and thermoregulation. Am J Physiol - Regul Integr Comp Physiol 2007.

[44] CaterinaMJ, SchumacherMA, TominagaM, RosenTA, LevineJD, JuliusD. The capsaicin receptor: A heat-activated ion channel in the pain pathway. Nature 1997.

[45] ChaM, KohanKJ, ZuoX, LingJX, GuJG. Assessment of chronic trigeminal neuropathic pain by the orofacial operant test in rats. Behav Brain Res 2012.

[46] ChangDS, HsuE, HottingerDG, CohenSP. Anti-nerve growth factor in pain management: Current evidence. J Pain Res 2016.

[47] ChenX, Alessandri-HaberN, LevineJD. Marked attenuation of inflammatory mediator-induced C-fiber sensitization for mechanical and hypotonic stimuli in TRPV4-/- mice. Mol Pain 2007.

[48] ChenY, WilliamsJ, DingI, HernadyE, LiuW, SmudzinT, FinkelsteinJN, RubinP, OkunieffP. Radiation pneumonitis and early circulatory cytokine markers. Seminars in Radiation Oncology.2002.

[49] ChenY, WilliamsSH, McNultyAL, HongJH, LeeSH, RothfuszNE, ParekhPK, MooreC, Gereau IVRW, TaylorAB, WangF, GuilakF, LiedtkeW. Temporomandibular joint pain: A critical role for Trpv4 in the trigeminal ganglion. Pain 2013;154:1295–1304.

[50] ChenZ, MalhotraPS, ThomasGR, OndreyFG, DuffeyDC, SmithCW, EnamoradoI, YehNT, KroogGS, RudyS, McCullaghL, MousaS, QuezadoM, HerscherLL, VanWaesC. Expression of proinflammatory and proangiogenic cytokines in patients with head and neck cancer. Clin Cancer Res 1999.

[51] ClyneB, OlshakerJS. The C-reactive protein. J Emerg Med 1999.

[52] Committee on Recognition and Alleviation of Pain in Laboratory Animals (National Research Council). Recognition and Alleviation of Pain in Laboratory Animals. Recognition and Alleviation of Pain in Laboratory Animals.2009.

[53] ConnollyI, ZaleonC, MontagniniM. Management of Severe Neuropathic Cancer Pain: An Illustrative Case and Review. Am J Hosp Palliat Med 2013.

[54] CostiganM, ScholzJ, WoolfCJ. Neuropathic Pain: A Maladaptive Response of the Nervous System to Damage. Annu Rev Neurosci 2009.

[55] CoussensLM, WerbZ. 860-Inflammation-Cancer.Pdf. Nature 2002.

[56] CoveñasR, MuñozM. Cancer progression and substance P. Histol Histopathol 2014.

[57] CriswellT, LeskovK, MiyamotoS, LuoG, BoothmanDA. Transcription factors activated in mammalian cells after clinically relevant doses of ionizing radiation. Oncogene 2003.

[58] CummingsBJ. Benefits of accelerated hyperfractionation for head and neck cancer. Acta Oncol (Madr) 1999.

[59] CunhaFQ, PooleS, LorenzettiBB, FerreiraSH. The pivotal role of tumour necrosis factor α in the development of inflammatory hyperalgesia. Br J Pharmacol 1992.

[60] CunhaJM, CunhaFQ, PooleS, FerreiraSH. Cytokine-mediated inflammatory hyperalgesia limited by interleukin-1 receptor antagonist. Br J Pharmacol 2000.

[61] CzeschikJC, HagenackerT, SchäfersM, BüsselbergD. TNF-α differentially modulates ion channels of nociceptive neurons. Neurosci Lett 2008.

[62] CzifraG, VargaA, NyesteK, MarincsákR, TóthBI, KovácsI, KovácsL, BíróT. Increased expressions of cannabinoid receptor-1 and transient receptor potential vanilloid-1 in human prostate carcinoma. J Cancer Res Clin Oncol 2009.

[63] DamascenoMBMV, DeMelo JúniorJDMA, SantosSAAR, MeloLTM, LeiteLHI, Vieira-NetoAE, MoreiraRDA, Monteiro-MoreiraACDO, CamposAR. Frutalin reduces acute and neuropathic nociceptive behaviours in rodent models of orofacial pain. Chem Biol Interact 2016.

[64] DavarG, HansG, FareedMU, SinnottC, StrichartzG. Behavioral signs of acute pain produced by application of endothelin-1 to rat sciatic nerve. Neuroreport 1998.

[65] DavisMP. Drug management of visceral pain: Concepts from basic research. Pain Res Treat 2012;2012.

[66] DeandreaS, MontanariM, MojaL, ApoloneG. Prevalence of undertreatment in cancer pain. A review of published literature. Ann Oncol 2008.

[67] DelanianS, LefaixJL, PradatPF. Radiation-induced neuropathy in cancer survivors. Radiother Oncol 2012.

[68] DenisF, GaraudP, BardetE, AlfonsiM, SireC, GermainT, BergerotP, RheinB, TortochauxJ, CalaisG. Final results of the 94-01 French head and neck oncology and radiotherapy group randomized trial comparing radiotherapy alone with concomitant radiochemotherapy in advanced-stage oropharynx carcinoma. J Clin Oncol 2004.

[69] DenkoNC. Hypoxia, HIF1 and glucose metabolism in the solid tumour. Nat Rev Cancer 2008.

[70] DeuisJR, DvorakovaLS, VetterI. Methods Used to Evaluate Pain Behaviors in Rodents. Front Mol Neurosci 2017.

[71] DinarelloCA, SimonA, Van DerMeerJWM. Treating inflammation by blocking interleukin-1 in a broad spectrum of diseases. Nat Rev Drug Discov 2012.

[72] DiogenesA, AkopianAN, HargreavesKM. NGF Up-regulates TRPA1: Implications for orofacial pain. J Dent Res 2007.

[73] DolanJC, LamDK, AchdjianSH, SchmidtBL. The dolognawmeter: A novel instrument and assay to quantify nociception in rodent models of orofacial pain. J Neurosci Methods 2010.

[74] DongY, Mao-YingQL, ChenJW, YangCJ, WangYQ, TanZM. Involvement of EphB1 receptor/ephrinB1 ligand in bone cancer pain. Neurosci Lett 2011.

[75] DonnellyJP, BellmLA, EpsteinJB, SonisST, SymondsRP. Antimicrobial therapy to prevent or treat oral mucositis. Lancet Infect Dis 2003.

[76] DuGJ, LiJH, LiuWJ, LiuYH, ZhaoB, LiHR, HouXD, LiH, QiXX, DuanYJ. The combination of TRPM8 and TRPA1 expression causes an invasive phenotype in lung cancer. Tumor Biol 2014.

[77] DubinAE, PatapoutianA. Nociceptors: The sensors of the pain pathway. J Clin Invest 2010.

[78] DubnerR, HargreavesKM, RuparelS. Role of Oxidized Lipids and TRP Channels in Orofacial Pain and Inflammation. J Dent Res 2016;95:1117–1123.

[79] DunnPM, LiuM, ZhongY, KingBF, BurnstockG. Diinosine pentaphosphate: An antagonist which discriminates between recombinant P2X3 and P2X(2/3) receptors and between two P2X receptors in rat sensory neurones. Br J Pharmacol 2000.

[80] EdwardsRR, DoleysDM, FillingimRB, LoweryD. Ethnic differences in pain tolerance: Clinical implications in a chronic pain population. Psychosom Med 2001.

[81] ElittCM, MalinSA, KoerberHR, DavisBM, AlbersKM. Overexpression of artemin in the tongue increases expression of TRPV1 and TRPA1 in trigeminal afferents and causes oral sensitivity to capsaicin and mustard oil. Brain Res 2008.

[82] ElittCM, McIlwrathSL, LawsonJJ, MalinSA, MolliverDC, CornuetPK, KoerberHR, DavisBM, AlbersKM. Artemin Overexpression in Skin Enhances Expression of TRPV1 and TRPA1 in Cutaneous Sensory Neurons and Leads to Behavioral Sensitivity to Heat and Cold. J Neurosci 2006;26:8578–8587. doi:10.1523/JNEUROSCI.2185-06.2006.

[83] EltingLS, KeefeDM, SonisST, GardenAS, SpijkervetFKL, BaraschA, TishlerRB, CantyTP, KudrimotiMK, Vera-LlonchM. Patient-reported measurements of oral mucositis in head and neck cancer patients treated with radiotherapy with or without chemotherapy: Demonstration of increased frequency, severity, resistance to palliation, and impact on quality of life. Cancer 2008.

[84] EvangelistaMC, WatanabeR, O'TooleE, PangDSJ, SteagallPV. Facial expressions of pain in cats: development of the Feline Grimace Scale. Abstracts presented at the spring meeting of the Association of Veterinary Anaesthetists, Grenada, West Indies – 10–13 th March, 2018, published in Veterinary Anaesthesia and Analgesia.2018.

[85] F.Y, E.L.Q, S.K, M.P. Expression of TNF and the 55-kDa TNF receptor in epidermis, oral mucosa, lichen planus and squamous cell carcinoma. Oral Dis 1996.

[86] FaucettJ, GordonN, LevineJ. Differences in postoperative pain severity among four ethnic groups. J Pain Symptom Manage 1994.

[87] FowlerJF, LindstromMJ. Loss of local control with prolongation in radiotherapy. Int J Radiat Oncol Biol Phys 1992.

[88] FrunzaA, SlavescuD, LascarI. Perineural invasion in head and neck cancers - a review. J Med Life 2014.

[89] GaoY, SunN, WangL, WuY, MaL, HongJ, RenJ, ZhuB, YuL, YanM. Bioinformatics analysis identifies p53 as a candidate prognostic biomarker for neuropathic pain. Front Genet 2018.

[90] GardnerEP, JohnsonKO. 22: The Somatosensory System: Receptors and Central Pathways. Principles of Neural Science.2012.

[91] GhilardiJR, RöhrichH, LindsayTH, SevcikMA, SchweiMJ, KubotaK, HalvorsonKG, PobleteJ, ChaplanSR, DubinAE, CarruthersNI, SwansonD, KuskowskiM, FloresCM, JuliusD, MantyhPW. Selective blockade of the capsaicin receptor TRPV1 attenuates bone cancer pain. J Neurosci 2005.

[92] GilletteEL, MahlerPA, PowersBE, GilletteSM, VujaskovicZ. Late radiation injury to muscle and peripheral nerves. Int J Radiat Oncol Biol Phys 1995.

[93] GiuffridaMA, BrownDC, EllenbergSS, FarrarJT. Development and psychometric testing of the Canine Owner-Reported Quality of Life questionnaire, an instrument designed to measure quality of life in dogs with cancer. J Am Vet Med Assoc 2018.

[94] GiuffridaMA, FarrarJT, BrownDC. Psychometric properties of the Canine Symptom Assessment Scale, a multidimensional owner-reported questionnaire instrument for assessment of physical symptoms in dogs with solid tumors. J Am Vet Med Assoc 2017.

[95] GokinAP, FareedMU, PanHL, HansG, StrichartzGR, DavarG. Local injection of endothelin-1 produces pain-like behavior and excitation of nociceptors in rats. J Neurosci 2001.

[96] GranovskyY, MatreD, SokolikA, LorenzJ, CaseyKL. Thermoreceptive innervation of human glabrous and hairy skin: A contact heat evoked potential analysis. Pain 2005.

[97] GrantAD, CottrellGS, AmadesiS, TrevisaniM, NicolettiP, MaterazziS, AltierC, CenacN, ZamponiGW, Bautista-CruzF, LopezCB, JosephEK, LevineJD, LiedtkeW, VannerS, VergnolleN, GeppettiP, BunnettNW. Protease-activated receptor 2 sensitizes the transient receptor potential vanilloid 4 ion channel to cause mechanical hyperalgesia in mice. J Physiol 2007.

[98] GrecoMT, RobertoA, CorliO, DeandreaS, BandieriE, CavutoS, ApoloneG. Quality of cancer pain management: An update of a systematic review of undertreatment of patients with cancer. J Clin Oncol 2014.

[99] GregoryNS, HarrisAL, RobinsonCR, DoughertyPM, FuchsPN, SlukaKA. An overview of animal models of pain: Disease models and outcome measures. J Pain 2013.

[100] GriffithsJR. Are cancer cells acidic? Br J Cancer 1991.

[101] GruberS, BozsakyE, DörrW, SchmidtM, WolframK, HaagenJ, HabeltB, PuttrichM. Modulation of radiation-induced oral mucositis by pentoxifylline: Preclinical studies. Strahlentherapie und Onkol 2015.

[102] GuilleminF, BombardierC, BeatonD. Cross-cultural adaptation of health-related quality of life measures: Literature review and proposed guidelines. J Clin Epidemiol 1993.

[103] GülerAD, LeeH, IidaT, ShimizuI, TominagaM, CaterinaM. Heat-Evoked Activation of the Ion Channel, TRPV4. J Neurosci 2002.

[104] GurujeyalakshmiG, GiriSN. Molecular mechanisms of antifibrotic effect of interferon gamma in bleomycin-mouse model of lung fibrosis: Downregulation of TGF-β and procollagen I and III gene expression. Exp Lung Res 1995.

[105] HaagenJ, KrohnH, RölligS, SchmidtM, WolframK, DörrW. Effect of selective inhibitors of inflammation on oral mucositis: Preclinical studies. Radiother Oncol 2009.

[106] HäblerHJ, JänigW, KoltzenburgM. Activation of unmyelinated afferent fibres by mechanical stimuli and inflammation of the urinary bladder in the cat. J Physiol 1990;425:545–562.

[107] HanahanD, WeinbergRA. Hallmarks of cancer: The next generation. Cell 2011.

[108] HandschelJ, ProttFJ, SunderkötterC, MetzeD, MeyerU, JoosU. Irradiation induces increase of adhesion molecules and accumulation of β2-integrin-expressing cells in humans. Int J Radiat Oncol Biol Phys 1999.

[109] HenryJL. Substance P and pain: an updating. Trends Neurosci 1980.

[110] HoltonL, ReidJ, ScottEM, PawsonP, NolanA. Development of a behaviour-based scale to measure acute pain in dogs. Vet Rec 2001.

[111] HoltonLL, ScottEM, NolanAM, ReidJ, WelshE, FlahertyD. Comparison of three methods used for assessment of pain in dogs. J Am Vet Med Assoc 1998.

[112] HondaK, ShinodaM, FurukawaA, KitaK, NomaN, IwataK. TRPA1 contributes to capsaicin-induced facial cold hyperalgesia in rats. Eur J Oral Sci 2014.

[113] HonoréP, SchweiMJ, RogersSD, Salak-JohnsonJL, FinkeMP, RamnaraineML, ClohisyDR, MantyhPW. Cellular and neurochemical remodeling of the spinal cord in bone cancer pain. Prog Brain Res 2000.

[114] HuangSM, LiX, YuY, WangJ, CaterinaMJ. TRPV3 and TRPV4 ion channels are not major contributors to mouse heat sensation. Mol Pain 2011.

[115] ItoR, ShinodaM, HondaK, UrataK, LeeJ, MarunoM, SomaK, OkadaS, GionhakuN, IwataK. Tumor Necrosis Factor Alpha Signaling in Trigeminal Ganglion Contributes to

Mechanical Hypersensitivity in Masseter Muscle During Temporomandibular Joint Inflammation. J Oral Facial Pain Headache 2018.

[116] Jeffrey T.L. Smith, Leon F. Garcia-MartinezALF. Anti-il-6 antibodies for the treatment of oral mucositis. 2019.

[117] JensenTS, BaronR. Translation of symptoms and signs into mechanisms in neuropathic pain. Pain 2003;102:1–8.

[118] JinX. Acute p38-Mediated Modulation of Tetrodotoxin-Resistant Sodium Channels in Mouse Sensory Neurons by Tumor Necrosis Factor- . J Neurosci 2006.

[119] DeJonghRF, VissersKC, MeertTF, BooijLHDJ, DeDeyneCS, HeylenRJ. The role of interleukin-6 in nociception and pain. Anesth Analg 2003.

[120] KanjuP, ChenY, LeeW, YeoM, LeeSH, RomacJ, ShahidR, FanP, GoodenDM, SimonSA, SpasojevicI, MookRA, LiddleRA, GuilakF, LiedtkeWB. Small molecule dual-inhibitors of TRPV4 and TRPA1 for attenuation of inflammation and pain. Sci Rep 2016.

[121] KatsaravaZ, AyzenbergI, SackF, LimmrothV, DienerHC, KaubeH. A novel method of eliciting pain-related potentials by transcutaneous electrical stimulation. Headache 2006.

[122] KatzNP, AdamsEH, BenneyanJC, BirnbaumHG, BudmanSH, BuzzeoRW, CarrDB, CiceroTJ, GourlayD, InciardiJA, JoransonDE, KesslickJ, LandeSD. Foundations of opioid risk management. Clin J Pain 2007.

[123] KhanAA, DiogenesA, JeskeNA, HenryMA, AkopianA, HargreavesKM. Tumor necrosis factor α enhances the sensitivity of rat trigeminal neurons to capsaicin. Neuroscience 2008.

[124] KhodorovaA, MontmayeurJP, StrichartzG. Endothelin Receptors and Pain. J Pain 2009.

[125] KimMJ, JohnsonWA. ROS-mediated activation of Drosophila larval nociceptor neurons by UVC irradiation. BMC Neurosci 2014.

[126] KnazovickyD, HelgesonES, CaseB, GruenME, MaixnerW, LascellesBDX. Widespread somatosensory sensitivity in naturally occurring canine model of osteoarthritis. Pain 2016.

[127] KnowltonWM, Bifolck-FisherA, BautistaDM, McKemyDD. TRPM8, but not TRPA1, is required for neural and behavioral responses to acute noxious cold temperatures and cold-mimetics in vivo. Pain 2010.

[128] Kosek E, Cohen M, Baron R, Gebhart GF, Mico JA, Rice AS, Rief WSA. Do we need a third mechanistic descriptor for chronic pain states? Pain 2016;157:1382–1386.

[129] KrzyzanowskaA, AvendañoC. Behavioral testing in rodent models of orofacial neuropathic and inflammatory pain. Brain Behav 2012.

[130] KwonJH, HuiD, ChisholmG, BrueraE. Predictors of Long-Term Opioid Treatment Among Patients Who Receive Chemoradiation for Head and Neck Cancer. Oncologist 2013.

[131] LacasB, BourhisJ, OvergaardJ, ZhangQ, GrégoireV, NankivellM, ZackrissonB, SzutkowskiZ, SuwińskiR, PoulsenM, O'SullivanB, CorvòR, LaskarSG, FallaiC, YamazakiH, DobrowskyW, ChoKH, GardenAS, LangendijkJA, ViegasCMP, HayJ, LotayefM, ParmarMKB, AupérinA, vanHerpenC, MaingonP, TrottiAM, GrauC, PignonJP, BlanchardP, BernierJ, LeQT, TrottiA, AgarwalJP, AngKK, AwwadHK, BacigalupoA, BartelinkH, BenhamouE, BudachW, ChitapanaruxI, ColletteL, DaniC, DischeS, DenhamJW, DriessenCM, GhoshalS, GregoireV, HayJH, HliniakA, JohansenJ, KristiansenCA, KrstevskaV, LapeyreM, MaciejewskiB, MichalskiW, MoonSH, NilssonP, OlmiP, NishiyamaK, PoulsenMG, RamadasK, RishiA, RosenthalDI, SanguinetiG,

SaundersMI, SireC, SkladowskiK, SouhamiL, SuwinskiR, TandonN, vanTinterenH, TorriV, TripconyL, WaldronJ, WidderJ, WongS, WuJS. Role of radiotherapy fractionation in head and neck cancers (MARCH): an updated meta-analysis. Lancet Oncol 2017.

[132] LamDK, DangD, ZhangJ, DolanJC, SchmidtBL. Novel animal models of acute and chronic cancer pain: A pivotal role for PAR2. J Neurosci 2012.

[133] LamDK, SchmidtBL. Serine proteases and protease-activated receptor 2-dependent allodynia: A novel cancer pain pathway. Pain 2010.

[134] LangDSP. Interventions for preventing oral mucositis for patients with cancer receiving treatment. Clin J Oncol Nurs 2013.

[135] LangfordDJ, BaileyAL, ChandaML, ClarkeSE, DrummondTE, EcholsS, GlickS, IngraoJ, Klassen-RossT, Lacroix-FralishML, MatsumiyaL, SorgeRE, SotocinalSG, TabakaJM, WongD, Van DenMaagdenbergAMJM, FerrariMD, CraigKD, MogilJS. Coding of facial expressions of pain in the laboratory mouse. Nat Methods 2010.

[136] LascellesBDX, BrownDC, ConzemiusMG, GillM, OshinskyML, SharkeyM. Measurement of chronic pain in companion animals: Discussions from the Pain in Animals Workshop (PAW) 2017. Vet J 2019.

[137] LeachMC, KlausK, MillerAL, Scotto di PerrotoloM, SotocinalSG, FlecknellPA. The assessment of post-vasectomy pain in mice using behaviour and the Mouse Grimace Scale. PLoS One 2012.

[138] LEASKA. TGF- signaling and the fibrotic response. FASEB J 2004.

[139] LebrecH, PonceR, PrestonBD, IlesJ, BornTL, HooperM. Tumor necrosis factor, tumor necrosis factor inhibition, and cancer risk. Curr Med Res Opin 2015.

[140] LeeE, NelsonOL, PuyanaC, TakitaC, WrightJL, ZhaoW, ReisIM, LinRY, HlaingWM, BakalarJL, YangGR, HuJJ. Association between C-reactive protein and radiotherapy-related pain in a tri-racial/ethnic population of breast cancer patients: A prospective cohort study. Breast Cancer Res 2019.

[141] LeeKM, KangBS, LeeHL, SonSJ, HwangSH, KimDS, ParkJS, ChoHJ. Spinal NF-kB activation induces COX-2 upregulation and contributes to inflammatory pain hypersensitivity. Eur J Neurosci 2004.

[142] LeungL, CahillCM. TNF-α and neuropathic pain - a review. J Neuroinflammation 2010.

[143] LEVI-MONTALCINIR. Effects of mouse tumor transplantation on the nervous system. Ann N Y Acad Sci 1952.

[144] Levi-MontalciniR, HamburgerV. Selective growth stimulating effects of mouse sarcoma on the sensory and sympathetic nervous system of the chick embryo. J Exp Zool 1951.

[145] LevineJD, Alessandri-HaberN. TRP channels: Targets for the relief of pain. Biochim Biophys Acta - Mol Basis Dis 2007.

[146] LiAJ, KatafuchiT, OdaS, HoriT, OomuraY. Interleukin-6 inhibits long-term potentiation in rat hippocampus slices. Brain Res 1997.

[147] LiF, HuangQ, ChenJ, PengY, RoopDR, BedfordJS, LiCY. Apoptotic cells activate the "phoenix rising" pathway to promote wound healing and tissue regeneration. Sci Signal 2010.

[148] LiJ, KanjuP, PattersonM, ChewWL, ChoSH, GilmourI, OliverT, YasudaR, GhioA, SimonSA, LiedtkeW. TRPV4-mediated calcium influx into human bronchial epithelia upon exposure to diesel exhaust particles. Environ Health Perspect 2011.

[149] LiedtkeW, ChoeY, Martí-RenomMA, BellAM, DenisCS, AndrejŠali, HudspethAJ, FriedmanJM, HellerS. Vanilloid receptor-related osmotically activated channel (VR-OAC), a candidate vertebrate osmoreceptor. Cell 2000.

[150] LiedtkeW, FriedmanJM. Abnormal osmotic regulation in trpv4-/- mice. Proc Natl Acad Sci 2003.

[151] LojaMN, LuoZ, Greg FarwellD, LuuQC, DonaldPJ, AmottD, TruongAQ, Gandour-EdwardsRF, NitinN. Optical molecular imaging detects changes in extracellular pH with the development of head and neck cancer. Int J Cancer 2013.

[152] Louca JoungerS, ChristidisN, SvenssonP, ListT, ErnbergM. Increased levels of intramuscular cytokines in patients with jaw muscle pain. J Headache Pain 2017.

[153] LynchS, Savary-BatailleK, LeeuwB, ArgyleDJ. Development of a questionnaire assessing health-related quality-of-life in dogs and cats with cancer. Vet Comp Oncol 2011.

[154] MaciejewskiB, Preuss-BayerG, TrottKR. The influence of the number of fractions and of overall treatment time on local control and late complication rate in squamous cell carcinoma of the larynx. Int J Radiat Oncol Biol Phys 1983.

[155] MaixnerW. Orofacial Pain Fact Sheets. 2016. Available: https://www.iasp-pain.org.

[156] MantyhPW. A mechanism based understanding of cancer pain. Pain 2002.

[157] MantyhPW, KoltzenburgM, MendellLM, TiveL, SheltonDL. Antagonism of nerve growth factor-TrkA signaling and the relief of pain. Anesthesiology 2011.

[158] MarincsákR, TóthBI, CzifraG, MártonI, RédlP, TarI, TóthL, KovácsL, BíróT. Increased expression of TRPV1 in squamous cell carcinoma of the human tongue. Oral Dis 2009;15:328–35. doi:10.1111/j.1601-0825.2009.01526.x.

[159] MartinM, PintonP, CrechetF, LefaixJL, DaburonF. Preferential Induction of c-fos versus c-jun Protooncogene during the Immediate Early Response of Pig Skin to γ-Rays. Cancer Res 1993.

[160] MathewsK, KronenPW, LascellesD, NolanA, RobertsonS, SteagallPVM, WrightB, YamashitaK. Guidelines for Recognition, Assessment and Treatment of Pain: WSAVA Global Pain Council members and co-authors of this document: J Small Anim Pract 2014;55.

[161] MatosR, WangK, JensenJD, JensenT, NeumanB, SvenssonP, Arendt-NielsenL, JensenJD, JensenT, NeumanB, SvenssonP. Quantitative sensory testing in the trigeminal region: Site and gender differences. J Orofac Pain 2011.

[162] McNicolE, Horowicz-MehlerN, FiskRA, BennettK, Gialeli-GoudasM, ChewPW, LauJ, CarrD. Management of opioid side effects in cancer-related and chronic noncancer pain: A systematic review. J Pain 2003.

[163] MehboobR, TanvirI, WarraichRA, PerveenS, YasmeenS, AhmadFJ. Role of neurotransmitter Substance P in progression of oral squamous cell carcinoma. Pathol Res Pract 2015.

[164] MichPM, HellyerPW. Objective, Categoric Methods for Assessing Pain and Analgesia. Handbook of Veterinary Pain Management.2009.

[165] MillerAL, LeachMC. The effect of handling method on the mouse grimace scale in two strains of laboratory mice. Lab Anim 2016.

[166] MonteiroBP, SteagallPV. Chronic pain in cats: Recent advances in clinical assessment. J Feline Med Surg 2019.

[167] MorganJR, GebhartGF. Characterization of a Model of Chronic Orofacial Hyperalgesia in the Rat: Contribution of NAV 1.8. J Pain 2008.

[168] MorrisR, ArgyrisTS, MorrisR. Epidermal Cell Cycle and Transit Times during Hyperplastic Growth Induced by Abrasion or Treatment with 12-O-TetradecanoylPhorbol-13-acetate. Cancer Res 1983.

[169] MoslemiD, NokhandaniAM, OtaghsaraeiMT, MoghadamniaY, KazemiS, MoghadamniaAA. Management of chemo/radiation-induced oral mucositis in patients with head and neck cancer: A review of the current literature. Radiother Oncol 2016.

[170] NagakuraY. Challenges in drug discovery for overcoming dysfunctional pain: An emerging category of chronic pain. Expert Opin Drug Discov 2015.

[171] NaranjoJR, MellströmB, AchavalM, Sassone-CorsitP. Molecular pathways of pain: Fos/Jun-mediated activation of a noncanonical AP-1 site in the prodynorphin gene. Neuron 1991.

[172] NelsonJ, BagnatoA, BattistiniB, NisenP. The endothelin axis: Emerging role in cancer. Nat Rev Cancer 2003.

[173] NeubertJK, WidmerCG, MalphursW, RossiHL, VierckCJ, CaudleRM. Use of a novel thermal operant behavioral assay for characterization of orofacial pain sensitivity. Pain 2005.

[174] NolanMW, LongCT, MarcusKL, SarmadiS, RobackDM, FukuyamaT, BaeumerW, LascellesBDX. Nocifensive Behaviors in Mice with Radiation-Induced Oral Mucositis. Radiat Res 2017;187:397–403. doi:10.1667/RR14669.1.

[175] ObataK, KatsuraH, MizushimaT, YamanakaH, KobayashiK, DaiY, FukuokaT, TokunagaA, TominagaM, NoguchiK. TRPA1 induced in sensory neurons contributes to cold hyperalgesia after inflammation and nerve injury. J Clin Invest 2005.

[176] OliveiraKG, vonZeidlerSV., LamasAZ, dePodestaJRV, SenaA, SouzaED, LenziJ, LemosEM, GouveaSA, BissoliNS. Relationship of inflammatory markers and pain in patients with head and neck cancer prior to anticancer therapy. Brazilian J Med Biol Res 2014.

[177] OliverV, DeRantereD, RitchieR, ChisholmJ, HeckerKG, PangDSJ. Psychometric assessment of the rat grimace scale and development of an analgesic intervention score. PLoS One 2014.

[178] OlsonTH, RiedlMS, VulchanovaL, Ortiz-GonzalezXR, EldeR. An acid sensing ion channel (ASIC) localizes to small primary afferent neurons in rats. Neuroreport 1998.

[179] PeiL, LinCY, DaiJP, YinGF. Facial pain induces the alteration of transient receptor potential vanilloid receptor 1 expression in rat trigeminal ganglion. Neurosci Bull 2007.

[180] PellmarTC, LepinskiDL. Gamma Radiation (5-10 Gy) Impairs Neuronal Function in the Guinea Pig Hippocampus. Radiat Res 1993.

[181] PetersCM, LindsayTH, PomonisJD, LugerNM, GhilardiJR, SevcikMA, MantyhPW. Endothelin and the tumorigenic component of bone cancer pain. Neuroscience 2004.

[182] PetrusM, PeierAM, BandellM, HwangSW, HuynhT, OlneyN, JeglaT, PatapoutianA. A role of TRPA1 in mechanical hyperalgesia is revealed by pharmacological inhibition. Mol Pain 2007.

[183] PhillipsDJ, NjokuIU, BrownKD, SelesnickSH. Radiation-Induced Necrosis of the Temporal Bone: Diagnosis and Management. Otol Neurotol 2015.

[184] PickeringV, Jay GuptaR, QuangP, JordanRC, SchmidtBL. Effect of peripheral endothelin-1 concentration on carcinoma-induced pain in mice. Eur J Pain 2008.

[185] PopivanovaBK, KitamuraK, WuY, KondoT, KagayaT, KanekoS, OshimaM, FujiiC, MukaidaN. Blocking TNF-α in mice reduces colorectal carcinogenesis associated with chronic colitis. J Clin Invest 2008.

[186] PradhanAD, MansonJE, RifaiN, BuringJE, RidkerPM. C-reactive protein, interleukin 6, and risk of developing type 2 diabetes mellitus. J Am Med Assoc 2001.

[187] PremkumarLS, AboojM. TRP channels and analgesia. Life Sciences.2013.

[188] RedvanlyRD, HudginsPA, GussackGS, LewisM, CrockerIR. CT of muscle necrosis following radiation therapy in a patient with head and neck malignancy. Am J Neuroradiol 1992.

[189] ReersS, PfannerstillAC, RadesD, MaushagenR, AndratschkeM, PriesR, WollenbergB. Cytokine changes in response to radio-/chemotherapeutic treatment in head and neck cancer. Anticancer Res 2013.

[190] ReichardtLF. Neurotrophin-regulated signalling pathways. Philos Trans R Soc B Biol Sci 2006.

[191] ReidJ, NolanAM, HughesJML, LascellesD, PawsonP, ScottEM. Development of the short-form Glasgow Composite Measure Pain Scale (CMPS-SF) and derivation of an analgesic intervention score. Anim Welf 2007.

[192] ReidJ, Wiseman-OrrL, ScottM. Shortening of an existing generic online health-related quality of life instrument for dogs. J Small Anim Pract 2018.

[193] Reyes-GibbyCC, AndersonKO, MerrimanKW, ToddKH, SheteSS, HannaEY. Survival patterns in squamous cell carcinoma of the head and neck: Pain as an independent prognostic factor for survival. J Pain 2014.

[194] RiceASC, FinnerupNB, KempHI, CurrieGL, BaronR. Sensory profiling in animal models of neuropathic pain: a call for back-translation. Pain 2018.

[195] RiedelF, ZaissI, HerzogD, GötteK, NaimR, HörmannK. Serum levels of interleukin-6 in patients with primary head and neck squamous cell carcinoma. Anticancer Res 2005.

[196] RipamontiCI, SantiniD, MaranzanoE, BertiM, RoilaF. Management of cancer pain: ESMO clinical practice guidelines. Ann Oncol 2012.

[197] RueffA, DrayA. Sensitization of peripheral afferent fibres in the in vitro neonatal rat spinal cord-tail by bradykinin and prostaglandins. Neuroscience 1993.

[198] SabinoMAC, LugerNM, MachDB, RogersSD, SchweiMJ, MantyhPW. Different tumors in bone each give rise to a distinct pattern of skeletal destruction, bone cancer-related pain behaviors and neurochemical changes in the central nervous system. Int J Cancer 2003.

[199] SatoJ, YamazakiY, SatohA, NotaniK, KitagawaY. Pain is associated with an endophytic cancer growth pattern in patients with oral squamous cell carcinoma before treatment. Odontology 2010;98:60–64. doi:10.1007/s10266-009-0107-6.

[200] SchaeferEAM, StohrS, MeisterM, AignerA, GudermannT, BuechTRH. Stimulation of the chemosensory TRPA1 cation channel by volatile toxic substances promotes cell survival of small cell lung cancer cells. Biochem Pharmacol 2013.

[201] SchäfersM, SorkinL. Effect of cytokines on neuronal excitability. Neurosci Lett 2008.

[202] SchmidtBL, HamamotoDT, SimoneDA, WilcoxGL. Mechanism of Cancer Pain. Mol Interv 2010;10:164–178. doi:10.1124/mi.10.3.7.

[203] SchnitzerTJ, EastonR, PangS, LevinsonDJ, PixtonG, ViktrupL, DavignonI, BrownMT, WestCR, VerburgKM. Effect of Tanezumab on Joint Pain, Physical Function, and Patient Global Assessment of Osteoarthritis among Patients with Osteoarthritis of the Hip or Knee: A Randomized Clinical Trial. JAMA - J Am Med Assoc 2019.

[204] SchweiMJ, HonoreP, RogersSD, Salak-JohnsonJL, FinkeMP, RamnaraineML, ClohisyDR, MantyhPW. Neurochemical and cellular reorganization of the spinal cord in a murine model of bone cancer pain. J Neurosci 1999;19:10886–10897. doi:10.1523/jneurosci.3300-10.2010.

[205] SethiRKV, PanthN, PuramSV., VarvaresMA. Opioid prescription patterns among patients with head and neck cancer. JAMA Otolaryngol - Head Neck Surg 2018;144:382–383.

[206] SeyboldVS, JiaYP, AbrahamsLG. Cyclo-oxygenase-2 contributes to central sensitization in rats with peripheral inflammation. Pain 2003.

[207] ShinodaM, OginoA, OzakiN, UranoH, HironakaK, YasuiM, SugiuraY. Involvement of TRPV1 in Nociceptive Behavior in a Rat Model of Cancer Pain. J Pain 2008.

[208] ShumanAG, TerrellJE, LightE, WolfGT, BradfordCR, ChepehaD, JiangY, McLeanS, GhanemTA, DuffySA. Predictors of pain among patients with head and neck cancer. Arch Otolaryngol - Head Neck Surg 2012.

[209] SiegelRL, MillerKD, JemalA. Cancer statistics, 2019 (US statistics). CA Cancer J Clin 2019.

[210] SonisST. Pathobiology of mucositis. Semin Oncol Nurs 2004;20:11–15. doi:10.1053/j.soncn.2003.10.003.

[211] SonisST, PetersonRL, EdwardsLJ, LuceyCA, WangL, MasonL, LoginG, YmamkawaM, MosesG, BouchardP, HayesLL, BedrosianC, DornerAJ. Defining mechanisms of action of

interleukin-11 on the progression of radiation-induced oral mucositis in hamsters. Oral Oncol 2000.

[212] SotocinalSG, SorgeRE, ZaloumA, TuttleAH, MartinLJ, WieskopfJS, MapplebeckJCS, WeiP, ZhanS, ZhangS, McDougallJJ, KingOD, MogilJS. The Rat Grimace Scale: A partially automated method for quantifying pain in the laboratory rat via facial expressions. Mol Pain 2011.

[213] SouterAJ, GarryMG. Spinal interleukin-1β reduces inflammatory pain. Pain 2000.

[214] SoyluL, ÖzcanC, ÇetikF, PaydaşS, KiroğluM, AydoğanB, SarginÖ, ÖzşahinogluC, SeyrekE. Serum levels of tumor necrosis factor in squamous cell carcinoma of the head and neck. Am J Otolaryngol Neck Med Surg 1994.

[215] SperryMM, YuY-H, WelchRL, GranquistEJ, WinkelsteinBA. Grading facial expression is a sensitive means to detect grimace differences in orofacial pain in a rat model. Sci Rep 2018.

[216] SprostonNR, AshworthJJ. Role of C-reactive protein at sites of inflammation and infection. Front Immunol 2018.

[217] StarkweatherAR, LyonDE, SchubertCM. Pain and Inflammation in Women With Early-Stage Breast Cancer Prior to Induction of Chemotherapy. Biol Res Nurs 2013.

[218] StathopoulouTR, KoukiM, PypendopBH, JohnstonA, PapadimitriouS, PelligandL. Evaluation of analgesic effect and absorption of buprenorphine after buccal administration in cats with oral disease. J Feline Med Surg 2018.

[219] StewartJ. Bradykinin Antagonists as Anti-Cancer Agents. Curr Pharm Des 2005.

[220] StollBA, AndrewsJT. Radiation-induced Peripheral Neuropathy. Br Med J 1966.

[221] StubblefieldMD. Radiation fibrosis syndrome: Neuromuscular and musculoskeletal complications in cancer survivors. PM R 2011.

[222] TatrowK, MontgomeryGH. Cognitive behavioral therapy techniques for distress and pain in breast cancer patients: A meta-analysis. J Behav Med 2006;29:17–27.

[223] TeodoroFC, Tronco JúniorMF, ZampronioAR, MartiniAC, RaeGA, ChichorroJG. Peripheral substance P and neurokinin-1 receptors have a role in inflammatory and neuropathic orofacial pain models. Neuropeptides 2013.

[224] ThompsonLDR. World health organization classification of tumours: Pathology and genetics of head and neck tumours. Ear, Nose Throat J 2006.

[225] TominagaM, CalerinaMJ. Thermosensation and pain. J Neurobiol 2004.

[226] TominagaM, CaterinaMJ, MalmbergAB, RosenTA, GilbertH, SkinnerK, RaumannBE, BasbaumAI, JuliusD. The cloned capsaicin receptor integrates multiple pain-producing stimuli. Neuron 1998.

[227] ToniT, DuaP, Van DerGraafPH. Systems pharmacology of the NGF signaling through p75 and TrkA receptors. CPT Pharmacometrics Syst Pharmacol 2014.

[228] TrottiA, BellmLA, EpsteinJB, FrameD, FuchsHJ, GwedeCK, KomaroffE, NalysnykL, ZilberbergMD. Mucositis incidence, severity and associated outcomes in patients with head and neck cancer receiving radiotherapy with or without chemotherapy: A systematic literature review. Radiother Oncol 2003.

[229] TsudaM, KoizumiS, KitaA, ShigemotoY, UenoS, InoueK. Mechanical allodynia caused by intraplantar injection of P2X receptor agonist in rats: involvement of heteromeric P2X2/3 receptor signaling in capsaicin-insensitive primary afferent neurons. J Neurosci 2000.

[230] TuttleAH, MolinaroMJ, JethwaJF, SotocinalSG, PrietoJC, StynerMA, MogilJS, ZylkaMJ. A deep neural network to assess spontaneous pain from mouse facial expressions. Mol Pain 2018.

[231] ValeTA, SymmondsM, PolydefkisM, ByrnesK, RiceASC, ThemistocleousAC, BennettDLH. Chronic non-freezing cold injury results in neuropathic pain due to a sensory neuropathy. Brain 2017.

[232] VardehD, NaranjoJF. Peripheral and central sensitization. Pain Medicine: An Essential Review.2017.

[233] VenkatesuluBP, MahadevanLS, AliruML, YangX, BoddMH, SinghPK, YusufSW, AbeJ, KrishnanS. Radiation-Induced Endothelial Vascular Injury. JACC Basic to Transl Sci 2018.

[234] VetterI, LewisRJ. Natural product ligands of TRP channels. Advances in Experimental Medicine and Biology.2011.

[235] VigneswaranN, WilliamsMD. Epidemiologic trends in head and neck cancer and aids in diagnosis. Oral Maxillofac Surg Clin North Am 2014.

[236] WalkerHK. Cranial Nerve V: The Trigeminal Nerve. 1990 p.

[237] WangR, ZhouT, LiuW, ZuoL. Molecular mechanism of bystander effects and related abscopal/ cohort effects in cancer therapy. Oncotarget 2018.

[238] WatkinsLR, GoehlerLE, ReltonJ, BrewerMT, MaierSF. Mechanisms of tumor necrosis factor-alpha (TNF-alpha) hyperalgesia. Brain Res 1995.

[239] WatsonJJ, AllenSJ, DawbarnD. Targeting nerve growth factor in pain: What is the therapeutic potential? BioDrugs 2008.

[240] WeinholdB, RütherU. Interleukin-6-dependent and -independent regulation of the human C-reactive protein gene. Biochem J 1997.

[241] WiegandS, ZimmermannA, WilhelmT, WernerJA. Survival after distant metastasis in head and neck cancer. Anticancer Res 2015.

[242] WilliamsHJ, DaviesAM. The effect of X-rays on bone: A pictorial review. Eur Radiol 2006.

[243] WilliamsSH, PeifferE, FordS. Gape and bite force in the Rodents Onychomys leucogaster and Peromyscus maniculatus: Does Jaw-Muscle anatomy predict performance? J Morphol 2009.

[244] WoolfCJ. Central sensitization: Implications for the diagnosis and treatment of pain. Pain 2011.

[245] WoolfCJ. What is this thing called pain? J Clin Invest 2010.

[246] WoolfCJ, SalterMW. Neuronal plasticity: Increasing the gain in pain. Science (80-) 2000.

[247] WuT, HongY, JiaL, WuJ, XiaJ, WangJ, HuQ, ChengB. Modulation of IL-1β reprogrammes the tumor microenvironment to interrupt oral carcinogenesis. Sci Rep 2016.

[248] Y.C, P.K, Q.F, S.H.L, P.K.P, W.L, C.M, D.B, R.W.G, F.W, W.L. TRPV4 is necessary for trigeminal irritant pain and functions as a cellular formalin receptor. Pain 2014.

[249] YazbekKVB, FantoniDT. Validity of a health-related quality-of-life scale for dogs with signs of pain secondary to cancer. J Am Vet Med Assoc 2005.

[250] YeY, DangD, ZhangJ, VietCT, LamDK, DolanJC, GibbsJL, SchmidtBL. Nerve growth factor links oral cancer progression, pain, and cachexia. Mol Cancer Ther 2011.

[251] YeY, OnoK, BernabéDG, VietCT, PickeringV, DolanJC, HardtM, FordAP, SchmidtBL. Adenosine triphosphate drives head and neck cancer pain through P2X2/3 heterotrimers. Acta Neuropathol Commun 2014.

[252] YinE, NelsonDO, ColemanMA, PetersonLE, WyrobekAJ. Gene expression changes in mouse brain after exposure to low-dose ionizing radiation. Int J Radiat Biol 2003.

[253] YowtakJ, LeeKY, KimHY, WangJ, KimHK, ChungK, ChungJM. Reactive oxygen species contribute to neuropathic pain by reducing spinal GABA release. Pain 2011.

[254] ZhouYQ, LiuZ, LiuZH, ChenSP, LiM, ShahveranovA, YeDW, TianYK. Interleukin-6: An emerging regulator of pathological pain. J Neuroinflammation 2016.

[255] ZieglgänsbergerW. Substance P and pain chronicity. Cell Tissue Res 2019.

[256] ZimmermanMA, HuangQ, LiF, LiuX, LiCY. Cell Death-Stimulated Cell Proliferation: A Tissue Regeneration Mechanism Usurped by Tumors During Radiotherapy. Semin Radiat Oncol 2013.

Table 1.1 Taxonomy for the classification of pain.

Type of pain	Definition [10,245]
Nociceptive pain	Pain arises from actual or threatened damage to non-neuronal tissues and is due to the activation of nociceptors.
Inflammatory pain	Pain induced by the activation of immune cells in respond to tissue injuries or infection.
Neuropathic pain	Pain causes by a lesion or disease of somatosensory nervous system.
Dysfunctional pain	Pain occurs when there is no damage of the nervous system but pain is evoked due to abnormal central processing.

Table 1.2 Pain mediators in head and neck cancers.

Mediators	Type	Origin and mechanism	Target nociceptor in cancer pain	Mechanism of pain initiation
Proton	ion	Tumor hypoxia, inflammatory infiltrate, cell death	TRPV1, ASIC-3	Induce Ca^{+2} influx into the sensory neurons
ATP	Nucleoside triphosphate	Cancer cells, damaged cells	P2X2, P2X3	Signal transduction
Endothelin-1	Vasoactive peptide	Cancer cells	ET_AR	Sensory fiber excitation
Bradykinin	Vasoactive peptide	Kallikerin secret from cancer cells, tissue damage	B_1, B_2	Sensory fiber excitation
Substance P	Neuropeptide	Cancer cells	NK_1	Promote impulse transmission
Protease	Enzyme	Cancer cells	PAR-2	Proteolysis of nerve tissues
NGF	Neuropeptide	Cancer cells, damaged cells	Trk	Activate nociceptors

Table 1.3 Pain-related TRP channels [17,185].

	Exogenous agonists	Endogenous agonists	Nociceptive function
TRPV1	Temperature >43ºC Capsaicin Resiniferatoxin Spider toxin Allicin Cannabidiol	proton (H^+) anandamide NADA Nitric oxide N-Oleoylethanolamide PUFAs	Thermal hypersensitivity, noxious heat nociception
TRPV2	Temperature > 52ºC Mechanical stretch 2-APB Cannabidiol	Osmic stimuli	Sensory transduction Noxious heat nociception
TRPV3	Temperature 30-35ºC Camphor Menthol Carvacrol Eugenol Insensol	Farnesyl pyrophosphate (FPP)	Innocuous and noxious heat
TRPV4	Temperature > 27ºC 4α-PDD GSK-1016790	Hypotonicity 5'6'-EET 8'9'-EET	Mechanical and acidic nociception
TRPM8	Temperature < 26ºC Menthol Icilin Eucalyptol	Lysophospholipids	Innocuous and noxious cold
TRPA1	Temperature < 17 ºC Mustard (isothiocyanate) Allium plant (thiosulfinate) Cannabidiol Cucurmin Streptozotocin THC	5'6'-EET Bradykinin Prostaglandins H_2O_2 Nitric oxide	Injury-evoked cold hypersensitivity

Table 1.4 Comparisons of orofacial pain test models in lab animals.

	Pros	Cons	Examples
Spontaneous pain model	• Without personnel interruption • Less stress to animals • Measure the pain-associated function loss • Realistic reflection in people	• Time consuming • Test general well-being	• Home cage monitoring • Facial expression • Dolognawmeter • Ugo Basile orofacial thermal/mechanical stimulation test
Reflexive pain model	• Faster • Mimic hyperalgesia or allodynia to stimuli • Test certain nociceptive receptor	• Requires interacting with researcher. • Stressful to animals • Testing local reflex without perception • Testing the change of sensitivity but not pain • The added stimuli are not natural	• Cold/heat stimulation • Mechanical stimuli (e.g. von Frey) • Chemical stimuli (e.g. histamine, acid)

CHAPTER 2: Upregulation of TRPV1 corresponds to sensory neuron sensitization in a refined rodent radiation-induced mucositis model

Introduction

Approximately 70% of head and neck cancer patients report pain at the end of their cancer treatment, either with radiation therapy, chemotherapy, or combined treatment [11]. Oral mucositis is one of the most common side effects induced by radiation therapy, but the management of painful mucositis is challenging [25]. Painful mucositis decreases the patients' quality of life and can necessitate unplanned breaks in radiotherapy that may significantly worsen the probability of locoregional tumor control [16,29]. Patients are prevented from obtaining proper care to relieve severe acute orofacial radiation-associated pain (RAP) because therapeutics that are effective but without significant side effects are limited in availability [2].

Understanding the mechanism(s) of RAP is critical for developing potential therapeutics to achieve better pain control. The first mouse model to investigate radiation-associated orofacial pain was established by Nolan *et al*. [26]. This novel and reproducible model showed altered behavior and sensory neuron responses in mice that had severe radiation-induced mucositis (RIM). However, several limitations should be addressed to maximize the utility of this model, and to ensure that experimental results are properly interpreted. In the study, RIM was induced using a linear accelerator-based high-dose single fraction lingual irradiation protocol; sham-irradiated mice were used as the experimental control. The decision to use sham-irradiated mice was based on the assumption that all measurable biological effects would have been the result of direct lingual irradiation. However, the investigators did not consider any potential contributions from the low doses of radiation that would have simultaneously been delivered to the rest of the body during lingual irradiation. Potential sources of that low-dose total body radiation exposure

include: (1) scatter from the accelerator head (primary collimator, flattening filter, the secondary collimator); (2) backscattering of photons and/or electrons from the device used to immobilize and position mice during lingual irradiation; and (3) internal scattering from within the tongue or bolus (a material that has equivalent properties to tissues that is used to adjust radiation dosing on the target) to the rest of body. Out-of-field scattering from a linear accelerator can be monitored in the clinical situation and is usually clinically negligible [21]. As their distance from the irradiated field increases, tissues should receive less dose. Thus, if comparing the size of human head and neck cancer patients versus rodents, the low dose scattered on surrounding tissues such as skin or normal oral mucosa in humans would cover the entire brain and body of a mouse. The distance of brain from the rostral tongue-irradiation field in mice is about 1.5 - 2 cm. With 10 × 10 cm field size, the off-axis dose at distance of 2 and 10 cm from the field size edge can be 2% (range from 1 - 10%) and 1% (range from 0.2 - 1.8%) of maximum dose (d_{max}), respectively [21]. The field size used in our previous published murine model was 20 × 20 to minimize the treatment time [26], but larger collimator field sizes result in slower dose fall-off rate at the edge of the field [17]; thus by using 27 Gy to introduce glossitis, the off-axis dose deposit in the brain or elsewhere in this murine body could range from 0.27 - 2.7 Gy (1 - 10% of 27 Gy), which creates biologically meaningful doses that are sufficiently high to warrant a formal investigation. For example, although one study showed that 0.5 Gy TBI does not appear to affect the body weight in adult mice [9], another study showed that a dose of 2 Gy total body irradiation (TBI) leads to an increase in the number of osteoclasts at bone metaphyses within 3 days of irradiation [35].

Low dose irradiation can also impact the central nervous system (CNS). It has been revealed that 0.1 - 2 Gy irradiation can alter expression of various genes in the brain; these genes

are involved in signal transduction (e.g., glutamate receptor genes), ion regulation (e.g., *Trpc1* and H^+ transporting enzyme genes) and synaptic signaling (e.g., transcripts of AMPA and NMDA) [36]. A dose of 2 Gy has also been shown to induce cognitive dysfunction in young mice [27] and reduce neural precursor cell proliferation in the hippocampus of adult rats [31]. However, it is unknown to what extent the scattered dose in our previously described murine model can affect the functioning and the processing of nociceptive signals in nearby sensory neurons.

Despite lacking a low-dose total body irradiation control group (to understand impacts of the doses that scatter outside of the lingual irradiation field), our prior publication showed that a high proportion of sensory neurons are sensitive to histamine, TNF-α and capsaicin in mice with RIM (vs. unirradiated control mice) [26]. However, it is uncertain if this hypersensitization of sensory neurons resulted from pain, or from the direct effects of low-dose radiation that scattered to the trigeminal ganglia (and thus the cell bodies of the tongue's afferent sensory nerves). The capsaicin receptor, transient receptor potential vanilloid type 1 (TRPV1), has been identified as a key biomarker of CNS inflammation and pain [23]. Thus, investigating the regulation of TRPV1 fuction and expression should help clarify the potential impact of low dose scattered radiation in this rodent model of RIM/RAP.

The primary objectives of this current study were to: (1) determine how much radiation dose is absorbed by the body when using our experimental setup for lingual irradiation in mice, and (2) investigate the potential influences of that total body irradiation on spontaneous behaviors and sensory neuronal function. As a secondary aim, we sought to refine the irradiation protocol to facilitate multi-fraction irradiation experiments.

Material and methods

Animals

Six- to eight-week-old female CD-1 mice (Charles River Laboratories, Raleigh, NC) were quarantined for at least 2 weeks prior to being used in this study. Mice were housed in a controlled environment (22 °C; humidity 50%) and maintained on a 12h light: dark cycle throughout the study. Four mice were housed per cage; they were given *ad libitum* access to water and a commercial pelleted diet. Nutra-Gel Diet (Bio-Serv, Flemington, NJ) and non-wetting water gel (HydroGel, ClearH2O, Westbrook, ME) were provided on the floor of the cage if the mice had more than 10% body weight loss. Mice that lost ≥20% of body weight were monitored at least twice daily. Mice with weight loss more than 30% were euthanized if signs of extreme morbidity were observed (i.e., dyspnea, or inability to ambulate well enough to reach food and/or water) or if serious adverse events failed to improve within 48 hours. Euthanasia was performed by flow-metered carbon dioxide in a closed chamber. The study protocol was approved by the Animal Care and Use Committee of NC State University (IACUC Protocol No. 16-275-B).

Experimental setup

The study included sequential 3 phases:

Phase 1: determination of scattering doses. Six hundred monitor units (MU) were applied to the tongue (see more details of mouse positioning in *Mouse cadaver irradiation* below). Thermoluminescent dosimeters (TLDs) were used to determine the exact dose delivered to the tongue, and to determine the dose that simultaneously scatters to the rest of the mouse

during lingual irradiation. A variety of field sizes and bolus thicknesses were used to determine the optimal setup.

Phase 2: reaffirmation of radiation dose required for glossitis induction. Using refined lingual-irradiation techniques, a radiation dose-response assay was performed to reaffirm the minimum dose required to induce recoverable grade 3 glossitis.

Phase 3: understanding the physiological and biological effects of low-dose TBI in the context of lingual irradiation. Physiological change was evaluated by monitoring body weight, and burrowing behavior. To characterize the neurobiological impacts of low dose scattering to the rest of the body in mice with radiation-induced mucositis, mice were euthanized on day 11 post-irradiation and sensory neuron biology (expression and function of relevant biomarkers) was evaluated.

Note: several supportive experiments were performed that do not directly address the study aims yet are relevant to interpretation of the results; detailed methods and results are beyond the scope of this manuscript but are included in an Appendix for completeness. To direct readers to the Appendix at appropriate times while reading, references to such experiments are highlighted in the text that follows.

Radiation dosimetry verifications

In order to understand how much radiation dose is deposited in tissues that lie outside of the radiation field, relative to those tissues within the radiation field, we performed a dosimetry study. Fresh, intact 6-week-old mouse cadavers were used; during tongue irradiation, TLDs were placed: (1) on the tongue; (2) within the calvarium; and (3) in the mid-abdomen of mouse cadavers. Six hundred MU was delivered from the linear accelerator. TLDs were then sent to the University of Wisconsin Radiation Calibration Laboratory to be read.

Tongue irradiation was performed as previously described [26]. Ionizing radiation was delivered using a clinical linear accelerator (Novalis TX, Varian Medical Systems, Palo Alto, CA) with a 6 megavoltage (MV) x-ray beam and dose rate of 1000 MU/min. The radiation field covered the rostral half of the tongue with a source-axis distance of 100 cm. The rest of the body was blocked by the collimator. Mouse cadavers were positioned in right lateral recumbency. Suture loops around the maxillary and mandibular incisors were used to hold the mouth open during irradiation (**Figure 2.1**).

In the original methods [26], the rostral tongue was penetrated by a 30-gauge hypodermic needle and anchored to dental putty (Sil-Tech Putty, Ivoclar Vivadent Inc., Amherst, NY) under the tongue. The dental putty was used to allow for backscatter. A 0.5 cm bolus (homogeneous tissue-equivalent gel, CIVCO Medical Solutions, Coralville, IA) was placed on the top of the tongue to allow for radiation dose build-up, and a field size of asymmetric 20 × 20 cm with the isocenter located where the tongue exits the mouth was used to minimize the treatment time (i.e., large fields deliver more radiation dose per MU).

Here, the methods were modified with hopes of reducing tongue trauma caused by the needle. To create a non-invasive approach, the rostral tongue was gently extracted from the mouth and held in place using a 1 mL serological pipet (Falcon, Franklin Lakes, NJ) connected to the medical vacuum (maintained between -500 and -700 mmHg). In the **phase 1 experiment**, boluses of 0.5 cm, 1 cm or 1.5 cm thickness were placed on top of the tongue during irradiation (**Figure 2.1**).

Asymmetric field sizes of: (1) 4 × 4 cm for irradiation of a single mouse at a time; or (2) 22 × 4 cm for simultaneous irradiation of three mice were evaluated in the phase 1 experiment. In the single mouse irradiation protocol (using a 4 × 4 cm field), the beam's central axis was

placed in the center of the tongue, right where it exited the oral cavity. In the three-mouse irradiation protocol (which was designed to improve experimental efficiency via reduction in irradiation time), the mice were aligned to have rostral tongues under the exposure of the 22 × 4 cm field. Again, the beam's central axis was placed at the junction of the rostral and caudal halves of the tongue. The treatment isocenter of both the 4 × 4 and 22 × 4 cm fields were located at the caudal margin of the light field (half-beam block, generated using the primary jaws). As was done using the original methods, the rest of the head and body was shielded by the primary jaw of the linear accelerator.

Radiation-induced glossitis

Based on results of the aforementioned dosimetry study performed in mouse cadavers, phase 2 experiment was performed using the following irradiation protocol: asymmetric field size of 4 × 4 cm for single mouse irradiation with a 1 cm bolus on the top of the tongue. Single fractions of 25, 27, 29, 31 or 33 Gy were applied to the rostral tongue. The goal was to determine the minimum dose required to induce grade 3 glossitis such that lesions heal and the accompanying body weight loss recovers as quickly as possible (see the method of "body weight and glossitis severity scoring"). Two mice were assigned to each of the 5 radiation dose groups. Mice were anesthetized with ketamine (100 mg/kg, Vedco, St. Louis, MO) and xylazine (16 mg/kg, AnaSed, Lake Forest, IL) via intraperitoneal injection for tongue irradiation. Body weight and glossitis severity scoring (see detailed description below) were evaluated daily until glossitis resolved, or mice met the euthanasia criteria.

Total body irradiation

Mice underwent total body irradiation in order to simulate the dose (with an equivalent dose rate) of radiation that would be absorbed by the entire body during our high-dose lingual irradiation procedure. X-rays (6 MV) from a linear accelerator were used to irradiate anesthetized mice that were placed in the center of a plastic pipette tip box. The anesthesia protocol was the same as the description above. Based on results of phase 1 experiments (see below), a total dose of 1.6 Gy was delivered over 3.07 minutes. To achieve homogeneous radiation distribution throughout the entire body, equally-weighted parallel-opposed beams was utilized, and mice were surrounded by at least 1 centimeter of bolus material.

Body weight and glossitis severity scoring

Body weight and glossitis severity scores were recorded daily, beginning before irradiation (baseline) and continuing until the day of euthanasia. The glossitis severity scoring criteria were modified from the Radiation Therapy Oncology Group system [26,34] as listed in (**Table 2.1**). The scoring was performed by a single veterinarian (YHL) trained by a board-certificated veterinary radiation oncologist (MN).

Burrowing assay and rotarod

Burrowing assays were performed as described previously [26]. The burrowing assay was only performed in phase 3 experiments. Individual mice were placed in a cage that contained a small amount of bedding. A PVC pipe of 5.08 cm (2 inches) diameter and 15.24 cm (6 inches) long with 150 grams of pelleted rabbit food (Prolab high-fiber diet, PMI, Brentwood, MO) was placed in each cage. The mass of food remaining in the tube after one hour was recorded. Mice

underwent two trials before experiments commenced; the average residual mass from the two trials served as the baseline value. The assay was repeated once daily in the morning during the experimental period. An additional test was performed to ensure the motility of mice was not impaired by radiation; to ensure that observed burrowing behavior changes were not due to abnormal motor function, the rotarod assay was performed on days 1, 5, and 10 post-irradiation in 27 Gy tongue-irradiated and sham-irradiated mice. For additional details and results of rotarod, see **Appendix A**.

Neuron tracing

With a goal of identifying tongue afferents in our calcium imaging experiments, we performed pilot studies to evaluate neuron retrograde tracing by injecting DiI into the tip of the tongue. Detailed descriptions of the methods and results are provided (**Supplemental Figure 2.1**) in **Appendix A**. However, because the DiI injection caused considerable grossly-evident lingual trauma that might affect afferent neuron sensitivity, this technique was not utilized in the main study.

Calcium imaging

Calcium imaging is a technique for measuring cellular function, as indicated by shifts in intracellular calcium concentrations. For this experimental procedure, Fura-2 AM is the calcium indicator; it undergoes conformational change when binding to calcium ions. When the cytosolic Fura-2 AM binds to free Ca^{2+}, the peak excitation wavelength changes from 380 nm (Ca^{2+} free Fura-2 AM) to 340 nm (Ca^{2+} bound Fura-2 AM). As a result, the ratio of fluorescent density detected at 340 and 380 nm (340/380 nm) can be used for quantifying the Ca^{2+} concentration in a

neuron [14]. After adding a stimulus, if Ca^{2+} flows into a neuron, that will induce an increase of 340/380 nm ratio. The peak of the 340/380 nm ratio indicates the maximum intracellular Ca^{2+} concentration.

For calcium imaging, trigeminal ganglia (TG) were isolated from euthanized mice and immediately digested with collagenase (Sigma-Aldrich, St. Louis, MO) and dispase (Sigma-Aldrich, St. Louis, MO) in Hanks' Balanced Salt Solution (HBSS, Grand Island, NY) at 37 °C, according to the procedures described by Nolan *et al.* [26]. Isolated cells were resuspended in 25 µL Dulbecco's Modified Eagle Medium (DMEM, Gibco, Paisley, UK), and placed onto an 18 mm coverslip coated with poly-L-lysine and laminin. Neurons were then incubated (at 37 °C with 5% CO_2) in 1 mL DMEM medium containing 10% fetal bovine serum (FBS, heat-inactivated, Gibco, Grand Island, NY) and 2% Pen Strep (Gibco, Grand Island, NY) overnight.

All calcium imaging was performed 12-24 hours after plating the neurons. In preparation for imaging, cultured neurons were incubated with Fura-2 AM (Biotium, Fremont, CA) in complete media for 30 minutes. The coverslip was held using a Quick Release Magnetic Imaging Chamber (Warner Instruments, Hamden, CT) and cells were visualized via inverted fluorescence microscopy (Nikon TE200, Melville, NY). Warm (37°C) Locke solution constantly flowed through the chamber and perfused the coverslip.

Stimuli for which we measured trigeminal neuron responses included: histamine (1 mmol/L, Sigma-Aldrich, St. Louis, MO) [12,13], TNF-α (1 µmol/L, Pepro Tech, Inc., Rockey Hill, NJ) [26], capsaicin (1 µmol/L, Sigma-Aldrich, St. Louis, MO) [12,13], and KCl (150 mmol/L, Fisher Scientific, Fair Lawn, NJ) [26], with at least 1 minute Locke solution flux between each stimulus. Neurons were identified in bright field based on the morphology with the diameter of 10 - 20 µm. A neuron was defined as having a positive response if the 340/380 nm

ratio was greater than 110% of the baseline (pre-stimulation) value. An increase of the 340/380 nm ratio indicated calcium influx. Neurons having positive responses to the various stimuli were counted and the total number of sensory neurons was defined by the number of KCl-responsive cells. For each stimulus (i.e., histamine, TNF-α, or capsaicin), the count of non-responding neurons was calculated by (number of total sensory neurons – number of neurons that had a positive response to certain stimulus). The proportion of neurons that had positive responses to various stimuli was also calculated.

As we have described, the fluorescent ratio of 340/380 nm can be used for quantifying intracellular Ca^{2+} intensity. The increase of intracellular fluorescent intensity (or Ca^{2+} intensity) is defined by the difference between the maximum of fluorescent intensity after adding stimuli and the baseline (pre-stimulation) intracellular fluorescent intensity. The baseline fluorescent intensity ($F_{baseline}$) is the mean of the 340/380 nm fluorescent ratio before adding stimulus; the maximum intracellular fluorescent intensity (F_{max}) is the maximum 340/380 nm fluorescent ratio after adding the stimulus. The percentage increase of the normalized intracellular fluorescent intensity ($\Delta F/F_{baseline}$) is then calculated by $(F_{max} - F_{baseline})/ F_{baseline} \times 100\%$ [3,32,33], which indicated the increased amplitude of intracellular Ca^{2+} intensity after adding the stimuli.

To confirm that the calcium imaging results were not affected by the order in which stimuli were applied, an additional experiment was performed where we randomly changed the order of histamine, TNF-α, and capsaicin. For additional details and results, see **Appendix A**.

Cellular immunofluorescence staining

After calcium imaging, TG neurons that had been grown on coverslips were immediately fixed in 4% neutral buffered formalin (for 5 minutes) then washed with PBS. The coverslips

were incubated in a blocking solution (5% goat serum and 0.05% Triton-X 100 in PBS) for 1 hour at room temperature. TRPV1 expression was detected by the primary antibody (mouse anti-mouse, 1:1000; Abcam, Cambridge, MA) at 4 °C overnight. The coverslips were washed with phosphate-buffered saline (PBS) three times, followed by incubation with secondary antibody (Alexaflour 594 conjugated goat anti-mouse, 1:1000; Invitrogen, Eugene, Oregon) for one hour at room temperature. The coverslips were then washed with PBS and mounted with ProLong Gold antifade reagent and DAPI (4',6-diamidino-2-phenylindole, Invitrogen, Eugene, Oregon) overnight at room temperature. The negative control was performed by omitted primary antibody or secondary antibody. Images were acquired from random fields by confocal microscopy (Olympus FV1000, Center Valley, PA) with 20X objectives. The cellular outline was drawn manually and area, mean fluorescence, and the adjacent background were measured by ImageJ software (US National Institutes of Health, Bethesda, MD) as previously described [24]. The corrected total cellular fluorescent (CTCF) = integrated density – (area of the selected cell × mean fluorescence of background readings) was calculated.

Western blot

The total protein lysates from snap-frozen lingual and TG tissues were extracted using a homogenizer and CHAPS reagent. Protease and Phosphatase Inhibitor Cocktail (EDTA-free, Thermo Scientific, Rockford, IL) was added into the solution prior to protein extraction. Total protein lysate concentration was determined via bicinchoninic acid assay using a kit (BCA, Thermo Scientific, Rockford, IL) and as instructed in the manual. Samples were heated in the Laemmili sample buffer (Bio-Rad, Hercules, CA) with 5% β-mercaptoethanol. Proteins were separated on 10% polyacrylamide gel during electrophoresis and then transferred to a

polyvinylidene difluoride (PVDF) membrane using a Trans-blot Turbo apparatus (7 min/25 V; Bio-Rad). Blocking was achieved with 5% bovine serum albumin (BSA) in TBST buffer. TRPV1 expression was detected via monoclonal antibody (C-terminal, mouse anti-TRPV1, 1:2000; Abcam, Cambridge, MA) in 5% BSA in TBST buffer at 4 °C overnight. Secondary antibody incubation was with peroxidase-conjugated goat anti-mouse (1:5000; Abcam, Cambridge, MA) at room temperature for 1 hour. Reference protein β-tubulin$_{III}$ (rabbit-anti mouse, 1:10000; Abcam, Cambridge, MA) served as the loading control. Signals on the membranes were visualized with the ChemiDoc MP (Bio-Rad, Hercules, CA) imaging system after adding chemiluminescence substrate (Pierce ECL, Thermo Scientific, Rockford, IL). The optical density of protein bands was analyzed using Image Lab software 6.1 (Bio-Rad, Hercules, CA).

Quantitative real-time PCR

To allow readers to readily discriminate expression results for protein versus gene, the TRPV1 protein expression are written in all capital letters; gene names are written in italics with a capital letter as the first character (*Trpv1*). Snap-frozen lingual and TG tissues were homogenized using Multi-Gen 7XL probes (PRO Scientific Inc., Oxford, CT). Total RNA was isolated using RNAeasy Mini Kits (Qiagen, Hilden, Germany) as described in the instruction manual. Total RNA (1 μg) was reverse transcribed to cDNA using a SuperScript III synthesis kit (Thermo Fisher Scientific, Carlsbad, CA). The synthesized cDNA was mixed with TaqMan Gene Expression Master Mix (Applied Biosystem, Austin, TX) and the TaqMan primer probe. TaqMan probes for *Trpv1* (#Mm01246300_m1; target gene) and *Gapdh* (#Mm99999915_g1; reference gene, Thermo Fisher Scientific, Pleasanton, CA) were used. Gene expression was

detected using a quantitative real-time PCR machine (Applied Biosystem, Austin, TX). The expression level was determined by the Ct threshold value and the relative expression was calculated by the ΔCt method.

Statistics

Linear regression was used to evaluate for correlation between changes in body weight and residual mass in the burrowing assay. To compare changes in body weight between treatment groups at various time points, we performed two-way ANOVA with Tukey's multiple comparisons post-hoc test. To compare proportions of responding cells in calcium imaging experiments, we used the Fisher's exact test. Calcium influx level from individual neurons was analyzed by one-way ANOVA. Results of the rotarod and various expression assays were analyzed using the non-parametric Mann-Whitney test. Significance was defined as $P < 0.05$. The data analysis was performed with Prism 7 (GraphPad Software, San Diego, CA).

Results

Phase 1: scatter dose determination

Potentially biologically meaningful dose scatters to the brain and body during high-dose lingual irradiation

We measured dose on the tongue, in the brain, and the abdomen during lingual irradiations that were performed with various experimental setups. With the larger (22 × 4 cm) field size used for simultaneous irradiation of 3 mice, the lingual dose was more variable and the abdomen dose was higher (**Table 2.2**). The tongue of the middle mouse received approximately 17% less dose than the tongue of the other two (outer) mice. The scattered dose measured in the

abdomen was 5.8% (versus 3.9% with 4 × 4 cm field size). Therefore, although slower, all subsequent irradiations were performed on a single mouse at a time. Fewer monitor units could be used to deliver a given dose of radiation as the bolus thickness increased; however, results were similar for 1 vs. 1.5 cm thick bolus (0.85 cGy/MU and 0.88 cGy/MU, respectively). Therefore, all subsequent irradiations were performed using 1 cm bolus.

Phase 2: reaffirmation of radiation dose required for glossitis induction

Confirmation of dose required for recoverable grade 3 glossitis using the modified lingual irradiation methods

By using 25 Gy, the worst glossitis was grade 2 on day 11 and glossitis was fully recovered by day 14. In mice irradiated with 31 Gy or 33 Gy irradiation, grade 3 glossitis began improving by day 13, but accompanying severe weight loss did not improve; due to ethical concerns regarding animal well-being, the mice were euthanized on day 14.

For mid-range doses (27 and 29 Gy), grade 3 glossitis developed and was most severe 11 days after irradiation; accompanying weight loss began to recover on day 14. With 29 Gy, the mean duration of glossitis ≥ grade 2 was 5.5 days, whereas the duration was 3.5 days with 27 Gy (**Table 2.3**). To enable studies of severe glossitis, while minimizing associated morbidity, we chose to use 27 Gy for all subsequent experiments.

Phase 3: investigation of the biological effects of low-dose (1.6 Gy) TBI in the context of high-dose single fraction lingual irradiation.

Low doses of total body irradiation that are absorbed during high dose lingual irradiation did not induce measurable acute physiological effects.

In the **phase 1 experiment**, we found that the brain is exposed to 5.87% of the lingual-irradiation dose, and in the **phase 2 experiment**, we verified that 27 Gy induces recoverable grade 3 glossitis. Mice who underwent high dose (27 Gy) tongue irradiation are hereafter referred to as "tongue-irradiated mice". Because we were interested in the potential neurobiological effects of total body exposures made during lingual irradiation, we opted to use 1.6 Gy (5.87% of 27 Gy) for our total body dose as one of the control groups for glossitis induction in the **phase 3 experiment**.

Tongue-irradiated mice (27 Gy) began to lose weight 7 days post-irradiation and developed grade 1 glossitis on day 9 (**Figure 2.2 A**). Each of the tongue-irradiated mice ultimately developed grade 2 glossitis, and 7/8 (87.5%) developed grade 3 lesions; in all mice, maximally severe glossitis and weight loss occurred 10-11 days post-irradiation. By contrast, neither sham irradiation nor TBI (1.6 Gy administered at 50 cGy/min) caused either glossitis or body weight loss during the first 11 days post-irradiation. In line with previous experimental results for the burrowing assay, mice with severe glossitis left significantly more pellets behind versus mice without severe glossitis [26]. Body weight loss was correlated with burrowing results; as mice lost weight, they left more pellets in the tube (**Figure 2.2 B**). There is no significant difference in motor function between tongue-irradiated mice and sham-irradiated mice (**Supplemental Figure 2.2**). The detailed results are described in the **Appendix A.**

Sensory neuron function was not acutely affected by low dose scattering

Calcium imaging revealed that a higher proportion of sensory neurons were sensitive to histamine, TNF-α, and capsaicin in mice with maximally severe radiation-induced glossitis; such changes were not observed in mice having undergone 1.6 Gy TBI. In the 324 trigeminal sensory

neurons that were imaged from mice with glossitis, the proportion of cells that responded to histamine, TNF-α, or capsaicin were 24%, 26%, and 40%, respectively, which was about two times higher than the other two control groups (**Figure 2.3 A**). A total of 349 and 207 individual neurons from the two control groups were imaged. Histamine induced significant Ca^{+2} influx into 16% and 11% of neurons in TBI and sham irradiated mice, respectively. Similarly, TNF-α opened ion channels in 16% (TBI) and 12% (sham) of neurons. More neurons were responsive to capsaicin than the other two stimuli, with 20% and 21% of neurons responding in the TBI and sham irradiated groups, respectively.

The order of stimulus application in calcium imaging did not significantly impact the proportion of neurons that responds to each stimulus in sham-irradiated mice (**Supplemental Figure 2.3**). Detailed results are described in the **Appendix A.**

The maximum cytosol Ca^{+2} influx was calculated in individual neurons. The greatest changes from baseline were seen in neurons harvested from mice with glossitis and stimulated by either histamine, TNF-α, and capsaicin (1.8-, 2-, and 2.6- fold higher than sham irradiated mice, respectively, **Figure 2.3 B** and **Table 2.4**). There was no significant difference in Ca^{+2} influx between neurons from sham and TBI group mice after stimulation with histamine or capsaicin. Interestingly, TNF-α induced a significantly higher averaged cytosol Ca^{+2} intensity increase in neurons from both mice with glossitis (9.04%) and TBI mice (6.3%), compared to neurons from sham irradiated mice (4.5%). However, this method includes all the imaged neurons that contains non-meaningful Ca^{+2} influx (i.e., cytosol Ca^{+2} intensity increase less than 10% than the baseline).

Since not all of the sensory neurons had functional histamine, TNF-α, or capsaicin receptors, we excluded non-responsive neurons (i.e. excitation 340/380 nm ratio increase from baseline < 10%) to characterize the neurons that had a positive response to a certain stimulus.

This evaluation of excitation ratios from responsive neurons showed no statistically significant difference between TBI, sham, or tongue-irradiated mice (**Figure 2.3 C**). No matter what treatment the mice had, histamine-responsive neurons had a 40.5-45% ratio increase, and capsaicin-responsive neurons had a 35-40% ratio increase, which was higher than that of TNF-α induced ratio increases (27-29%) in responding neurons.

As assessed using immunolabeling and Western blot, we found significantly higher TRPV1 protein expression in trigeminal neurons from mice with severe glossitis (**Figure 2.4**). The mean CTCF (corrected total cell fluorescence) in mice with RAP was 1.6-fold and 1.5-fold higher than sham and TBI mice, respectively, but there was no significant difference between the sham and TBI groups (**Figure 2.4 A**). The average fluorescent signal in sham-irradiated mice was $9.069 \pm 3.531 \times 10^4$. The distribution of TRPV1 included cytoplasm and cell membrane. Neurons that had a fluorescence signal that was higher than the average value from sham-irradiated mice were evaluated. Using this method, the fluorescence signal density was elevated in 148/309 (48%) neurons from tongue-irradiated mice (**Figure 2.4 B**). Moreover, the proportion of TRPV1-upregulated neurons from mice with tongue-irradiation was significantly higher than sham ($P = 0.0008$) and TBI ($P = 0.0026$). Only 45/145 (31.03%) and 79/228 (34.65%) neurons had higher TRPV1 signals than the average in sham-irradiated mice and TBI, respectively (**Figure 2.4 C-E**), and there was no significant difference between the two groups. The Western blotting results for TG agreed with cellular immunostaining. Higher expression of TRPV1 was present in TG homogenates from mice with severe glossitis. The expression level in mice with glossitis was 5-fold and 4.5-fold higher than sham and TBI, respectively (both $P = 0.0286$). By contrast, TRPV1 expression in TG from the TBI group was indistinguishable from the sham-irradiated group on day 11 (**Figure 2.4 F**).

At the time of maximally severe glossitis, quantitative RT-PCR showed a significantly higher (2.5-fold) expression of the *Trpv1* gene in the TG of high-dose (27 Gy) tongue-irradiated mice versus sham-irradiated mice ($P = 0.0286$, **Figure 2.5**). The expression of *Trpv1* in TBI mice was not significantly different from either sham- or tongue-irradiated mice ($P = 0.8857$).

Discussion

Earlier work relied on fixation of the tongue using a hypodermic needle in order to effect exposure. That was very effective, and allowed reliable irradiation of the rostral tongue; however, the lingual tissues are full of capillaries and rich with peripheral nerve endings. The puncture may induce hemorrhage and pain that could interfere with the observation of RAP [5]. In the present study, we developed a method of tongue exposure and stabilization by using a vacuum to gently hold the tip of the tongue. Although we did not perform histopathology to compare tissue damage between the two methods, the vacuum method used in the present study was non-invasive did not induce visible tissue damage. However, there is risk that the tongue may become detached from the pipette tip during irradiation; this should be closely monitored via camera, to ensure proper irradiation.

The field size and bolus used in the present work differed from previous work. The large field sizes we previously used were designed to minimize treatment time. Another potential advantage of using a large field is that it could enable simultaneous irradiation of multiple mice. However, as shown in the data, when using a 22 × 4 cm field size to treat 3 mice, the mouse at the middle received less radiation than the other two mice, and the scattering at the abdomen was nearly 2% higher than with the smaller field size. The inconsistent dosing on the tongue could induce different levels of glossitis. It may also impact the neurobiological study since radiation-

induced injuries are generally dose-dependent. Therefore, all other *in vivo* experiments utilized a single-mouse irradiation technique, and a field size of 4 × 4 cm to minimize the variability in tongue-dosing and to minimize scattering. With the 6 MV beam, the maximum dose deposits at the depth of 1.4 cm. In the setup of this study, 0.88 cGy/MU and 0.85 cGy/MU can be delivered when using 1 cm and 1.5 cm bolus respectively, which was not a significant difference. The similarity may due to the softening of the energy near the edge of the beam in the penumbra [18]. As the beam softens, the depth of maximum dose deposition becomes shallower and this may account for the small difference between the two thicknesses of bolus.

With a goal of understanding whether sham-irradiated animals provide sufficient control data for studies of radiation-associated pain, the current study quantified the amount, and neurobiological effects, of the radiation that inadvertently scatters to the rest of the body (which lies outside of the primary beam and is shielded) in mice undergoing this high-dose lingual irradiation protocol. Exposure of the entire mouse to 1.6 Gy at a relatively high dose rate in the present study has no measurable impact on general well-being (as indicated by stable body weight and burrowing activity) in the first 11 days post-irradiation. Although Kondo *et al*. showed compromised trabecular bone microarchitecture as early as 3 days following irradiation of adult mice with 1-2 Gy [20], another study showed that doses lower than 6 Gy did not significantly change the body weight over 30 days in mice [19]. We did not see body weight changes in the period of the present study, but this low-dose may still induce microscopic change such as bone atrophy.

Hematological side effects induced by total body irradiation could lead to immune compromise thus under the risk of opportunistic infection that could affect body weight. Based on literature reports, total body exposure to 1-2 Gy can induce bone marrow stem cell reduction,

mild lymphocytopenia and reduce cytokine production in T cells [8]. These hematopoietic changes induced by low-dose TBI could increase the risk of fever and infection [30], thus potentially influence animal health.

TBI-treated mice in our study displayed normal burrowing behavior. By contrast, mice with tongue-irradiation had reduced burrowing behavior, which is consistent with the previous study [26]. To clarify that this behavior change is due to pain rather than impaired motor function, we performed an additional experiment of rotarod (**Supplemental Figure 2.2**). The results of the rotarod assay provided evidence that the motor function of mice was not affected by the irradiation, thus supporting our conclusion that the reduced burrowing activity in mice with severe glossitis is due to discomfort. Notably, in both tongue-irradiated and sham-irradiated mice, we saw that in the rotarod assay, the latency to fall had an increasing trend from day 1 to day 5. This indicates that rotarod performance can be affected by training; the more practice mice have, the longer they may stay on the rotating rod.

The results of calcium imaging supported the previous study that a higher proportion of neurons from mice with glossitis were responsive to the stimuli used, but the proportion of sensitized neurons were different [26]. This may due to the different radiosensitivities of the various mouse strain (Balb/c vs. CD-1 in the present study) [10]. However, despite differences between our results and previous results, the comparison between groups in the present study is valid as all neurons were treated under similar conditions. Overall, the relative pattern of responsiveness between neurons from mice with RIM and sham irradiation still agreed with the previous study [26]. Both studies showed that an increased proportion of sensory neurons responded to capsaicin, TNF-α and histamine from tongue-irradiated mice, when compared to sham irradiated mice. As capsaicin is the activator of the TRPV1 channel, we further evaluated

the expression of TRPV1 in the trigeminal ganglia. Supporting our calcium imaging results, we have now shown that TRPV1 expression in mice with severe radiation-induced glossitis is upregulated (versus the other two control groups).

The expression of TRPV1 protein was not impacted by low-dose TBI. The non-statistically significant increase in *Trpv1* gene expression in TGs from low-dose TBI mice may due to statistical error. The small sample (4 mice) may lead to a type II error that we were not able to detect the increase of *Trpv1.* Type I error may result from cross-contamination, but the negative control (blank well without cDNA samples) and the sham irradiated group has ruled out the possibility of false-positives in the TBI group. The discrepancy of protein and mildly increased gene expression can be due to DNA damage by ionizing irradiation, or the indirect impact on transcriptional signaling [22,28]. The transcriptional response could be radiation dose-dependent [28]. Transcription and pre-mRNA splicing of some genes can be affected by doses as low as 0.1 Gy [22]. Yin *et al.* investigated a panel of brain genes and showed alteration of gene expression after 0.1 or 2 Gy low dose ionizing radiation [36]. In that study, one of the Trp family associate genes, *Trpc1*, was evaluated and shown to be downregulated 30 min post-irradiation [36]. In the present study, a non-significant increase of *Trpv1* transcripts in TG of TBI mice was observed at day 11 post-irradiation, but neither the translation of TRPV1 channels nor their function was affected. TRPV1-selective microRNA (miRNA) in neurons may play a role in regulating the functional translation of TRPV1 [23]. The downregulation of miRNAs, miR-199, has been revealed to promote TRPV1 signaling in mice with visceral pain [38]. Another study showed that miR-141-3p, miR-6802-3p, miR-511b-5p, and miR-6807-3p can post-translationally regulate TRPV1 mRNA expression [37]. Different radiation dose could affect the quantity of miRNA in animals; with a sublethal dose total body irradiation in mice, Acharya *et al.* have

shown the signature of the altered miRNA in mouse serum, and the alteration was different under the exposure of 2 Gy or 6.5 Gy radiation [1]. Therefore, with the 1.6 Gy irradiation, the miRNA that regulates the TRPV1 mRNA translation may not significantly be changed, whereas a high dose on the tongue can cause the downregulation of miRNA in trigeminal sensory neurons and promote TRPV1 expression. Investigation of the relevant miRNA would be needed to test this theoretical role of miRNA in RAP.

Another member in TRP family, TRPV4, could also play a role in radiation-associated discomforts. TRPV4 channel is known to respond to a histaminergic stimulus that induced calcium influx [6]. As we saw the proportion of neurons that responded to histamine stimulation were increased from tongue-irradiated mice compared to two control groups, the expression of TRPV4 should be further investigated. By comparing sham and TBI, the proportion of neurons that responded to histamine and TNF-α was not significantly different. It has been revealed that ionizing radiation induced-CNS toxicity is correlated to increased gene expression of pro-inflammatory cytokines including TNF-α and INF-γ in the normal brain microenvironment [4]. TNF-α is known to be linked to inflammatory hypernociception [7] and the expression of TNF-α gene may directly be activated by ionizing radiation [15]. Although our study has shown that TNF-α can induce a higher calcium influx level in sensory neurons from low dose TBI (1.6 Gy) mice than sham-irradiated mice, but that includes all the imaged neurons; not all of the neurons include in this analysis had meaningful Ca^{+2} influx (i.e. influx level increase 10% from baseline); when evaluating those TNF-α positive neurons, the calcium influx level was the same among all three treatment groups. Moreover, the proportion of activated neurons was not significantly different from sham-irradiated mice.

In conclusion, we confirmed the dose that can efficiently induce RIM in CD-1 mice with refined murine model. The amount of out-of-field scattering was determined and an additional control group with low-dose TBI was evaluated. The low-dose scattering did not significantly impact body weight or burrowing behavior. It may subtly alter the expression of pain-related genes such as *Trpv1* in neurons, but in our study, the function and protein expression of TRPV1 were not changed by low dose TBI at 11 days post-irradiation (the time at which maximally severe glossitis occurs in this mouse strain and with our methodologies for high dose rostral tongue irradiation). Our experiments showed the serendipitous observation that TNF-α induced more Ca^{+2} influx in sensory neurons from mice exposed to low dose TBI than sham irradiated mice, which indicates that those mice may potentially be more sensitive to inflammatory pain. In the future, measuring TNF-α in mouse serum and/or irradiated tissue (e.g., by ELISA, Western blot, or immunofluorescent staining) may provide useful insight regarding general pro- or/ anti-inflammatory responses induced by low dose irradiation. The lack of low-dose TBI as control may jeopardize the evaluation of mild systemic change in cytokines, but sham-irradiated control mice should be sufficient to investigate the acute pain that is induced by high-dose lingual irradiation.

REFERENCES

[1] AcharyaSS, FendlerW, WatsonJ, HamiltonA, PanY, GaudianoE, MoskwaP, BhanjaP, SahaS, GuhaC, ParmarK, ChowdhuryD. Serum microRNAs are early indicators of survival after radiation-induced hematopoietic injury. Sci Transl Med 2015.

[2] AstrupGL, RustøenT, MiaskowskiC, PaulSM, BjordalK. Changes in and predictors of pain characteristics in patients with head and neck cancer undergoing radiotherapy. Pain 2015.

[3] Barreto-ChangOL, DolmetschRE. Calcium imaging of cortical neurons using Fura-2 AM. J Vis Exp 2009.

[4] BelkaC, BudachW, KortmannRD, BambergM. Radiation induced CNS toxicity - Molecular and cellular mechanisms. Br J Cancer 2001.

[5] CasanovaF, CarneyPR, SarntinoranontM. Effect of needle insertion speed on tissue injury, stress, and backflow distribution for convection-enhanced delivery in the rat brain. PLoS One 2014.

[6] ChenY, FangQ, WangZ, ZhangJY, MacLeodAS, HallRP, LiedtkeWB. Transient receptor potential vanilloid 4 ion channel functions as a pruriceptor in epidermal keratinocytes to evoke histaminergic itch. J Biol Chem 2016.

[7] CunhaFQ, PooleS, LorenzettiBB, FerreiraSH. The pivotal role of tumour necrosis factor α in the development of inflammatory hyperalgesia. Br J Pharmacol 1992.

[8] DainiakN. Hematologic consequences of exposure to ionizing radiation. Exp Hematol 2002.

[9] DalkeC, NeffF, BainsSK, BrightS, LordD, ReitmeirP, RößlerU, SamagaD, UngerK, BraselmannH, WagnerF, GreiterM, GomolkaM, HornhardtS, KunzeS, KempfSJ, GarrettL,

HölterSM, WurstW, RosemannM, AzimzadehO, TapioS, AubeleM, TheisF, HoeschenC, SlijepcevicP, KadhimM, AtkinsonM, ZitzelsbergerH, KulkaU, GrawJ. Lifetime study in mice after acute low-dose ionizing radiation: a multifactorial study with special focus on cataract risk. Radiat Environ Biophys 2018.

[10] DörrW, SpeklK, MartinM. Radiation-induced oral mucositis in mice: Strain differences. Cell Prolif 2002.

[11] EpsteinJB, HongC, LoganRM, BaraschA, GordonSM, Oberlee-EdwardsL, McGuireD, NapenasJJ, EltingLS, SpijkervetFKL, BrennanMT. A systematic review of orofacial pain in patients receiving cancer therapy. Support Care Cancer 2010.

[12] FukuyamaT, GanchingcoJR, MishraSK, OlivryT, RzagalinskiI, VolmerDA, BäumerW. Janus kinase inhibitors display broad anti-itch properties: A possible link through the TRPV1 receptor. J Allergy Clin Immunol 2017.

[13] FukuyamaT, MartelBC, LinderKE, EhlingS, GanchingcoJR, BäumerW. Hypochlorous acid is antipruritic and anti-inflammatory in a mouse model of atopic dermatitis. Clin Exp Allergy 2018.

[14] GrienbergerC, KonnerthA. Imaging Calcium in Neurons. Neuron 2012.

[15] HallahanDE, SpriggsDR, BeckettMA, KufeDW, WeichselbaumRR. Increased tumor necrosis factor α mRNA after cellular exposure to ionizing radiation. Proc Natl Acad Sci U S A 1989.

[16] HarrisDJ. Cancer treatment-induced mucositis pain: Strategies for assessment and management. Ther Clin Risk Manag 2006.

[17] HuangY, Alfredo SiochiR, BayouthJE. Dosimetric properties of a beam quality-matched 6 MV unflattened photon beam. J Appl Clin Med Phys 2012.

[18] Khan, Faiz M. GibbonsJP. Treatment Planning I: Isodose Distributions. In: PineJW, editor. Khan's The Physics of Radiation Therapy. Philadelphia, PA: LIPPINCOTT WILLIAMS & WILKINS, 2014. pp. 170–194.

[19] KochA, GulaniJ, KingG, HieberK, ChappelM, OssetrovaN. Establishment of early endpoints in mouse total-body irradiation model. PLoS One 2016.

[20] KondoH, SearbyND, MojarrabR, PhillipsJ, AlwoodJ, YumotoK, AlmeidaEAC, LimoliCL, GlobusRK. Total-Body Irradiation of Postpubertal Mice with 137 Cs Acutely Compromises the Microarchitecture of Cancellous Bone and Increases Osteoclasts . Radiat Res 2009.

[21] KrySF, BednarzB, HowellRM, DauerL, FollowillD, KleinE, PaganettiH, WangB, WuuCS, George XuX. AAPM TG 158: Measurement and calculation of doses outside the treated volume from external-beam radiation therapy. Med Phys 2017.

[22] MacaevaE, SaeysY, TaburyK, JanssenA, MichauxA, BenotmaneMA, DeVosWH, BaatoutS, QuintensR. Radiation-induced alternative transcription and splicing events and their applicability to practical biodosimetry. Sci Rep 2016.

[23] MarroneMC, MorabitoA, GiustizieriM, ChiurchiùV, LeutiA, MattioliM, MarinelliS, RigantiL, LombardiM, MuranaE, TotaroA, PiomelliD, RagozzinoD, OddiS, MaccarroneM, VerderioC, MarinelliS. TRPV1 channels are critical brain inflammation detectors and neuropathic pain biomarkers in mice. Nat Commun 2017.

[24] McCloyRA, RogersS, CaldonCE, LorcaT, CastroA, BurgessA. Partial inhibition of Cdk1 in G2 phase overrides the SAC and decouples mitotic events. Cell Cycle 2014.

[25] MoslemiD, NokhandaniAM, OtaghsaraeiMT, MoghadamniaY, KazemiS, MoghadamniaAA. Management of chemo/radiation-induced oral mucositis in patients with head and neck cancer: A review of the current literature. Radiother Oncol 2016.

[26] NolanMW, LongCT, MarcusKL, SarmadiS, RobackDM, FukuyamaT, BaeumerW, LascellesBDX. Nocifensive Behaviors in Mice with Radiation-Induced Oral Mucositis. Radiat Res 2017;187:397–403. doi:10.1667/RR14669.1.

[27] RolaR, RaberJ, RizkA, OtsukaS, VandenbergSR, MorhardtDR, FikeJR. Radiation-induced impairment of hippocampal neurogenesis is associated with cognitive deficits in young mice. Exp Neurol 2004.

[28] RouchkaEC, FlightRM, FasciottoBH, EstradaR, EatonJW, PatibandlaPK, WaigelSJ, LiD, KirtleyJK, SethuP, KeyntonRS. Transcriptional profile of immediate response to ionizing radiation exposure. Genomics Data 2016.

[29] RussoG, HaddadR, PosnerM, MachtayM. Radiation Treatment Breaks and Ulcerative Mucositis in Head and Neck Cancer. Oncologist 2008.

[30] StorekJ, ZhaoZ, LinE, BergerT, McSweeneyPA, NashRA, AkatsukaY, MetcalfMD, LuH, KalinaT, ReindlM, StorbR, HansenJA, SullivanKM, KraftGH, FurstDE, MaloneyDG. Recovery from and consequences of severe iatrogenic lymphopenia (induced to treat autoimmune diseases). Clin Immunol 2004.

[31] TadaE, ParentJM, LowensteinDH, FikeJR. X-irradiation causes a prolonged reduction in cell proliferation in the dentate gyrus of adult rats. Neuroscience 2000.

[32] TakahashiA, CamachoP, LechleiterJD, HermanB. Measurement of intracellular calcium. Physiol Rev 1999.

[33] TinningPW, FranssenAJPM, HridiSU, BushellTJ, McconnellG. A 340/380 nm light-emitting diode illuminator for Fura-2 AM ratiometric Ca2+ imaging of live cells with better than 5 nM precision. J Microsc 2018.

[34] TrottiA. Toxicity in head and neck cancer: A review of trends and issues. Int J Radiat Oncol Biol Phys 2000.

[35] WilleyJS, LloydSAJ, RobbinsME, BourlandJD, Smith-SielickiH, BowmanLC, NorrdinRW, BatemanTA. Early Increase in Osteoclast Number in Mice after Whole-Body Irradiation with 2 Gy X Rays. Radiat Res 2008.

[36] YinE, NelsonDO, ColemanMA, PetersonLE, WyrobekAJ. Gene expression changes in mouse brain after exposure to low-dose ionizing radiation. Int J Radiat Biol 2003.

[37] ZhangJ, ZhouZ, ZhangN, JinW, RenY, ChenC. Establishment of preliminary regulatory network of TRPV1 and related cytokines. Saudi J Biol Sci 2017.

[38] ZhouQ, YangL, LarsonS, BasraS, MerwatS, TanA, CroceC, Nicholas VerneG. Decreased miR-199 augments visceral pain in patients with IBS through translational upregulation of TRPV1. Gut 2015.

Table 2.1 Glossitis severity scoring.

Score	Lesion description
0	no change over baseline
1	erythema, redness, vascular dilation, 1-2 small blister-like lesions, mild thickened and edema
2	patchy ulceration and/or pseudomembrane/ plaque formation, >2 blister-like lesions, hypersalivation, moderate edema
3	confluent ulceration or fibrinous membrane formation within the irradiated field
4	hemorrhage or necrosis
5	death

Table 2.2 Radiation scattering to the brain and abdomen after delivery of 600 monitor was delivered to the center of the tongue.

# of mice irradiated	Field size (cm)	Bolus thickness (cm)	TLD location	Absolute dose (cGy)	Relative dose (% of prescribed lingual dose)
3	22 × 4	1.5	Tongue (mouse at right)	590.3	
3	22 × 4	1.5	Tongue (mouse at middle)	472	
3	22 × 4	1.5	Tongue (mouse at left)	555.5	
1	4 × 4	0.5	Tongue	474.2	
1	4 × 4	1.0	Tongue	510.8	
1	4 × 4	1.5	Tongue	530.1	
1	4 × 4	0.5	Brain	41.1	8.67%
1	4 × 4	1.5	Brain	32	5.87%
1	4 × 4	0.5	Abdomen	17.9	3.93%
1	4 × 4	1.5	Abdomen	21.7	3.98%
3	22 × 4	1.5	Abdomen (mouse at middle)	27.4	5.81%

Table 2.3 Glossitis severity and duration as a function of radiation dose.

Dose (Gy)	Worst glossitis score (grade)	Duration of glossitis ≥ grade 2 (days)
25	2	1.5
27	3	3.5
29	3	5.5
31	3	4.5
33	3	6

Table 2.4 Excitation 340/380 ratio increase from baseline after adding the stimulus. All sensory neurons in each group were included. Values were presented as percentage % (95% CI).

	Sham	TBI 1.6 Gy	Lingual 27 Gy
Histamine	6.1 (3.5 – 8.5%)	7.8 (5.7 - 9.9%)	11.1 (8.5 - 13.8%)
TNF-α	4.5 (3.0 – 5.9%)	6.3 (5.1 – 7.5%)	9.0 (7.3 – 10.8%)
Capsaicin	6.8 (5.1 – 8.4%)	8.9 (7.0 – 10.8%)	17.6 (14.8 – 20.3%)

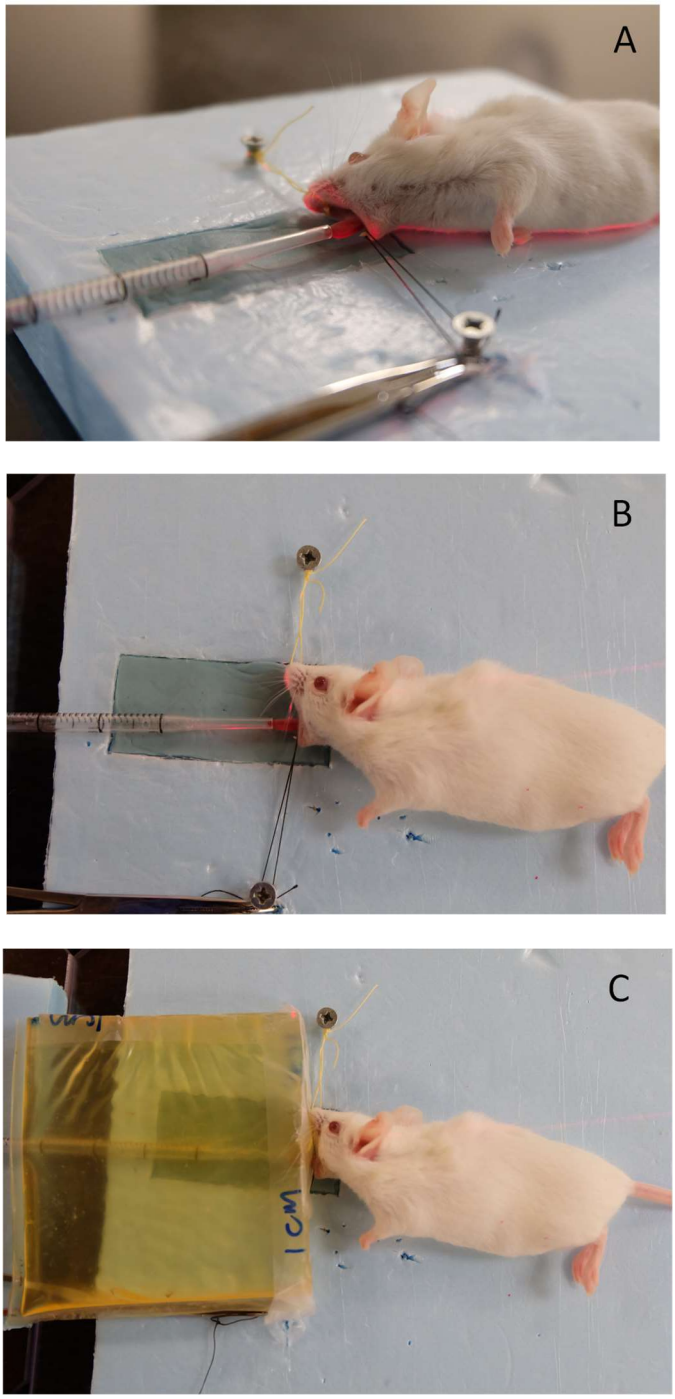

Figure 2.1 The improved rodent model setup. (A) and (B) The incisors were retracted to make the mouth open, and the tongue was gently held by a pipette. (C) A piece of bolus was placed on the top of the tongue.

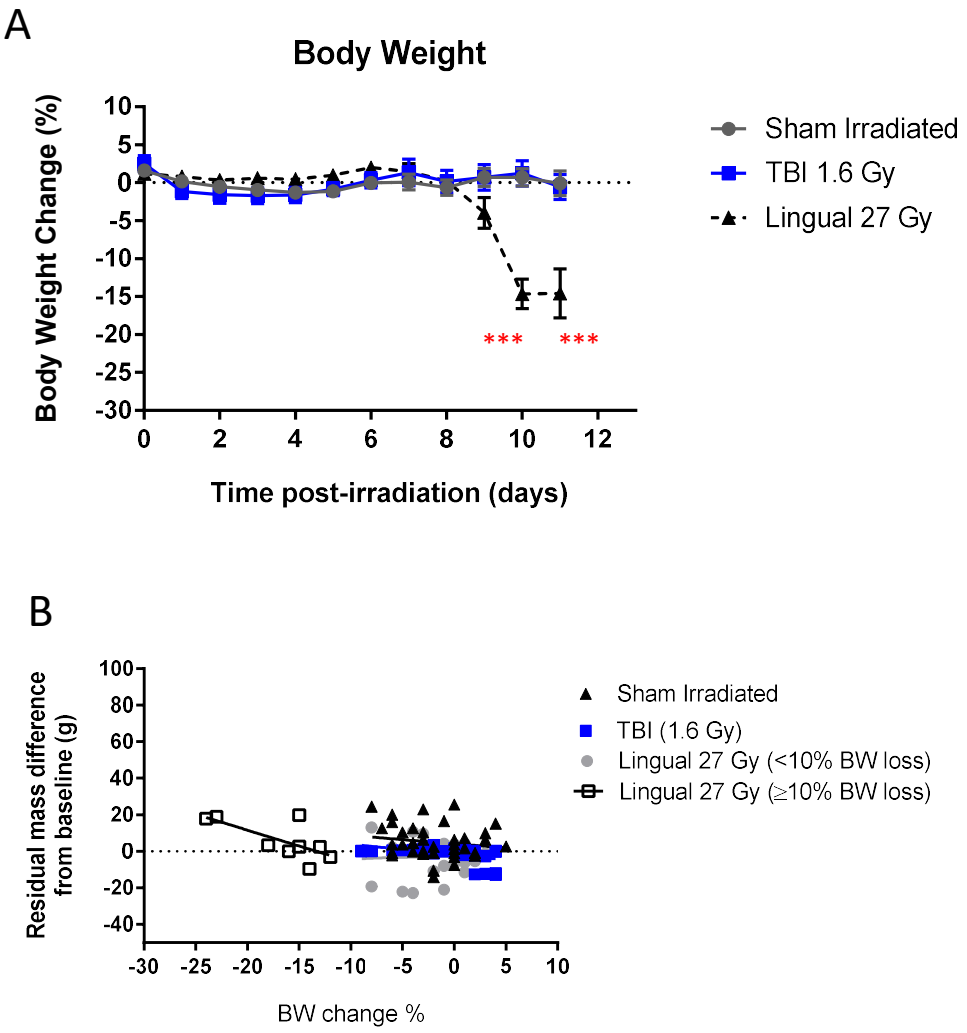

Figure 2.2 Body weight change after the irradiation and its correlation to the burrowing behavior. (A) The body weight change of sham and TBI mice varies from -10% to + 5% from the baseline during the study period. High-dose (27 Gy) lingual irradiated mice had significant body weight loss at day 10 and day 11 (14.67 ± 5.548 and 14.58 ± 9.118, % ± SD, respectively). ***$P < 0.001$, Mann-Whitney test, n = 8-10 in each group, error bars depict SEM. (B) In lingual 27Gy irradiated mice, the body weight loss greater than 10% were correlated to the less burrowing behavior (r^2= 0.4872, $P = 0.0365$).

Figure 2.3 The proportion of neurons that responded to the tested stimuli, and the magnitude of Ca^{+2} influx in calcium imaging. (A) In mice with severe glossitis, the proportion of sensory neuron responded to histamine, TNF-α, or capsaicin was significantly higher than the other two control groups. The proportion of neurons from TBI mice that responded to histamine, TNF-α, or capsaicin was not significantly different from sham-irradiated mice. Neurons were from 8 mice, Fisher's exact test. (B) In all imaged neurons, the average increased intensity when either stimulated by histamine, TNF-α, or capsaicin in RIM group were significantly higher than sham group (1.8, 2, and 2.6-fold higher, respectively). Interestingly, TNF-α induced a 1.4-fold higher intensity increase in TBI than sham group; Mann-Whitney test. (C) Only the responsive neurons were included in this analysis. There was no significant difference between TBI, sham, or lingual irradiated group. Histamine-responsive neurons had 40.5-45% intensity increase in average among three groups; neurons responded to TNF-α had 27-29% ratio increase, and capsaicin-responsive neurons had 35-40% ratio increase when the stimuli were applied; Mann-Whitney test. All error bars depict SEM, $*P < 0.05$, $**P < 0.01$, $***P < 0.001$, $****P < 0.0001$.

A

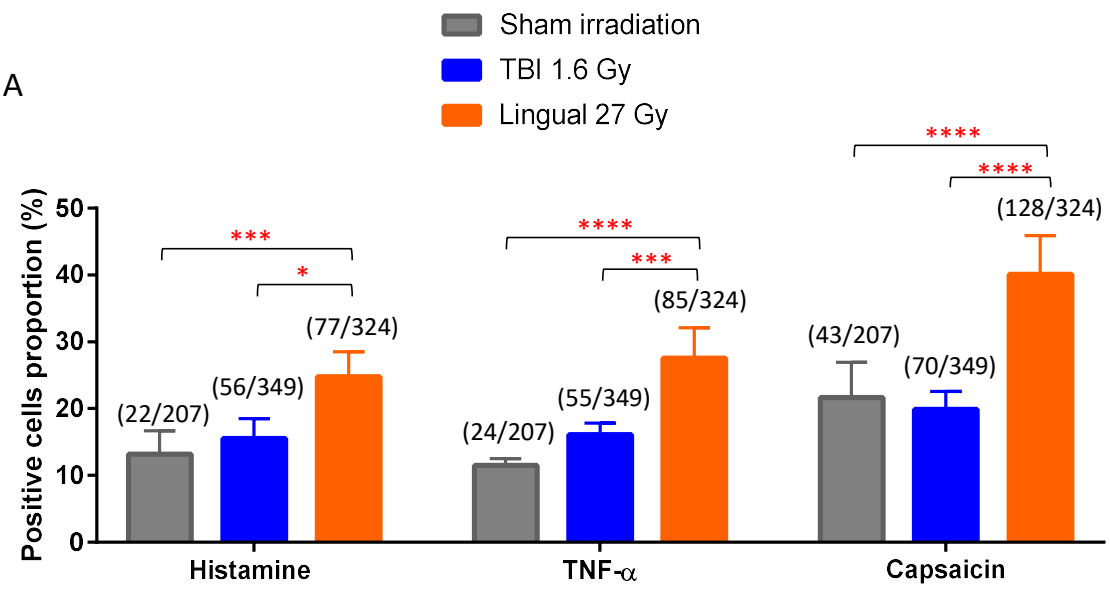

B All sensory neurons

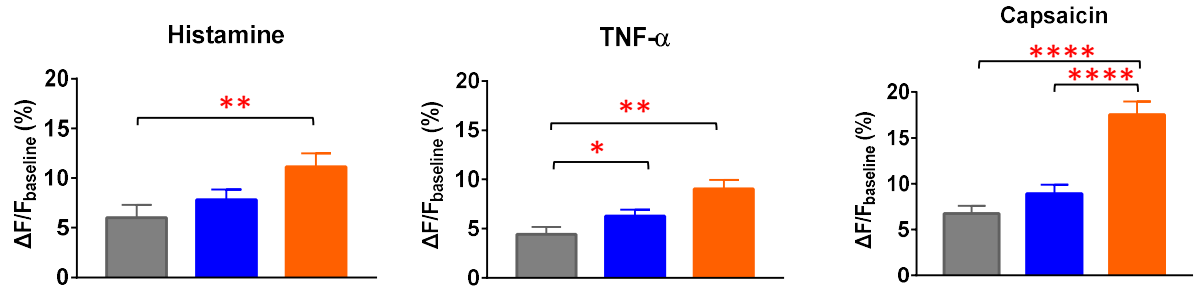

C Only responsive neurons included

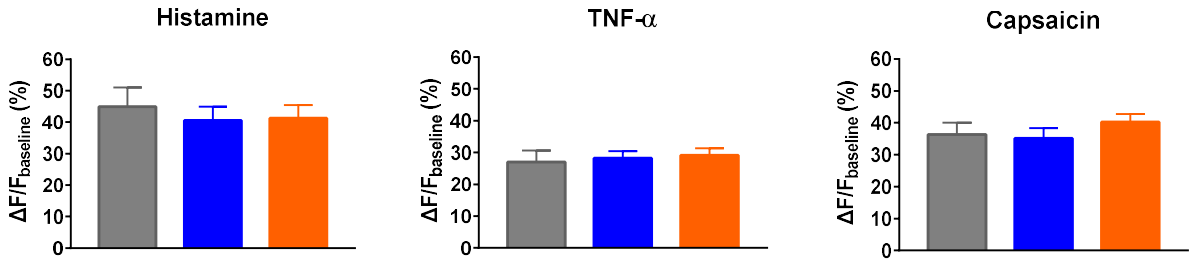

Figure 2.4 Cellular immunofluorescent labeling also supported the TRPV1 expression pattern in Western blot. (A) Significant higher TRPV1 immuno-active signals were detected in the sensory neurons of lingual irradiated mice. (neurons were pooled from 4 mice, each spot represents the mean cellular fluorescent density of a random 20X microscopic field; in average, 3 – 4 spots were used from each mouse, scale = 50 μm) (B) Cellular immunofluorescent labeling showed more neurons had higher TRPV1 expression than the average signal density in sham irradiated mice. The proportion of TRPV1-upregulated neurons in mice with TBI was similar to sham irradiated mice. (C) - (E) The neurons count of CTCF (corrected total cellular fluorescent) in sham, TBI, and lingual 27 Gy-irradiated mice. (F) Western blot showed tongue-irradiated mice had significant increase of TRPV1 expression than other two controls. $*P < 0.05$, $**P < 0.01$, Mann-Whitney test; error bars depict SEM.

A

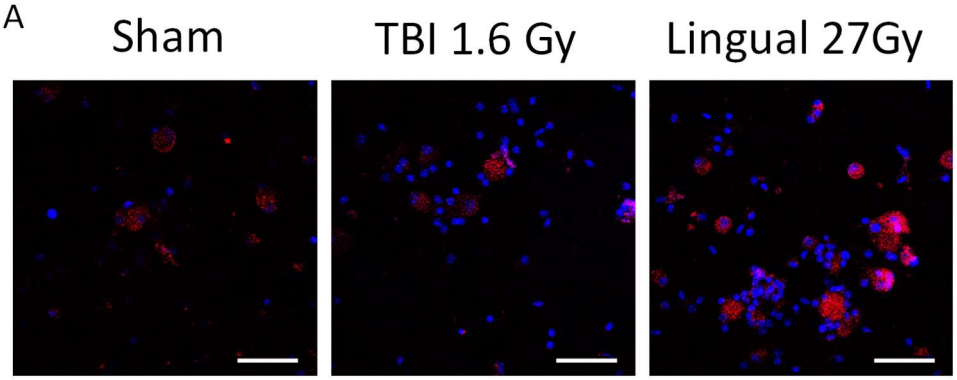

Scale: 50 µm

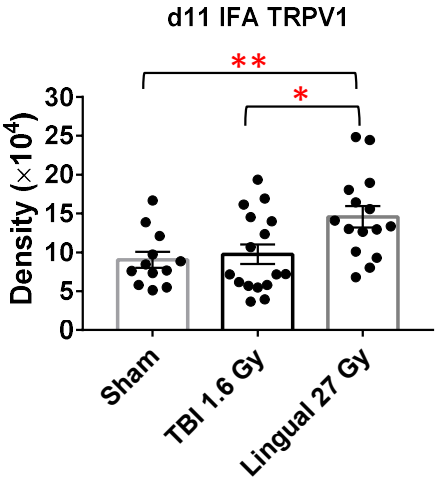

B

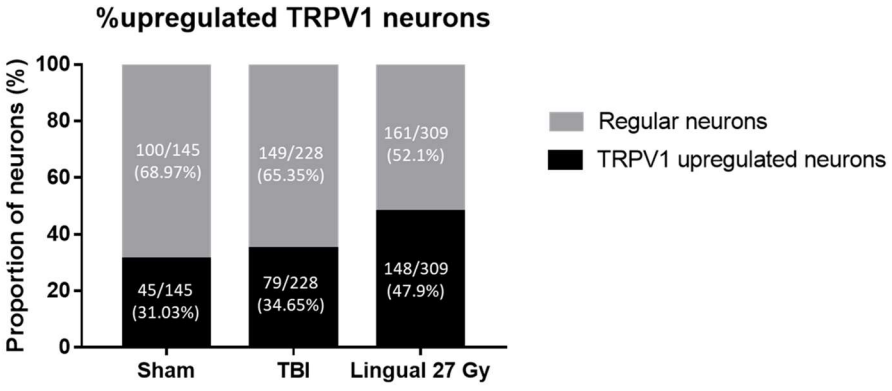

C

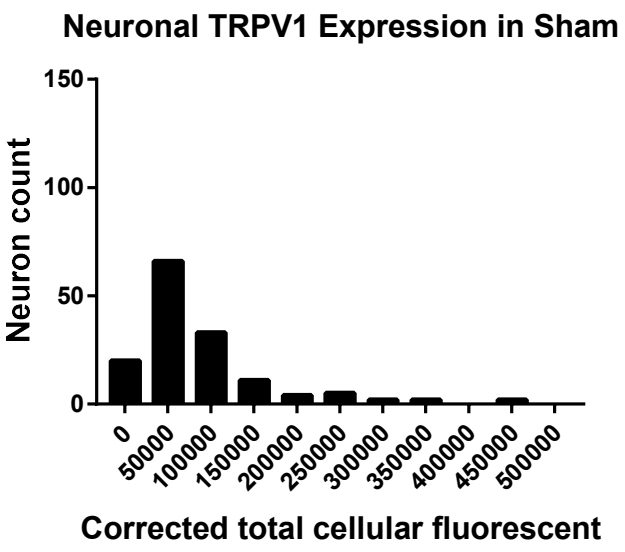
Neuronal TRPV1 Expression in Sham
Neuron count
150
100
50
0
0
50000
100000
150000
200000
250000
300000
350000
400000
450000
500000
Corrected total cellular fluorescent

D

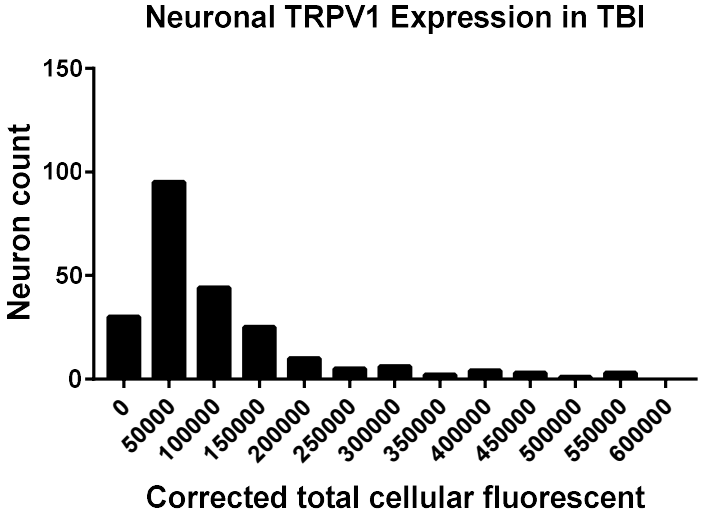
Neuronal TRPV1 Expression in TBI
Neuron count
150
100
50
0
0
50000
100000
150000
200000
250000
300000
350000
400000
450000
500000
550000
600000
Corrected total cellular fluorescent

E

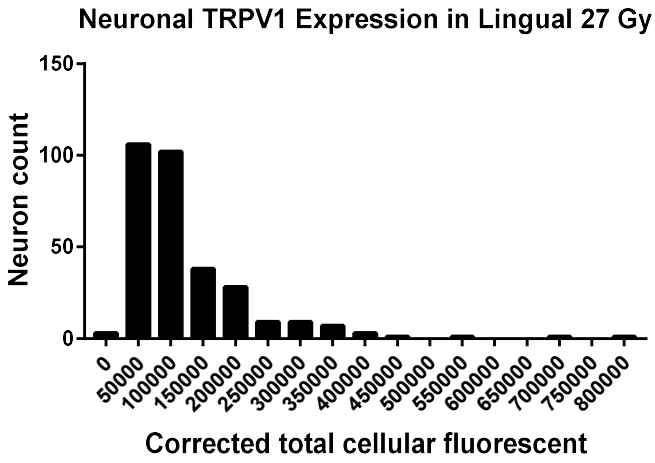
Neuronal TRPV1 Expression in Lingual 27 Gy
Neuron count
150
100
50
0
0
50000
100000
150000
200000
250000
300000
350000
400000
450000
500000
550000
600000
650000
700000
750000
800000
Corrected total cellular fluorescent

F

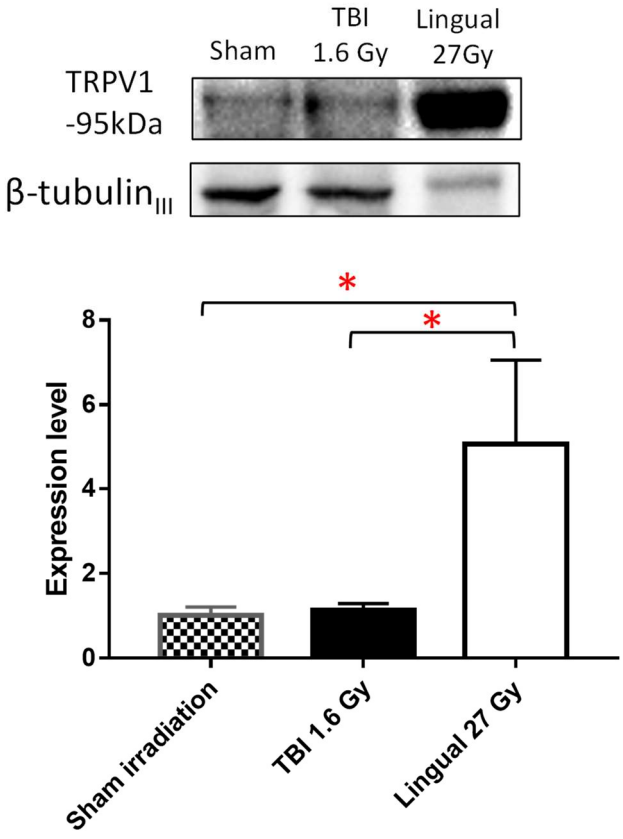
Sham
TBI
1.6 Gy
Lingual
27Gy
TRPV1
-95kDa
β-tubulin III
*
*
Expression level
8
6
4
2
0
Sham irradiation
TBI 1.6 Gy
Lingual 27 Gy

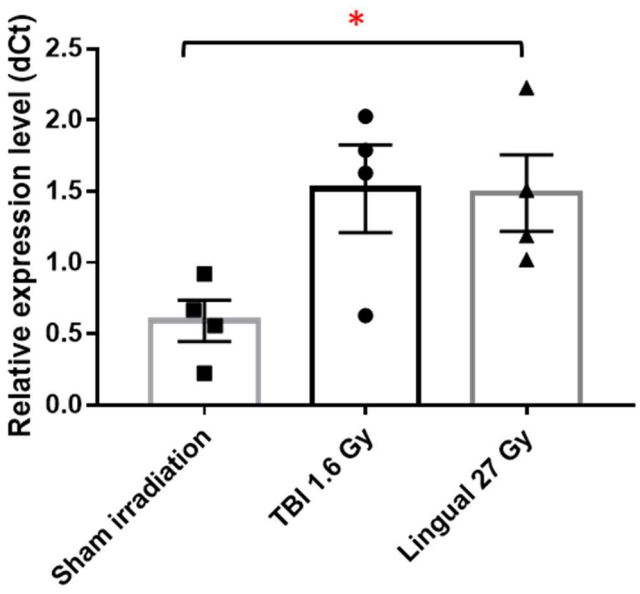

Figure 2.5 *Trpv1* gene expression of trigeminal ganglia in mice. *Trpv1* gene expression was significantly increased in mice had sever mucositis, but there was no significant difference between sham and TBI group. n = 4 per group; **P* < 0.05, Mann-Whitney test; error bars depict SEM.

CHAPTER 3: Upregulation of TRPV1 and TRPV4 may contribute to radiation-associated pain and itch

Introduction

In the most recent cancer statistics report, there are about 650,000 newly diagnosed head and neck cancer cases globally each year, and 65,000 in the United States [9,47]. Either radiation therapy or chemoradiotherapy is used to treat 55% of head and neck cancer (HNC) cases. Nearly one-hundred percent of the patient develop acute mucositis and/or dermatitis [23]. These radiation-induced acute injuries can be painful. A survey has shown that severe pain is reported by 80% of HNC patients at some time during radiation therapy [23]. Radiation-associated orofacial pain in HNC patients can result in unplanned interruption of treatment that may adversely affect the likelihood of tumor control [8]. Mucositis lesions typically heal within 2-4 weeks after the last dose of radiation therapy [31], but it has also reported that the radiation-associated pain (RAP) persists in approximately 60% of the patients three months after the locally visible mucositis has resolved [5].

Seventy percent of HNC patients with severe RAP are treated with opioids. Unfortunately, RAP seems to be relatively resistant to the analgesic effects of opioids [23]. Moreover, long-term use of opioid in this population of cancer patients is associated with adverse effects, such as sedation, hallucination, addiction, and gastrointestinal problems [37]. The limited efficacy of opioids, undesirable side effects, and lack of other effective analgesic options make it critical to identify new and better strategies to manage RAP. Having a mechanistic understanding of RAP could help guide therapeutic development. However, the mechanism of RAP is currently unknown.

Orofacial nociception is initiated in free endings of the afferent branches of the trigeminal

nerve; these free nerve endings are located in the skin and oral tissues. Impulses that begin in the periphery are transmitted to the cell bodies of the afferent nerves, located in the trigeminal ganglia. The impulses then move to second order neurons in the brainstem. The family of transient receptor potential (TRP) ion channels represents a set of pivotal membrane proteins; these channels regulate cations that influence the transmission of impulses in sensory neurons, and contribute to both hypersensitivity and pathological pain [36]. The vanilloid subfamily (TRPV) plays a role in sensation of heat, osmolarity changes, chemicals, and mechanical stimuli [39]. Because many acute radiation side effects (e.g., oral mucositis and dermatitis) are associated with burning painful sensations, we theorized that activation and/or upregulation of TRP family proteins in sensory neurons contributes to RAP.

The TRPV1 channel was first cloned, and its sensory properties were first identified in 1997 [12,16]. Since then, TRPV1 has become one of the most widely reviewed analgesic targets [50]. TRPV1 can be activated by stimuli such as capsaicin, acid (H^+), heat (> 43 °C), and certain bioactive lipids [43]. Capsaicin is a vanilloid compound present in chili peppers; capsaicin can induce sensations similar to that of thermal heat. By utilizing *Trpv1* gene knockout mice models, TRPV1 was shown to be highly associated with thermal hyperalgesia and chronic pain prior to, or during inflammatory responses [10,18]. Recently, Wang *et al*. revealed that in a rodent model, TRPV1 expression mediates the orofacial pain produced from mechanical irritation of orthodontic force and masseter muscle inflammation [58,59]; they found that blockade or knockout of TRPV1 significantly attenuated pain behaviors (i.e., reducing TRPV1 reduced mouse grimace scale scores and increased bite-force).

TRPV4 is another member of the TRPV subfamily that appears to be involved in orofacial pain. This ion channel is present in trigeminal ganglia neurons and appears to regulate

cation permeability, especially Ca^{2+}[14,40]. Studies have shown that various inflammatory and mechanical stimuli can sensitize TRPV4 in afferent sensory neurons; this sensitization induces nociception and hyperalgesia [1,3]. A murine study has revealed that TRPV4 plays an important role in temporomandibular joint orofacial pain and inflammation [14]. That study showed strong expression of TRPV4 in trigeminal ganglia during orofacial inflammation, and *Trpv4* gene knockout mice tended to display fewer nocifensive behaviors. TRPV4 also functions as a signal transducer in keratinocytes. After ultraviolet exposure on the skin, keratinocytes transmit signals to the primary sensory neurons that generate the sensations of itch and pain [7,13,15]. Chen *et al*. further revealed that histamine pruritogens can evoke Ca^{2+} influx into keratinocytes by activating TRPV4 channels [13]. However, this study did not investigate the sensitization status of TRPV4 in sensory neurons. In our previous work, trigeminal sensory neurons from mice with severe glossitis were sensitive to histamine, which indicated that TRPV4 channels may be activated [41].

The molecular biological mechanisms of pain associated with radiation-induced oral mucositis is unclear. Here, we utilize a rodent model to investigate trigeminal pain pathways after lingual irradiation. Since TRPV1 and TRPV4 have been shown to play critical roles in orofacial pain, we focus on the expression and functional changes of these two channels in both the trigeminal sensory neurons and the irradiated organs. To characterize the time course of biological changes that occur after irradiation, we also explore the expression of TRP channels at several time points.

Material and methods

Animals

All the mice were quarantined for at least 2 weeks prior to use. Eight- to ten-week-old female CD1 mice (Charles River Laboratories, Raleigh, NC) weighing 20-25 g at the beginning of the experiment were housed four per cage in climate-controlled rooms (temperature 21 ± 1 °C, humidity 55 ± 10%), and a 12:12 light/dark cycle. Standard rodent diet (LabDiet 5001, PMI, Brentwood, MO) and water were available *ad libitum* during the study. Mice with glossitis and pain lose weight quickly; to support their health, mice with weight loss ≥ 10% of their baseline were provided both gel diet (Nutra-Gel Diet, Bio-Serv, Flemington, NJ) and non-wetting water gel (HydroGel, ClearH2O, Westbrook, ME) on the floor of their cage [41]. Twice daily monitoring was performed if mice suffered 20% body weight loss or more. Mice with weight loss exceeding 30% of baseline were euthanized if the body weight loss failed to improve within 48 hours. Euthanasia was performed using flow metered carbon dioxide in a closed chamber. All work was approved by the Institutional Animal Care and Use Committee of NC State University (protocol No. 16-275).

Animal irradiations

Mice were randomly allocated to one of 3 treatment groups: (1) high-dose irradiation of the rostral tongue [hereafter referred to as "tongue-irradiated mice"]; (2) low-dose total body irradiation [to simulate the dose that is absorbed by the rest of the body during high-dose lingual irradiation; see Chapter 2 for additional details, mice who underwent low-dose total body irradiation hereafter referred to as "TBI mice"]; (3) sham irradiation. For each procedure, mice underwent general anesthesia with ketamine (100 mg/kg; Vedco, St. Louis, MO) and xylazine

(16 mg/kg; AnaSed, Lake Forest, IL) via intraperitoneal injection. All irradiations were performed using a clinical linear accelerator (Novalis TX; Varian Medical Systems, Palo Alto, CA) and 6 MV X-ray beams. For high-dose irradiation of the rostral tongue, individual animals were positioned in right lateral recumbency atop a purpose-designed Styrofoam assembly for experimental irradiation. The mouth was held open with pieces of suture that were looped around the maxillary and mandibular incisors. The tongue was gently retracted using a 1 mL serological pipet (Falcon, Franklin Lakes, NJ) connected to a medical vacuum in order to hold the rostral half of the tongue out of the mouth. The tongue was positioned atop a block of a dental putty (Sil-Tech Putty, Ivoclar Vivadent Inc., Amherst, NY) and underneath bolus material (1 cm thick sheet of solid, homogeneous, tissue-equivalent gel, CIVCO Medical Solutions, Coralville, IA). A single dose of 27 Gy was delivered to the rostral tongue at a dose rate of 1000 MU/min (3.07 minutes, 3068 MU). The treatment isocenter was located at the margin of the light field (half-beam block, generated using the primary jaws) and at the center of the tongue. The radiation field size was 4 x 4 cm (asymmetric). While the rostral half of the tongue was within the radiation field, the rest of the body was blocked by the primary collimator. In group 2, anesthetized mice were positioned in a plastic box and surrounded by bolus materials; 1.6 Gy was delivered to the entire body using equally weighted parallel-opposed beams with a dose rate of 60 MU/min (2.5 min, 150 MU). In group 3, mice were positioned just as they would be for high-dose lingual irradiation, but did not receive any radiation dose. Radiation dose verifications were performed using thermoluminescent dosimeters, as described in Chapter 2.

Body weight, glossitis severity scoring

Body weight and glossitis severity scores were determined daily, beginning before

irradiation (baseline) and continuing until day 25 post-irradiation. After that, the body weight and glossitis severity score were evaluated three times per week until day 45. The glossitis severity scoring criteria were modified from Radiation Therapy Oncology Group system as listed in (**Table 2.1** in **Chapter 2**) [41,55]. The scoring was performed by a single veterinarian (YHL) trained by a board-certified veterinary radiation oncologist (MN).

Orofacial mechanical stimulation test

To quantify orofacial radiation-associated pain, the orofacial mechanical stimulation test was performed in 27 Gy high-dose tongue-irradiated mice, using commercially available equipment (Orofacial Stimulation Test, Ugo Basile, Gemonio, Italy); 1.6 Gy low-dose total body irradiated mice served as the controls. Due to the time-consuming nature of this spontaneous pain test, and limited access to the testing device, we were not able to perform this test in sham irradiated mice. For detailed materials, methods and results, see **Supplemental Figure 3.1** in **Appendix B**.

Endpoints

Based on published data [41], grade 1 glossitis developed starting from day 7-8 after high-dose tongue irradiation; the most severe glossitis developed on day 10-12 and was fully recovered on day 17 post-irradiation. To characterize the time course of the trigeminal ganglia neurons' biological change after lingual irradiation, mice in each group were euthanized on day 1, 5, 11, 21, and 45. Trigeminal ganglia and lingual tissues were collected for further investigation (i.e. calcium imaging, qPCR, Western blot, and cellular immunofluorescent).

Calcium imaging

Trigeminal ganglia were isolated immediately after euthanasia and digested in collagenase (Sigma-Aldrich, St. Louis, MO) and dispase (Sigma-Aldrich, St. Louis, MO) in Hanks' Balanced Salt Solution (HBSS, Grand Island, NY) at 37 °C as described previously [41]. Briefly, isolated cells were resuspended in 25 µL Dulbecco's Modified Eagle Medium (DMEM, Gibco, Paisley, UK), placed onto an 18 mm coverslip coated with poly-L-lysine and laminin. Neurons were further incubated in 1 mL complete media that contained DMEM medium with 10% fetal bovine serum (FBS, heat inactivated, Gibco, Grand Island, NY) and 2% Pen Strep (Gibco, Grand Island, NY) at 37 °C with 5% CO_2.

All calcium imaging was performed 12-24 hours after plating the neurons. Neurons were incubated with Fura-2AM (Biotium, Fremont, CA) in complete media for 30 min before imaging. The coverslip was held by a Quick Release Magnetic Imaging Chamber (Warner Instruments, Hamden, CT) and cells were visualized using an inverted microscope (Eclipse TE2000, Nikon, Melville, NY). Warm (37°C) Locke solution flowed through the chamber continuously and perfused the coverslip during the imaging. Fura-2AM is a calcium indicator that undergoes conformal change when it binds calcium ions. Cytosolic free Ca^{2+} can be assessed by alternating the two channel wavelengths because Fura-2AM and its Ca^{2+} bound complex have their excitation peaks at different wavelengths (380 nm and 340 nm, respectively). The excitation wavelength alternated every 100 ms between 380 nm and 340 nm to acquire the fluorescent intensity of Ca^{2+} free Fura-2 AM and Ca^{2+} bound Fura-2 AM. The ratiometric measurement of fluorescent intensity at 340 and 380 nm wavelength (340/380 nm) therefore indicated intracellular Ca^{2+} concentration. The peak of the 340/380 nm ratio indicates the maximum intracellular Ca^{2+} concentration. Trigeminal ganglia (TG) neurons were manually circled –

identification was based on morphology and size (diameter of 10 - 20 μm). Neurons were stimulated by the order of histamine (1 mmol/L, Sigma-Aldrich, St. Louis, MO), TNF-α (1 μmol/L, Pepro Tech, Inc., Rockey Hill, NJ), capsaicin (1 μmol/L, Sigma-Aldrich, St. Louis, MO), and KCl (150 mmol/L, Fisher Scientific, Fair Lawn, NJ), with at least 1 minute between stimulations. Only cells that responded to KCl were included in the analysis. A positive response was defined as a neuron that had a maximum 340/380 nm ratio greater than 110% of the baseline (pre-stimulation) 340/380 nm ratio, and other neurons were defined as unresponsive (negative). The proportion of neurons that had positive response to certain stimuli was calculated and compared by Fisher exact test.

Cellular immunofluorescence staining

After calcium imaging, neurons on the coverslips were immediately fixed using 4% neutral buffered formalin (for 5 minutes), then washed with phosphate-buffered saline (PBS). The coverslips were incubated in blocking solution (5% goat serum and 0.05% Triton-X 100 in PBS) for 1 hour at room temperature. TRPV1 (mouse anti-mouse, 1:1000; Abcam, Cambridge, MA) and TRPV4 (rabbit anti-mouse, 1:2000; Alomone Labs, Jerusalem, Israel) expression was detected by applying primary antibody at 4 °C overnight. The coverslips were washed with PBS three times followed by incubation with secondary antibody (Alexaflour 594 conjugated goat anti-mouse, 1:1000, for TRPV1; FITC conjugated goat anti-rabbit, 1:1000, for TRPV4; Invitrogen, Eugene, Oregon) for one hour at room temperature. The coverslips were then washed with PBS and mounted using ProLong Gold antifade reagent with DAPI (Invitrogen, Eugene, Oregon) overnight at room temperature. Images were acquired by confocal microscopy (Olympus FV1000, Center Valley, PA) and the neurons were manually contoured by ImageJ

software (US National Institutes of Health, Bethesda, MD) to measure the area, mean fluorescence and adjacent background. The corrected total cell fluorescence (CTCF) of individual neurons was calculated by the equation: integrated density – (area of selected cell × mean fluorescence of background readings). To discriminate protein from gene expression results, the protein expression was written in all capital letters (e.g., TRPV1); murine gene names were written in italic with capital letter at first character (e.g., *Trpv1*).

Histology

Lingual tissues from four 27 Gy tongue-irradiated mice were excised for histologic examination on day 11 and 21 post-irradiation. The tongue samples were fixed in 10% neutral buffered formalin solution. Paraffin-embedded tissue sections were sectioned in the sagittal plan at 2 μm and stained with hematoxylin-eosin (H&E). The histopathologic change of glossitis was qualitatively evaluated and quantitatively graded according to the published grading criteria for oral mucositis in a murine model (**Table 3.1**) [52].

Quantitative real-time PCR

Lingual and TG tissues were homogenized (Multi-Gen 7XL probes; PRO Scientific Inc., Oxford, CT). Total RNA was isolated using the RNAeasy Mini Kit (Qiagen, Hilden, Germany) as described in the instruction manual. Total RNA (1 μg) was reverse transcribed to cDNA using the SuperScript III synthesis kit (Thermo Fisher Scientific, Carlsbad, CA). The synthesized cDNA was mixed with TaqMan Gene Expression Master Mix (Applied Biosystem, Austin, TX) and gene expression was detected by quantitative real-time PCR (Applied Biosystem, Austin, TX) with TaqMan probes (Thermo Fisher Scientific, Pleasanton, CA), listed in (**Table 3.2**). The

rationale for targeting those genes is as follows: TRPV1, -V2, -V4, -A1 and -M8 are expressed in afferent sensory neurons, and have been associated with pain sensitization [32]. TRPV1, -V2, and -V4 are the most well-characterized TRP channels in terms of their involvement in heat and pain [14,21,27,54]. TRPA1 channel is in another subfamily that contains a large number of ankyrin repeats in the structure. In mammalian animals, TRPA1 is the only member of this subfamily that is activated by noxious cold (17 °C) [51]. The function of TRPV1 and TRPA1 channel can be upregulated and/or enhanced by artemin, resulting in sensitization of the nociceptive afferent [19,34]. Artemin is a neurotrophic factor that contributes to acute inflammatory hypersensitivity through binding to the receptor GFRα3 [53]. Therefore, upregulation or activation of TRPV1 may be correlated to increased activity of artemin-GFRα3 interaction. There is another TRP channel that responds to cold stimuli, TRPM8. TRPM8 is in the TRPM subfamily and is activated by noxious cold stimuli such as menthol, icilin and cool temperatures (< 30 °C in neurons) [42]. Mas-related G-protein coupled receptor D (MrgprD) has been implicated in initiating mechanical hypersensitivity and cold allodynia [57,61]. A recent study also showed the upstream role of MrgprD in activating TRPA1 in sensory neurons [57]. The expression level was determined by the Ct threshold value and the relative expression was calculated by the ΔCt method, with GAPDH as the housekeeping gene.

Western blot

The proteins from snap-frozen lingual and TG tissues were immersed in CHAPS lysis buffer and homogenized (Multi-Gen 7XL probes, PRO Scientific Inc., Oxford, CT). Protease and phosphatase inhibitor cocktail (EDTA-free, Thermo Scientific, Rockford, IL) was added into the solution prior to protein extraction. Total protein lysate concentration was determined by BCA

(Thermo Scientific, Rockford, IL) as instructed in the manual. The protein lysates were heated in Laemmili sample buffer (Bio-Rad, Hercules, CA) with 5% β-mercaptoethanol. Mouse cerebellum lysates served as positive control (for both TRPV1 and TRPV4); negative control (sample buffer without protein sample) was also loaded. Proteins were separated in 10% polyacrylamide gel during electrophoresis (200V) and transferred to PVDF membranes by Trans-blot Turbo (7 min/25V; Bio-Rad). Membranes were blocked with 5% bovine serum albumin in TBST buffer. Protein expression was detected by monoclonal TRPV1 (C-terminal, mouse anti-TRPV1, 1:2000; Abcam, Cambridge, MA) or polyclonal TRPV4 (rabbit anti-TRPV4, 1:2000; Alomone Labs, Jerusalem, Israel) primary antibody in 5% BSA in TBST buffer at 4°C overnight. Secondary antibody incubation was made by peroxidase-conjugated goat anti-mouse (1:5000, for TRPV1; Abcam, Cambridge, MA) or goat anti-rabbit (1:5000, for TRPV4; Jackson ImmunoResearch) at room temperature for 1 hour. Housekeeping protein β-tubulin$_{III}$ (rabbit-anti mouse, 1:10000; Abcam, Cambridge, MA) served as the loading control. Signals on the membranes were visualized by ChemiDoc MP (Bio-Rad, Hercules, CA) imaging system after adding chemoluminescence substrate (Pierce ECL, Thermo Scientific, Rockford, IL). The optical density was analyzed by Image Lab software 6.1 (Bio-Rad, Hercules, CA).

Statistics

All data are expressed as mean ± SD, unless otherwise noted in the figures. Statistical significance of differences between groups was determined with a threshold of *P* value at 0.05. Unpaired two-tailed student t-test was carried out for the comparison between two treatment groups. Of the assays that were not normally distributed, the statistical significance was defined by nonparametric Mann-Whitney test. For multiple comparisons, two-way ANOVA was carried

out followed by Tukey post hoc test. The proportion comparisons were made by Fisher exact test. Statistical analysis was performed with the software Prism 7 (GraphPad Software, San Diego, CA).

Results

Body weight and glossitis severity

Glossitis severity scores in lingual 27Gy irradiated group showed that glossitis starting from day 7-8 and fully recovered at day 17 (Figure 3.1 A), in agreement with previous work [41]. The histopathology of the lingual tissue at day 11 showed ulceration (complete loss of epithelial and keratinized cell layers), leukocytic infiltration and edema at the dermis layer on the rostral tongue. According to the grading system (**Table 3.1**), all mice on day 11 had grade 4 histopathological mucositis. On day 21, the rostral tongue had grade 0 histopathological mucositis -- the epithelial layer was repopulated and thickened, and the basal layer was intact (**Figure 3.1 A**). In 27 Gy tongue-irradiated mice, the body weight was significantly decreased in conjunction with glossitis. Controls (sham or TBI) and lingual irradiation groups differed significantly from day 10. The body weight of mice with glossitis was back to baseline at day 16. On days 20, 21, 24, and 35-39, the body weight of mice that had 27 Gy lingual irradiation was still significantly lower than sham irradiated mice. Additionally, the average body weight gain in mice with 1.6 Gy irradiation was slower than sham irradiated mice starting from day 19 (**Figure 3.1 B**) and the body weight was significantly lower from day 35 to 39 ($P = 0.0008 – 0.0021$). Significant differences in body weight between TBI and mice with RIM were only present on days 10-14; thereafter, the body weight growth pattern was similar in these two groups. Orofacial stimulation behavioral test was performed to evaluate acute radiation-associated pain in 27 Gy

tongue-irradiated mice. Interestingly, mice with severe glossitis more frequently inserted their snout into the window with metal wires; for additional detailed results, see **Supplemental Figure 3.1** in **Appendix B**).

Calcium imaging

TGs were harvested on days 1, 5, 11, 21, and 45 post-irradiation to evaluate the responsiveness of sensory neurons via calcium imaging. Lingual irradiation induced significant increases in the proportion of trigeminal neurons that were sensitive to capsaicin from day 1 to 21 (Figure 3.2 A). In sham-irradiated animals, 21.65 ± 8.3% (mean of five time points) of neurons responded to capsaicin; by comparison, higher proportions of neurons were capsaicin-responsive in the high-dose tongue-irradiated mice: 34.26 ± 5.98%, 37.65 ± 4.27%, 44.43 ± 4.11%, and 34.34 ± 4.66% on days 1, 5, 11 and 21 respectively, with the maximum response at day 11. On day 45 post-irradiation, the proportion of neurons responsive to capsaicin were comparable in sham and lingual 27 Gy irradiated groups (28.06 ± 18.11% vs. 29.05 ± 5.13%). Calcium imaging showed no difference between TBI and sham in capsaicin response from day 1-21 (P = 0.38 - 0.8) and on day 45.

The proportion of neurons responsive to histamine was increased in mice after high-dose lingual irradiation (**Figure 3.2 B**). There was a statistically significant increase on day 1 (19.6 ± 3.03%), day 11 (29.21 ± 9.6%), and day 21 (16.52 ± 1.98%), compared to the averaged proportion of responsive neurons in the sham irradiated group of 12.8 ± 4.23%. Although we did not see the statistical difference between lingual irradiated and sham group on day 5 and day 45 (P = 0.58 and 0.83, respectively), the average proportion of histamine-responsive neurons in lingual irradiated mice was higher than sham irradiated mice. In the 1.6 Gy TBI control group,

we saw an increased proportion of responsive neurons at day 11 (18.09 ± 9.8%, $P = 0.66$) and a significantly increased proportion at day 21 (19.76 ± 13.11%, $P = 0.0063$) compared to the sham group. The proportion of responsive neurons from the high-dose tongue-irradiated mice was 11.38 ± 0.1% on day 45.

The pattern of the neuronal response to TNF-α was similar to histamine (**Figure 3.2 C**). Mice that had high-dose lingual irradiation had a significantly increased proportion of neurons that responded to TNF-α at day 1 (19.5 ± 7.86%), 11 (24.03 ± 4.9%) and 21 (17.51 ± 5.14%) than the averaged proportion in the sham group (10.9 ± 4.9%). Interestingly, the neuronal response to TNF-a in the TBI group was significantly lower at day 1 (10.6 ± 3.19% versus 14.79 ± 7.01% in sham group mice) but the proportion was significantly increased (16.47 ± 4.08%) than the sham group at day 21.

We further evaluated the characteristics of neuronal responsiveness to different stimuli (**Figure 3.3**). Among imaged neurons, a higher proportion of neurons was sensitive to all 3 stimuli (11% vs. 3.4%, lingual irradiated vs. sham) at the time of maximally severe glossitis (day 11), demonstrating increased activation via the TRPV1 channel, histamine (or TRPV4 channel), and TNF-α receptors. A higher proportion of the histamine- or TNF-alpha-responsive neurons were also sensitive to capsaicin on days 11 (11%, versus 3.4% in controls). Neurons that were responsive to either histamine, TNF-alpha, or capsaicin (termed the "responsive neurons") comprised 47%, 41%, 55%, 40%, and 39% at five endpoints from day 1 to day 45 in lingual irradiated mice, but in sham group, only 30 ± 4.5% of neurons were responsive neurons to one or more stimuli. A higher proportion of responsive neurons in RAP mice were activated by all three stimuli. From day 11 to day 45, the proportion of trigeminal ganglia neurons that responded to all three stimuli was 20% in mice that had undergone lingual irradiation, versus only 10.7% in

control animals. In mice with TBI, the proportion of responsive neurons were similar to sham irradiated mice (**Supplemental Figure 3.2**).

TRP expression in trigeminal ganglia

TRPV1 was significantly upregulated at day 11 and day 21 in Western blot (5- and 2.8-fold increase, respectively, both $P = 0.0286$) (**Figure 3.4**). To describe the neuronal expression pattern, immunofluorescent staining was performed on sensory neurons at day 11 and day 21 (**Figure 3.5 A**). The evaluated neurons showed the significantly increased TRPV1 expression at both time points (**Figure 3.5 B**) and there was immunoreactivity in both cytoplasm and cell membranes (**Figure 3.5 C**). The size distribution of the TG neurons that expressed TRPV1 from mice with RAP was similar to the sham irradiated group (**Figure 3.5 D**); there are 76% and 67% of the neurons had the size between 200 to 400 μm^2 from lingual-irradiated mice and sham-irradiated mice, respectively.

The gene expression of *Trpv1* in TGs had approximately 2.5-fold increase at day 11 and 21 post-irradiation in lingual 27 Gy irradiated mice comparing to sham-irradiated mice (both $P = 0.0286$, **Figure 3.6**), which supported the results of Western blotting and immunofluorescent staining.

We did not see a statistically significant difference of TRPV4 expression in trigeminal ganglia between lingual- and sham-irradiated group via Western blot (**Figure 3.7 A**) or immunofluorescent staining (**Figure 3.7 B and C**). However, compared to day 11, the trigeminal ganglia expression of TRPV4 in the lingual-irradiated group was slightly higher at day 21 ($P = 0.1$). The transcripts of the *Trpv4* gene in TGs were much lower than *Trpv1* (**Figure 3.6** and **Figure 3.8**). The mean Ct value of *Trpv4* in sham irradiated mice was 11.60 compared to *Trpv1*

of 7.57, which indicated the expression level of *Trpv4* in TGs was 16 (or 2^4) times less than that of *Trpv1*. Significant statistical difference was not detected in qPCR at those five endpoints, but the expression of *Trpv4* was 2.8-fold higher than the sham irradiated group at d11 post-irradiation when comparing to sham-irradiated mice ($P = 0.1$).

To evaluate the possible impact of scattering dose in this rodent RIM model, we used 1.6 Gy for total body irradiation. We did not detect a statistically significant increase of either TRPV1 or TRPV4 gene/protein expression in mice with TBI 1.6 Gy, but we saw a slightly higher of *Trpv1* expression on day 11 ($P = 0.1$) (**Figure 3.9**). The expression of the *Trpv4* gene in TG was low in mice had TBI 1.6 Gy but comparing to the sham-irradiated mice, the expression was slightly higher at day 11 ($P = 0.1$).

Quantitative PCR was performed to evaluate other thermal or mechanical pain-associated genes (**Figure 3.10**). The trigeminal ganglia harvested from mice with glossitis showed significantly upregulated *Trpa1* (3-fold increase, $P = 0.0286$), *Trpm8* (4-fold increase, $P = 0.0286$), and *GFRα3* (2-fold increase, $P = 0.0286$) at day 11 post-irradiation. On day 21, the expression of *Trmp8* and *GFRα3* were persistently higher in high-dose tongue-irradiated mice than the sham group (both $P = 0.0286$). The average expression of *Trpa1* was still higher than sham-irradiated mice but the difference was not statistically significant ($P = 0.0571$). Although *Trpv2* and *Mrgprd* were not significantly increased in mice with lingual-irradiation at day 11 or 21, the transcripts level in TGs were still higher than sham irradiated mice.

Of all the genes we investigated (i.e., *Trpv1*, *Trpv2*, *Trpv4*, *Trpa1*, *Trpm8*, *Gfra3*, and *Mrgprd*), the expression did not show a statistically significant increase at day 1 and day 5 post-irradiation, but the increasing expression trend until day 11 or 21 post-irradiation was presented (**Supplemental Figure 3.3**).

We evaluated the possible effect of scattering irradiation on pain-related genes other than *Trpv1* and *Trpv4*. There was no statistical difference between sham irradiation and TBI 1.6 Gy at all time points (For additional details on the results of TBI 1.6 Gy, see **Supplemental Figure 3.4 and 3.5** in **Appendix B**). However, scattered irradiation may subtly increase the gene expression in the central nerve system, especially Trp family genes (i.e. *Trpv2*, *Trpa1*, and *Trpm8*).

To the last time point at day 45 post-irradiation, we compared the gene expression of TGs in sham, TBI 1.6 Gy and mice with lingual 27Gy irradiation group. Although we did not see the statistical difference between the treatment, one of three mice experienced RIM had persistent 2-3 folds higher *Trpm8*, *Gfrα3*, and *Mrgprd* gene expression, and one of the mice had 2-fold increased *Mrgprd* expression (**Supplemental Figure 3.5**).

Molecular expression pattern at irradiated target (lingual tissue)

We collected the irradiated lingual tissue to investigate the TRP gene/protein change over time. The TRPV1 expression difference between sham and lingual-irradiated mice did not reach statistical significance at all times (**Figures 3.11**). However, compared to sham irradiated mice, tongue-irradiated mice had an average of 3.2- and 8-fold increase of TRPV1 expression in Western blot ($P = 0.3429$) and *Trpv1* expression in qPCR ($P = 0.0571$) at day 11 post-irradiation, respectively. The TRPV4 protein expression was gradually increased and had a 2.5-fold increase at day 11 ($P = 0.0286$, **Figure 3.12A**). In agreement with Western blotting, expression of the *Trpv4* gene was 6.8-times upregulated ($P = 0.0286$, **Figure 3.12B**) on day 11 post-irradiation, compared to sham-irradiated mice, but did not significantly change at other endpoints.

In lingual tissue with acute radiation injuries, the expression of *Trpv2* had a 10-fold increase ($P = 0.0286$) at day 11 post-irradiation (**Figure 3.13 A**). The transcripts of *Trpa1* was

trace and undetectable in the lingual tissues (8/16, 50%) of sham irradiated mice. However, after the lingual irradiation, *Trpa1* was increased and detectable in 17/19 (90%) of the samples. Although the statistical significances were not detected, the mRNA level of *Trpa1* in tongue-irradiated mice had 2.4-, 1.6-, and 1.9-fold higher than sham-irradiated group at day 11 (P = 0.2571), 21 (P = 0.3143), and 45 (P = 0.4) post-irradiation, respectively (**Figure 3.13 B**). The expression of *Trpm8*, *GFRα3*, and *Mrgprd* was not statistically significantly increased, but the expression level at day 11 had 3-, 2.4, and 2.4-fold increase in tongue-irradiated mice than sham-irradiated mice (**Figure 3.13 C-E**).

Low dose scattering did not impact the expression of pain-associated gene expression in lingual tissues. The expressions of TRPV1 and TRPV4 were not statistically changed over the time, either (For additional details on the results of TBI 1.6 Gy, see **Supplemental Figure 3.6 and 3.7** in **Appendix B**).

Discussion

This is the first study to have explored the role of TRP ion channels, particularly TRPV1 and TRPV4, in the setting of acute and severe orofacial pain induced by ionizing irradiation. We have now demonstrated that changes in TRPV1 and TRPV4 expression and functional activation in sensory neurons starts very soon after irradiation and lasts long after clinically evident pain and glossitis have resolved. The expression of a wide range of pain-related, thermal sensitive TRP channel genes (*Trpv2*, *Trpa1*, *Trpm8*, and *Gfra3*) are enhanced by radiation, with the most dramatic changes coincident with maximally severe glossitis.

Glossitis severity scoring and body weight monitoring showed that high-dose (27 Gy) lingual irradiation-induced clinically observed acute glossitis began on day 7 post-irradiation,

and weight loss started on day 8. These observations are in agreement with a previously published study, which reported epithelial breakdown and inflammatory infiltration approximately 1 week after tongue irradiation [49]. In our study, we saw that a significantly higher proportion of trigeminal neurons were activated to painful mediators (i.e., the agonists of TRPV1, TRPV4, and TNF-α) prior to the appearance of grossly visible glossitis. Although tongue tissues from days 1 and 5 were not available for histopatologic evaluation, with a high-dose such as 27 Gy, radiation-induced cell damage or death (that may affect peripheral neurons) can happen within 3-8 hours [26,38]; intracellular materials such as K^+, H^+, glutamate, cytosol ATP, neurotrophins, and bradykinin that are released during cell damage have been shown to induce neuronal hypersensitization [4,6,17].

Radiation-induced DNA damage can also trigger the transcription of specific mRNAs in neurons (e.g., TNF-α) and also alter the function of neurons [28,60]. DNA damage can activate transcription factors such as nuclear factor-κB (NF-κB) and promote cytokine production including TNF-α as well as TNF-α receptors gene expression [48]. Although we did not investigate TNF-α expression in this study, we observed that a high proportion of trigeminal neurons from 27 Gy tongue-irradiated mice were sensitive to TNF-α.

Trigeminal neurons from high-dose tongue-irradiated mice had functional activation of TRPV1 that was accompanied by TRPV1 upregulation. The increased trend of TRPV1 expression started from day 1 and was significantly higher than sham-irradiated mice when glossitis was most severe. The overexpression of TRPV1 persisted even after the glossitis was resolved, which indicated a possible mechanism by which patients experience pain even after cancer has been cured and mucositis has resolved; a longitudinal study has shown that there are approximately 65% of cancer patients who received radiation therapy still feel painful 6 months

after the first treatment, and another study showed the pain could last for 20 years, with a median of 1.5 years [5,25].

The high proportion of neurons that responded to histamine suggests that TRPV4 channels may contribute to radiation-associated pain and inflammation [44]. Furthermore, Chen *et al.*, have shown that the *Trpv4* gene and the TRPV4 channel in epidermal keratinocytes are necessary for scratching behavior [13], which has previously been observed in mice with RIM [41]. Upregulation of TRPV4 in trigeminal sensory neurons has been shown to be associated with orofacial pain in temporomandibular disorders [14]. We did not detect a statistically significant increase of *Trpv4*/TRPV4 expression in TGs from high-dose tongue-irradiated mice; however, via mRNA quantification, out study demonstrates an increase of *Trpv4* in lingual tissue at day 11 post-tongue irradiation when compared to sham-irradiated mice. Furthermore, increased protein expression of TRPV4 was observed at day 21. This discrepancy of *Trpv4*/TRPV4 expression level has also been described in a database of normal tissues [56]; the database showed that *Trpv4* transcripts are scarce in the central nervous system (CNS), but they are abundant in kidney and urinary bladder; However, at the level of protein expression, TRPV4 is abundant in CNS and muscle tissues. The reason for the discrepancy is unclear since the post-transcriptional regulation of TRPV4 is largely unknown [56]. Nevertheless, together with the higher TRPV4 expression in TG and irradiated region, our results suggest that upregulation of TRPV4 may contribute to radiation-associated pain and inflammation.

In addition to the aforementioned changes in *Trpv1* and *Trpv4* expression, we also found that *Trpv2* was upregulated in mice with high-dose lingual-irradiation. TRPV2 is activated by a higher threshold temperature at ~ 52^{o}C (versus TRPV1 at 43^{o}C) [11], and both TRPV2 and TRPV4 are required for mechanical nociception [2,30]. The gene overexpression of *Trpv1*, *Trpv2*

and *Trpv4* indicated mice had RAP may be sensitive to heat and mechanical stimulation. Moreover, our exploration of pain-related TRP gene revealed that the upregulated thermal sensitive receptors also involved cold (i.e. *Trpm8* and *Trpa1*) receptors in tongue-irradiated mice. The cold sensitization of TRPA1 and TRPM8 is associated with artemin. The binding of artemin to its receptor, GFR-α3, enhances TRPM8-dependent cold sensitization and upregulates TRPA1 [19,33,34]. Our observation of upregulated *Trpa1*, *Trpm8*, and *Gfra3*, suggests that the tongue-irradiated mice may be sensitive to cold stimulation. Together with TRPA1, the overexpression of artemin has been shown to upregulate TRPV1 [22]. With the blockade of the artemin-TRP pathway, we may be able to mitigate RAP.

In addition to using sham-irradiated mice as a control, to rule out the possible physiological effect of scattering dose in this rodent model, we also used TBI 1.6 Gy as another control. Compared to sham irradiated mice, the weight growth curve in this group showed reduced body weight gain starting from day 19 until day 39, suggested that the medium-term (i.e., 2 weeks to one-month post-irradiation) observation of behavior may be altered by the scattering dose in this model due to physiological change. However, this difference may be negligible for a longer investigation (i.e., 1.5 months). The low-dose radiation can induced or inhibit various cytokines and molecules that affect the balance between inflammation and healing [46]; a low dose (2 Gy) radiation on inflamed lesion has been shown to reduce TNF-α production in the first 24-48 hours; however, TNF-α production started to increase again, 72 hours after the irradiation [45]. Here, we did not measure the serum TNF-α level in mice with RIM, but we did observe a similar trend in fluctuating neuronal sensitivity in the calcium imaging studies -- a reduced proportion of neurons were sensitive to TNF-α after the total body 1.6 Gy irradiation in the first 24 hours, but an increased proportion of neurons was sensitive to

TNF-α on day 21. The delayed sensitization that we observed may be due to the site (CNS) and/or the cell type (neurons). The reduced neuron sensitivity to TNF-α from TBI 1.6 Gy mice on day 1 may also suggest that low-dose irradiation could reduce pain that associated with reduced neuronal sensitivity toward TNF-α.

In our study, we described significant changes in TRPV1 and TRPV4 expression and function that suggest a role for these ion channels in RAP, but the limited sample numbers used herein resulted in relatively low statistical power in the molecular assays. Nonetheless, we still saw a trend of increased expression level of TRPV1 in irradiated lingual tissues over time. We also saw upregulated TRPV4 in lingual tissues; immunofluorescent staining of the lingual tissues should be reviewed to identify the expression pattern on peripheral afferents. Ideally, the evaluations of pain-related receptors should be supported investigations of pain behavior. A previous study has shown pain behaviors in mice with RIM that could support the molecular findings presented here [41]. Furthermore, we have performed limited spontaneous pain testing (i.e., orofacial stimulation test) that demonstrate abnormal behavior in mice had severe glossitis (See **supplemental Figure 3.1** in **Appendix B**). Further optimization of that assay is needed, to ensure that it robustly reports on orofacial pain. In the future, using *Trpv1/4*-gene knockout mice, miRNA to reduce TRPV1/4 expression, or the TRPV1/4 antagonist may allow us to confirm the blockade of TRPV1/4 pathway can reduce pain behavior induced by radiation injuries.

The strategy of blocking TRPV1/4 to reduce RAP is expected to help human patients, and may also benefit veterinary patients. Pet owners pursue radiation therapy as part of the treatment program when their pets have unresectable oral or nasal cancers [20,24]. Acute side effects are dose-dependent; and even when using highly conformal irradiation techniques such as intensity-modulated radiation therapy (IMRT) and stereotactic body radiation therapy (SBRT) to treat

canine nasal tumors, radiation induced-dermatitis (25-26%) and oral mucositis (16.7-30%) remain problematic [29,35].

In conclusion, our study indicates that sensitization and upregulation of TRPV1 in trigeminal ganglia and TRPV4 in irradiated tongue are associated with orofacial pain induced by irradiation. The sensitization of neurons began before the RIM was clinically evident, and continued even after the lesions had visually healed. Other TRP-related genes were also upregulated in mice with RIM. Together, our results indicate that the TRP channels may be promising targets for relief RAP. The blockade of TRP channels should be further investigated to confirm their roles in orofacial RAP signaling.

REFERENCES

[1] Alessandri-HaberN. A Transient Receptor Potential Vanilloid 4-Dependent Mechanism of Hyperalgesia Is Engaged by Concerted Action of Inflammatory Mediators. J Neurosci 2006.

[2] Alessandri-HaberN. Transient Receptor Potential Vanilloid 4 Is Essential in Chemotherapy-Induced Neuropathic Pain in the Rat. J Neurosci 2004.

[3] Alessandri-HaberN, DinaOA, JosephEK, ReichlingDB, LevineJD. Interaction of Transient Receptor Potential Vanilloid 4, Integrin, and Src Tyrosine Kinase in Mechanical Hyperalgesia. J Neurosci 2008.

[4] AmayaF, IzumiY, MatsudaM, SasakiM. Tissue Injury and Related Mediators of Pain Exacerbation. Curr Neuropharmacol 2013.

[5] AstrupGL, RustøenT, MiaskowskiC, PaulSM, BjordalK. Changes in and predictors of pain characteristics in patients with head and neck cancer undergoing radiotherapy. Pain 2015.

[6] BasbaumAI, BautistaDM, ScherrerG, JuliusD. Cellular and Molecular Mechanisms of Pain Introduction: Acute Versus Persistent Pain. 2009:1–22. doi:10.1016/j.cell.2009.09.028.

[7] BautistaDM, WilsonSR, HoonMA. Why we scratch an itch: The molecules, cells and circuits of itch. Nat Neurosci 2014.

[8] BeseNS, HendryJ, JeremicB. Effects of Prolongation of Overall Treatment Time Due To Unplanned Interruptions During Radiotherapy of Different Tumor Sites and Practical Methods for Compensation. Int J Radiat Oncol Biol Phys 2007.

[9] BrayF, FerlayJ, SoerjomataramI, SiegelRL, TorreLA, JemalA. Global cancer statistics 2018: GLOBOCAN estimates of incidence and mortality worldwide for 36 cancers in 185 countries. CA Cancer J Clin 2018.

[10] CaterinaMJ, LefflerA, MalmbergAB, MartinWJ, TraftonJ, Petersen-ZeitzKR, KoltzenburgM, BasbaumAI, JuliusD. Impaired nociception and pain sensation in mice lacking the capsaicin receptor. Science (80-) 2000.

[11] CaterinaMJ, RosenTA, TominagaM, BrakeAJ, JuliusD. A capsaicin-receptor homologue with a high threshold for noxious heat. Nature 1999.

[12] CaterinaMJ, SchumacherMA, TominagaM, RosenTA, LevineJD, JuliusD. The capsaicin receptor: A heat-activated ion channel in the pain pathway. Nature 1997.

[13] ChenY, FangQ, WangZ, ZhangJY, MacLeodAS, HallRP, LiedtkeWB. Transient receptor potential vanilloid 4 ion channel functions as a pruriceptor in epidermal keratinocytes to evoke histaminergic itch. J Biol Chem 2016.

[14] ChenY, WilliamsSH, McNultyAL, HongJH, LeeSH, RothfuszNE, ParekhPK, MooreC, Gereau IVRW, TaylorAB, WangF, GuilakF, LiedtkeW. Temporomandibular joint pain: A critical role for Trpv4 in the trigeminal ganglion. Pain 2013;154:1295–1304.

[15] ChenY, YehI, SteinhoffM, LiedtkeWB, KongW, MooreC, LeeSH, ParekhP, CevikbasF, JokerstNM, KontchouN-A, FuchsE, KempkesC, PasolliHA. UVB radiation generates sunburn pain and affects skin by activating epidermal TRPV4 ion channels and triggering endothelin-1 signaling. Proc Natl Acad Sci 2013.

[16] ColbertHA, SmithTL, BargmannCI. OSM-9, a novel protein with structural similarity to channels, is required for olfaction, mechanosensation, and olfactory adaptation in Caenorhabditis elegans. J Neurosci 1997.

[17] CookSP, McCleskeyEW. Cell damage excites nociceptors through release of cytosolic ATP. Pain 2002.

[18] DavisJB, GrayJ, GunthorpeMJ, HatcherJP, DaveyPT, OverendP, HarriesMH, LatchamJ, ClaphamC, AtkinsonK, HughesSA, RanceK, GrauE, HarperAJ, PughPL, RogersDC, BinghamS, RandallA, SheardownSA. Vanilloid receptor-1 is essential for inflammatory thermal hyperalgesia. Nature 2000.

[19] DeBerryJJ, SalomanJL, DragooBK, AlbersKM, DavisBM. Artemin Immunotherapy Is Effective in Preventing and Reversing Cystitis-Induced Bladder Hyperalgesia via TRPA1 Regulation. J Pain 2015.

[20] DennebergNÅ, EgenvallA. Evaluation of dog owners' perceptions concerning radiation therapy. Acta Vet Scand 2009.

[21] DubnerR, HargreavesKM, RuparelS. Role of Oxidized Lipids and TRP Channels in Orofacial Pain and Inflammation. J Dent Res 2016;95:1117–1123.

[22] ElittCM, MalinSA, KoerberHR, DavisBM, AlbersKM. Overexpression of artemin in the tongue increases expression of TRPV1 and TRPA1 in trigeminal afferents and causes oral sensitivity to capsaicin and mustard oil. Brain Res 2008.

[23] EltingLS, KeefeDM, SonisST, GardenAS, SpijkervetFKL, BaraschA, TishlerRB, CantyTP, KudrimotiMK, Vera-LlonchM. Patient-reported measurements of oral mucositis in head and neck cancer patients treated with radiotherapy with or without chemotherapy: Demonstration of increased frequency, severity, resistance to palliation, and impact on quality of life. Cancer 2008.

[24] FanVC, MayerMN, SukutSL, GustafsonNR, MauldinGN, WaldnerCL. Retrospective survey of owners' experiences with palliative radiation therapy for pets. J Am Vet Med Assoc 2018.

[25] FathersE, ThrushD, HusonSM, NormanA. Radiation-induced brachial plexopathy in women treated for carcinoma of the breast. Clin Rehabil 2002.

[26] GobbelGT, BellinzonaM, VogtAR, GuptaN, FikeJR, ChanPH. Response of postmitotic neurons to x-irradiation: Implications for the role of DNA damage in neuronal apoptosis. J Neurosci 1998.

[27] GülerAD, LeeH, IidaT, ShimizuI, TominagaM, CaterinaM. Heat-Evoked Activation of the Ion Channel, TRPV4. J Neurosci 2002.

[28] HallahanDE, SpriggsDR, BeckettMA, KufeDW, WeichselbaumRR. Increased tumor necrosis factor α mRNA after cellular exposure to ionizing radiation. Proc Natl Acad Sci U S A 1989.

[29] HunleyDW, Neal MauldinG, ShiomitsuK, MauldinGE. Clinical outcome in dogs with nasal tumors treated with intensity-modulated radiation therapy. Can Vet J 2010.

[30] KatanosakaK, TakatsuS, MizumuraK, NaruseK, KatanosakaY. TRPV2 is required for mechanical nociception and the stretch-evoked response of primary sensory neurons. Sci Rep 2018.

[31] LallaRV., SonisST, PetersonDE. Management of Oral Mucositis in Patients Who Have Cancer. Dent Clin North Am 2008.

[32] LevineJD, Alessandri-HaberN. TRP channels: Targets for the relief of pain. Biochim Biophys Acta - Mol Basis Dis 2007.

[33] LippoldtEK, ElmesRR, McCoyDD, KnowltonWM, McKemyDD. Artemin, a Glial Cell Line-Derived Neurotrophic Factor Family Member, Induces TRPM8-Dependent Cold Pain. J Neurosci 2013.

[34] MalinS, MolliverD, ChristiansonJA, SchwartzES, CornuetP, AlbersKM, DavisBM. TRPV1 and TRPA1 Function and Modulation Are Target Tissue Dependent. J Neurosci 2011.

[35] MayerMN, DewaltJO, SidhuN, MauldinGN, WaldnerCL. Outcomes and adverse effects associated with stereotactic body radiation therapy in dogs with nasal tumors: 28 cases (2011-2016). J Am Vet Med Assoc 2019.

[36] McKemyDD, NeuhausserWM, JuliusD. Identification of a cold receptor reveals a general role for TRP channels in thermosensation. Nature 2002.

[37] McNicolE, Horowicz-MehlerN, FiskRA, BennettK, Gialeli-GoudasM, ChewPW, LauJ, CarrD. Management of opioid side effects in cancer-related and chronic noncancer pain: A systematic review. J Pain 2003.

[38] MeynRE. Apoptosis and Response to Radiation: Implications for Radiation Therapy. Oncology 1997.

[39] MontellC. The TRP Superfamily of Cation Channels. Sci Signal 2005.

[40] NiliusB, VriensJ, PrenenJ, DroogmansG, VoetsT. TRPV4 calcium entry channel: A paradigm for gating diversity. Am J Physiol - Cell Physiol 2004.

[41] NolanMW, LongCT, MarcusKL, SarmadiS, RobackDM, FukuyamaT, BaeumerW, LascellesBDX. Nocifensive Behaviors in Mice with Radiation-Induced Oral Mucositis. Radiat Res 2017;187:397–403. doi:10.1667/RR14669.1.

[42] PeierAM, MoqrichA, HergardenAC, ReeveAJ, AnderssonDA, StoryGM, EarleyTJ, DragoniI, McIntyreP, BevanS, PatapoutianA. A TRP channel that senses cold stimuli and menthol. Cell 2002.

[43] DePetrocellisL, DiMarzoV. Lipids as regulators of the activity of transient receptor potential type V1 (TRPV1) channels. Life Sciences.2005.

[44] RosaAC, FantozziR. The role of histamine in neurogenic inflammation. Br J Pharmacol 2013.

[45] SchaueD, JahnsJ, HildebrandtG, TrottKR. Radiation treatment of acute inflammation in mice. Int J Radiat Biol 2005.

[46] SchaueD, MicewiczED, RatikanJA, XieMW, ChengG, McBrideWH. Radiation and Inflammation. Semin Radiat Oncol 2015.

[47] SiegelRL, MillerKD, JemalA. Cancer statistics, 2019 (US statistics). CA Cancer J Clin 2019.

[48] SonisST. Pathobiology of mucositis. Semin Oncol Nurs 2004;20:11–15. doi:10.1053/j.soncn.2003.10.003.

[49] SonisST, PetersonRL, EdwardsLJ, LuceyCA, WangL, MasonL, LoginG, YmamkawaM, MosesG, BouchardP, HayesLL, BedrosianC, DornerAJ. Defining mechanisms of action of interleukin-11 on the progression of radiation-induced oral mucositis in hamsters. Oral Oncol 2000.

[50] SpicarovaD, NerandzicV, PalecekJ. Update on the role of spinal cord TRPV1 receptors in pain modulation. Physiol Res 2014.

[51] StoryGM, PeierAM, ReeveAJ, EidSR, MosbacherJ, HricikTR, EarleyTJ, HergardenAC, AnderssonDA, HwangSW, McIntyreP, JeglaT, BevanS, PatapoutianA. ANKTM1, a TRP-

like channel expressed in nociceptive neurons, is activated by cold temperatures. Cell 2003.

[52] Sunavala-DossabhoyG, AbreoF, Timiri ShanmugamPS, CalditoG. Histopathologic grading of oral mucositis. Oral Dis 2015.

[53] ThorntonP, HatcherJP, RobinsonI, SargentB, FranzénB, MartinoG, KitchingL, GloverCP, AndersonD, Forsmo-BruceH, LowCP, CusdinF, DosanjhB, WilliamsW, SteffenAC, ThompsonS, EklundM, LloydC, ChessellI, HughesJ. Artemin-GFRα3 interactions partially contribute to acute inflammatory hypersensitivity. Neurosci Lett 2013.

[54] TominagaM, CalerinaMJ. Thermosensation and pain. J Neurobiol 2004.

[55] TrottiA. Toxicity in head and neck cancer: A review of trends and issues. Int J Radiat Oncol Biol Phys 2000.

[56] UhlénM, FagerbergL, HallströmBM, LindskogC, OksvoldP, MardinogluA, SivertssonÅ, KampfC, SjöstedtE, AsplundA, OlssonIM, EdlundK, LundbergE, NavaniS, SzigyartoCAK, OdebergJ, DjureinovicD, TakanenJO, HoberS, AlmT, EdqvistPH, BerlingH, TegelH, MulderJ, RockbergJ, NilssonP, SchwenkJM, HamstenM, VonFeilitzenK, ForsbergM, PerssonL, JohanssonF, ZwahlenM, VonHeijneG, NielsenJ, PonténF. Tissue-based map of the human proteome. Science (80-) 2015.

[57] WangC, GuL, RuanY, GengX, XuM, YangN, YuL, JiangY, ZhuC, YangY, ZhouY, GuanX, LuoW, LiuQ, DongX, YuG, LanL, TangZ. Facilitation of MrgprD by TRP-A1 promotes neuropathic pain. FASEB J 2019.

[58] WangS, BrigoliB, LimJ, KarleyA, ChungMK. Roles of TRPV1 and TRPA1 in Spontaneous Pain from Inflamed Masseter Muscle. Neuroscience 2018.

[59] WangS, KimM, AliZ, OngK, PaeE-K, ChungM-K. TRPV1 and TRPV1-Expressing Nociceptors Mediate Orofacial Pain Behaviors in a Mouse Model of Orthodontic Tooth Movement. Front Physiol 2019.

[60] WuPH, CoultrapS, PinnixC, DaviesKD, TailorR, AngKK, BrowningMD, GrosshansDR. Radiation induces acute alterations in neuronal function. PLoS One 2012.

[61] ZylkaMJ, LeeH, BasbaumAI, ShieldsSD, LoL, CavanaughDJ, AndersonDJ. Distinct subsets of unmyelinated primary sensory fibers mediate behavioral responses to noxious thermal and mechanical stimuli. Proc Natl Acad Sci 2009.

Table 3.1 Histopathologic grading criteria for oral mucositis

Grade	Histopathologic manifestation
0	No radiation injury; normal mucosa
1	Focal or diffuse alteration of basal cell layer with nuclear atypia and ≤ 2 dyskeratoic squamous cells
2	Epithelial thinning (2-4 cell layer) and/or ≥ 3 dyskeratoic squamous cells in the epithelium
3a	Loss of epithelium without a break in keratinization, or presence of atrophied eosinophilic epithelium
3b	Subepithelial vesicle or bullous formation
4	Complete loss epithelial and keratinized cell layers; ulceration

Table 3.2 TaqMan Gene Expression Assay probes

Gene	Assay ID
Trpv1	Mm01246300_m1
Trpv2	Mm00449223_m1
Trpv4	Mm00499025_m1
Trpa1	Mm01227437_m1
Trpm8	Mm01299593_m1
Gfra3	Mm00494589_m1
Mrgprd	Mm01701850_s1
Gapdh	Mm99999915_g1

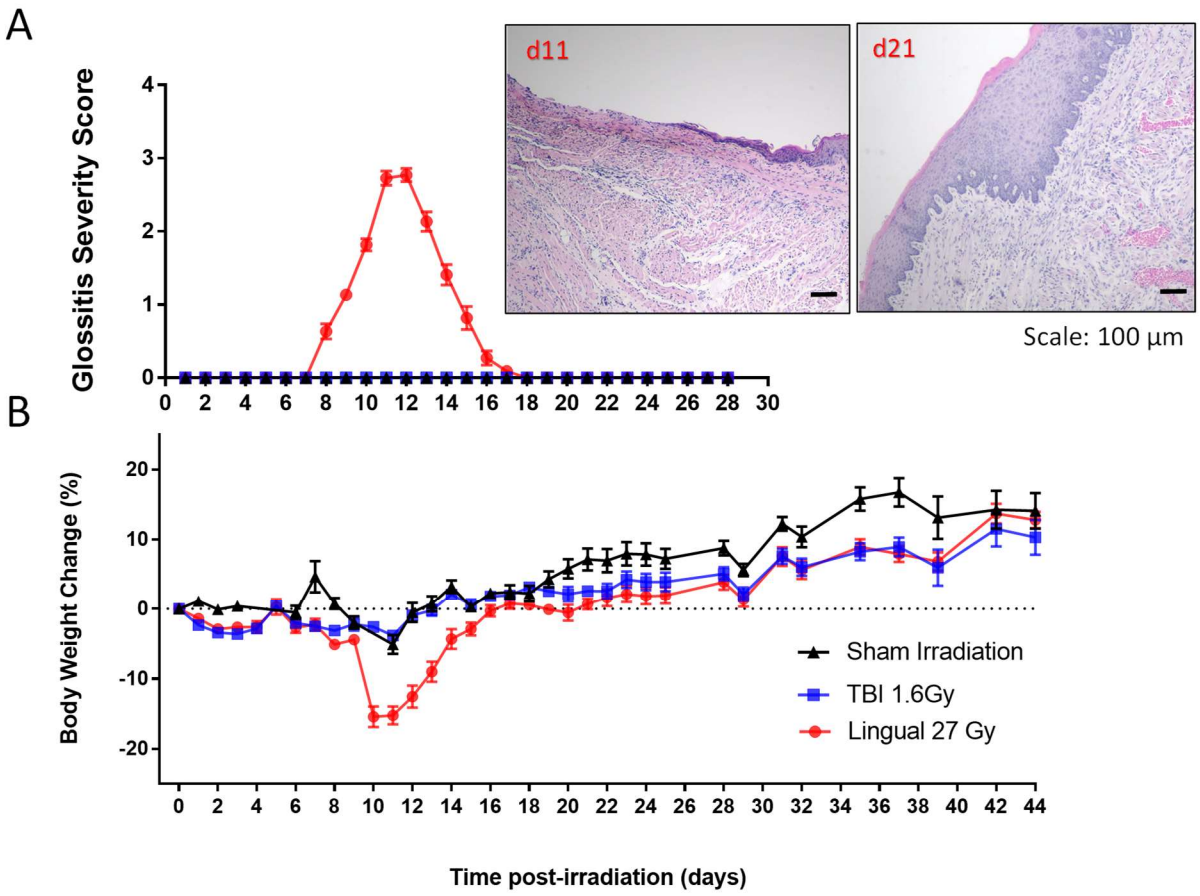

Figure 3.1 Glossitis severity scoring and body weight change over 45 days. (A) The glossitis was presented starting at day 7-8 and reach to the most severe glossitis at day 11, but healed by day 18. The five endpoints at day 1, 5, 11, 21, and day 45 was according on the time-course of RIM (immediate after irradiation, before RIM development, most severe RIM, fully recover RIM, and 1 month after RIM recovered). (B) The body weight change from mice with lingual irradiation was corresponded to the development of RIM. Mice with tongue irradiation and TBI 1.6 Gy had statistically significant lower body weight than sham irradiated mice from day 35 to 39 (P = 0.0008 – 0.0021). Two-way ANOVA, n=8-10 in each group, error bars depict SEM.

Figure 3.2 Calcium imaging showed the proportion of responsive TG neurons was increased in mice that had lingual irradiation compared to sham-irradiated mice and mice with TBI (A) Mice having undergone lingual irradiation had a higher proportion of sensory neurons that were responsive to capsaicin from day 1 to day 21. (B) The proportion of neurons that responded to histamine and (C) TNF-α was increased in tongue-irradiated mice at day 1, 11, and 21 (n= 8-10 in either TBI or tongue irradiated group per time point; n = 4-8 in sham control per time point. Approximately of 30-50 neurons were imaged on each coverslip; a total of 6-10 coverslips were imaged in each group per time point). Error bar = SEM, $*P < 0.05$, $**P < 0.01$, $***P < 0.001$, Fisher's exact test.

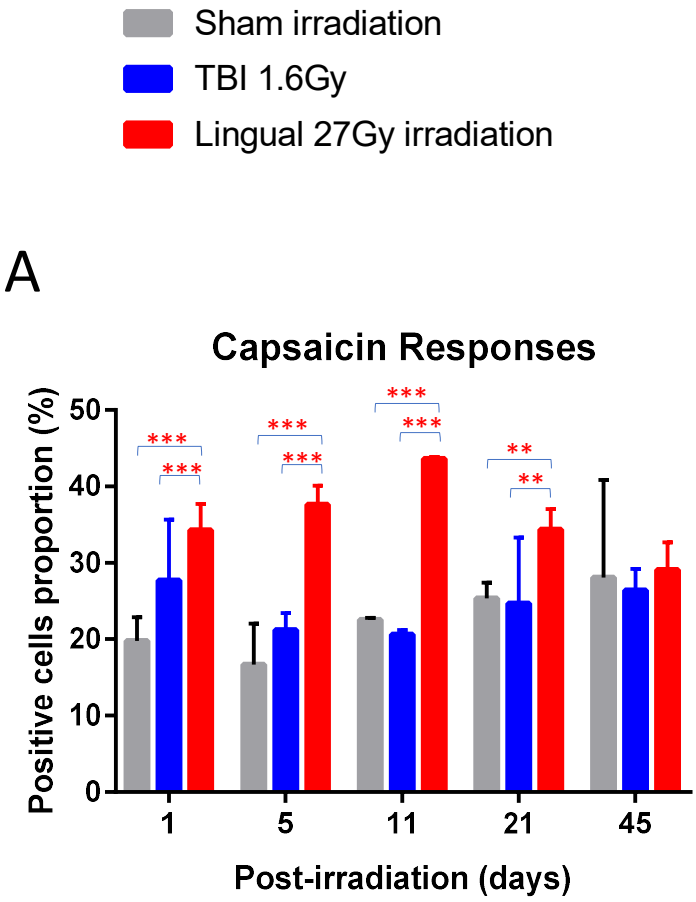
Sham irradiation
TBI 1.6Gy
Lingual 27Gy irradiation
A
Capsaicin Responses
Positive cells proportion (%)
50
40
30
20
10
0
***
***
***
***
***
***
**
**
1
5
11
21
45
Post-irradiation (days)

B

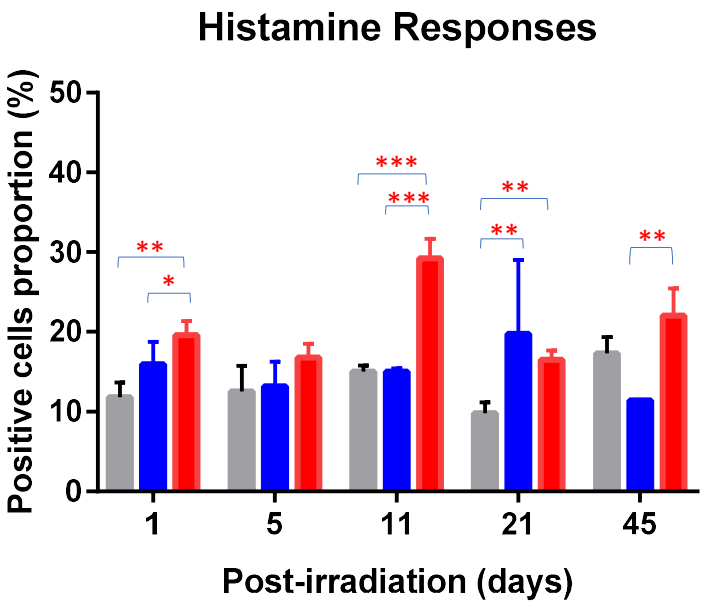
Histamine Responses
Positive cells proportion (%)
50
40
30
20
10
0
**
*
***
***
**
**
**
1
5
11
21
45
Post-irradiation (days)

C

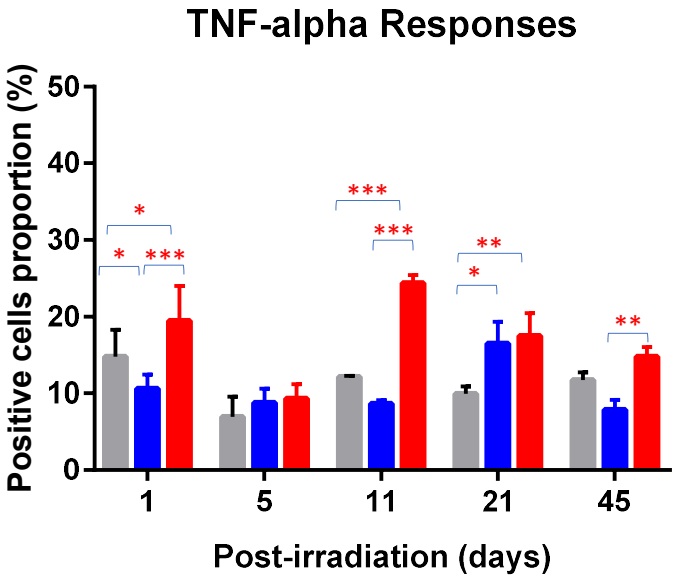
TNF-alpha Responses
Positive cells proportion (%)
50
40
30
20
10
0
*
*
***
***
***
**
*
**
1
5
11
21
45
Post-irradiation (days)

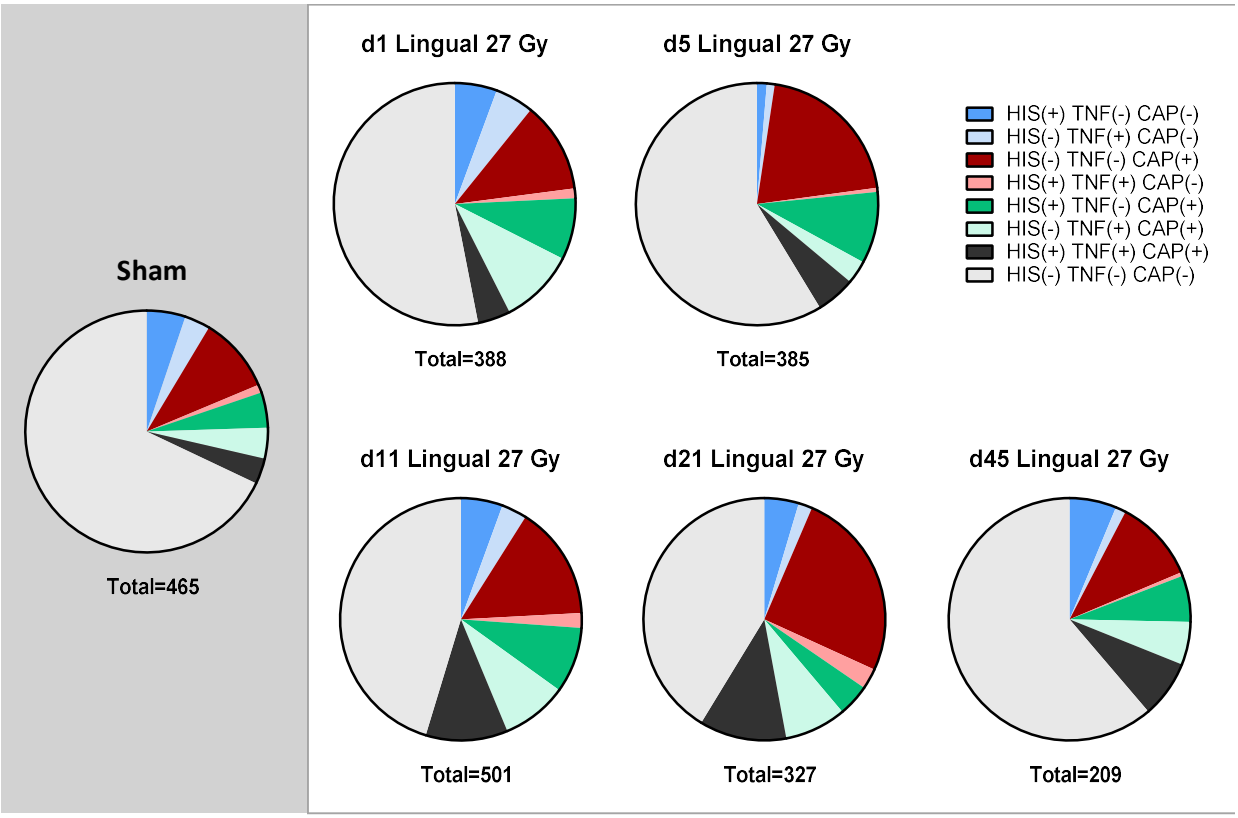

Figure 3.3 The characteristics of neurons that responded to stimuli in calcium imaging. A majority of the responsive neurons were sensitive to capsaicin after lingual irradiation (red). The proportion of neurons that responded to histamine (blue) and TNF-α (light blue) was lower than capsaicin. Most of the neurons that responded to histamine or TNF-α also responded to capsaicin (green and light green). Only a few cells responded to histamine and TNF-α but not capsaicin (pink). A higher proportion of neurons responded to all three stimuli (black) at day 11 (11%) and day 21 (11.6%) in tongue-irradiated mice versus sham-irradiated mice (3.4%).

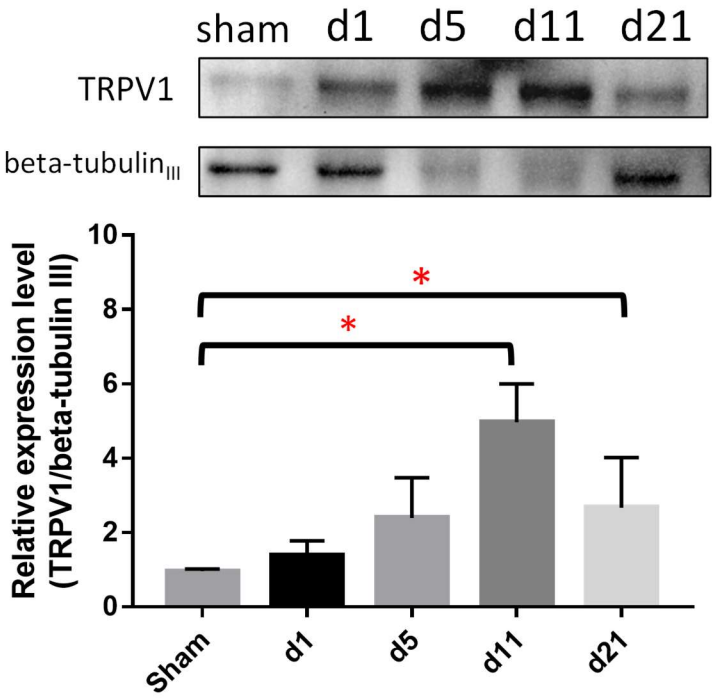

Figure 3.4 Increased expression of TRPV1 in TG from tongue-irradiated mice. The increased trend was observed in TRPV1 protein expression, but the expression was decreased at day 21. The expression on day 45 was not shown, because the sample was pooled from 5 trigeminal ganglia and the sample size was one. The time-course of TRPV1 expression was paralleled to the clinical presented RIM *$P < 0.05$, Mann-Whitney test; n = 3 to 4 per time point; error bar = SEM.

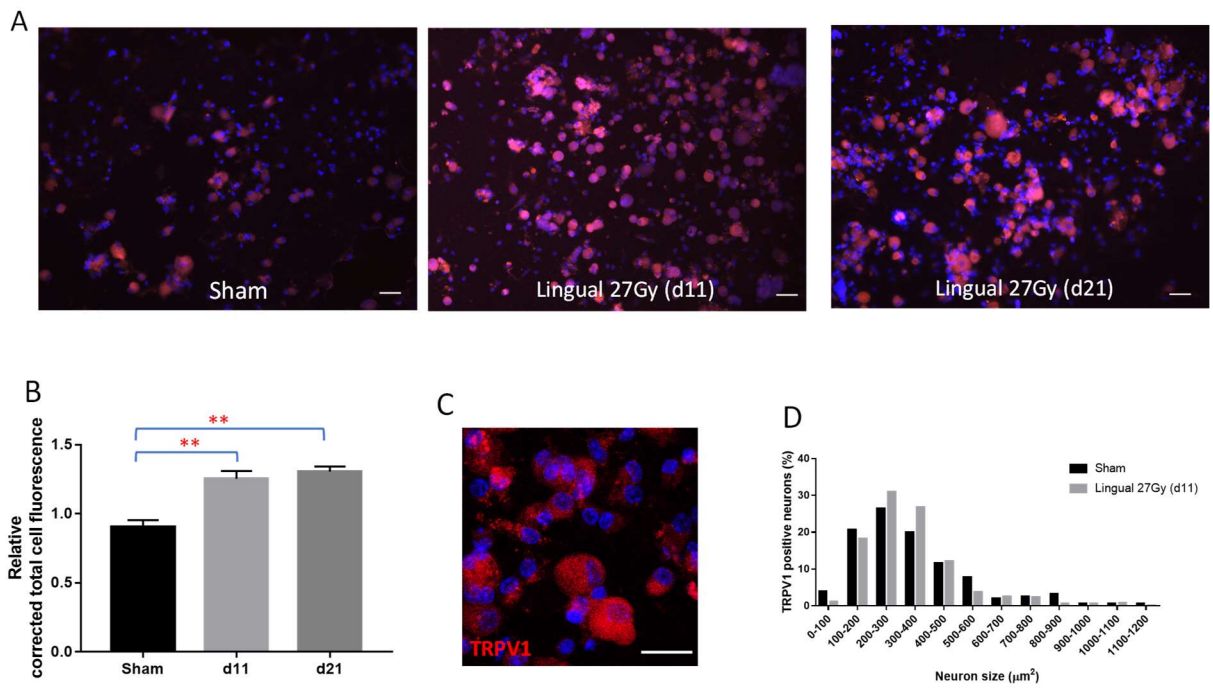

Figure 3.5 Immunostaining of TRPV1 in isolated neurons. (A) After calcium imaging, the neurons on the coverslips were immediately fixed using 4% neutral buffered formalin for immunostaining of TRPV1 (red color) and DAPI (nuclei, blue color). Scale bar = 25 μm. (B) Quantification of corrected total cell fluorescence (CTCF) showed that neurons from tongue-irradiated mice had significantly higher TRPV1 expression at day 11 and day 21 (vs. sham-irradiated mice). The quantification was acquired from 320, 309, and 864 neurons from sham irradiated, day 11, and day 21 lingual irradiated mice, respectively. The imaged neurons were pooled from 4 mice in each group; error bar = SEM, $^{**}P < 0.01$ (C) TRPV1 is expressed in cytoplasm and on cell membrane. Note that not all of the neurons had upregulated TRPV1 expression. Scale bar = 20 μm. (D) The size distribution of TRPV1-label neurons. The majority of the TRPV1 positive neurons were small to medium in size (0-600 μm^2).

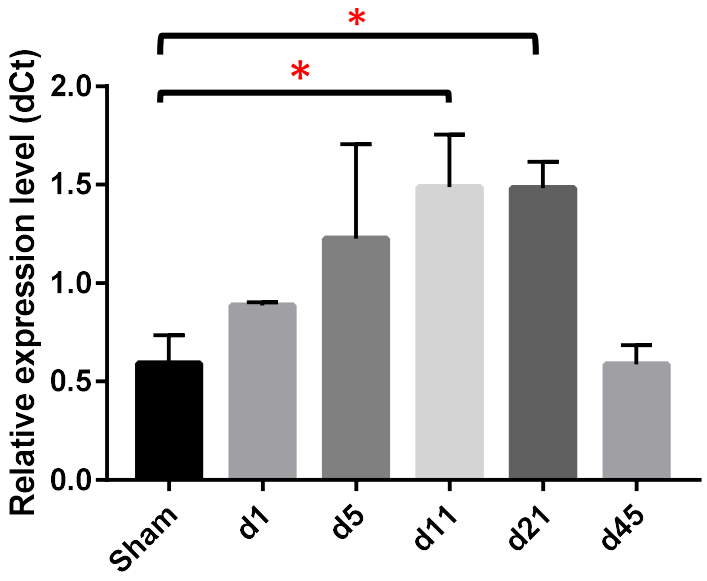

Figure 3.6 Increased expression of *Trpv1* gene in TG from tongue-irradiated mice. The expression of *Trpv1* gene was gradually increased after lingual irradiation and reached statistical significance at day 11 and day 21. *$P < 0.05$, Mann-Whitney test; n = 3 - 4 per time point; error bar = SEM.

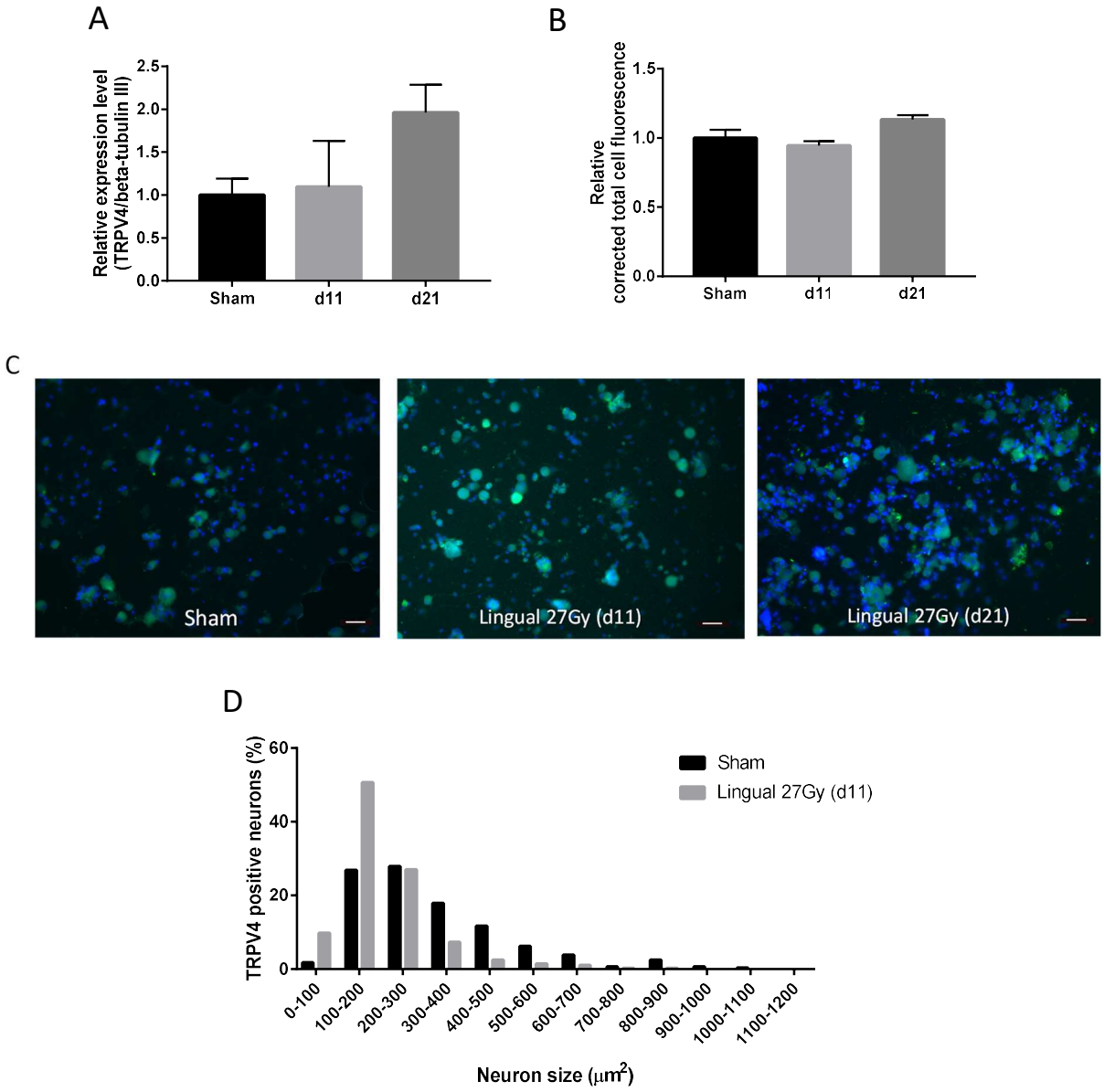

Figure 3.7 The expression of TRPV4 in TG from tongue-irradiated mice. (A) Western blot and (B, C) immunolabeling of trigeminal ganglia showed an increasing trend of TRPV4 expression at day 21, with 2-fold increase ($P = 0.1$) in Western blot detection. (D) The size distribution of TRPV4-label neurons. The majority of the TRPV4 positive neurons were small to medium in size (0-500 μm^2). Mann-Whitney test, n= 3-4; individual neurons were evaluated via cellular immunostaining. The imaged neurons were pooled from 4 mice in each group; sham (n= 320 neurons), lingual 27 Gy at d11 (n= 482 neurons), d21 (n= 863 neurons). Scale bar = 25 µm. All error bar = SEM.

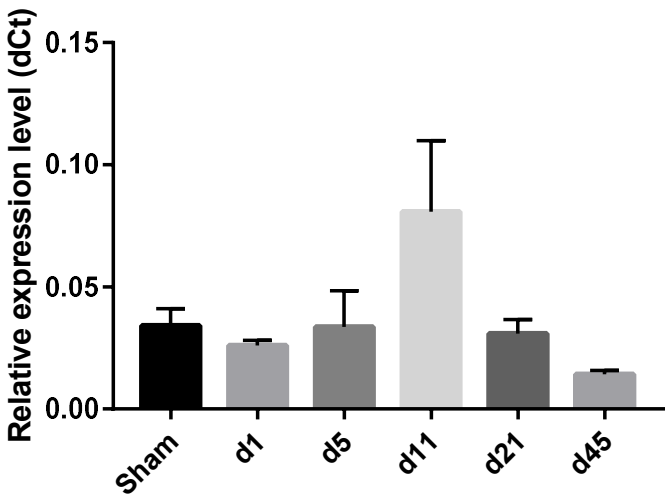

Figure 3.8 The expression of *Trpv4* in TG from tongue-irradiated mice. *Trpv4* gene was increased at day 11, but not it was a statistically significant change ($P = 0.1$, Mann-Whitney test, n=3-4). Note the dCt was used rather than ddCt in order to compare the mRNA transcripts of different genes in the same type of tissue. All error bar = SEM.

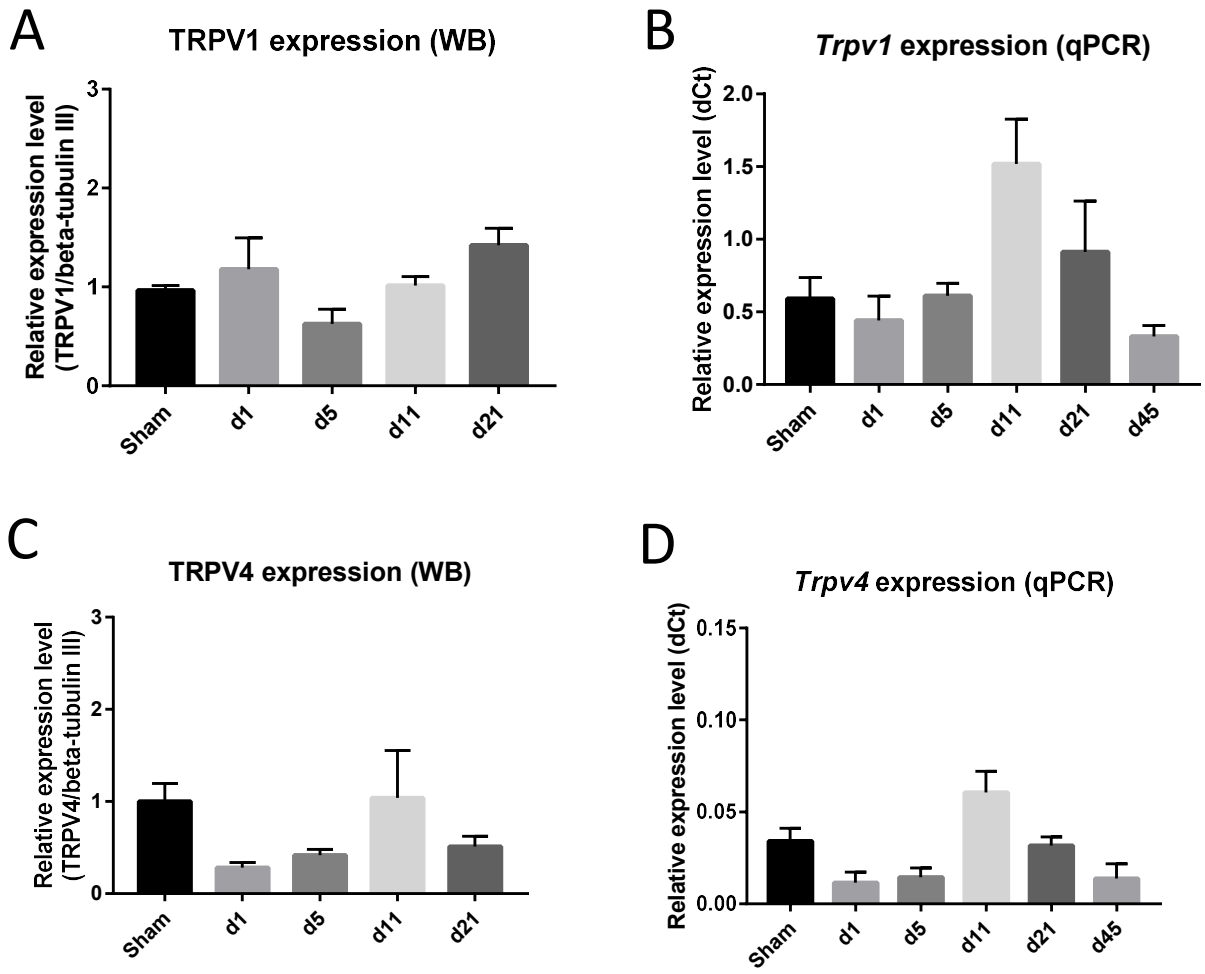

Figure 3.9 The expression of TRPV1 and TRPV4 in mice TG after 1.6 Gy TBI. (A) The protein expression of TRPV1 was not significantly changed over the time. (B) The *Trpv1* gene expression showed a slightly increased pattern at day 11 post-irradiation, but was not significantly different than sham group ($P = 0.1$). (C) (D) the expression of TRPV4/*Trpv4* in TG was low in mice had TBI 1.6 Gy and did not show significant differences from sham-irradiated mice. All error bar = SEM, Mann-whiteney test, n = 3-4 per group at each endpoint.

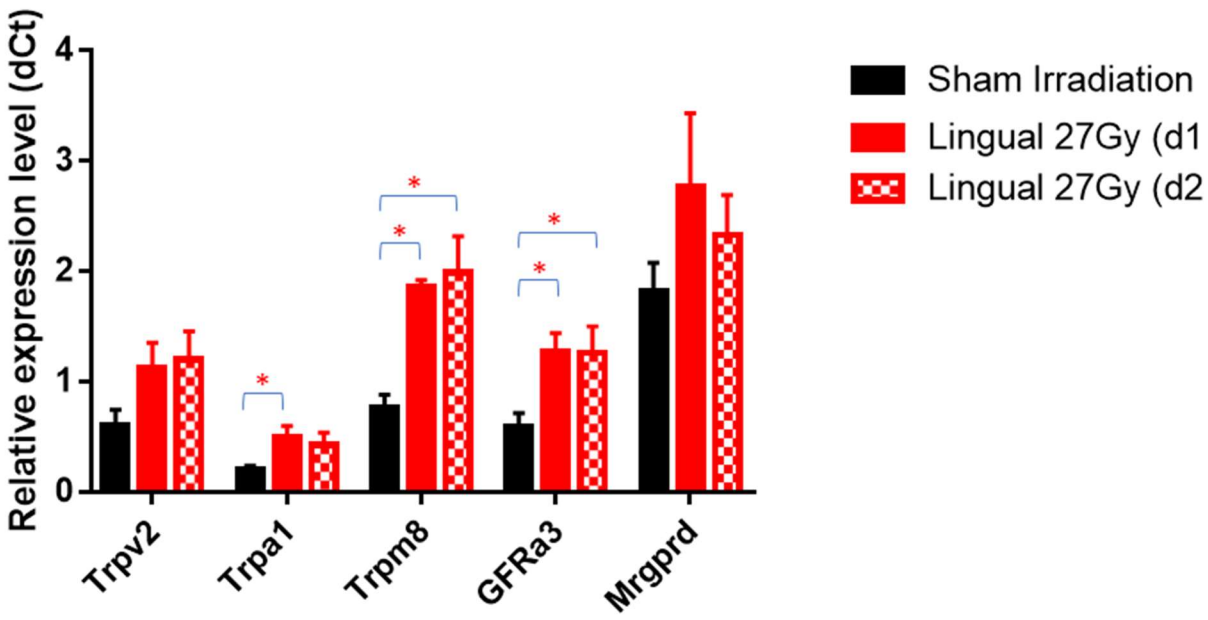

Figure 3.10 Thermal and mechanical pain-related gene expression changes in TG from 27 Gy tongue-irradiated mice. Compared to sham-irradiated mice, *Trpa1*, *Trpm8* and *Gfra3* were significantly increased when the severe glossitis was developed, and the higher expression persisted even the glossitis was resolved at day 21. (*$P < 0.05$, Mann-Whitney test, n=4 mice per group per at each time point; error bar = SEM). *Gapdh* was served as the housekeeping gene.

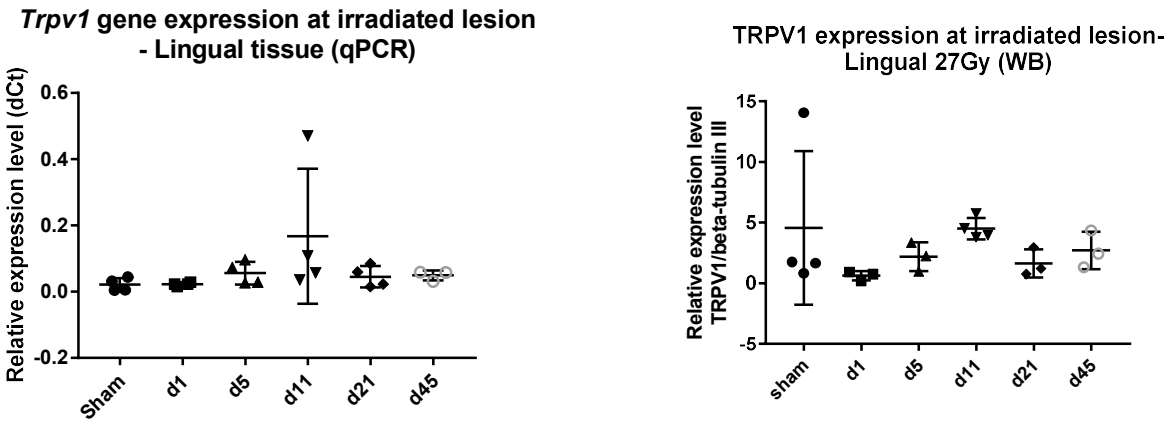

Figure 3.11 The expression of TRPV1 in high-dose irradiated tongue tissue had a non-significant increase at day 11, compared to sham-irradiated mice. Mann-Whitney test, n= 3-4 mice per group per at each time point; error bar = SEM.

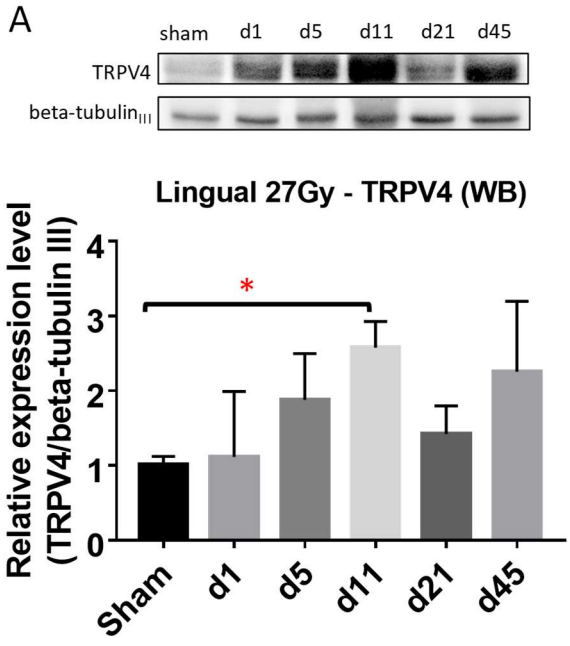
A
sham
d1
d5
d11
d21
d45
TRPV4
beta-tubulin III
Lingual 27Gy - TRPV4 (WB)
Relative expression level (TRPV4/beta-tubulin III)
0
1
2
3
4
*
Sham
d1
d5
d11
d21
d45

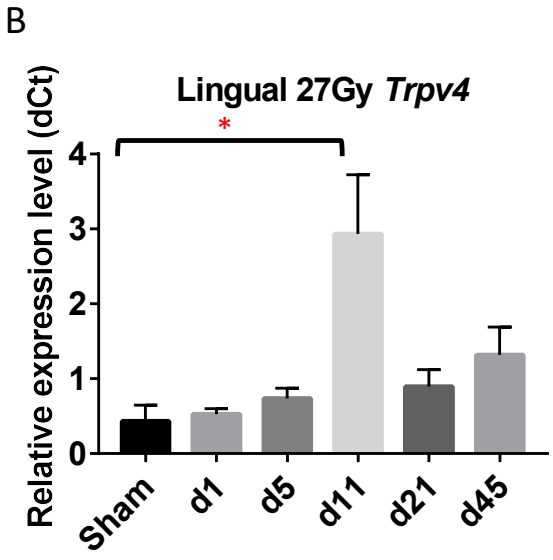
B
Lingual 27Gy Trpv4
Relative expression level (dCt)
0
1
2
3
4
*
Sham
d1
d5
d11
d21
d45

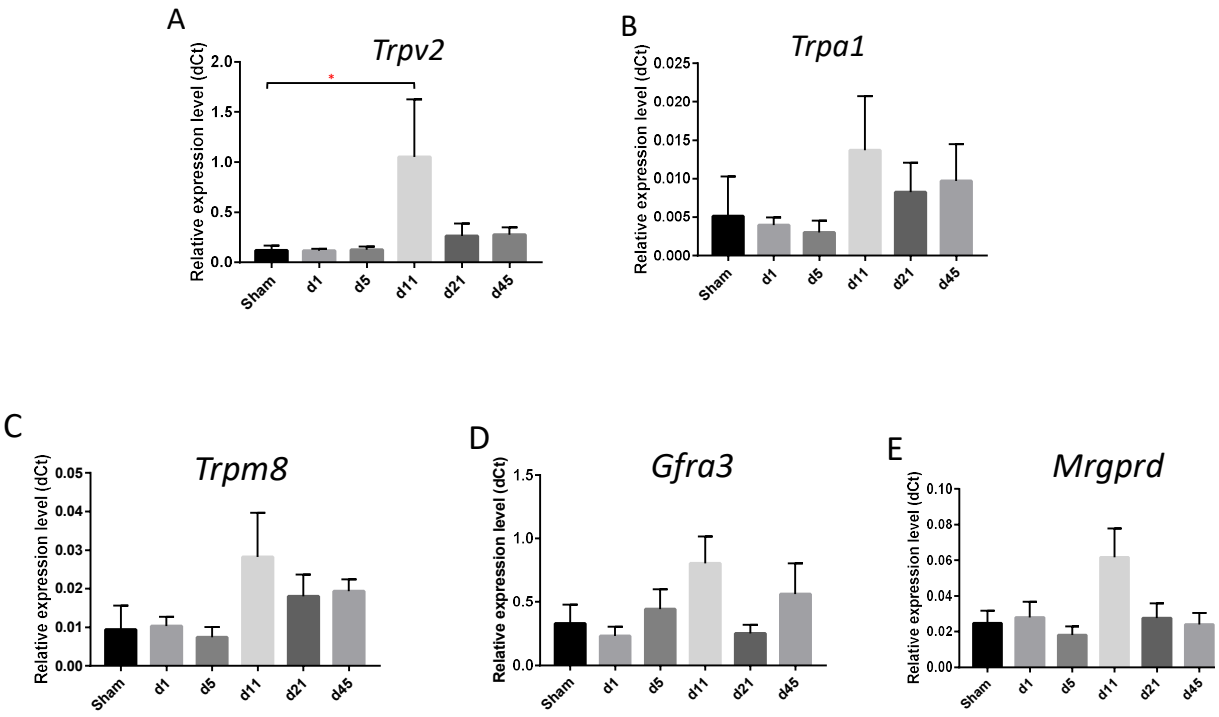

Figure 3.12 Thermal and mechanical pain-related gene expression in 27 Gy irradiated tongue tissue. (A) After high-dose lingual irradiation, the expression of *Trpv2* was significantly increased at day 1, with a 10-fold increase. (B) *Trpa1* was undetectable in the tongue in 50% of sham-irradiated mice; the expression was increased and detectable in mice with high-dose lingual irradiation, and the increased expression level was detected at day 11, 21 and 45, although there was not a significant difference between sham and irradiated mice. (C) The expression pattern of the cold pain-related gene, *Trpm8*, was similar to *Trpa1* (which itself is also cold-related). (D) *Gfra3* gradually increased until day 11 and decreased when the RIM was resolved. (E) The expression of *Mrgprd* was increased when the RIM was developed, but did not reach a statistically significant difference (P=0.1). *$P < 0.05$, Mann-Whitney test, n= 3-4 mice per group per at each time point; error bar = SEM. *Gapdh* was served as a housekeeping gene.

CHAPTER 4: The assessment of orofacial pain in patients with head and neck cancers: developing the domesticated cat as a translational clinical model.

Introduction

Pain is a common symptom of human head and neck cancers (HNC). Approximately three in five HNC patients report pain [38]. As we have discussed in Chapter 1, moderate to severe cancer pain is commonly treated with opioid medications [45,49]. Unfortunately, opioids are addictive, cause significant side effects, and have significant abuse potential [40]. It has been shown that at least one in five cancer patients is at risk of opioid misuse or abuse [18]. The need for improved HNC analgesics is underscored by the fact that more than 650,000 people are diagnosed with HNC each year worldwide [6].

Development of effective, non-addictive HNC pain treatments would benefit from animal model(s) that closely recapitulate human HNC pain; it also requires robust outcome measures for measuring pain and pain relief in that model system. Translational pain research based solely on induced rodent models and then human clinical trials is not producing new analgesic therapies – indicating that this type of "unidimensional" translational research is not successful [36]. Using an animal model in which the disease is naturally occurring and similar to the human condition may be more predictive of human clinical efficacy [36]. Feline oral SCC (FOSCC) has been proposed as a model of human HNC [62] because FOSCC is one of the most common and locally aggressive cancers in cats, and it is a disease that is relatively resistant to treatment with both chemotherapy and radiotherapy [4]. Many cats with FOSCC rapidly succumb to the local and regional progression of their cancer [4]. In these ways, FOSCC is quite similar to human papilloma virus-negative head and neck SCC (HPV negative HNSCC) [62]. It is likely that FOSCC also causes pain which is similar to that experienced by people with HNC, including

HPV negative HNSCC. While some work suggests cats with FOSCC have decreased QOL [37], the incidence and severity of FOSCC-associated pain has not been reported. This gap in the literature is attributable at least in part to the fact that methods for quantifying FOSCC-associated pain are limited. To address this gap, the goal of this study was to begin assessing methods to measure FOSCC-associated pain. We opted to evaluate 3 different types of pain and/or sensitivity assessment methods: client questionnaires, clinician-based pain scales and quantitative sensory testing (QST).

Several methods and instruments have been used in human HNC patients for measuring pain. The most common instruments are numeric or visual analogue scales as a part of quality of life (QOL) questionnaires [38]. In veterinary patients, owner-reported questionnaires have been used to measure QOL and pain-associated behaviors in canine cancer patients [19,20,37,48,63] and one has been reported for use in both dogs and cats [37]. However, none of them are specific for orofacial cancers, or specific for cats. Therefore, we developed an owner-reported QOL questionnaire modified from a canine cancer pain study [19] to evaluate QOL in cats with oral cancer. QOL is affected by many factors, one of which is pain [46].

Acute pain assessment in veterinary patients is often performed by attending clinicians. However, there are only a few validated clinician pain scoring instruments for cats [12]. Pain scales such as the Glasgow composite measure pain scale for felines (CMPS-F) [12,47] and the Botucatu multidimensional composite pain scale (MCPS) [8,9] were developed and validated around acute pain (i.e. surgery or trauma-induced pain) in cats. The Botucatu MCPS is the clinician pain scoring instrument that has undergone the most comprehensive testing of validity, reliability, and sensitivity [9,12]. Clinical instruments for measuring chronic pain in cats have been developed - the Feline Musculoskeletal Pain Index (FMPI) [2,3], Client-Specific Outcome

Measures (COSM) [23,35], and Montreal Instrument for Cat Arthritis Testing (MI-CAT) [30–32]. These instruments have been developed specifically for evaluating osteoarthritis pain. Despite an increasing number of studies investigating different types of pain in cats, none have yet been designed for orofacial pain. Recently, Stathopoulou *et al*. used a modified Botucatu MCPS to identify the analgesic effect of buprenorphine in cats with gingivostomatitis [53]. Based on this, we felt there was a reasonable chance that it might also provide a robust measure of feline oral cancer pain. A multi-dimensional assessment may be required to fully characterize orofacial cancer pain. Comparing Botucatu MCPS and Glasgow CMPS-F, the former has been modified and showed good feasibility in orofacial pain, hence it was further modified to test the validity of oral cancer pain evaluation in the present study.

Pain affects multiple dimensions [34], and not necessarily all equally. Therefore, in developing a model with associated outcome measures, it is important to assess differing methodology. Mechanical/thermal quantitative sensory testing (QST) is methodology that has been used to measure local tissue sensitivity (e.g., wounds) and sensitivity remote from injured tissues [7,33,39] – sensitivity that may relate to central plasticity of pain processes. In humans, thermal and mechanical QST has been shown to be a highly reliable instrument to detect orofacial somatosensory abnormalities including hyperalgesia or allodynia at intra- and extraoral sites [15,43]. The trigeminal nerve mediates the somatosensory input from most of the orofacial region, and so input from one area of the face may result in changes in sensitivity in another facial region [28]. The mandible and tongue are innervated by the mandibular branches, and the maxillary cutaneous region is innervated by maxillary branches, of the trigeminal nerve. The afferent impulses of corneal reflexes are mediated by the ophthalmic division of the trigeminal nerve. Cochet-Bonnet aesthesiometer is another example of QST that has been used for testing

the corneal sensitivity in dogs and cats that are innervated by ophthalmic division [1,5,13]. The filament on the aesthesiometer applies a mechanical stimulation on the corneal surface and elicits a reflex to determine corneal touch threshold (CTT).

Together, the use of owner-reported questionnaires, clinician-based pain scales, and QST may be useful for characterizing cancer-related pain, and abnormalities in orofacial sensitivity, of cats with oral SCC. The resultant data should help to define a pain phenotype for FOSCC.

The present study was performed in order to better define the features of oral cancer pain in cats, and to evaluate the potential utility of FOSCC as a model for human HNC associated pain, We hypothesized that an owner-reported QOL questionnaire, clinician pain scoring instrument, and mechanical QST would be able to discriminate between states of normal orofacial sensory processing in healthy cats and abnormal sensory processing in cats with oral cancers.

Material and Methods

Animals

Pet cats aged > 1 year and weighing > 2.5 kg were eligible for the study. Fractious cats were excluded during screening. Cats were enrolled into two experimental cohorts: (1) tumor-bearing cats; and (2) healthy controls. In the group of cancer-bearing patients, only the cats with confirmed diagnosis of sublingual SCC (either cytology or histopathology) were included. Biopsy was performed after the pain and sensitivity measurements if the cats only had cytology diagnosis. Enrolled cats were required to discontinue systemically administered non-steroid anti-inflammatory drug or corticosteroid for 72 hours prior to the enrollment. Short-term opioids (i.e. buprenorphine) were discontinued at least 48 hours before the pain and sensitivity measurement.

Complete blood count, serum biochemical analysis, and voided urinalysis were performed in each cat with oral cancer. To be enrolled as a healthy control subject for this, complete physical examination was performed by a veterinarian to ensure the cat was outwardly healthy and free of clinically overt oral disease. The study protocol and all procedures were approved by the Institutional Animal Care and Use Committee of North Carolina State University (protocol #18-079-O and #18-082-O).

Outcome measures

A. Owner-Reported Quality of Life (QOL) questionnaire for cats with oral SCC

A recently published scale for evaluating QOL in dogs with cancer (CORQ) [19,20] was modified into the FORQ -- **F**eline oral cancer **O**wner-**R**eported quality of life **Q**uestionnaire (**Appendix 4.1**). There are 17 question items in the published CORQ scale, each scored on an 8-point scale (0-7). We rearranged the order of the questions to fit into four categories: behavior, activity, interaction, and orofacial discomfort. We changed the presentation of the items from how they are presented in the CORQ; each item in CORQ consists of a descriptive statement of an observable behavior and then the respondent is asked to indicate (1) whether that behavior has been seen in the last week; (2) how many days within the past week their pet showed that particular behavior; finally (3) how severe the signs were. If a behavior had been seen, the frequency was scored on a 5-point scale (0-4), as was the severity. We removed the item "treatment interfered with his/her enjoyment of life" because not all cats are undergoing cancer treatment when enrolled into studies. The "playful" evaluation was moved into the "do what he/she like to do". We added questions about "altered mood", "growling or groaned when resting", "ability able to maintain hygiene", "drank less water" and "had trouble positioning to

defecate/urinate" in the behavior category. In the orofacial discomfort category, we included questions about "excessive drooling", "difficulty eating normal food", "trouble eating soft food", "trouble resting their head down", "discomfort or pain near mouth", and "defensiveness when head was touched". We believed these questions may be important in evaluating cats with oral cancers.

In summary, the FORQ included a total of 24 questions grouped within four categories: general behavior, activity, interaction, and orofacial discomfort. The pet owners were requested to score each question with regards to frequency and severity; responses were based on behaviors observed over the preceding 7 days. If a behavior had been seen, the frequency was categorized as: none, rarely (1-2 days), sometimes (3-4 days), usually (5-6 days), or always (every day). Severity was scored as: none, mild, moderate, severe, or very severe. The research team later assigned responses numbers, ranging from 0 to 4 with zero reflecting a response of "none" and 4 being either "always" or "very severe". A total score was calculated the simple summing of individual scores, with higher scores reflecting lower QOL. A 100 mm visual analog scale (VAS) item was also included at the end of the questionnaire to serve as a single measure of overall QOL; respondents were asked to mark along a line representing somewhere between the "worst imaginable quality of life" (0 mm) and "perfect quality of life" (100 mm).

To refine the instrument, the individual items in the QOL questionnaire were analyzed by the non-parametric Mann-Whitney test to evaluate whether the item discriminated between the two groups. Any score comparison with a P-value > 0.5 would be removed from the QOL questionnaire. This threshold was set due to the small sample size in this study.

B. Clinician pain scoring instrument for assessing orofacial pain in cats with oral SCC

The UNESP-Botucatu MCPS for cats with oral diseases was modified to generate a scale that assesses orofacial cancer pain in cats (**F**eline **O**rofacial **P**ain **S**cale for **C**ancers, or FOPS-C, **Appendix 4.2**) [9,53]. In the category of miscellaneous behavior, the abnormal behavior of "lick and/or bites the surgical wound" was changed to "licks, has ptyalism and/or chattering (jaw shakes). Categories or items in the instrument pertained to miscellaneous behavior, reaction to palpation around the mouth and on the head, vocalization, posture, comfort, activity, attitude, and appetite. Categories or items were scored on a 4-point scale, with 0 indicating normal or no change and 3 denoting significantly altered behavior. The categories (miscellaneous behavior and attitude) were scored differently to the other items (e.g., activity) (**Appendix 4.2**). For example, the first item evaluated miscellaneous behavioral abnormalities in 4 categories: A- lying down but moving the tail; B- contract thoracic limbs and/or neck muscles; C- partially closed eyes; D- lick, ptyalism, and/or chattering. If the cat had none of those behaviors, the score would be 0 conversely, a score of 3 indicated the cat had three or more abnormal behaviors on the list. The clinician was requested to label A, B, C, or D if any of the abnormal behaviors were observed when the score was higher than 0. Similar to the miscellaneous behavior category, in the attitude category there were five mental statuses (A, B, C, D or E: satisfied, uninterested, indifferent, anxious, or aggressive, respectively). Score 0 indicated the cat had mental state A; score 1 indicated the cat had one of the mental states B, C, D, or E; score 3 indicated the cat had three of mental states B, C, D, or E. For the other categories, the clinician gave a score based on the description provided. In the evaluation of appetite, a small amount of canned food was provided. When fasting was performed at the time of the pain scoring, the scores were based on the amount of food they consumed at the previous meal.

C. Mechanical sensitivity

An electronic von Frey (EVF) apparatus (BIO-EVF3, Bioseb, Chavillecedez, France) was used to assess mechanical sensitivity threshold (MST). A plastic pipette tip was loaded on the mounting accessory of a hand-held device that can record the applied force (**Figure 4.1 A**). The force was gradually increased manually until a response was elicited, with the upper cut-off limit set as 500 g. The test was terminated when a positive reaction was elicited. Responses deemed a positive reaction included vocalization, head withdrawal, paw withdrawal, attempt to 'bat' or paw at the device, or trying to bite the device. Tests were repeated five times with an interstimulus interval of approximately 1 minute. The mean of all five trials was used for data analysis. Lower thresholds indicate greater sensitivity. Measurements were applied at anatomic sites based on the branches of trigeminal nerves (**Figure 4.1 B**): (1 and 2) just medial to the bilateral mandibulae (intermandibular space), (3) the ipsilateral maxilla, where the maxillary branch innervated, and (4) on the dorsal aspect of the right metacarpus, where serve as the control. For subjects in the healthy cat cohort, the right maxilla was always tested.

D. Cochet-Bonnet aesthesiometer

Corneal touch thresholds (CTT) were measured using a Luneau Cochet-Bonnet (COBO) aesthesiometer (Western Ophthalmics, Lynwood, WA) with a monofilament nylon fiber of 0.12 mm diameter, as previously described (**Figure 4.1 B**) [5]. Testing was performed on all enrolled cats, unless they had pre-existing corneal diseases (e.g., corneal scarring, ulcers). The cats were gently restrained with their head up and their body parallel to the chest of the restrainer (assistant) such that their body was cradled between the restrainer's chest and forearm. All measurements were made by a single veterinarian, in a quiet and well-lit room. The

aesthesiometer was applied centrally on the left corneas; the stimulus intensity was increased in 5-mm step increments, starting with a filament length of 60 mm and progressively shortening the filament to increase resistance. The instrument was held perpendicular to the cornea with a filament. The filament was touched to the cornea in an attempt to elicit a response. The filament was shortened for 5 mm until a corneal blink reflex occurred. A CTT was defined by a consistent blink reflex in 2 of 3 applications. As a safeguard, corneal integrity was confirmed via fluorescein staining at the conclusion of each testing session.

Experimental design

Within the scope of one prospective clinical study, we performed 3 experiments to address the following questions related to validity: (1) reliability; (2) discriminatory ability; and (3) responsiveness.

To test reliability (test-re-test reliability), experiment 1 included two measurements on the same subject in both cancer-bearing cats and healthy cats. Except for the owner-reported QOL questionnaire (FORQ), other pain/sensitivity assessments (i.e. FOPS-C, EVF, and COBO aesthesiometer) were repeated with at least 8 hours between two tests. The assessments were performed in the same environment on each subject by the same person (YHL) each time.

Experiment 2 examined cats with oral cancers compared to healthy cats without oral diseases to examine the discriminative validity of assessments. We performed the FORQ, FOPS-C, EVF, and COBO aesthesiometer on cats with and without sublingual SCC. Upon enrollment into the study, the owners of healthy cats were requested to answer the questionnaire. Cats with sublingual SCC completed the questionnaire after the confirmed diagnosis was given but before the consultation with the oncologist (MN). All assessments, except for FORQ, were conducted

by a single veterinarian (YHL).

Experiment 3 investigated the responsiveness validity of the assessments using cats with sublingual SCC. Assessments were conducted three times at baseline, 30 min after buprenorphine, and lastly, on the second day. The buprenorphine was administered buccally once with a dose of 0.02 mg/kg as described previously [50].

Statistics

Normality of the data was evaluated by the Shapiro-Wilk test. Test-re-test repeatability (experiment 1) evaluation was performed using the Wilcoxon matched-pairs signed rank test, comparing data between two repeated data within the same cat. The Bland-Altman analysis and correlation of test and re-test data were also performed. The mean values of the two repeated tests were used for analysis in experiment 2. Comparisons of FORQ and FOPS-C between healthy control and cancer cats were analyzed using the non-parametric Mann-Whitney U-test. Student *t*-tests were used to compare the results of MST and CTT between two groups. In experiment 3, the Wilcoxon matched-paired test or paired *t*-test were performed on data collected before buprenorphine and 30 min after buprenorphine; and the results at 30 min after buprenorphine and the test on the second day. The level of significance was defined as $P < 0.05$. All the statistical analysis was performed by Prism 7 (GraphPad Software, San Diego, CA).

Results

Animals

A total of 14 healthy cats and 6 cats with sublingual SCC were included in the study. Healthy client-owned cats were recruited from the staff and students at the NC State College of

Veterinary Medicine. The sublingual SCC patients were referred from veterinary practices in North Carolina (n = 5) and Massachusetts (n = 1) between September 2018 and May 2019. The signalments of the cats are detailed in **Table 4.1**. Two healthy cats and one cancer-bearing cat were uncompliant for the EVF assessment; the two healthy cats did not complete the assessment on the orofacial region and one cancer cat was not able to finish the assessment on the right forelimb; thus, complete pain evaluations were feasible in 12/14 (86%) healthy cats and 5/6 (83%) cats with oral tumors.

Experiment 1: Test – re-test reliability

The test – re-test reliability of all pain assessment (FOPS-C, EVF, and COBO aesthesiometer) for enrolled cats were found to be good. In FOSP-C, the Wilcoxon matched-pair test showed that there was no difference between first scoring and second scoring in neither control nor cats with sublingual SCC (**Figure 4.2 A**). The Bland-Altman analysis (**Figure 4.2 B**) showed the mean ± SD of the differences between two tests (Test 1 - Test 2) was 0.588 ± 2.12 and the correlation coefficient (**Figure 4.2 C**) showed two tests were positively correlated (r^2 = 0.73, $P < 0.0001$).

In mechanical QST, there were no statistical differences between test and re-test of EVF test performed at sites between the mandibles, on the right maxilla, and over the right metacarpus in Wilcoxon matched-pairs signed rank test (**Figure 4.3**, left panel, and **Supplemental Figure 4.1 and 4.2** in **Appendix 4.3**). The Bland-Altman plot showed most of the differences between the two tests lay between the 95% limits of agreement (**Figure 4.3**, middle panel). However, the variability was greater at higher thresholds. The correlations between test and re-test were statistically significant at four testing sites (P = 0.0006 – 0.0365, see **Figure 4.3**, right panel),

which indicated good test – re-test reliability of EVF. There was no significant difference between the two CTT tests on the same cats (**Figure 4.3** and **Supplemental Figure 4.1 and 4.2** in **Appendix 4.3**) and all of the differences on the Bland-Altman plots were within the 95% limits of agreement (**Figure 4.3**). The mean difference between the two tests ± SD was 0.029 ± 1.007. The correlation between the two tests was not statistically significant ($P = 0.4162$), but the CTT in cats with sublingual cancers were generally higher than control cats.

Experiment 2: Discriminatory validity

FORQ

The mean total score of the QOL questionnaire in cats with sublingual SCC was significantly higher than healthy cats ($P = 0.0002$, **Figure 4.4 A**). The VAS QOL score was significantly lower in cats with sublingual SCC than healthy controls (**Figure 4.4 B**). The mean ± SD VAS QOL score in cancer cats was 52.0 ± 24.6 mm, compared to 94.3 ± 8.6 mm in healthy cats. The correlation of QOL questionnaire total score and VAS from all respondents was statistically significant ($r^2 = 0.6$, $P = 0.0002$, **Figure 4.4 C**). The (mean ± SD) subtotal scores in terms of frequency and severity were both significantly higher in cancer patients (26.2 ± 7.05 and 22.4 ± 3.782, respectively, **Figure 4.4 D** and **E**) than healthy cats (mean = 2.25 ± 3.934 and 1.667 ± 3.025, respectively).

Frequency and severity of the abnormal behavior were evaluated separately. Regarding frequency of clinical signs, 4 out of 6 items (67%) in the "orofacial discomfort" category had significantly elevated scores in sublingual SCC cats compared to healthy cats, followed by the category of "general behaviors" (5 out of 9 items, 56%) and "activity " (2 out of 6 items, 33%). Similarly, the severity evaluation showed cats with sublingual SCC had more items that had a

significantly higher score in the categories orofacial discomfort (4 out of 6 items, 67%), activity (3 out of 6 items, 50%) and general behaviors (4 out of 9 items, 44%). None of the items in the “interaction" category had significantly different frequency or severity scores between healthy cats and cancer cats.

Each question item was assigned a code (**Table 4.2**) for analysis. By reviewing the heat plot, the most frequent observations in cats with sublingual SCC were excessive drooling and trouble eating normal food (QF-19 and -20, **Figure 4.5 A**); in regards to severity, the mean score in hygiene (poor hygiene) and drooling were the highest in cats with sublingual SCC when compared to other questions (QS-06 and -19, **Figure 4.5 B**). The total score for each category of general behavior, activity, and orofacial discomfort was significantly higher in cats with sublingual SCC than healthy controls for both frequency and severity evaluation (**Table 4.3**), but the difference between healthy cats and cats with sublingual SCC for the “interaction” category was not significant.

Individual question item analysis showed 21 of 48 items (44%, 10/24 items in frequency evaluation and 46%, 11/24 items in severity evaluation) were able to discriminate between cats with cancer and healthy controls (**Table 4.4**). Questions #2, 3, 5, 8, 9, 10, 11, 14, 15, 16, 17, 18, 22, and 24 in Frequency evaluation were not able to distinguish between cats with sublingual SCC and healthy cats. The scores of questions #2, 3, 5, 8, 9, 10, 11, 15, 16, 17, 18, 22 and 24 in cancer cats were not significantly different from healthy cats. These items were reluctance to wake up (Q-02), mood alternation (Q-03), noise when sleeping (Q-05), less drinking (Q-08), trouble in urination/defecation (Q-09), trouble in mobility (Q-10), lost balance (Q-11), decrease enjoyment in life (Q-14), poor sleep quality (Q-15), less interaction with the owner (Q-16, 17, 18), trouble lying down the head (Q-22), and defensive behavior when touching the head (Q-24).

The only discrepancy in the non-significant items in frequency and severity was the question of "decrease enjoyment in life" (Q-14). There were no differences in frequency of decreased enjoyment in life, but cats had that cancer were significantly more severely affected (decreased enjoyment of life) than healthy cats.

We removed those items that may not distinguish between cancer cats and healthy cats to obtain a refined FORQ for the future investigation. Due to the small sample size that decreased the statistical power, we only exclude those items with a p-value greater than 0.5 in both frequency and severity evaluation. The refined 19-item questionnaire was then developed (**Appendix 4.4**). The removed questions were lost balance (Q-11), unwilling to be accompanied (Q-16), decreased affection (Q-17), unwanted to be pet (Q-18), and defensive behavior when touching the head (Q-24).

FOPS-C

The average score of the test and re-test in each subject was used for statistical analysis (**Figure 4.6 A**). The median (range) of the scores in healthy cats and cats with sublingual SCC are detailed in (**Table 4.5**). An increased score indicates more pain-related behaviors. Cats with sublingual SCC had significantly higher scores in miscellaneous behavior ($P = 0.0002$), mouth palpation ($P = 0.0205$), comfort ($P = 0.0021$), activity ($P = 0.0273$), attitude ($P = 0.006$), and appetite ($P = 0.0021$), as shown in (**Figure 4.6 B**). However, head palpation, vocalization, and posture evaluation did not show significant differences between healthy cats and cats with sublingual SCC (P-value range from 0.13 to 0.54). The total score of FOPS-C was significantly correlated to the original FORQ score ($r^2 = 0.55$, $P = 0.0007$, **Figure 4.6 C**) and the proposed, refined FORQ score ($r^2 = 0.66$, $P < 0.0001$).

The (**Table 4.6**) details the pain score of each cancer cat - note the scores were the average score of test and re-test. In the miscellaneous behavioral category, most of the observations in cats with sublingual SCC were licks, ptyalism, or chattering (n = 4/5), and laying down and quiet (n = 4/5) (see **Appendix 4.2**). In attitude evaluation, four out of five cats with sublingual SCC were uninterested in interacting with the observer and one cat showed both disinterest in the observer and indifference to its surroundings. Cats with sublingual SCC tended to show interest in provided food, but did not continue consumption after a few bites.

Electronic von Frey and Cochet-Bonnet Aesthesiometer

Lower QST thresholds indicated the cats were more sensitive to mechanical pressure. Cats with sublingual SCC were significantly more sensitive to pressure at both sides of intermandibular area (**Table 4.7** and **Figure 4.7 A** and **B**, $P = 0.0001$ and 0.0002 on right and left side, respectively), but not to pressure over the maxillary region (**Figure 4.7 C**, $P = 0.2043$). However, the mean ± SD of the MST at the maxillary region in tumor-bearing cats was lower (174.5 ± 62.03 g) than control (231.3 ± 86.3 g). Interestingly, decreased thresholds were observed at the right metacarpal site ($P = 0.0268$) in cats with sublingual SCC compared to controls (**Figure 4.7 D**). In cancer-bearing cats, four out of five cats had tumors that originated from the right side and one out of the five cats had a tumor originating from the left side. However, all of the cats had masses that crossed the midline and occupied the base of the tongue. There was no significant difference between the MST values at ipsilateral and contralateral sides of the intermandibular region in cats with sublingual SCC (**Figure 4.7 E**, $P = 0.6745$).

Previous work has demonstrated similar CTT values measured at right and left eyes in healthy Domestic Short Hair cats [5]. To reduce procedure time and stress on animals, we only

performed the COBO aesthesiometer on the left corneas. In contrast to the threshold value measured by EVF, the higher CTT values indicated the subjects were more sensitive to corneal touches. The COBO aesthesiometer results from the left cornea showed cats with sublingual SCC were more sensitive (**Figure 4.8**, $P = 0.0006$). The mean ± SD of the recorded filament length in tumor-bearing cats was (3.18 ± 0.58 cm) compared to controls (2.04 ± 0.53 cm).

Sex difference have been shown in measuring orofacial sensitivity using QST in humans [15]. We compared the MST values between healthy castrated males (n =5) and spayed females (n = 7) via student *t*-test and CTT via Mann-Whitney test, but did not identify statistically significant differences between the two groups either in EVF or CTT in healthy cats (**Figure 4.9**). There were too few cancer-bearing cats to make a statistically relevant comparison.

Experiment 3: Responsiveness validity

FOPS-C, EVF, and COBO aesthesiometer measurements were performed before and 30 minutes after administering an analgesic (buprenorphine 0.02 mg/kg, buccally) in five cats with oral cancers. Although not significant, FOPS-C, orofacial region EVF, and COBO aesthesiometer all showed a trend of decreased pain/sensitization after buprenorphine administration, and the pain/sensitivity returned (to pre-buprenorphine levels) on the next day (**Figure 4.10** and **Table 4.8**). There were four out of five cats had improved orofacial pain sensitization.

Discussion

While others have reviewed the value of feline oral SCC as a comparative oncology model [62], this is the first-time cats with oral SCC have ever been considered as a potential model for studying cancer pain. Through our research, we have identified methods that appear to

be reliable (i.e., produce repeatable results within individual cats), responsive to analgesic therapy, and discriminate between healthy and tumor-bearing cats. Interestingly, our results also suggest that cats with sublingual cancer not only develop pain, but also seem to have regional peripheral sensitization, and widespread sensitization.

One goal of this study was to develop a method for assessing the well-being of cats with oral cancer. This is generally achieved by measuring either QOL or health-related QOL (HR-QOL). Both can be measured with questionnaires. HR-QOL focuses on the impact that treating a specific illness has on QOL, whereas QOL measures are more general assessments that cover all aspects of an animal's life such as social environment and mood. [46]. In our study, we attempted to measure QOL rather than HR-QOL because overall QOL affects pet owners' decision of undergoing euthanasia or treatment. Initially, we took a published canine owner-reported QOL questionnaire for cancer patients and modified it to evaluate the QOL of cats with oral cancers. We then created an initial version of the FORQ which we believe had face validity – that is, our team agreed it was an appropriate questionnaire. Our initial version of the FORQ showed good discriminative function; it distinguished healthy cats from those with sublingual SCC. However, some of the questions did not show a significant difference between the two groups. In our study, cats with oral cancers did not have significant "mood alteration" and they had normal interactions with the owners, which is different from the observation previously made in canine cancer patients [19]. This discrepancy may due to the natural characteristics of different species. We also found "Less drinking" did not appear to be a good indicator in cats with sublingual cancers. Although cats with sublingual cancers decreased their normal food intake, water may help them to relieve some pain and replace the food if they had dysphagia. Mouth dryness and pain are common in human patients with advanced cancers but usually

underreported [42]. Therefore, increased water intake could possibly indirectly indicate mouth dryness and/or pain in those cancer-bearing cats.

Overall, about half of the questions in FORQ were able to distinguish cats with oral cancers from healthy cats, and the score was consistently correlated with the VAS. However, this questionnaire-based evaluation has some limitations. Scoring by individual owners is subjective and may be affected by their backgrounds; for example, most of the owners of healthy cats used in our study work in the field of veterinary medicine/research; veterinary personnel may likely view and assess QOL differently than the general public. Another concern is related to the design of the questionnaire; the way that questions are worded and the order in which questions are presented can influence the way that individuals respond to those questions [55]. These factors can result in variable estimates of pain prevalence; for example, in a meta-analysis of questionnaire-based pain evaluations, while most studies reported a pain prevalence of at least 30%, the range was 9% to 98% across 82 studies of HNC patients [38]..

In the second iteration of the FORQ, we removed the items that did not well distinguish between healthy cats and cats with oral cancers. We set the threshold of $P > 0.5$ that we removed the items showed there are more than 50% chance that the difference is not exist. Since we saw the question of lost balance (Q-11), unwilling to be accompanied (Q-16), decreased affection (Q-17), unwanted to be pet (Q-18), and defensive behavior when touching the head (Q-24) were not able to discriminate two groups of cats, those items suggest the cats had sublingual cancer did not influent their gait, interaction with their owners and still like to be pet on the head. In future work, we should increase the sample size. A ratio of 3:1 sample size to number of items has been recommended for questionnaire sampling [19,29]. Therefore, with 19 items (questions) left in the second version of the FORQ, this means that at least 57 cats should be included in future studies.

A holistic quality of life has been developed by the World Health Organization that evaluate six categories including physical health, psychological healthy, level of independence, social relationships, environment, and spirituality/religion [61]. Since not all of them are applicable to animals, we believe the FORQ covers most of the facets that measures QOL of the cats. We evaluate the patients' physical health such as energy, sleep quality and discomfort near mouth; in psychological health facet, we evaluated the altered mood, and if they do what they like to do; in level of independence aspect, we evaluated mobility and eat their normal food; in social relations, we assess the interaction between the owner and their cats. The other two categories (environment and spirituality/religion) may not affected by the cancer or not applicable to animals.

In our study, we tested a clinician-based multi-dimensional evaluation. The scores of FOPS-C were significantly greater for cancer-bearing cats than control cats, and the FOPS-C scoring was highly correlated to FORQ responses. The FOPS-C assesses various pain categories: miscellaneous behavior, reaction to palpation around the mouth and on the head, vocalization, posture, comfort, activity, attitude, and appetite. Most of the cancer cats had high scores for abnormal miscellaneous behaviors that include licking, ptyalism or chattering; this makes sense because each of these have been reported as clinical signs in FOSCC patients [4]. An important consideration is that these clinical signs are not necessarily specific to FOSCC; they are also common in other painful oral diseases such as gingivitis-stomatitis [25]. Interestingly, this lack of FOP-C specificity means that in addition to measuring cancer pain, the instrument may also be appropriate for measuring cancer treatment-associated pain. That is relevant because, in addition to human HNC-associated pain, radiation-associated pain is also common in this patient population; it has been reported that 80% of the HNC patients undergoing full course radiation

can develop moderate to severe orofacial pain [16]. Similarly, FOSCC patients appear to have painful oral mucositis after radiation therapy; cats that underwent hypofractionated radiation therapy were reported to have grade 2 mucositis (patchy ulcerations) [44]. Another category evaluated by the FOPS-C is mouth palpation; mouth palpation scores were higher in cats with oral cancers, which is consistent with the QST results for the maxillary and intermandibular regions. In the activity category, most of the cancer cats moved normally, which also agreed with the evaluation of mobility in the FORQ. Three of the cats were quieter and had less activity, which may reflect in the question of less energy in the FORQ. Most cancer-bearing cats maintained interest in food; however, tumor-associated dysphagia is known to be a problem that reduces food intake (which is reflected in the data of difficulty eating food in FORQ); thus, in future iterations of the FOPS-C, we may consider revising the appetite scoring to reflect this disconnect between appetite and ability to successfully prepend food. The definition of "normal" appetite in each cat should probably be based on the owner's reported history, particularly as some cats may not eat normally outside of the home in an unfamiliar environment. Fasting before the in-clinic evaluation could also be considered to aid in judging a cat's ability to eat, and their interest in food. Additionally, the value of FOPS-C may be improved through the incorporation of facial expression assessment. The ear position and the shape of the muzzle have been used as a part of the Glasgow CMPS-F evaluation [26,47]. Recently, the Feline Grimace Scale has been shown to be a valid and reliable instrument for evaluating acute pain in cats [17,41].

We found no significant difference in "posture", "head palpation", and "vocalization" category evaluation between the two groups in our study. The evaluation of posture could be affected by attitude (e.g., cats who are nervous when in-clinic may adopt an abnormal/hunched

posture). In fact, a previous study has indicated that certain demeanors (such as shyness, fearfulness, or aggressiveness) can influence the scoring for Botucatu MCPS [11]. A quiet room that allows the cats to explore their surroundings may help in clinician scoring, but would add to the time taken to perform the scoring. The head palpation response was not significantly different between control cats and cancer-bearing cats, which is in line with the FORQ item 24 (defensive when the head was touched). Vocalization in cats with oral cancer was only seen in two of five cancer cats, with growling but not hissing. The lack of difference between groups for vocalization indicates that this is not likely to be a useful measure. It can also be biased by subject selection since fractious cats were excluded from this study. In the present study, FOPS-C was evaluated by a single clinician; this was done to avoid the bias from differences in scoring between individuals. Now, additional work should be done to verify the reproducibility/inter-rater reliability of the scoring [56].

We used EVF and COBO aesthesiometer to evaluate each cat's response to varying mechanical stimuli. The EVF showed that cats with sublingual cancer were more sensitive to mechanical pressure at both the oral region and the region outside of tumor location such (metacarpal region). Sensitivity around the mandibular region and maxilla may be partly related to peripheral sensitization driven by nociceptor sensitizers, but part may be driven by more central changes affecting multiple branches of the trigeminal nerve [57,60]. This peripheral sensitization may be due to inflammation, tumor cells infiltrating into the nerve fibers or other tumor-related factors (trauma, acidification, etc.) that increases the responsiveness and activity of nociceptors [57]. The MST measured on the maxilla of healthy cats were variable. This could be due to the presence of highly sensitive tactile hairs of the vibrissal pad [21,22]. The von Frey aesthesiometer has been used for evaluating paw withdrawal threshold in cats with osteoarthritis

[24]; this study showed that the von Frey is able to detect the reduced threshold of paw withdraw in cats with osteoarthritis. In our study, we tested withdrawal threshold at the right metacarpus. Cats with sublingual SCC had relatively low nociception thresholds; this may indicate central sensitization in our study population, or a generalized peripheral sensitization [57,60]. Central and peripheral sensitization have been shown in bone cancers [27]. As there was no tumor or other tissue injuries around the metacarpal region of the cats in our study, these results support the conclusion that lingual cancer can induce central sensitization, decreasing the threshold of nociception and increasing responsiveness at non-tumor sites. Other anatomical sties, for example, metatarsus, should be performed to verify the presence of central sensitization.

We found that QST measures appeared to distinguish healthy cats and cats with oral cancer. However, it must be remembered that QST results are likely affected by the 'pain history'. Procedures that may be associated with pain such as biopsy, venipuncture or intravenous catheter placement or other painful diseases such as osteoarthritis all have the potential to affect somatosensory processing. Sex could be another factor that influences the QST results. Sex differences have been in QST-based somatosensory assessments of human at orofacial pain [15,39]; although we did not detect differences between male and female cats, this may be due to the fact that animals in the study were neutered, or attributable to the small sample size.

The COBO aesthesiometer is another example of mechanical QST and it measures corneal sensitivity. The reason for measuring corneal sensitivity in this study was to determine whether there is cross-sensitization of nerves that innervate the tongue. The tongue is innervated by the mandibular branch of the trigeminal nerve; another branch (the ophthalmic branch) innervates the eye. Tactile stimulation produces a signal that begins at the nerve ending, travels

along the peripheral nerve branch to the trigeminal ganglia; impulses are then transmitted to the secondary-order neuron in the spinal cord [59]. Our CTT test suggests cross-sensitization between trigeminal branches in cats with oral cancers. Most of literature used COBO aesthesiometer to investigate corneal sensitization [10,14] or ocular pain [52], and there is very little in the human literature on using COBO aesthesiometer to assess head pain sensitization; Vijayan *et al.* used this instrument and revealed the cluster headache pain did not involve trigeminal sensory pathway [58]. The present study showed cats with oral cancers had decreased corneal touch thresholds, which suggests that COBO could be used for assessing all sorts of cat orofacial pain that related to trigeminal sensory pathway.

As an initial evaluation of whether the methods used in the present study are able to detect reduced cancer pain after administration of an analgesic, we performed assessments before and after the administration of buprenorphine. Buprenorphine has been used as an analgesics that provides moderate analgesia for cats after ovariohysterectomy (acute pain) [54]. Although we did not detect statistically significant pain/sensitivity reduction, 4/5 cats had a trend of hyperalgesia improvement after buprenorphine administration in regards to FOPS-C scoring, MST at orofacial region, and the cornea touch (**Figure 4.9**); these results indicate that buprenorphine is able to provide at least some pain relief in cats with sublingual SCC and the pain relief can be detected during the pain assessments. However, buprenorphine can also cause sedation that affects pain measurement. Additionally, buprenorphine, although considered effective for perioperative pain, may not be as effective for cancer pain, possibly due to differing underlying mechanisms. A review from 19 studies indicated the efficacy of buprenorphine in cancer pain relief is still undetermined, but continues to be used as a fourth-line option compared to morphine, oxycodone, and fentanyl in human patients [51]. The incomplete reversal of sensitization/pain in

our study suggests more effective analgesics are needed.

We have shown that these methods can be used together to provide what we believe is a comprehensive pain assessment of orofacial pain phenotypes in cats with oral cancers. However, there are some limitations. We only enrolled cats with sublingual SCC, and it is unknown if the results are generalized to all oral cancers. For example, cats with mandibular or maxillary SCC often involve bone invasion and these may be associated with different types of behavioral changes and patterns of sensitivity. Moreover, due to the subjective nature of owner and clinician assessments, the responses can be affected by knowledge of the condition, visual cues such as a visible mass, bleeding or ptyalism. The way these factors would influence the assessment of response to treatments is unknown. If these instruments are to be successfully used to assess the efficacy of treatments, then they need to be evaluated under blinded, placebo-controlled conditions. Although our data indicated the subjective instruments appeared to be 'stable' in test – re-test conditions, it is unknown whether the variability we saw is greater or less than the changes associated with treatments. Such evaluation will also contribute to understanding the stability of the instruments over time. Other possible factors impacting our results include sex, breed and age; fortunately, the demographics were similar for our two groups. A major concern of the study is the sample size. The small sample size in with the group of oral cancers reduced the power of the statistics and increased the likelihood of type II error; results of our work should be verified using a larger sample size and/or in the second population of patients to ensure instrument's reliability and accuracy. Large scale institutional and inter-institutional consistency and verification should be performed to review the reproducibility of those measurements in cats with oral cancers.

In conclusion, initial validation of feline oral pain assessments was performed in the present study; we found evidence of test re-test, discriminatory and responsiveness validity when evaluating our methods in healthy cats and cats with sublingual SCC. This work should be extended to evaluate all sorts of head and neck region pain in cats, such as pain induced by brain disease or dental problems that could potentially serve as a spontaneous translational model. As patients with oral cancers may pursue treatment like radiation therapy or surgery, we should further evaluate pain sensitization associated with cancer treatment. These approaches will help in the development of cats with oral cancer as a translational model for oral cancer pain. Additionally, the methods we have described may assist the clinical veterinary team in measuring orofacial pain in cats with oral cancer, and thus enhance their ability to provide appropriate analgesia.

REFERENCES

[1] BarrettP, ScagliottiR, MeridethR, JacksonP, AlarconF. Absolute corneal sensitivity and corneal trigeminal nerve anatomy in normal dogs. Prog Vet Comp Ophthalmol 1991.

[2] BenitoJ, DePuyV, HardieE, ZamprognoH, ThomsonA, SimpsonW, RoeS, HansenB, LascellesBDX. Reliability and discriminatory testing of a client-based metrology instrument, feline musculoskeletal pain index (FMPI) for the evaluation of degenerative joint disease-associated pain in cats. Vet J 2013.

[3] BenitoJ, HansenB, DepuyV, DavidsonGS, ThomsonA, SimpsonW, RoeS, HardieE, LascellesBDX. Feline musculoskeletal pain index: Responsiveness and testing of criterion validity. J Vet Intern Med 2013.

[4] BilgicO, DudaL, SánchezMD, LewisJR. Feline oral Squamous cell carcinoma: Clinical manifestations and literature review. J Vet Dent 2015.

[5] BlockerT, Van DerWoerdtA. A comparison of corneal sensitivity between brachycephalic and Domestic Short-haired cats. Vet Ophthalmol 2001.

[6] BrayF, FerlayJ, SoerjomataramI, SiegelRL, TorreLA, JemalA. Global cancer statistics 2018: GLOBOCAN estimates of incidence and mortality worldwide for 36 cancers in 185 countries. CA Cancer J Clin 2018.

[7] BrileyJD, WilliamsMD, FreireM, GriffithEH, LascellesBDX. Feasibility and repeatability of cold and mechanical quantitative sensory testing in normal dogs. Vet J 2014.

[8] BrondaniJT, LunaSPL, PadovaniCR. Refinement and initial validation of a multidimensional composite scale for use in assessing acute postoperative pain in cats. Am J Vet Res 2011.

[9] BrondaniJT, MamaKR, LunaSPL, WrightBD, NiyomS, AmbrosioJ, VogelPR,

PadovaniCR. Validation of the English version of the UNESP-Botucatu multidimensional composite pain scale for assessing postoperative pain in cats. BMC Vet Res 2013.

[10] BrooksDE, ClarkCK, LesterGD. Cochet-Bonnet aesthesiometer-determined corneal sensitivity in neonatal foals and adult horses. Vet Ophthalmol 2000.

[11] BuismanM, HasiukMMM, GunnM, PangDSJ. The influence of demeanor on scores from two validated feline pain assessment scales during the perioperative period. Vet Anaesth Analg 2017.

[12] CalvoG, HoldenE, ReidJ, ScottEM, FirthA, BellA, RobertsonS, NolanAM. Development of a behaviour-based measurement tool with defined intervention level for assessing acute pain in cats. J Small Anim Pract 2014.

[13] Chan-LingT. Sensitivity and neural organization of the cat cornea. Investig Ophthalmol Vis Sci 1989.

[14] ChaoC, StapletonF, BadarudinE, GolebiowskiB. Ocular surface sensitivity repeatability with Cochet-Bonnet esthesiometer. Optom Vis Sci 2015.

[15] CostaYM, deAraújo-JúniorENS, FiedlerLS, deSouzaPRJ, SilvaLLCP, FerreiraDMAO, ContiPCR, BonjardimLR. Reproducibility of quantitative sensory testing applied to musculoskeletal orofacial region: Site and sex differences. Eur J Pain (United Kingdom) 2019.

[16] EltingLS, KeefeDM, SonisST, GardenAS, SpijkervetFKL, BaraschA, TishlerRB, CantyTP, KudrimotiMK, Vera-LlonchM. Patient-reported measurements of oral mucositis in head and neck cancer patients treated with radiotherapy with or without chemotherapy: Demonstration of increased frequency, severity, resistance to palliation, and impact on quality of life. Cancer 2008.

[17] EvangelistaMC, WatanabeR, O'TooleE, PangDSJ, SteagallPV. Facial expressions of pain in cats: development of the Feline Grimace Scale. Abstracts presented at the spring meeting of the Association of Veterinary Anaesthetists, Grenada, West Indies – 10–13 th March, 2018, published in Veterinary Anaesthesia and Analgesia.2018.

[18] DelFabbroE, CarmichaelA-N, MorganL. Identifying and assessing the risk of opioid abuse in patients with cancer: an integrative review. Subst Abuse Rehabil 2016.

[19] GiuffridaMA, BrownDC, EllenbergSS, FarrarJT. Development and psychometric testing of the Canine Owner-Reported Quality of Life questionnaire, an instrument designed to measure quality of life in dogs with cancer. J Am Vet Med Assoc 2018.

[20] GiuffridaMA, FarrarJT, BrownDC. Psychometric properties of the Canine Symptom Assessment Scale, a multidimensional owner-reported questionnaire instrument for assessment of physical symptoms in dogs with solid tumors. J Am Vet Med Assoc 2017.

[21] GoganP, GuéritaudJP, Horcholle-BossavitG, Tyc-DumontS. The vibrissal pad as a source of sensory information for the oculomotor system of the cat. Exp Brain Res 1981.

[22] GrantRA, HaidarliuS, KennerleyNJ, PrescottTJ. The evolution of active vibrissal sensing in mammals: Evidence from vibrissal musculature and function in the marsupial possum Monodelphis domestica. J Exp Biol 2013.

[23] GruenME, GriffithEH, ThomsonAE, SimpsonW, LascellesBDX. Criterion validation testing of clinical metrology instruments for measuring degenerative joint disease associated mobility impairment in cats. PLoS One 2015.

[24] GuillotM, MoreauM, HeitM, Martel-PelletierJ, PelletierJP, TroncyE. Characterization of osteoarthritis in cats and meloxicam efficacy using objective chronic pain evaluation tools. Vet J 2013.

[25] HealeyKAE, DawsonS, BurrowR, CrippsP, GaskellCJ, HartCA, PinchbeckGL, RadfordAD, GaskellRM. Prevalence of feline chronic gingivo-stomatitis in first opinion veterinary practice. J Feline Med Surg 2007.

[26] HoldenE, CalvoG, CollinsM, BellA, ReidJ, ScottEM, NolanAM. Evaluation of facial expression in acute pain in cats. J Small Anim Pract 2014.

[27] HonoréP, SchweiMJ, RogersSD, Salak-JohnsonJL, FinkeMP, RamnaraineML, ClohisyDR, MantyhPW. Cellular and neurochemical remodeling of the spinal cord in bone cancer pain. Prog Brain Res 2000.

[28] JääskeläinenSK. Clinical neurophysiology and quantitative sensory testing in the investigation of orofacial pain and sensory function. J Orofac Pain 2004.

[29] JungS. Exploratory factor analysis with small sample sizes: A comparison of three approaches. Behav Processes 2013.

[30] KlinckMP, GruenME, delCastilloJRE, GuillotM, ThomsonAE, HeitM, LascellesBDX, TroncyE. Development and preliminary validity and reliability of the montreal instrument for cat arthritis testing, for use by caretaker/owner, MI-CAT(C), via a randomised clinical trial. Appl Anim Behav Sci 2018.

[31] KlinckMP, MonteiroBP, LussierB, GuillotM, MoreauM, OtisC, SteagallPVM, FrankD, Martel-PelletierJ, PelletierJP, delCastilloJRE, TroncyE. Refinement of the Montreal Instrument for Cat Arthritis Testing, for Use by Veterinarians: detection of naturally occurring osteoarthritis in laboratory cats. J Feline Med Surg 2018.

[32] KlinckMP, RiallandP, GuillotM, MoreauM, FrankD, TroncyE. Preliminary validation and reliability testing of the montreal instrument for cat arthritis testing, for use by veterinarians, in a colony of laboratory cats. Animals 2015.

[33] KnazovickyD, HelgesonES, CaseB, GruenME, MaixnerW, LascellesBDX. Widespread somatosensory sensitivity in naturally occurring canine model of osteoarthritis. Pain 2016.

[34] LascellesBDX, BrownDC, ConzemiusMG, GillM, OshinskyML, SharkeyM. Measurement of chronic pain in companion animals: Discussions from the Pain in Animals Workshop (PAW) 2017. Vet J 2019.

[35] LascellesBDX, HansenBD, RoeS, DePuyV, ThomsonA, PierceCC, SmithES, RowinskiE. Evaluation of client-specific outcome measures and activity monitoring to measure pain relief in cats with osteoarthritis. J Vet Intern Med 2007.

[36] Lascelles DX, Flecknell PAS. Do Animal Models Tell Us about Human Pain? IASP Pain Clin Updat 2010.

[37] LynchS, Savary-BatailleK, LeeuwB, ArgyleDJ. Development of a questionnaire assessing health-related quality-of-life in dogs and cats with cancer. Vet Comp Oncol 2011.

[38] MacfarlaneTV., WirthT, RanasingheS, Ah-SeeKW, RennyN, HurmanD. Head and Neck Cancer Pain: Systematic Review of Prevalence and Associated Factors. J Oral Maxillofac Res 2012.

[39] MatosR, WangK, JensenJD, JensenT, NeumanB, SvenssonP, Arendt-NielsenL, JensenJD, JensenT, NeumanB, SvenssonP. Quantitative sensory testing in the trigeminal region: Site and gender differences. J Orofac Pain 2011.

[40] McNicolE, Horowicz-MehlerN, FiskRA, BennettK, Gialeli-GoudasM, ChewPW, LauJ, CarrD. Management of opioid side effects in cancer-related and chronic noncancer pain: A systematic review. J Pain 2003.

[41] MonteiroBP, SteagallPV. Chronic pain in cats: Recent advances in clinical assessment. J Feline Med Surg 2019.

[42] OneschukD, HansonJ, BrueraE. A survey of mouth pain and dryness in patients with advanced cancer. Support Care Cancer 2000.

[43] PiggM, Baad-HansenL, SvenssonP, DrangsholtM, ListT. Reliability of intraoral quantitative sensory testing (QST). Pain 2010.

[44] PoirierVJ, Kaser-HotzB, VailDM, StrawRC. Efficacy and toxicity of an accelerated hypofractionated radiation therapy protocol in cats with oral squamous cell carcinoma. Vet Radiol Ultrasound 2013.

[45] PortenoyRK. Treatment of cancer pain. Lancet 2011.

[46] ReidJ, NolanAM, ScottEM. Measuring pain in dogs and cats using structured behavioural observation. Vet J 2018.

[47] ReidJ, ScottEM, CalvoG, NolanAM. Definitive Glasgow acute pain scale for cats: validation and intervention level. Vet Rec 2017.

[48] ReidJ, Wiseman-OrrL, ScottM. Shortening of an existing generic online health-related quality of life instrument for dogs. J Small Anim Pract 2018.

[49] RipamontiCI, SantiniD, MaranzanoE, BertiM, RoilaF. Management of cancer pain: ESMO clinical practice guidelines. Ann Oncol 2012.

[50] RobertsonSA, LascellesBDX, TaylorPM, SearJW. PK-PD modeling of buprenorphine in cats: Intravenous and oral transmucosal administration. Journal of Veterinary Pharmacology and Therapeutics.2005.

[51] Schmidt-HansenM, BromhamN, TaubertM, ArnoldS. Buprenorphine for treating cancer pain. Cochrane Database Syst Rev 2013.

[52] SpiererO, FelixER, McClellanAL, ParelJM, GonzalezA, FeuerWJ, SarantopoulosCD, LevittRC, EhrmannK, GalorA. Corneal mechanical thresholds negatively associate with

dry eye and ocular pain symptoms. Investig Ophthalmol Vis Sci 2016.

[53] StathopoulouTR, KoukiM, PypendopBH, JohnstonA, PapadimitriouS, PelligandL. Evaluation of analgesic effect and absorption of buprenorphine after buccal administration in cats with oral disease. J Feline Med Surg 2018.

[54] SteagallPVM, TaylorPM, RodriguesLCC, FerreiraTH, MintoBW, AguiarAJA. Analgesia for cats after ovariohysterectomy with either buprenorphine or carprofen alone or in combination. Vet Rec 2009.

[55] StrackF. “Order Effects” in Survey Research: Activation and Information Functions of Preceding Questions. Context Effects in Social and Psychological Research.1992.

[56] StreinerDL, NormanGR. Health Measurement Scales: A practical guide to their development and use. 2008 p.

[57] VardehD, NaranjoJF. Peripheral and central sensitization. Pain Medicine: An Essential Review.2017.

[58] VijayanN, WatsonC. Corneal Sensitivity in Cluster Headache. Headache J Head Face Pain 1985.

[59] WalkerHK. Cranial Nerve V: The Trigeminal Nerve. 1990 p.

[60] WoolfCJ. Central sensitization: Implications for the diagnosis and treatment of pain. Pain 2011.

[61] World Health Organization. WHOQOL Measuring Quality of Life. Psychol Med 1998.

[62] WypijJM. A naturally occurring feline model of head and neck squamous cell carcinoma. Patholog Res Int 2013.

[63] YazbekKVB, FantoniDT. Validity of a health-related quality-of-life scale for dogs with signs of pain secondary to cancer. J Am Vet Med Assoc 2005.

Table 4.1 Summary of demographics of cats with sublingual SCC and healthy controls.

	FOSCC (n = 5)	Control (n = 12)	All (n = 17)	*P* value
Sex				
Male castrated	2	5	7	
Female spayed	3	7	10	
Age				**0.005**
Median	10	4.5	5	
Range (min-max)	9-14	1.5-15	1.5-15	
Mean	10.6	5.042	6.676	
SD	1.949	3.72	4.157	
SEM	0.8718	1.074	1.008	
Bodyweight				0.0761
Median	4.35	3.43	4.13	
Range (min-max)	3.3-5.05	3.05-4.59	3.05-5.05	
Mean	4.351	3.71	4.162	
SD	0.6322	0.6313	0.6819	
SEM	0.1825	0.2823	0.1654	
Breed				
Domestic short hair	4	9	13	
Domestic long har	1	1	2	
Bengal	0	2	2	

Table 4.2 Codes assigned to each item in client questionnaire.

Question items	Code-Frequency	Code- Severity
General behavior		
· Had low energy?	QF-01	QS-01
· Was reluctant to wake up?	QF-02	QS-02
· Had altered mood?	QF-03	QS-03
· Had trouble getting comfortable?	QF-04	QS-04
· Growled or groaned when resting?	QF-05	QS-05
· Could not maintain hygiene (i.e., grooming)?	QF-06	QS-06
· Had decreased appetite?	QF-07	QS-07
· Drank less water than usual?	QF-08	QS-08
· Had trouble positioning to defecate/urinate?	QF-09	QS-09
Activity		
· Had trouble with mobility?	QF-10	QS-10
· Fell or lost balance?	QF-11	QS-11
· Did not do what he/she likes (e.g. chasing, playing, etc.)?	QF-12	QS-12
· Did not act like his/her normal self?	QF-13	QS-13
· Had decreased enjoyment of life?	QF-14	QS-14
· Did not sleep well?	QF-15	QS-15
Interaction		
· Was unwilling to be near me?	QF-16	QS-16
· Showed a decreased amount of affection?	QF-17	QS-17
· Did not like to be pet or touched?	QF-18	QS-18
Orofacial discomfort		
· Had excessive drooling?	QF-19	QS-19
· Had difficulty eating his/her normal food?	QF-20	QS-20
· Was offered and had trouble eating soft food?	QF-21	QS-21
· Had trouble lying down his/her head?	QF-22	QS-22
· Felt discomfort or pain near the mouth?	QF-23	QS-23
· Was defensive when their head was touched?	QF-24	QS-24

Table 4.3 QOL questionnaire category scores of median (range) value between the healthy control and cats with oral SCC in QOL questionnaire.

Question item	Frequency			Severity		
	Control	FOSCC	*P*-value	Control	FOSCC	*P*-value
General behavior	0 (0-3)	8 (6-14)	0.0002	0 (0-3)	7 (6-8)	0.0002
Activity	0 (0-3)	6 (3-8)	0.0003	0 (0-3)	5 (2-8)	0.0005
Interaction	0 (0-3)	0 (0-3)	>0.9999	0 (0-2)	0 (0-3)	0.9644
Orofacial discomfort	0 (0-5)	13 (6-16)	0.0002	0 (0-2)	11 (6-13)	0.0002
Subtotal	0 (0-11)	25 (18-37)	0.0002	0 (0-9)	21 (18-28)	0.0002

Table 4.4 Comparisons of the median (range) value between the healthy control and cats with oral SCC in QOL questionnaire.

Question item	Frequency			Severity		
	Control	FOSCC	*P*-value	Control	FOSCC	*P*-value
General behavior						
Q-01	0 (0-2)	2 (0-3)	**0.0079**	0 (0-1)	1 (0-2)	**0.0047**
Q-02	0 (0-0)	0 (0-1)	0.0735	0 (0-0)	0 (0-1)	0.2353
Q-03	0 (0-2)	0 (0-2)	0.4916	0 (0-2)	0 (0-1)	>0.9999
Q-04	0 (0-1)	2 (0-3)	**0.004**	0 (0-1)	1 (0-2)	**0.0168**
Q-05	0 (0-0)	0 (0-2)	0.2941	0 (0-0)	0 (0-1)	0.2778
Q-06	0 (0-0)	3 (2-3)	**0.0002**	0 (0-0)	3 (1-3)	**0.0001**
Q-07	0 (0-1)	1 (0-2)	**0.0399**	0 (0-1)	1 (0-2)	**0.0229**
Q-08	0 (0-0)	0 (0-2)	0.25	0 (0-0)	0 (0-2)	0.2353
Q-09	0 (0-0)	0 (0-3)	0.2941	0 (0-0)	0 (0-3)	0.2778
Activity						
Q-10	0 (0-0)	0 (0-1)	0.2941	0 (0-0)	0 (0-1)	0.2778
Q-11	0 (0-0)	0 (0-0)	>0.9999	0 (0-0)	0 (0-0)	>0.9999
Q-12	0 (0-1)	2 (0-3)	**0.004**	0 (0-1)	1 (0-3)	**0.0047**
Q-13	0 (0-1)	2 (0-3)	**0.0021**	0 (0-1)	2 (0-2)	**0.0032**
Q-14	0 (0-2)	1 (0-4)	0.0632	0 (0-1)	1 (0-2)	**0.035**
Q-15	0 (0-0)	0 (0-1)	0.0735	0 (0-0)	0 (0-2)	0.0654
Interaction						
Q-16	0 (0-1)	0 (0-0)	>0.9999	0 (0-1)	0 (0-0)	>0.9999
Q-17	0 (0-1)	0 (0-2)	0.6765	0 (0-1)	0 (0-2)	0.6814
Q-18	0 (0-3)	0 (0-1)	0.7689	0 (0-1)	0 (0-1)	>0.9999
Orofacial discomfort						
Q-19	0 (0-0)	3 (1-4)	**0.0002**	0 (0-0)	3 (2-4)	**0.0001**
Q-20	0 (0-1)	3 (1-4)	**0.0003**	0 (0-1)	2 (1-4)	**0.0002**
Q-21	0 (0-0)	3 (1-4)	**0.0002**	0 (0-0)	2 (1-3)	**0.0001**
Q-22	0 (0-0)	0 (0-2)	0.0735	0 (0-0)	0 (0-2)	0.0654
Q-23	0 (0-2)	2 (0-4)	**0.006**	0 (0-1)	2 (0-4)	**0.0016**
Q-24	0 (0-3)	0 (0-0)	0.5588	0 (0-1)	0 (0-0)	0.5752

Table 4.5 FOPS-C scores, median (range) and comparisons of the median value between the healthy control and cats with oral SCC.

Category	Control	FOSCC	Median difference (95% CI)	*P*-value
Miscellaneous behavior	0 (0-0)	2 (1-3)	2 (1, 3)	**0.0002**
Palpation around the mouth cavity	0 (0-3)	1 (0-1.5)	1 (0, 1.5)	**0.0205**
Reaction to palpation of the head	0 (0-0)	0 (0-0.5)	0 (0, 0.5)	0.2941
Vocalization	0 (0-1)	0 (0-0.5)	0 (0, 0.5)	0.5378
Posture	0 (0-0.5)	0 (0-1)	0 (0, 0.5)	**0.1324**
Comfort	0 (0-1)	0.5 (0-1.5)	0.5 (0, 1.5)	**0.0021**
Activity	0 (0-1)	1 (0-3)	1 (0, 2)	**0.0273**
Attitude	0 (0-0.5)	0.5 (0-2)	0.5 (0, 1.5)	**0.006**
Appetite	0 (0-0)	1 (0-2)	1 (0, 2)	**0.0021**
Total score	0 (0-7)	6 (4-13)	6 (4, 8)	**0.0011**

Table 4.6 Mean score of FOPS-C in the individual cats with oral SCC.

Category	FOSCC#1	FOSCC#2	FOSCC#3	FOSCC#4	FOSCC#5
Miscellaneous behavior	1.5	2	2	1	3
Palpation around the mouth cavity	0	1.5	0.5	1.5	1
Reaction to palpation of the head	0.5	0	0	0	0
Vocalization	0	0	0	0.5	0.5
Posture	0	0	0.5	0	1
Comfort	0.5	0.5	1	0	1.5
Activity	0	3	1	0	2
Attitude	0.5	0.5	1	0	2
Appetite	1	0.5	0	2	2
Total score	4	8	6	5	13

Table 4.7 Descriptive statistics (mean ± SD and range) and comparisons of the mean value between the healthy control and cats with oral SCC in mechanical sensitive threshold (MST, measured by EVF) and CTT (measured by COBO aesthesiometer).

Category	Control	FOSCC	Mean difference (95% CI)	*P*-value
MST (g)				
Right intermandibular space	260.7 ± 58.7	115.1 ± 29.5	-145.6 ± 27.95 (-205.2, 86.0)	0.0001
Left intermandibular space	212.8 ± 47.5	96.67 ± 38.4	-116.1 ± 24.1 (-167.5, -64.7)	0.0002
Right maxilla	231.3 ± 86.0	174.5 ± 62.0	-56.76 ± 42.8 (-147.9, 34.4)	0.2043
Right metacarpus	346 ± 37.3	249.3 ± 91.5	-96.72 ± 30.4 (-161.4, -32)	0.0061
CCT (cm)	2.04 ± 0.53	3.18 ± 0.58	1.14 ± 0.29 (0.5, 1.8)	0.0013

Table 4.8 Descriptive statistics (mean ± SD and range) and comparisons of orofacial pain measurement results before buprenorphine administration (Test 1), after buprenorphine administration (BUP), and the following day (Test 2).

Pain test	Test 1 (Baseline)	BUP	Test 2	Mean difference between Test 1 and BUP (95% CI)	*P*-value	Mean difference between BUP and Test 2 (95% CI)	*P*-value
FOPS-C							
Total score	7.4 ± 4.0	4.4 ± 3.4	7 ± 3.61	-3 ± 2.9 (-6.62, 0.62)	0.1875	2.6 ± 1.14 (1.184, 4.016)	0.0625
MST (g)							
Ipsilateral intermandibular space	102.7±34.7	172.6±59.3	114.3±39.96	69.87±66.52 (-12.72, 152.5)	0.0786	-58.3 ±82.64 (-160.9, 44.3)	0.1898
Contralateral intermandibular space	110.6±47.3	147.4±53.4	95.96±33.18	36.76±50.84 (-26.37,99.89)	0.1813	-51.43±53.11 (-117.4, 14.5)	0.0963
Ipsilateral maxilla	181.6±59.9	258.5±126.9	167.4±88.99	76.89±89.55 (-34.3,188.1)	0.1273	-91.08±83.1 (-194.3,12.1)	0.0704
Right metacarpus	225.7±81.8	221.8±118.8	209.9±67.26	-3.9±179.1 (-288.9,281.1)	0.9680	-11.89±141.9 (-237.7,213.9)	0.8776
CCT (cm)	3±0.41	2±1.08	2.88±0.48	-1±1.08 (-2.72, 0.72)	0.1612	0.875±1.49 (-1.5, 3.25)	0.3258

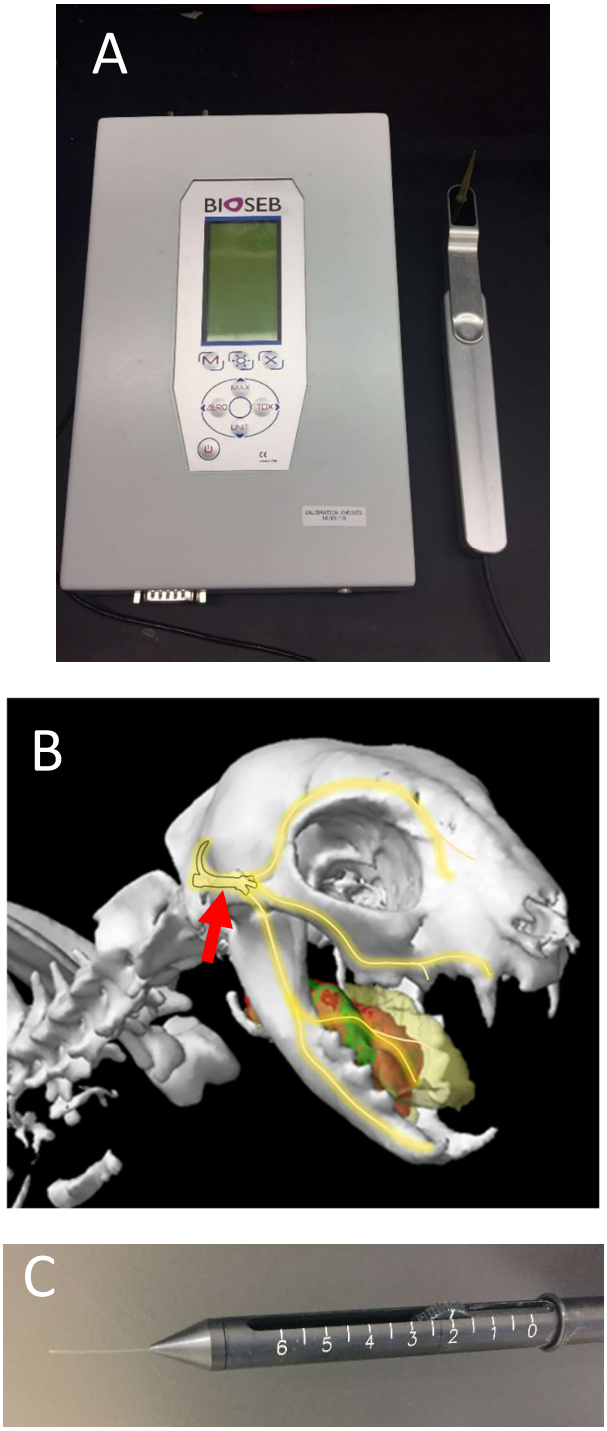

Figure 4.1 Mechanical QST test device (A) Electronic von Frey (B) Test sites were based on the branches of the trigeminal nerve. The afferent nerve transfers impulses from the first order neurons (in the trigeminal ganglia; arrow), to the thalamus. (C) Cochet-Bonnet aesthesiometer was used for measuring corneal touch threshold on the left eye.

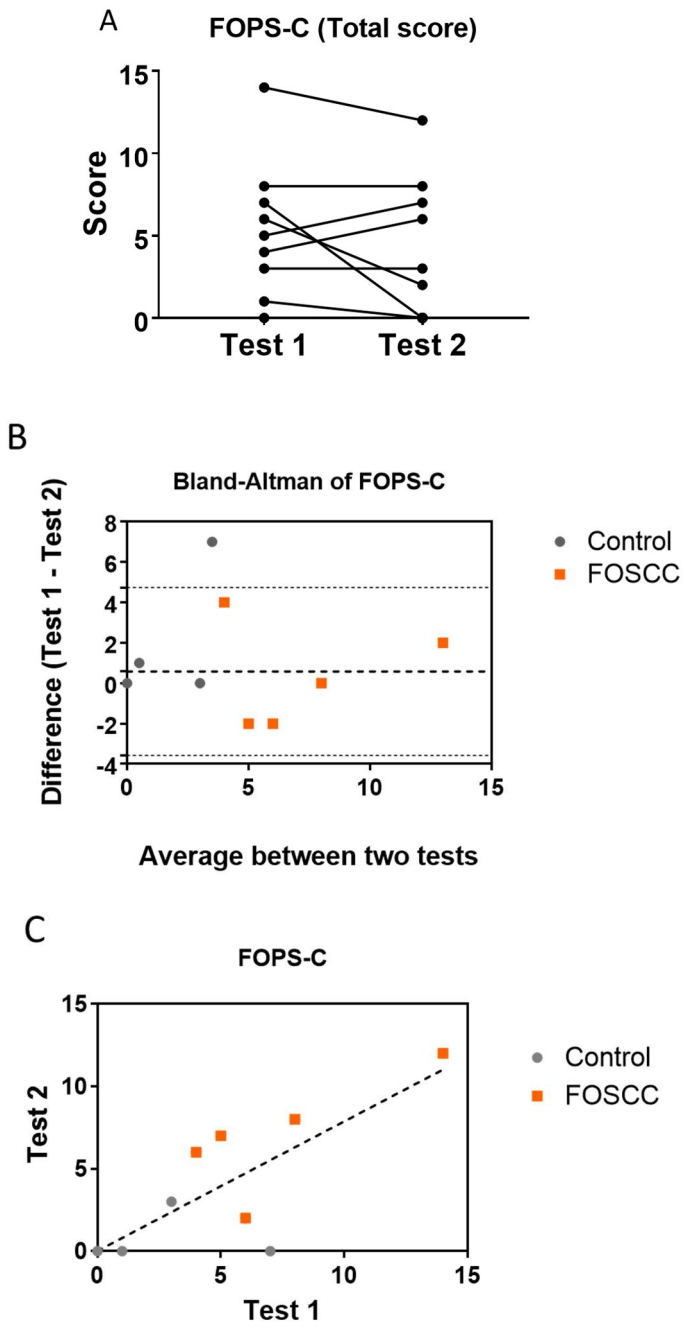

Figure 4.2 Test – re-test reliability evaluation of clinician-based feline orofacial cancer pain scoring (A) Wilcoxon matched-pairs signed rank test showed non-significant difference between the first and the second scoring. (B) The mean difference between two scores was 0.5882 ± SD 2.123. (C) The two scores had good, and statistically significant correlation (r^2 = 0.728, $P < 0.0001$)

Figure 4.3 Test – re-test reliability analysis of EVF measurements and COBO aesthesiometer measurements. The Wilcoxon matched-pairs test (left) the mean ± SD of the differences between two tests were 5.46 ± 69.21. The Bland-Altman plot (middle) and the correlation (right) between test 1 and test 2. Orange points, cats with sublingual SCC; gray points, control cats.

Right intermandibular space (EVF)

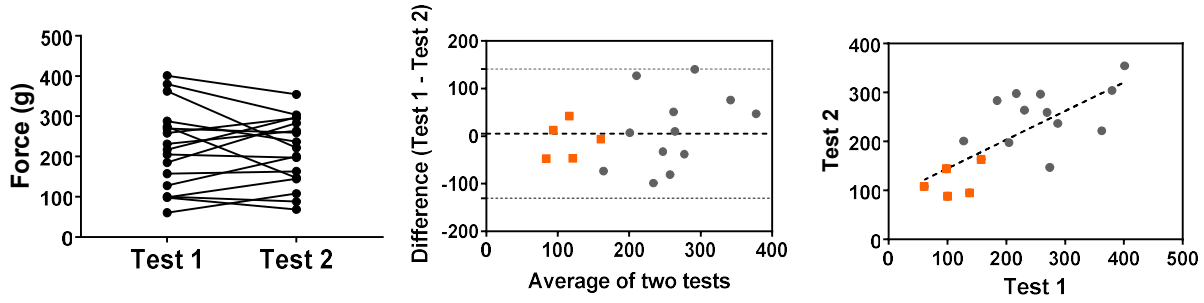

Left intermandibular space (EVF)

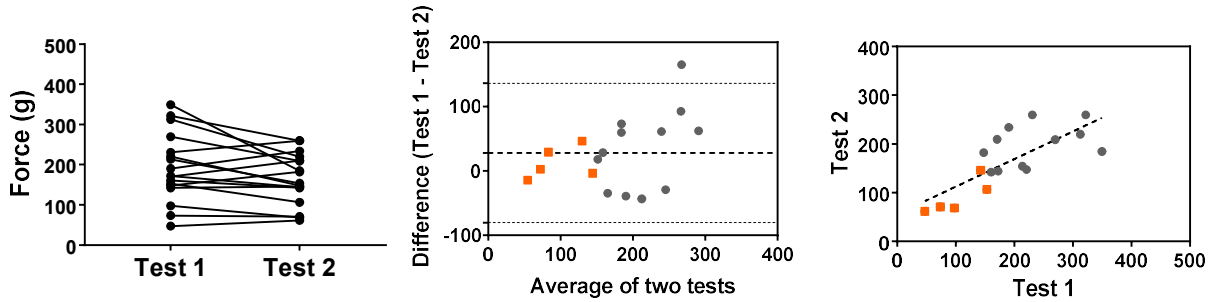

Right maxilla (EVF)

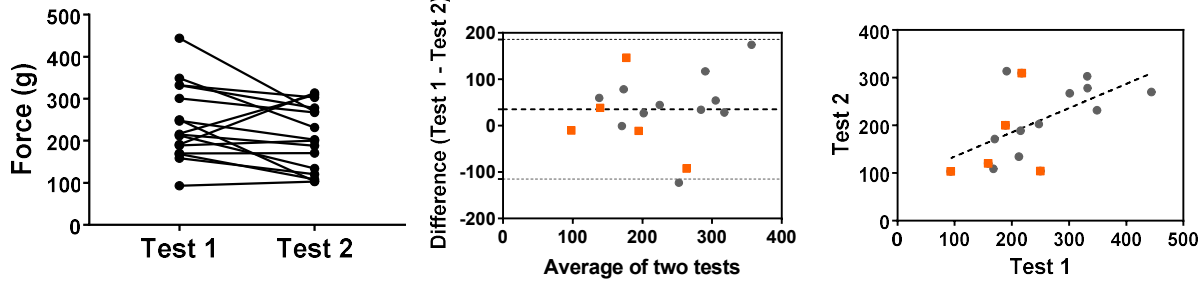

Right metacarpus (EVF)

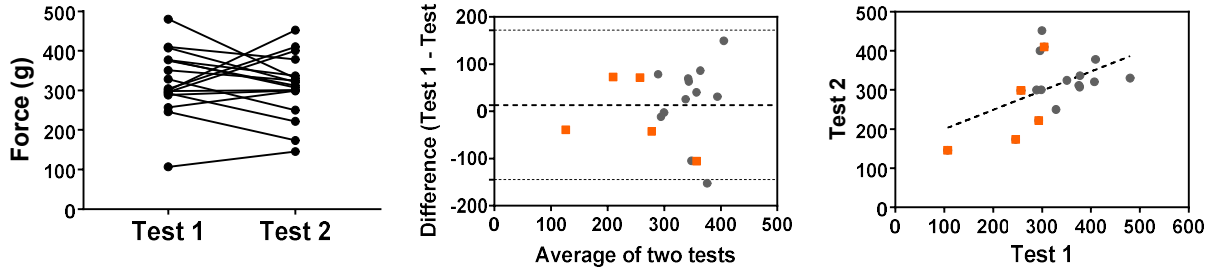

Left cornea (COBO aesthesiometer)

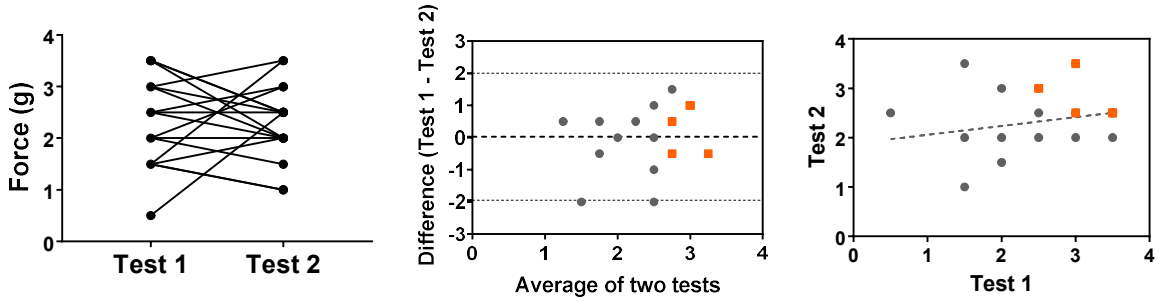

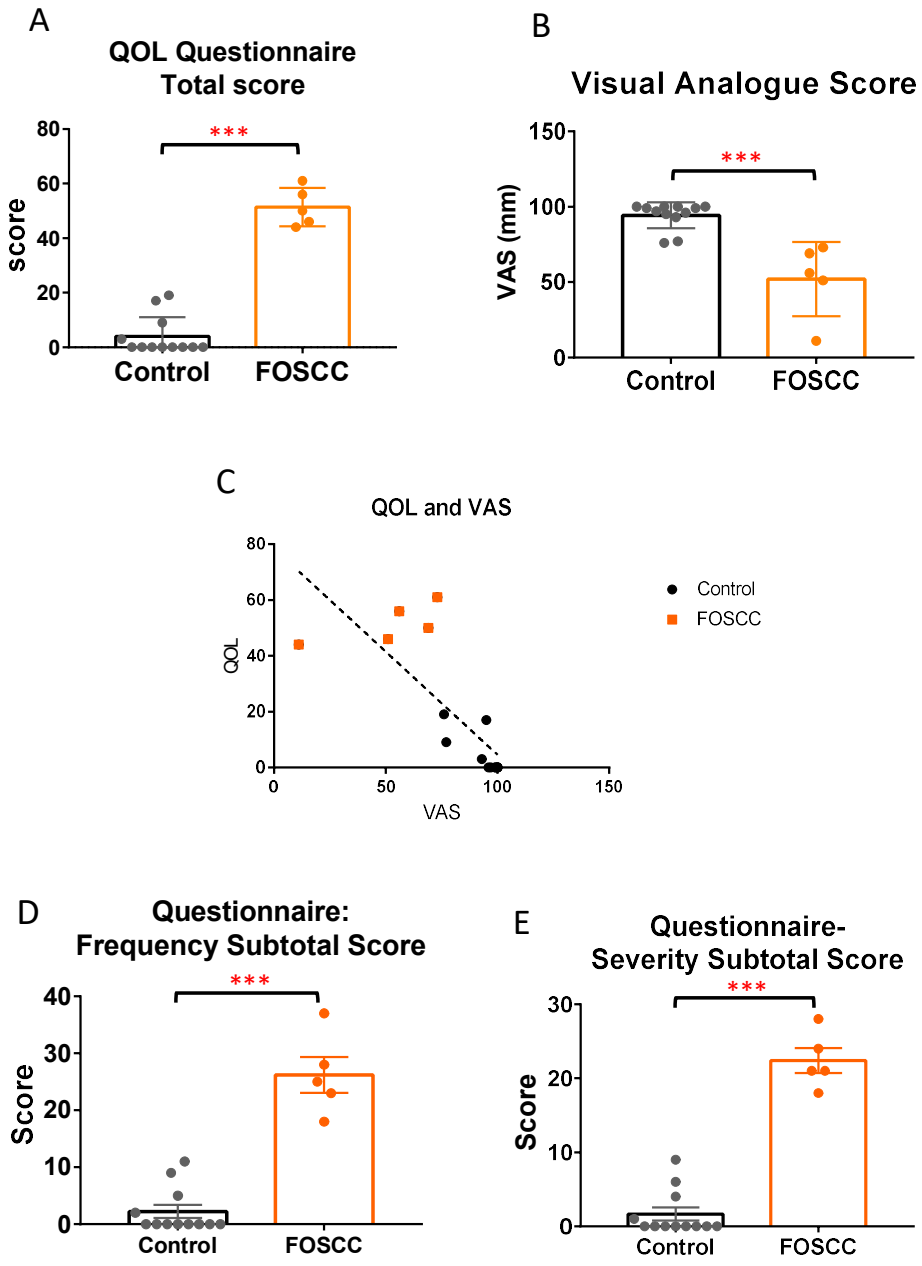

Figure 4.4 Statistical analysis of owner-reported QOL questionnaire (A) The VAS was significantly lower and (B) the total score of questionnaires was significantly higher in cat with oral cancer pain. (C) The correlation of total score of QOL questionnaire and VAS was statistically significant ($P = 0.0002$). The subtotal score of (D) frequency and (E) severity evaluation also found higher scores in cats with oral cancer pain. ***$P < 0.001$, Mann-Whitney test, each dot represents the score of individual cats. All error bars depict SD.

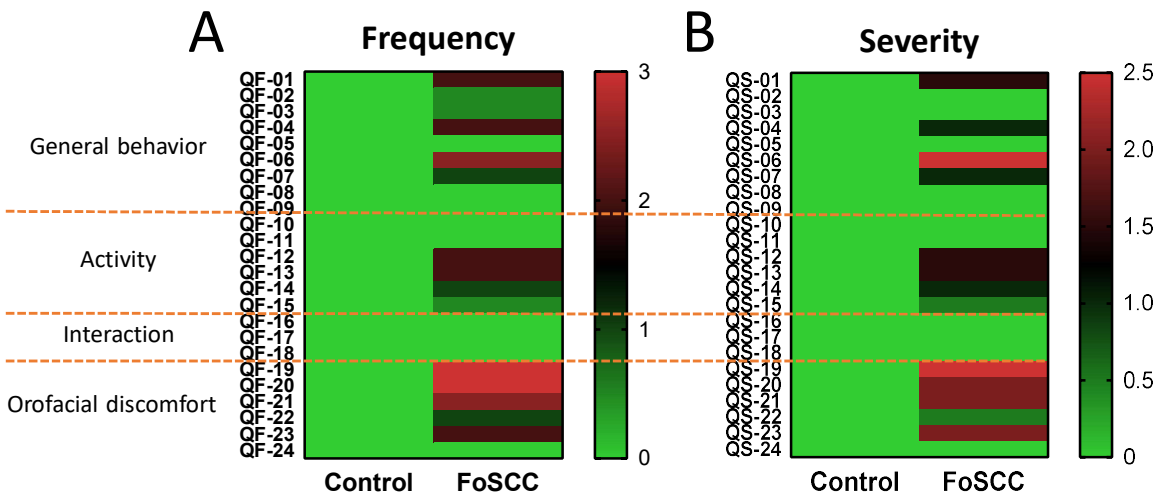

Figure 4.5 The frequency and severity of observations in the owner-reported QOL questionnaire. The represented questions and codes are listed in (**Table 4.2**). The most frequent observations (A) were excessive drooling, and trouble eating normal food; with regards to severity (B), the mean scores for hygiene and drooling were the highest in cats with oral cancers when compared to other questions.

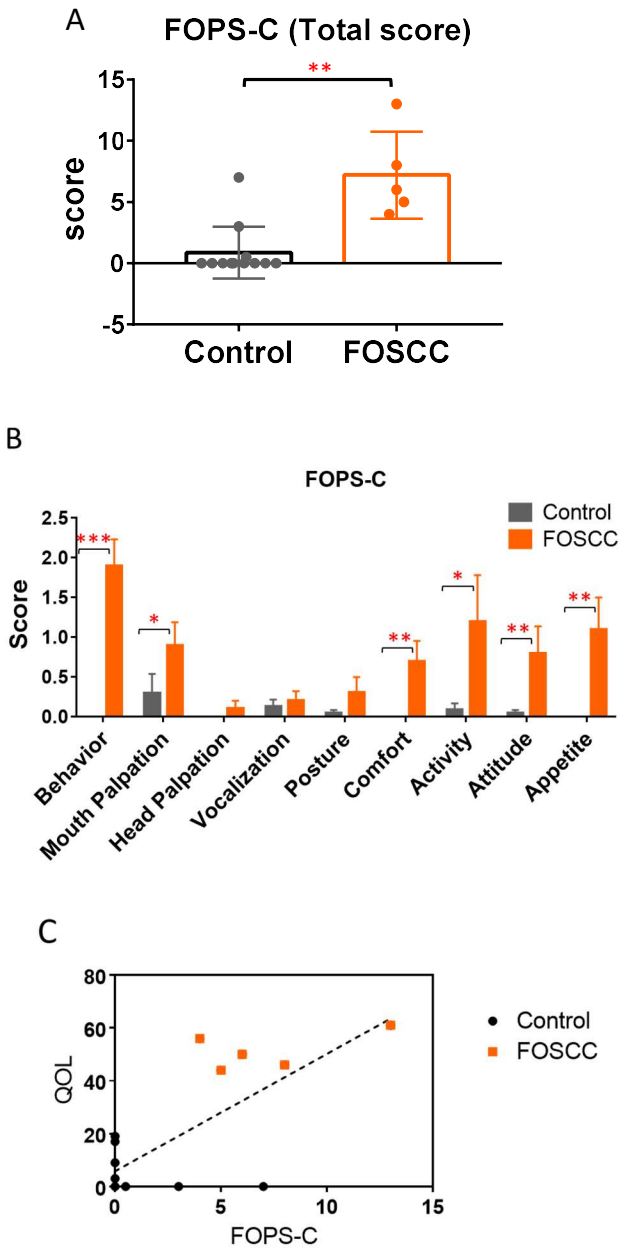

Figure 4.6 Clinician-based feline orofacial cancer pain scoring. (A) Cats with oral cancers showed a significantly higher total score than healthy cats. (B) Cats with oral tumors had significantly higher score in the category of miscellaneous behavior, mouth palpation, comfort, activity, attitude and appetite. (C) The FOPS-C scores were significantly correlated to QOL questionnaire score ($P = 0.0007$). *$P < 0.05$, **$P < 0.01$ ***$P < 0.001$, Mann-Whitney test, each dot represents the score of individual cats. All error bars depict SD.

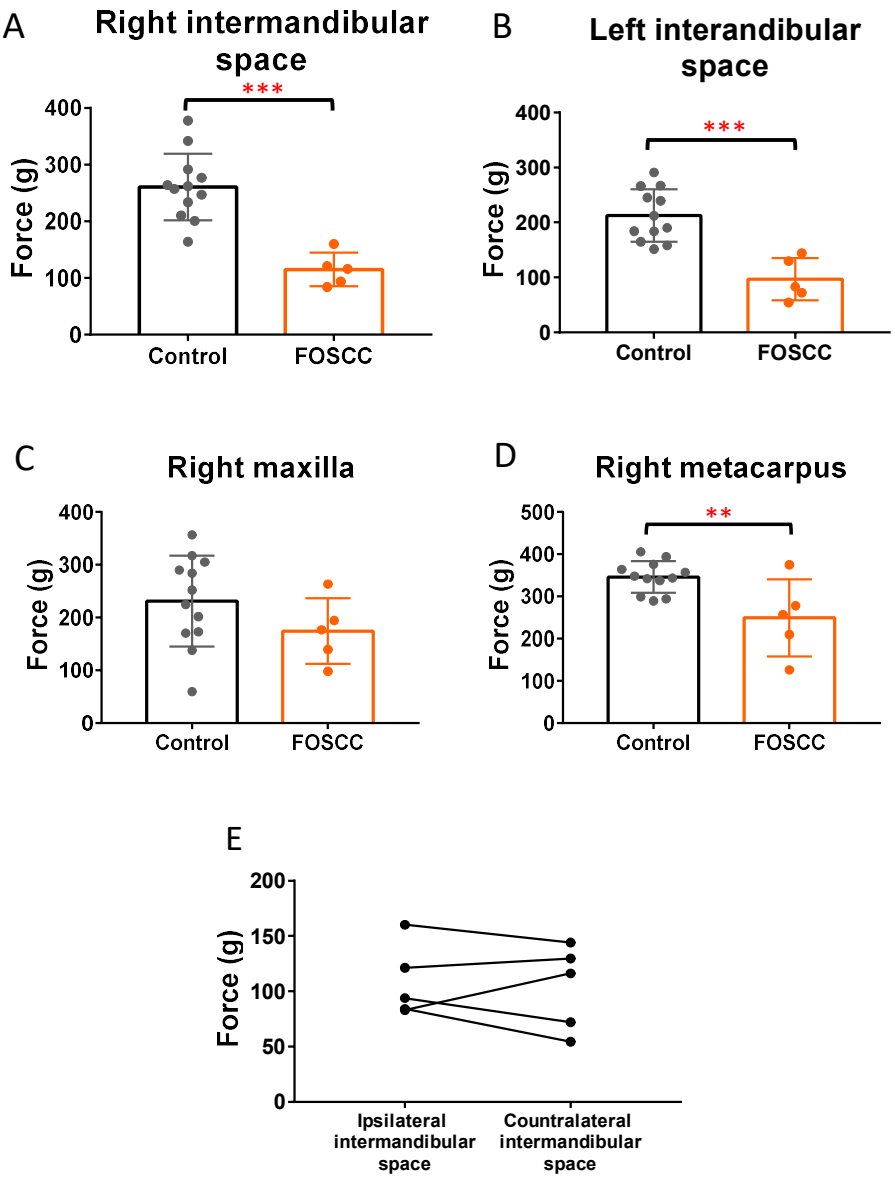

Figure 4.7 Electronic von Frey showed that cats with sublingual SCC were more sensitive to pressure in the (A) right and (B) left intermandibular areas. (C) Thresholds measured over the maxillary region were not statistically different between the two groups. (D) Cancer cats had more prominent general pain sensitization far outside of the tumor location at right metacarpal region. (E) There is no significant difference between the QST values at tumor side and the opposite side of mandibular region in cats with sublingual SCC. $*P < 0.05$, $**P < 0.01$, $***P < 0.001$, *t*-test, each dot represents the measurement of individual cats. All error bars depict SD.

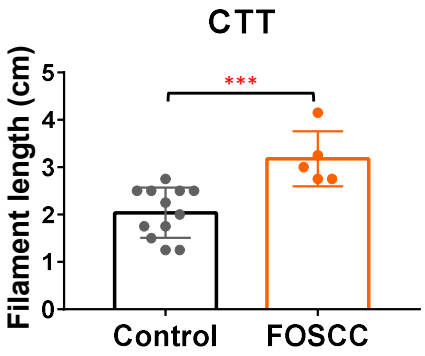

Figure 4.8 COBO aesthesiometer tested on the left cornea showed that cats with oral cancers were more sensitive on central corneal touch, which provides evidence for peripheral sensitization in the facial region. ***$P < 0.001$, *t*-test, each dot represents the measurement of individual cats. All error bars depict SD.

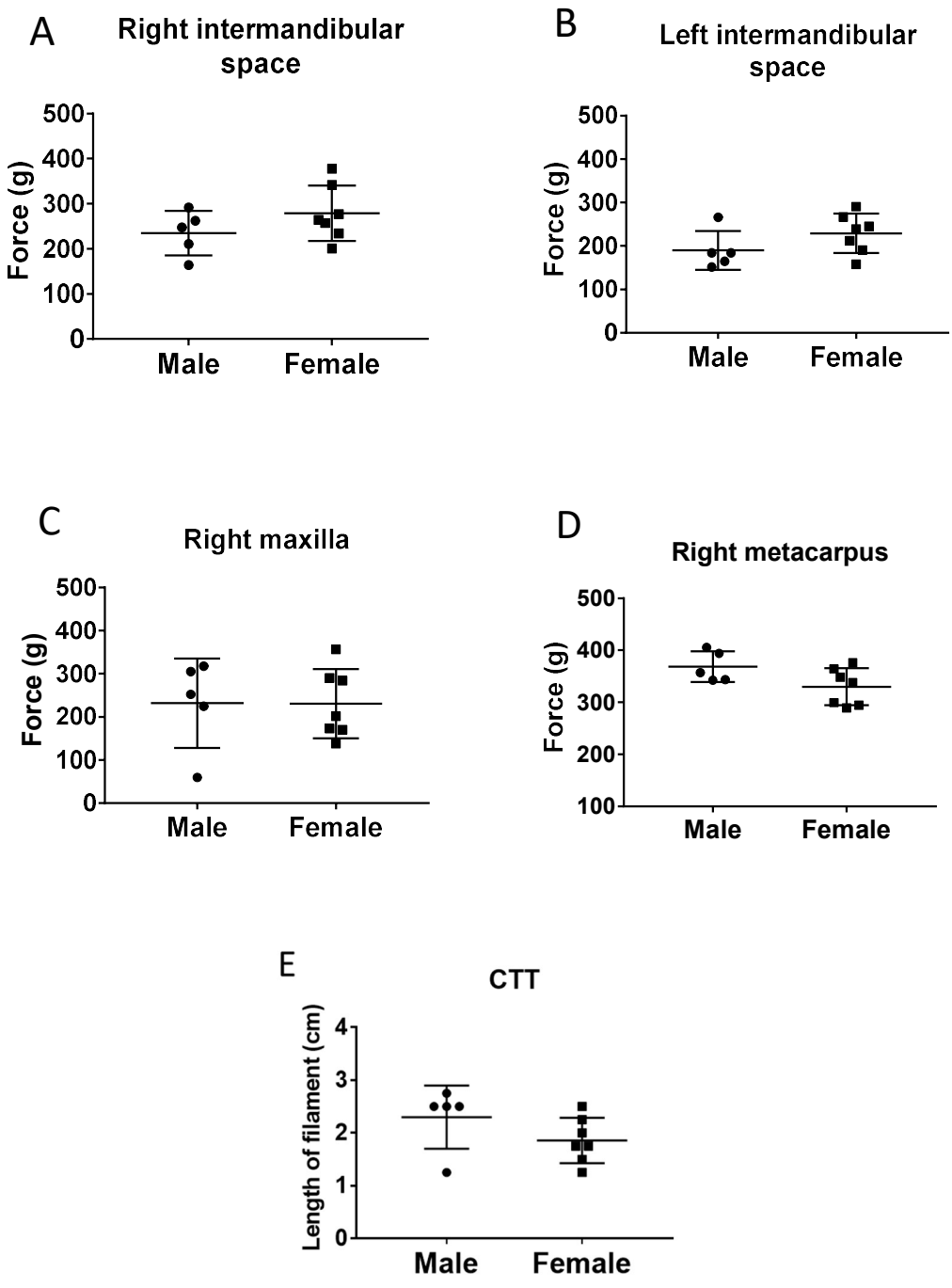

Figure 4.9 The sex differences of EVF (A-D) and COBO aesthesiometer (E) measurement in healthy cats. There was no significant difference of mean ± SD between male (n=5) and female (n=7) in orofacial mechanical QST measured in healthy cats.

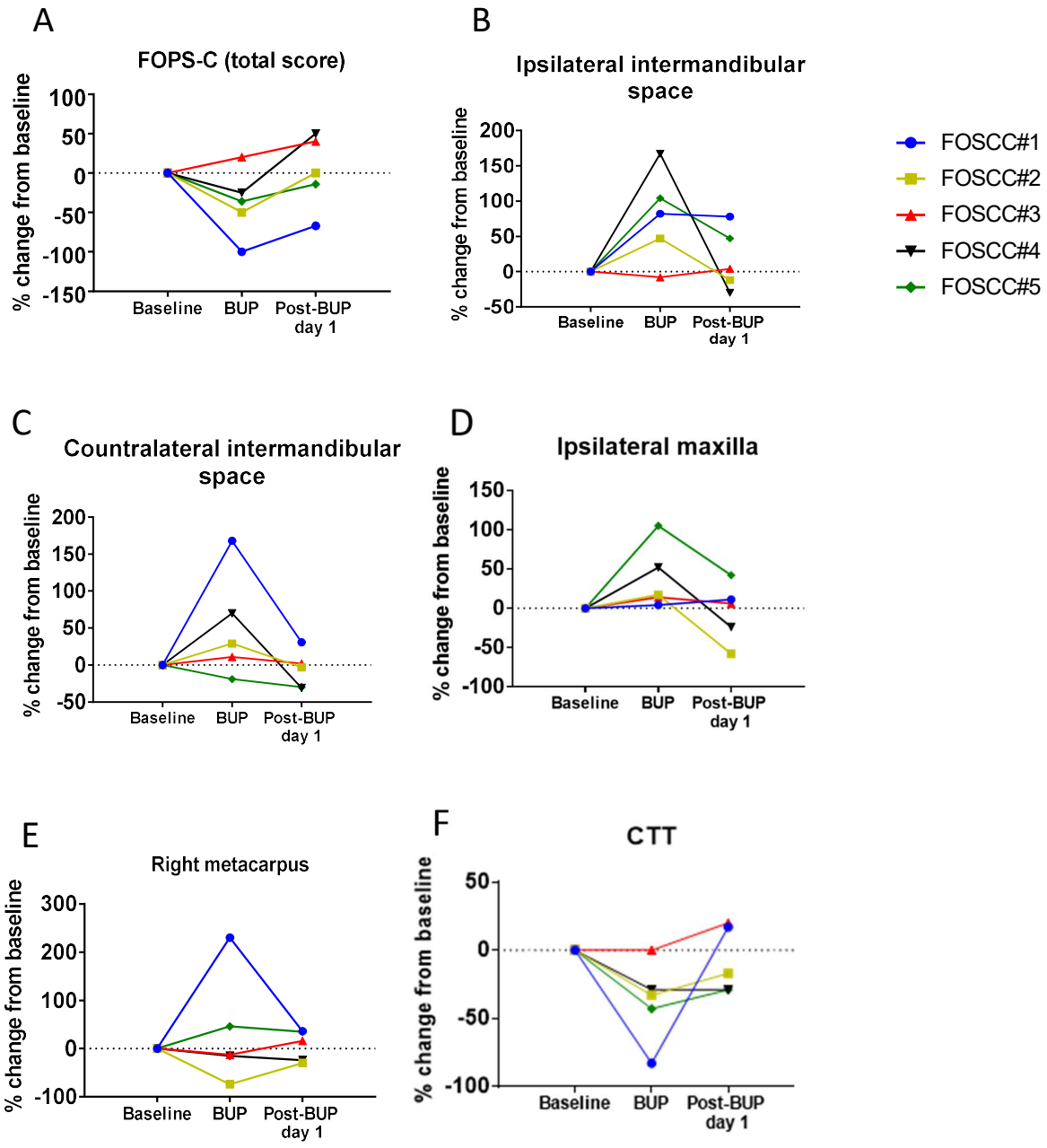

Figure 4.10 Sensitivity testing was performed in the cats with oral cancers via the (A) FOPS-C test, (B-E) EVF test, and (F) COBO aesthesiometer test. Most of the cats (4/5) had decreased hypersensitization in orofacial pain measurements. Buprenorphine did not reduce the QST at right metacarpal region in (3/5) cats.

CHAPTER 5: Conclusions and Future Direction

The purposes of this work were to: (1) identify the role of TRP channels in radiation-associated orofacial pain; and (2) develop and credential tools that can be used in modeling of the orofacial pain experienced by HNC patients. The present work developed a system for non-invasive induction of reversible grade 3 glossitis in CD-1 female mice using 27 Gy in a single fraction. We also found that in this model, TRPV1 in trigeminal ganglia is upregulated when glossitis is most severe. Those results were compared to two control groups: (1) sham irradiation; and (2) low-dose total body irradiation (to mimic scattering of radiation dose outside of the oral cavity when mice undergo high dose lingual irradiation). With the latter control group, we have demonstrated that scattered dose does not significantly impact either TRPV1 function or protein expression. To characterize the impact of lingual irradiation on TRP channel biology, we further evaluated TRPV1 and TRPV4 expression and function in the time course of day 1 to day 45 post-irradiation. The present study (Chapter 3) has shown that TRPV1 and TRPV4 are activated before glossitis is clinically observed; that activation is persistent even after glossitis has healed. Moreover, not only the expression of TRPV1 and TRPV4 are upregulated, but we also found *Trpa1*, *Trpm8,* and *Gfra-3* gene expressions are increased when glossitis is severe. The present work suggests that the upregulated function and expression of nociceptors induced by high-dose irradiation can be potential targets for treating RAP.

This dissertation summarizes work that was done to improve the utility of experimental tools for studying acute radiation-induced orofacial pain in mice; it also builds upon previous work to investigate possible mechanisms of RAP [5]. Here, we also investigated orofacial pain in pet cats that had spontaneously-occurring locally-advanced lingual SCC. Several instruments were developed to characterize pain in pet cats with oral cancers; our results showed the FORQ

(owner-reported QOL questionnaire), FOPS-C (clinician-based pain scale), electronic von Frey (mechanical sensory threshold), and Cochet-Bonnet Aesthesiometer (corneal touch threshold) were capable of discriminating healthy cats from those with oral cancer. Those instruments were also reliable in the test-retest scenario and capable of measuring the effect of pain medication (as shown by their responsiveness to opioid analgesics) in cats. In our study, we showed that cats with sublingual SCC had decreased QOL and increased multidimensional pain; we found evidence that pain sensitization in feline oral cancer patients involves not only peripheral sensitization, but also central sensitization.

Overall, we showed that TRP channels are associated with radiation-induced pain sensitization and we were able to detect pain in pet cats with spontaneous lingual SCC. In future studies, knockout mice should be used to determine if those TRP channels are necessary for pain induction after irradiation. Because we found upregulation of the *Trpm8* and *Gfrα-3* genes, it would also be interesting to know if the function of TRPM8 and GFR-α3 receptors in sensory neurons is activated after lingual irradiation. Understanding this could be achieved by using calcium imaging with the stimuli: menthol and artemin; these compounds are the agonists of TRPM8 and GFR-α3, respectively. We have performed some pilot studies (data not shown) that provide preliminary evidence that TRPM8 functional changes accompany the gene expression changes. As it has been shown the artemin, the agonist of GFR-α3, can induce both TRPM8 and TRPV1 activation in sensory neurons [2,4], future work might target GFR-α3 blockade and evaluate the role of GFR-α3 in radiation-induced pain. To support the molecular biological observations made herein, orofacial pain behavioral tests can be refined and performed (see Chapter 3) to more comprehensively evaluate orofacial hypersensitivity.

We have provided initial validation for feline orofacial cancer pain assessment using

various instruments; this study has set the stage for potential future use of cats as a RAP model. However, as we had a limited sample number, a larger population should be studied to confirm assay reliability between observers and institutions. In the future, those instruments used in our study could also be applied to cats with orofacial cancers at different sites other than sublingual SCC (e.g., mandibular SCC). With standardized pain measurement, we can compare the level of pain mitigation from different therapeutics in cancer patients. This translational research could be applied for development of novel analgesics. For example, TRPV1/4 has been shown to be a potential therapeutic target for RAP in our murine model; with the instruments we've developed, we may now be able to study cats with RAP, to help understanding if targeting TRPV1/4 will benefit patients with naturally occurring cancer; this could provide convincing data to compel human clinical trials. In addition to cats, pet dogs could be another good translational model for investigating cancer pain and RAP. The clinical pain instruments presented in this study can be modified for dog patients. Dogs having oronasal tumors could be enrolled for assessing pain sensitization by questionnaire, clinician pain scale, and thermal/mechanical QST. Since there is a higher number of dogs that are treated with radiation therapy, versus cats (approximately four times more dog patients, based on a 2010 survey) [3], pet dogs may be a better translational model for investigating radiation-induced orofacial pain.

REFERENCES

[1] BoriaAJ, Perez-TorresCJ. Minimal difference between fractionated and single-fraction exposure in a murine model of radiation necrosis. Radiat Oncol 2019.

[2] ElittCM, MalinSA, KoerberHR, DavisBM, AlbersKM. Overexpression of artemin in the tongue increases expression of TRPV1 and TRPA1 in trigeminal afferents and causes oral sensitivity to capsaicin and mustard oil. Brain Res 2008.

[3] FarrellyJ, McenteeMC. A survey of veterinary radiation facilities in 2010. Vet Radiol Ultrasound 2014.

[4] LippoldtEK, ElmesRR, McCoyDD, KnowltonWM, McKemyDD. Artemin, a glial cell line-derived nurotrophic factor family member, induces TRPM8-dependent cold pain. J Neurosci 2013.

[5] NolanMW, LongCT, MarcusKL, SarmadiS, RobackDM, FukuyamaT, BaeumerW, LascellesBDX. Nocifensive behaviors in mice with radiation-induced oral mucositis. Radiat Res 2017;187:397–403. doi:10.1667/RR14669.1.

APPENDICES

APPENDIX A: Chapter 2 Supplemental Data

Material and methods

Rotarod

The rotarod device (Rota Rod Rotamex 5, Columbus Instrument, Columbus, OH) was used to ensure that the observed changes in burrowing behavior were not due to impaired motor function in irradiated mice. Four mice were randomly assigned into 27 Gy tongue-irradiated group and four into the sham-irradiated group. For each run, the mouse was placed on an accelerating rod whose speed started from 4 revs/min, and increased by 1.5 rev/min every 10 seconds, with a cut-off speed of 41.5 revs/min. The time to fall from the rod was recorded. The mean of the four trials performed at each time point was used for data analysis. Two training runs were performed on each mouse before the experiment. The test was performed at baseline (one day before irradiation), day 1, 5, and 10 post-irradiation with 4 trials per time point per mouse.

Nerve tracing

DiI (1,1'-dioctadecyl-3,3,3',3'-tetramethylindocarbocyanine perchlorate) is a lipophilic carbocyanine dye that has been used as a neuron-tracer [2]. It has been shown that a higher proportion of trigeminal neurons are sensitized after high-dose lingual irradiation, compared to sham, but it is unknown where the peripheral terminals of these neurons are located [5]. The purpose of neuron retrograde tracing was to confirm that the sensitized neurons were from the nerve afferents of the tongue. The DiI was dissolved in DMSO to obtain a final concentration of 5 mg/mL (0.5% w/v). The mice were anesthetized (isoflurane) and 5 μL of DiI solution was injected into the tip of the tongue via 31 G insulin needle. To determine how soon after injection

the fluorescent DiI label can be detected, the mice were euthanized at 1, 2, 3, and 4 days (2 mice in each time point) after injection. Trigeminal ganglia were collected and cultured for imaging (see the description of calcium imaging in the main body). As the trauma induced by the DiI injection may affect the results of tongue irradiation-associated pain, this assay was not performed in the main study.

Order effect of added stimuli in calcium imaging

To confirm that the calcium imaging results were not significantly affected by the order in which compounds (stimuli) were added, an additional experiment was performed wherein the order of histamine, TNF-α, and capsaicin addition was randomized. The compound KCl was applied as a positive control at the end of imaging. The methods of calcium imaging were described in Chapter 2. Four mice (without irradiation) were used in this experiment. The results were compared to the data from the sham irradiated group (n = 8), in which the stimuli with the order of: (1) histamine, (2) TNF-α, and (3) capsaicin.

Results

Nerve tracing

In TG, the proportions (percentages) of DiI-labeled neurons on day 1-4 after injection were 1/256 (0.4%), 5/134 (3.7%), 9/213 (4.2%), and 10/92 (10.9%), respectively (**Supplemental Figure 2.1**). However, the wound caused by the injection took approximately five days to recover. To avoid biasing our results with tongue-injection associated pain, DiI injection was not performed in subsequent tongue-irradiation experiments.

Rotarod

There were no significant differences in latency to fall between tongue-irradiated and sham-irradiated mice at any of the tested time points (**Supplemental Figure 2.2**). The mean latency to fall in tongue-irradiated and sham-irradiated mice was increased on day 1 (288.9 and 303.4 seconds, respectively) and day 5 (312.8 and 327.6 seconds, respectively) from baseline (203.5 and 219.9 seconds, respectively). On day 10, the latency was shorter than day 5 in both groups, but the mice still stayed 37.3 % and 29.5% longer than the baseline in tongue-irradiated and sham-irradiated mice, respectively. There was no significant difference between the two groups at any time point, as evaluated using the Mann-Whitney test. Although the latency to fall in these two groups showed an increasing trend from baseline to day 5, there was no significant difference between baseline and each time point (Wilcoxon matched-pairs test).

Substance order effect in calcium imaging

The order in which stimuli were added did not affect the calcium imaging results. With the order of histamine, TNF-α, and capsaicin, the proportion of neuron that responded was 13, 12, and 22%, respectively. With the random order of added stimuli, there were 16, 9, and 25% of the neurons responded to histamine, TNF-α, and capsaicin, respectively.

Conclusion of nerve tracing

Retrograde DiI labeling was performed to identify TG neurons that innervate the tongue. The proportion of labeled TG neurons increased, daily. However, we observed DiI injection-associated trauma that may bias the results from the radiation-induced damage. The fluorescence signals of DiI were also low, suggesting that without significant assay optimization, this technique was insufficient for our needs.

We observed that the fluorescence of DiI in mouse TG neurons can last at least 4 days after injection; but it is unclear how long the fluorescence can last. If the fluorescence lasts for weeks *in vivo*, then DiI injection at the tip of the tongue could theoretically be performed 1-2 weeks prior to irradiation. This would allow injection-associated trauma and pain to subside before irradiation, and thus allow us to more robustly study the impact of radiation on specific/identifiable tongue-derived TG neurons. Alternatively, one could inject the neuron tracer into the superficial nerves of both the ophthalmic (V1) and maxillary branches (V2), at the supraorbital foramen and infraorbital foramen, to label neurons from those branches, but without traumatizing lingual tissues. With this technique, the assumption would be that unlabeled neurons are derived from the mandibular branch. Another strategy would be to use resiniferatoxin (RTX), which can mediate ablation of TRPV1-positive nerve fibers [3,4,6]. As described before, we can use RTX to ablate the afferent neurons of ophthalmic and maxillary branch that express TRPV1; afterwards, most remaining TRPV1-positive neurons in the trigeminal ganglia would be from mandibular branch, thus theoretically allowing us to investigate the proportion of responsive sensory neurons in calcium imaging that are from the mandibular branch.

REFERENCES

[1] BrämersonA, NymanJ, NordinS, BendeM. Olfactory loss after head and neck cancer radiation therapy. Rhinology 2013.

[2] HeilingoetterCL, JensenMB. Histological methods for ex vivo axon tracing: A systematic review. Neurol Res 2016.

[3] JeffryJA, YuSQ, SikandP, PariharA, EvansMS, PremkumarLS. Selective targeting of TRPV1 expressing sensory nerve terminals in the spinal cord for long lasting analgesia. PLoS One 2009.

[4] MishraSK, HoonMA. Ablation of TrpV1 neurons reveals their selective role in thermal pain sensation. Mol Cell Neurosci 2010.

[5] NolanMW, LongCT, MarcusKL, SarmadiS, RobackDM, FukuyamaT, BaeumerW, LascellesBDX. Nocifensive Behaviors in Mice with Radiation-Induced Oral Mucositis. Radiat Res 2017;187:397–403. doi:10.1667/RR14669.1.

[6] OlahZ, SzaboT, KaraiL, HoughC, FieldsRD, CaudleRM, BlumbergPM, IadarolaMJ. Ligand-induced Dynamic Membrane Changes and Cell Deletion Conferred by Vanilloid Receptor 1. J Biol Chem 2001.

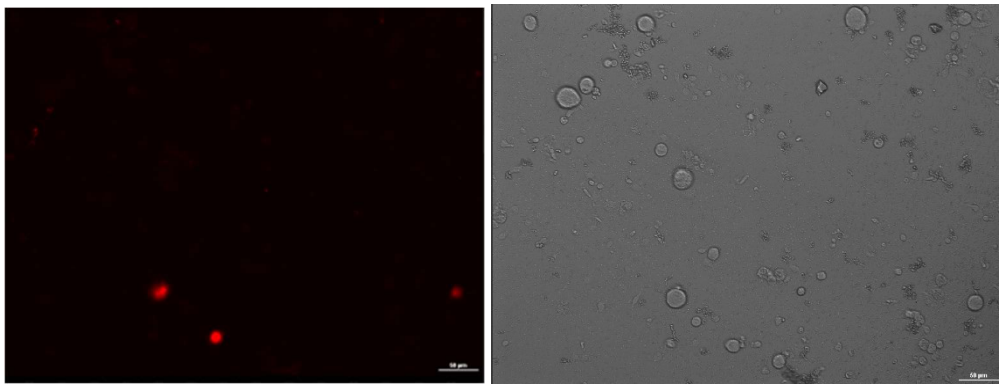

Supplemental Figure 2.1 Example of neurons labeled with DiI. The DiI solution was injected into the tip of the tongue. The trigeminal neurons from this representative animal were isolated and cultured on day 4 post-DiI injection. The same field of view was imaged with fluorescent channel of excitation wavelength 594 nm (left pane) and bright field (right pane).

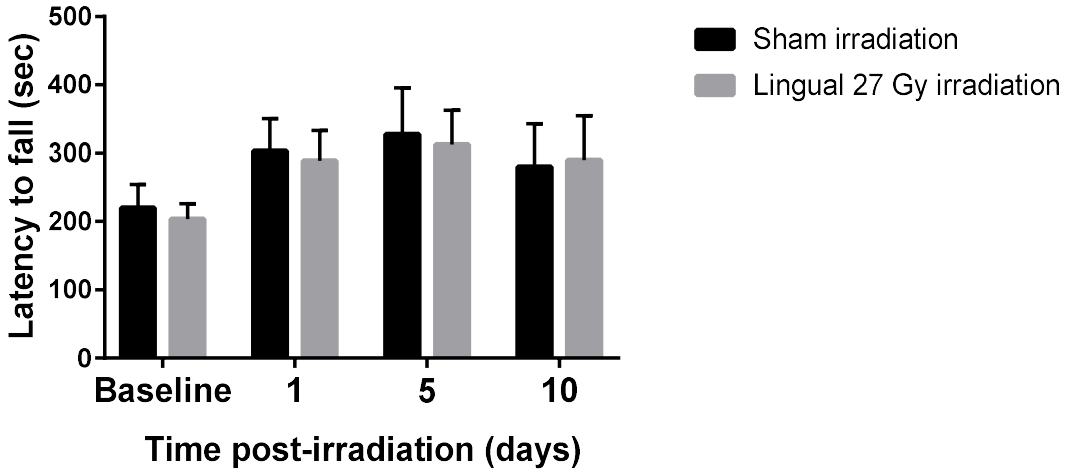

Supplemental Figure 2.2 The latency to fall in rotarod (mean and SEM) after lingual irradiation. There is no significantly difference of rotarod performance between these two groups. Mann-Whitney test; n = 4, all error bars depict SEM. In each group, there is no significant difference between baseline and other three time points; the comparisons were made by Wilcoxon matched-pairs test.

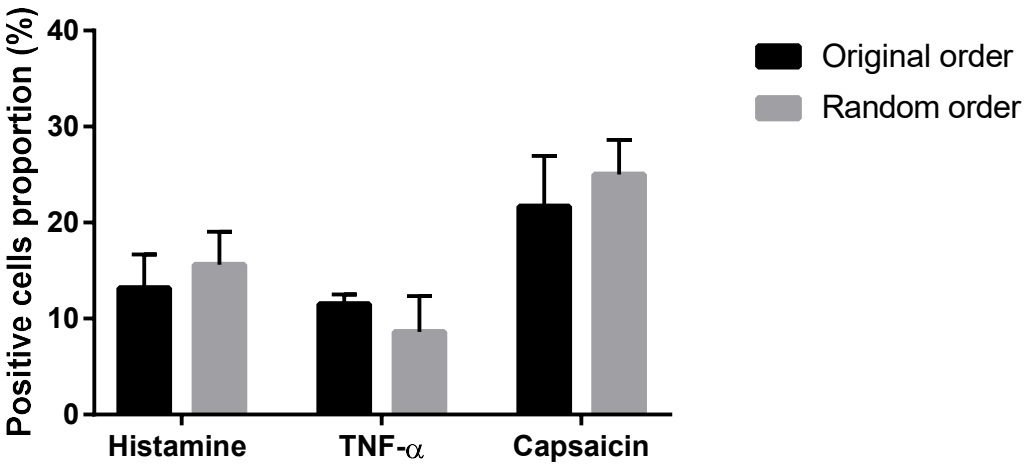

Supplemental Figure 2.3 The impact of stimulus addition on calcium imaging results. The order of the stimuli between histamine, TNF-α, and capsaicin did not affect the proportion of responsive neurons. The neurons were pooled from 8 mice (total neuron number = 207) in original order (histamine, TNF-alpha, and capsaicin) group; 4 mice (total neurons number = 210) in random order group. Fisher's exact test, all error bars depict SEM.

APPENDIX B: Chapter 3 Supplemental Data

Orofacial mechanical stimulation assay

Spontaneous pain was measured using the orofacial stimulation test (Ugo Basile, Gemonio, Italy). A water bottle containing a solution of 2:1 water to sweetened condensed milk was provided in a cage. A plate with an opening was set close to the end of the sipper tube. By inserting their snout into the opening of the plate, the mouse is able to lick the sipper tube and drink sweetened milk from the bottle. Thin metal wires are attached to the opening of the plate; these apply (presumably mildly noxious) mechanical stimulation to the face. Thus, this assay is intended to report on the animal's willingness/ability to withstand mild discomfort in order to get a treat. An optical sensor was built behind the plate to count the duration of beam break, which indicated the amount of time the mouse spends drinking the reward. A total of 16 mice were equally assigned to 27 Gy tongue irradiated group and total body 1.6 Gy irradiated group. Single mouse was acclimated in the cage for 10 minutes, then tested for 10 minutes. The test was performed once before the irradiation, and every other day after irradiation starting from day 1 to day 28 post-irradiation. The statistical analysis was made by two-way ANOVA test with Sidak's multiple comparisons test.

Results and discussion of orofacial mechanical stimulation assay

On day 11 post-irradiation, mice that had severe glossitis significantly drank (or attempted to drink) more than control mice (TBI 1.6 Gy, $P = 0.002$, **Supplemental Figure 3.1**). This was surprising, as we had expected that mice with orofacial radiation-associated pain would avoid inserting their snout into the window with thin metal wires. However, one possible explanation for the seemingly paradoxical result is that sweetened milk may provide pain relief for mice with

painful glossitis; this suggests that mice may have been self-medicating. A study investigating neonatal pain showed that glucose can reduce pain intensity of infants after lancing [1]. Here, we used a sweetened liquid in hopes that it would maximize fluid intake during a short test-period. However, using water instead of sweetened milk may be better for directly quantifying orofacial radiation pain. Another possible explanation for our unexpected result is that the wires may mimic the effect of scratching; this is logical to consider because in the previous study, mice with RIM more frequently scratch than sham-irradiated mice [2]. Therefore, attempts to rub their snout in this mechanical stimulation test may have indicated itch and discomfort.

Additional discussion of molecular assays

In calcium imaging, the comparisons of 27 Gy lingual-irradiation, TBI 1.6 Gy and sham-irradiation were made within the same time point. We used a different way to compare the expression level in qPCR, Western blot and IFA; the samples from day 11, sham-irradiated mice served as controls due a relatively high sample number (n =4); and because these samples were most consistently analyzed on multiple plates, using them as a control also helped avoid issues associated with comparing between various batches. In qPCR, the sham-irradiated mice on days 1 and 5 had a high expression levels in all genes (data not shown), which may due to the use of a different batch of qPCR primer. Those samples were obtained after we completed the qPCR experiments on samples from TBI and 27 Gy tongue-irradiated mice. In Western blot, there were more samples from day 11 sham-irradiated mice than other time points. Mann-Whitney test was used to compare the expression level of TRPV1/4 on day 11 in sham-irradiated mice to other time points, and it showed that there is no statistical significance, which indicates that aging did not affect TRPV1/4 expression in our study. Due to those technical errors and issue of low

sample numbers on other time points, we decided to use sample from day 11, sham-irradiated mice as the control in qPCR, Western blot, and IFA, so that the materials used among the samples were the same batch and from the same company; this maximized internal experimental consistency, and also ensured that the sample numbers were high enough for a reasonable statistical analysis.

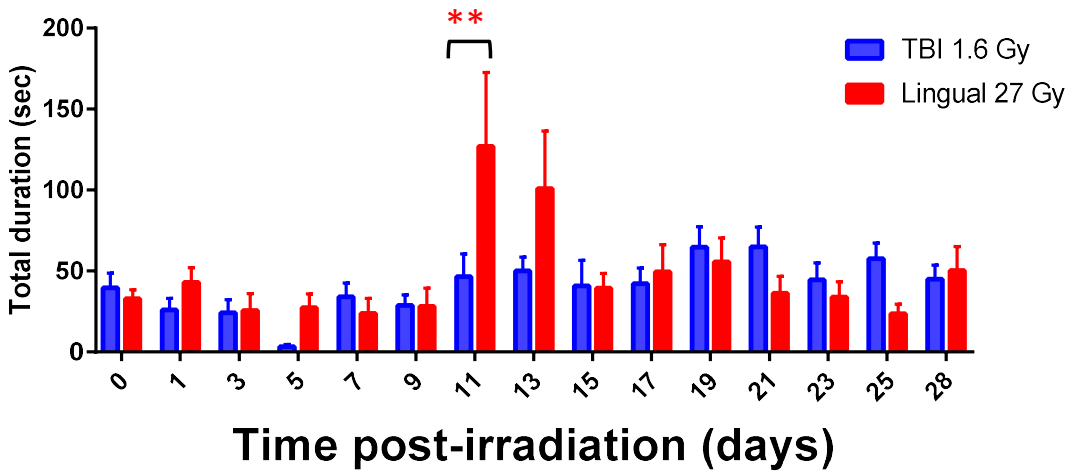

Supplemental Figure 3.1 Orofacial mechanical stimulation assay. On day 11 post-irradiation, mice having undergone tongue-irradiation place their snouts into the window significantly longer than mice having had TBI 1.6 Gy. $^{**}P < 0.01$, n=8, two-way ANOVA test.

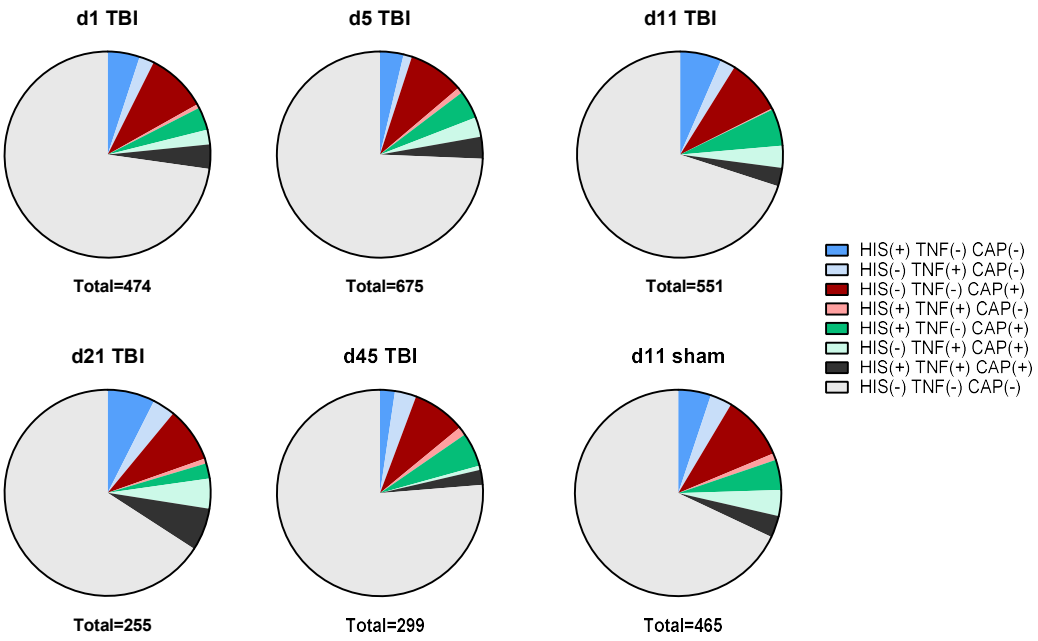

Supplemental Figure 3.2 The pie chart of neurons from mice having undergone TBI 1.6 Gy that responded to certain stimuli in calcium imaging. The proportion of neurons that responded to all three stimuli was consistent from day 1 (3.8%), 5 (3.4%), 11 (2.9%) and 45 (2.3%), but was slightly higher at day 21 (6.7%).

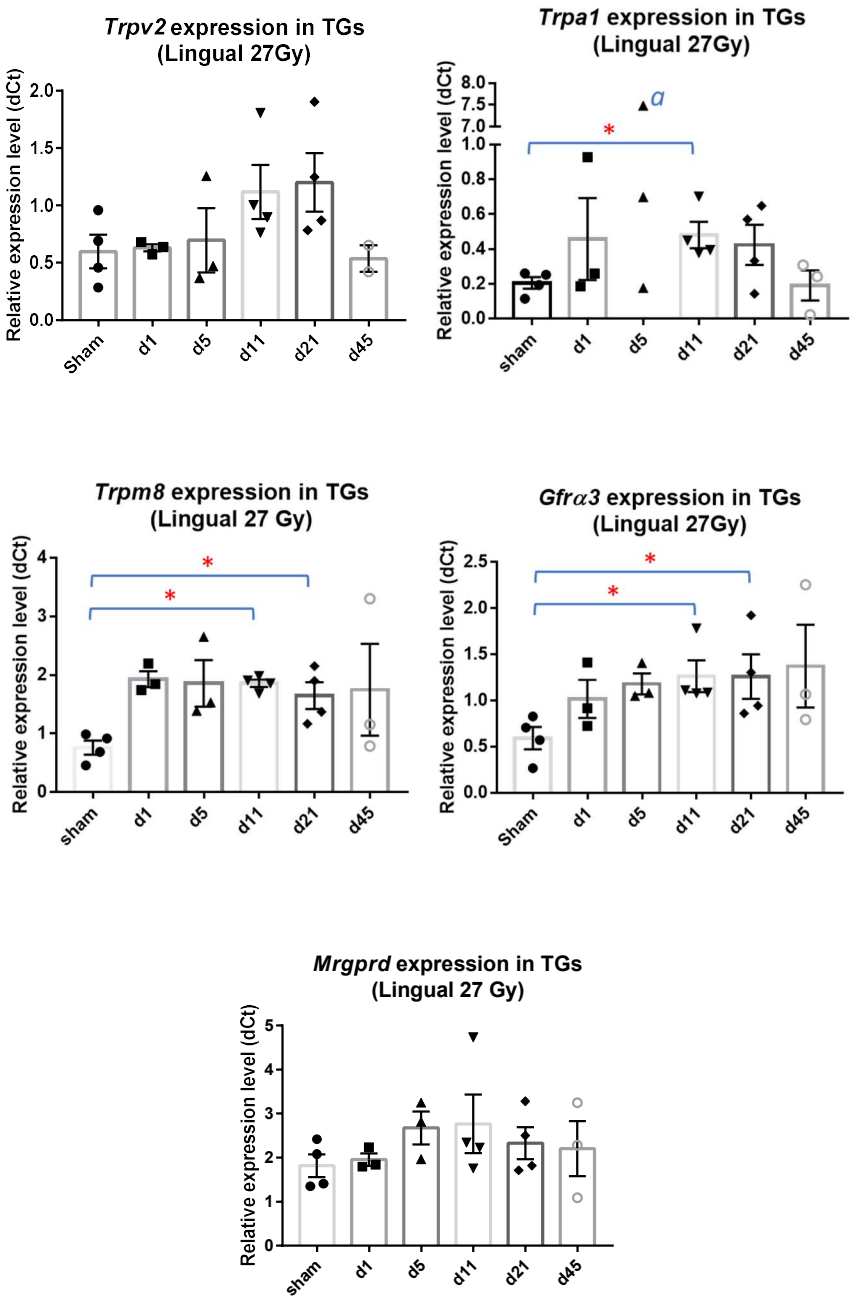

Supplemental Figure 3.3 Gene expression on TGs following high-dose lingual irradiation. These genes were not significantly increased at days 1 and 5 post-irradiation, but there was trend toward increased expression. However, the low sample number on day 1 and day 5 (n=3) may be the reason for observation of a non-significant difference. Mann-Whitney test, n=3-4 mice per group per at each time point; error bar = SEM. *Gapdh* was served as a housekeeping gene.*$P < 0.05$; *a*, outlier

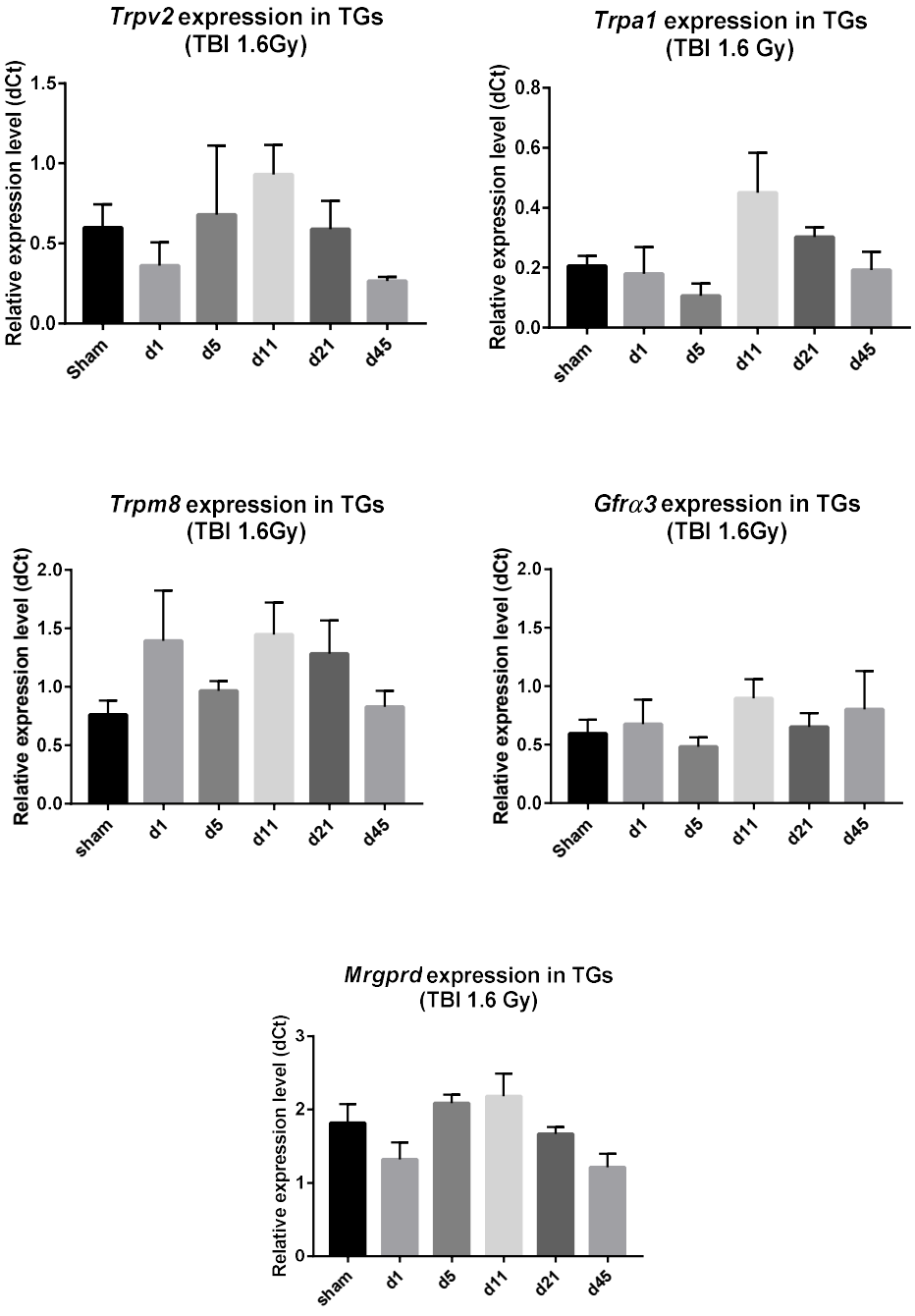

Supplemental Figure 3.4 Thermal and mechanical pain-related gene expression in TG from mice had 1.6 Gy TBI. This low dose of radiation, modeling that which scatters to the body during 27 Gy lingual irradiation, did not show a statistically significant difference in gene expression when compared to sham-irradiated mice. Mann-Whitney test, n= 3-4 mice per group per at each time point; error bar = SEM. *Gapdh* was served as a housekeeping gene.

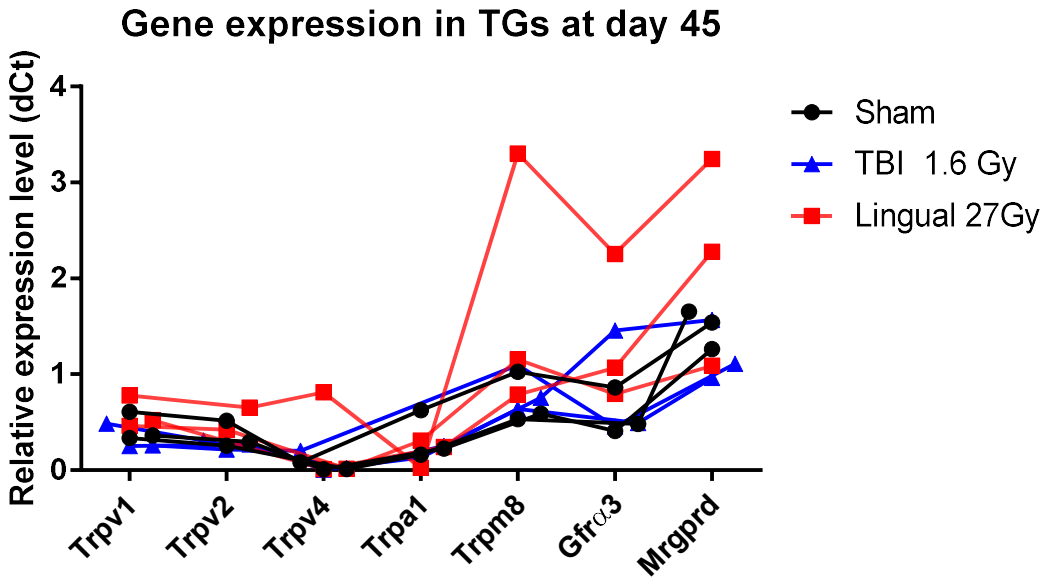

Supplemental Figure 3.5 Gene expression on TG neurons in three groups on day 45. Although we did not see a statistically significant difference between the treatment groups, the outliers may provide useful insight: one of the RIM mice had persistent 2-3-fold higher *Trpm8*, *GFRa3*, and *Mrgprd* gene expression, and another mouse had 2-fold increased *Mrgprd* expression. *Gapdh* was served as a housekeeping gene.

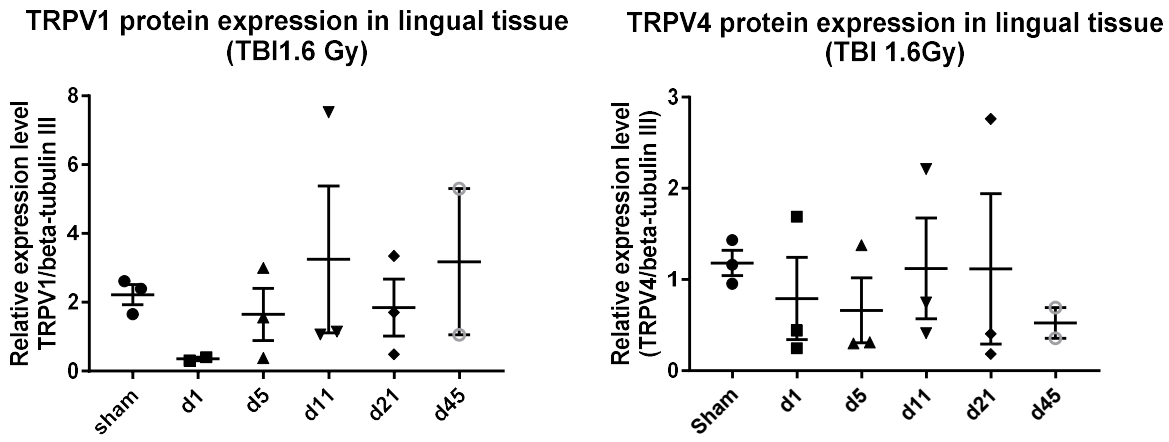

Supplemental Figure 3.6 The total body low dose irradiation did not significantly impact the TRPV1 and TRPV4 protein expression in lingual tissues.

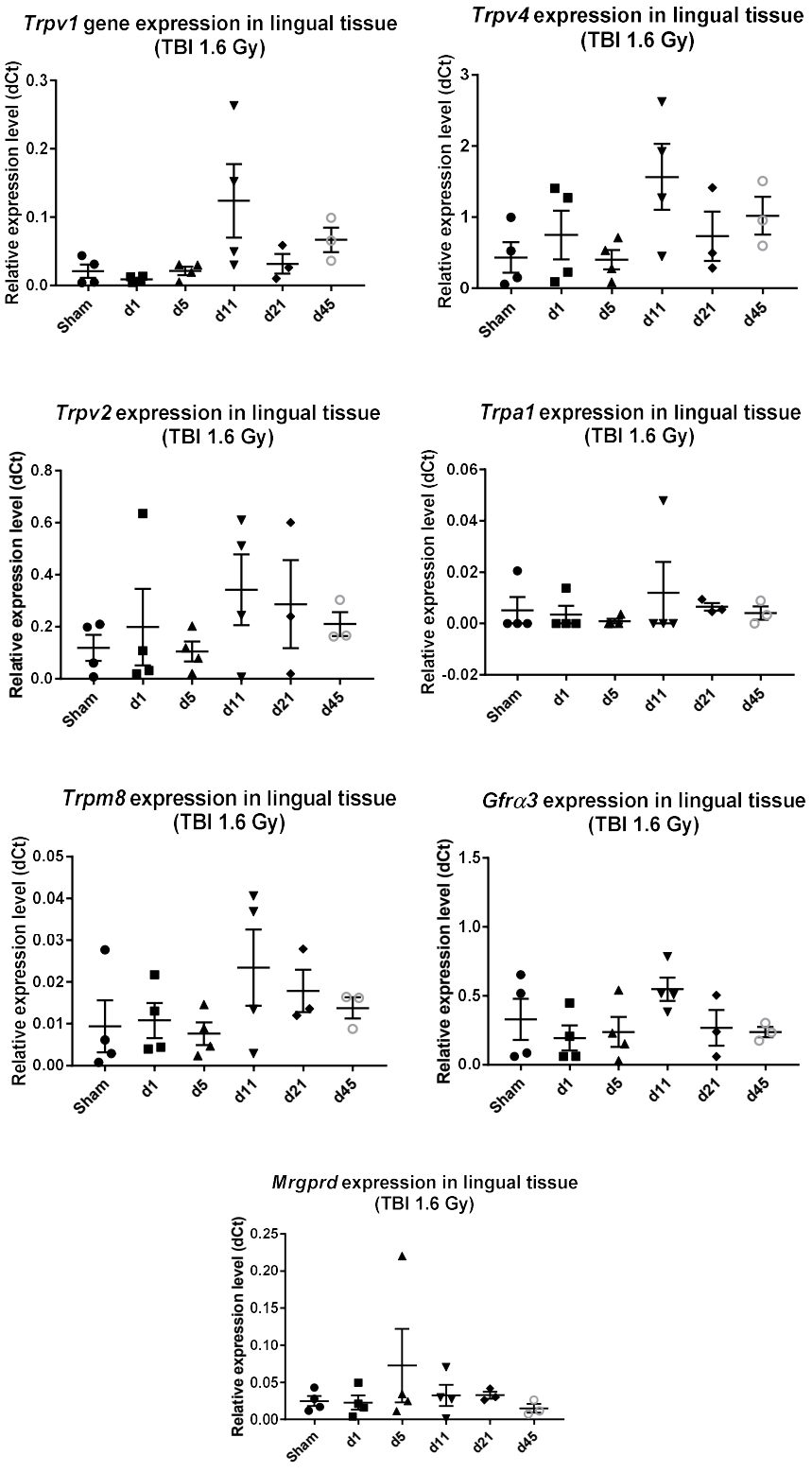

Supplemental Figure 3.7 Total body low dose irradiation did not significantly impact the expression of pain-related genes in lingual tissues.

REFERENCES

[1] BuenoM, StevensB, DeCamargoPP, TomaE, KrebsVLJ, KimuraAF. Breast milk and glucose for pain relief in preterm infants: A noninferiority randomized controlled trial. Pediatrics 2012.

[2] NolanMW, LongCT, MarcusKL, SarmadiS, RobackDM, FukuyamaT, BaeumerW, LascellesBDX. Nocifensive Behaviors in Mice with Radiation-Induced Oral Mucositis. Radiat Res 2017;187:397–403. doi:10.1667/RR14669.1.

APPENDIX C: Chapter 4 Supplemental Data

Appendix 4.1

Feline Orofacial Cancer Pain Questionnaire

- Patient name: _____
- Chose the answers which most closely match your cat's status in the past week.
- The questionnaire should be filled out by the same person throughout the study.

During the past 7 days, my cat:	No	If YES, ***how often*** did your cat have it?				If YES, ***how severe*** was it usually?			
		Rarely	Sometimes	Usually	Always	Mild	Moderate	Severe	Very severe
Behavior									
• Had low energy?	O	O	O	O	O	O	O	O	O
• Was reluctant to wake up?	O	O	O	O	O	O	O	O	O
• Had altered mood?	O	O	O	O	O	O	O	O	O
• Had trouble getting comfortable?	O	O	O	O	O	O	O	O	O
• Growled or groaned when resting?	O	O	O	O	O	O	O	O	O
• Could not maintain hygiene (i.e., grooming)?	O	O	O	O	O	O	O	O	O
• Had decreased appetite?	O	O	O	O	O	O	O	O	O
• Drank less water than usual?	O	O	O	O	O	O	O	O	O
• Had trouble positioning to defecate/urinate?	O	O	O	O	O	O	O	O	O
Activity									
• Had trouble with mobility?	O	O	O	O	O	O	O	O	O
• Fell or lost balance?	O	O	O	O	O	O	O	O	O
• Did not do what he/she likes (e.g. chasing, playing, etc.)?	O	O	O	O	O	O	O	O	O
• Did not act like his/her normal self?	O	O	O	O	O	O	O	O	O
• Had decreased enjoyment of life?	O	O	O	O	O	O	O	O	O
• Did not sleep well?	O	O	O	O	O	O	O	O	O
Interaction									
• Was unwilling to be near me?	O	O	O	O	O	O	O	O	O
• Showed a decreased amount of affection?	O	O	O	O	O	O	O	O	O
• Did not like to be pet or touched?	O	O	O	O	O	O	O	O	O
Oral/facial discomfort									
• Had excessive drooling?	O	O	O	O	O	O	O	O	O
• Had difficulty eating his/her normal food?	O	O	O	O	O	O	O	O	O
• Was offered and had trouble eating soft food?	O	O	O	O	O	O	O	O	O
• Had trouble lying down his/her head?	O	O	O	O	O	O	O	O	O
• Felt discomfort or pain near the mouth?	O	O	O	O	O	O	O	O	O
• Was defensive when their head was touched?	O	O	O	O	O	O	O	O	O

For this final question, please mark an ***X*** along the line to show your cat's overall ***current*** quality of life.

Appendix 4.2

Clinician Feline Orofacial Pain Scale for Cancers

Subscale 1: PAIN EXPRESSION (0-12)		
Miscellaneous behavior	Observe and mark the presence of the behaviors listed below **A** - The cat is laying down and quiet, but moving its tail **B** - The cat contracts and extends its thoracic limbs and/or contracts its neck muscles **C** - The cat's eyes are partially closed (eyes half closed) **D** - The cat licks, has ptyalism, and/or chattering (jaw shakes)	
	• All above behaviors are absent	0
	• Presence of one of the above behaviors	1
	• Presence of two of the above behaviors	2
	• Presence of three of the above behaviors	3
Reaction to palpation of the area around the mouth cavity	• The cat does not react when the mouth is touched or pressed	0
	• The cat does not react when the area around the mouth is touched, but does react when it is touched and pressed. It may vocalize and/or try to bite	1
	• The cat reacts when the mouth is touched and when pressed. It may vocalize and/or try to bite.	2
	• The cat reacts when the observer approaches the mouth. It may vocalize and/or try to bite. The cat does not allow palpation around mouth cavity.	3
Reaction to palpation of the head	• The cat does not react when the head is touched	0
	• The cat does not react when the head and neck are touched, but does react when it is pressed. The neck is tense	1
	• The cat reacts when the head and neck are touched and when pressed. The neck is tense	2
	• The cat reacts when the observer approaches the head. It may vocalize and/or try to bite. The cat does not allow palpation of the head and neck	3
Vocalization	• The cat is quiet, purring when stimulated, or meows interacting with the observer, but does not growl, groan, or hiss	0
	• The cat purrs spontaneously (without being stimulated or handled by the observer)	1
	• The cat growls, howls, or hisses when handled by the observer (when its body position is changed by the observer)	2
	• The cat growls, howls, hisses spontaneously (without being stimulated or handled by the observer)	3
	Subtotal	
Subscale 2: PSYCHOMOTOR CHANGE (0-12)		
Posture	• The cat is in a natural posture with relaxed muscles (it moves normally)	0
	• The cat is in a natural posture but is tense (it moves little or is reluctant to move)	1
	• The cat is sitting or in sternal recumbency with its back arched and head down; or The cat is in dorso-lateral recumbency with its pelvic limbs extended or contracted	2
	• The cat frequently alters its body position in an attempt to find a comfortable posture	3
Comfort	• The cat is comfortable, awake or asleep, and interacts when stimulated (it interacts with the observer and/or is interested in its surroundings)	0
	• The cat is quiet and slightly receptive when stimulated (it interacts little with the observer and/or is not very interested in its surroundings)	1

	• The cat is quiet and "dissociated from the environment" (even when stimulated it does not interact with the observer and/or has no interest in its surroundings) The cat may be facing the back of the cage	2
	• The cat is uncomfortable, restless (frequently changes its body position), and slightly receptive when stimulated or "dissociated from the environment" The cat may be facing the back of the cage	3
Activity	• The cat moves normally (it immediately moves when the cage is opened; outside the cage it moves spontaneously when stimulated or handled)	0
	• The cat moves more than normal (inside the cage it moves continuously from side to side)	1
	• The cat is quieter than normal (it may hesitate to leave the cage and if removed from the cage tends to return, outside the cage it moves a little after stimulation or handling)	2
	• The cat is reluctant to move (it may hesitate to leave the cage and if removed from the cage tends to return, outside the cage it does not move even when stimulated or handled)	3
Attitude	Observe and mark the presence of the mental states listed below A- **Satisfied:** The cat is alert and interested in its surroundings (explores its surroundings), friendly and interactive with the observer (plays and/or responds to stimuli) - *The cat may initially interact with the observer through games to distract it from the pain. Carefully observe to distinguish between distraction and satisfaction games* B- **Uninterested:** The cat does not interact with the observer (not interested by toys or plays a little; does not respond to calls or strokes from the observer) - *In cats, which don't like to play, evaluate interaction with the observer by its response to calls and strokes* C- **Indifferent:** The cat is not interested in its surroundings (it is not curious; it does not explore its surroundings) - *The cat can initially be afraid to explore its surroundings. The observer needs to handle the cat and encourage it to move itself (take it out of the cage and/or change its body position)* D- **Anxious:** The cat is frightened (it tries to hide or escape) or nervous (demonstrating impatience and growling, howling, or hissing when stroked and/or handled) E- **Aggressive:** The cat is aggressive (tries to bite or scratch when stroked or handled)	
	• Presence of the mental state A	0
	• Presence of one of the mental states B, C, D, or E	1
	• Presence of two of the mental states B, C, D, or E	2
	• Presence of three or all of the mental states B, C, D, or E	3
	Subtotal	
	Subscale 3: PHYSIOLOGICAL VARIABLES (0-3)	
Appetite	• The cat is eating normally	0
	• The cat is eating more than normal	1
	• The cat is eating less than normal	2
	• The cat is not interested in food	3
	Subtotal	
	Total Score	

Appendix 4.3

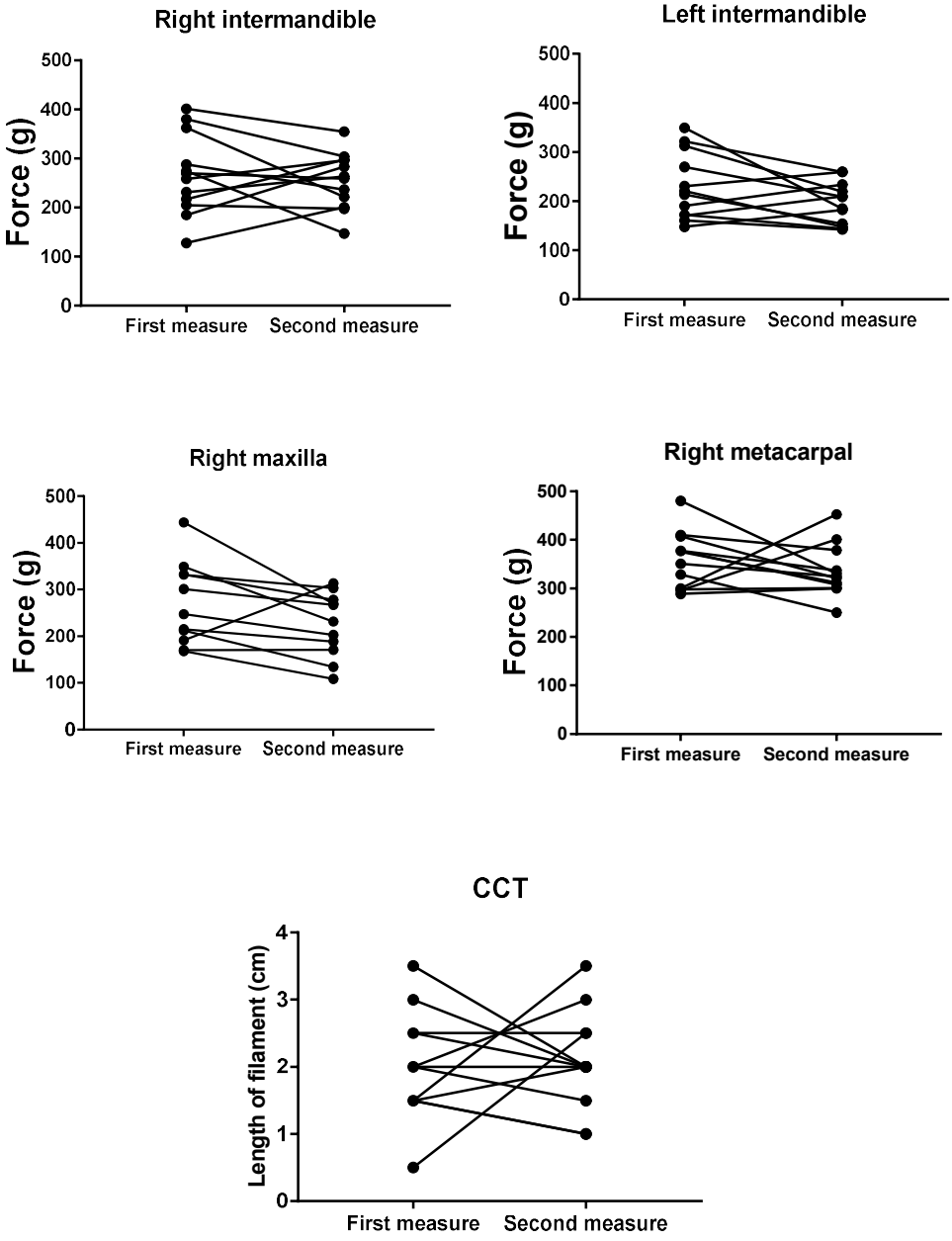

Supplemental Figure 4.1 Reliability test of EVF and COBO aesthesiometer (CTT) in healthy control cats. There was no significant difference between two measurements (Mann-Whitney test).

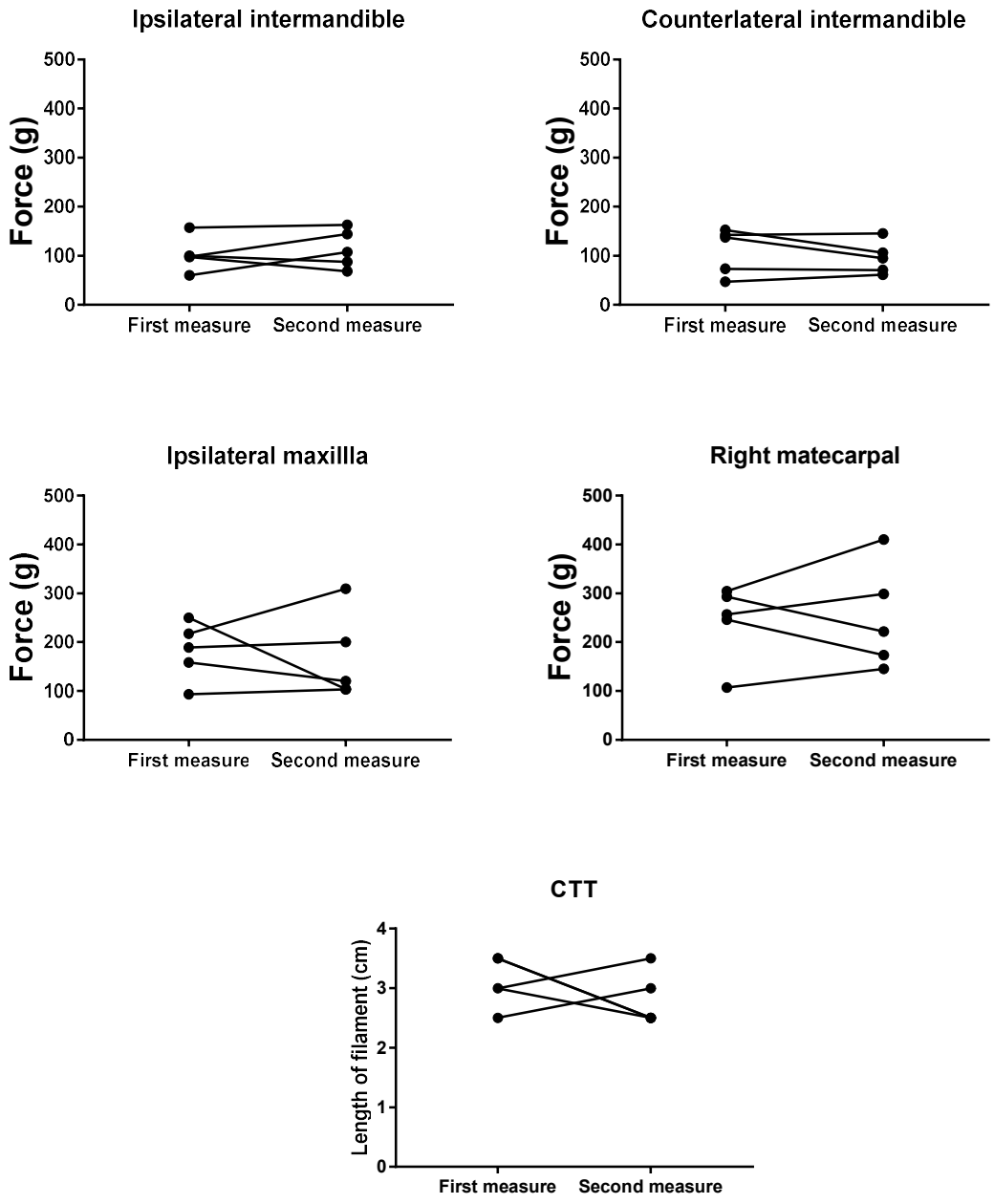

Supplemental Figure 4.2 Repeatability test of EVF and COBO aesthesiometer (CTT) in cats with sublingual SCC. There was no significant difference between two measurements (Mann-Whitney test).

Appendix 4.4

Feline Orofacial Cancer Pain Questionnaire

- Patient name: _____
- Chose the answers which most closely match your cat's status in the past week.
- The questionnaire should be filled out by the same person throughout the study.

During the past 7 days, my cat:	No	If YES, ***how often*** did your cat have it?				If YES, ***how severe*** was it usually?			
		Rarely	Sometimes	Usually	Always	Mild	Moderate	Severe	Very severe
Behavior									
• Had low energy?	○	○	○	○	○	○	○	○	○
• Was reluctant to wake up?	○	○	○	○	○	○	○	○	○
• Had altered mood?	○	○	○	○	○	○	○	○	○
• Had trouble getting comfortable?	○	○	○	○	○	○	○	○	○
• Growled or groaned when resting?	○	○	○	○	○	○	○	○	○
• Could not maintain hygiene (i.e., grooming)?	○	○	○	○	○	○	○	○	○
• Had decreased appetite?	○	○	○	○	○	○	○	○	○
• Drank less water than usual?	○	○	○	○	○	○	○	○	○
• Had trouble positioning to defecate/urinate?	○	○	○	○	○	○	○	○	○
Activity									
• Had trouble with mobility?	○	○	○	○	○	○	○	○	○
• Did not do what he/she likes (e.g. chasing, playing, etc.)?	○	○	○	○	○	○	○	○	○
• Did not act like his/her normal self?	○	○	○	○	○	○	○	○	○
• Had decreased enjoyment of life?	○	○	○	○	○	○	○	○	○
• Did not sleep well?	○	○	○	○	○	○	○	○	○
Oral/facial discomfort									
• Had excessive drooling?	○	○	○	○	○	○	○	○	○
• Had difficulty eating his/her normal food?	○	○	○	○	○	○	○	○	○
• Was offered and had trouble eating soft food?	○	○	○	○	○	○	○	○	○
• Had trouble lying down his/her head?	○	○	○	○	○	○	○	○	○
• Felt discomfort or pain near the mouth?	○	○	○	○	○	○	○	○	○

For this <u>final question</u>, please mark an ***X*** along the line to show your cat's overall ***current*** quality of life.